Retina Atlas
Series Editors:
Sandeep Saxena · Richard F. Spaide · Eric H. Souied · Timothy Y. Y. Lai

Ivana K. Kim
Editor

Macular Disorders

Springer

Retina Atlas

Series Editors

Sandeep Saxena, MS, FRCSEd, FRCS, FRCOphth
Department of Ophthalmology,
King George's Medical University,
Lucknow, Uttar Pradesh, India

Richard F. Spaide, MD
Vitreous Retina Macula Consultants of New York,
New York, NY, USA

Eric H. Souied, MD
Department of Ophthalmology,
University Paris-Est Créteil,
Créteil Cedex, France

Timothy Y. Y. Lai, MD, FRCS, FRCOphth
Department of Ophthalmology and Visual Sciences,
Chinese University of Hong Kong,
Hong Kong, Hong Kong

The 9-volume atlas covers validated and comprehensive information on retinal imaging, retinal vascular disorders, macular disorders, vitreoretinal surgical diseases, infectious and inflammatory disorders, retinal degenerations and dystrophies, pediatric retinal diseases, oncology, and trauma. This atlas with over 100 chapters is well supported with hundreds of high-quality images and text notes providing in-depth details and information in a well-organized manner.

The editors Sandeep Saxena (India), Richard F Spaide (USA), Eric Souied (France) and Timothy Y Y Lai (Hong Kong), volume editors and contributing authors are reputed eye physicians in their field with vast clinical experience.

This series has a full dedicated volume on imaging and includes various imaging technologies like optical coherence tomography, fluorescein angiography, etc. It provides global perspective of vitreoretinal diseases extensively covering medical and surgical aspects of the disease. Uncommon retinal findings in diseases such as Dengue hemorrhagic fever, malaria etc. are also covered well.

Retina Atlas is a useful go-to series meant for ophthalmology residents, retina fellows, and retina specialists as well as general ophthalmologists.

Key Features

Features coverage of retina in 9 volumes and more than hundred chapters enabling selective reading

Covers full spectrum of retinal diseases and includes recent advances in imaging techniques

Provides global perspective of vitreoretinal diseases for the first time covering extensively medical and surgical aspects of the disease

Presents global expertise and knowledge of reputed experts working at high-volume centers of excellence

'Retina Atlas' series includes the following 9 Volumes:

1. Retinal Imaging
2. Retinal Vascular Disorders
3. Macular Disorders
4. Surgical Retina
5. Inflammatory and Infectious Ocular Disorders
6. Hereditary Chorioretinal Disorders
7. Pediatric Retinal Diseases
8. Ocular Oncology
9. Trauma and Miscellaneous Disorders in Retina

More information about this series at http://www.springer.com/series/16451

Ivana K. Kim
Editor

Macular Disorders

Springer

Editor
Ivana K. Kim
Massachusetts Eye and Ear
Harvard Medical School
Boston, MA
USA

ISSN 2662-5741 ISSN 2662-575X (electronic)
Retina Atlas
ISBN 978-981-15-3000-5 ISBN 978-981-15-3001-2 (eBook)
https://doi.org/10.1007/978-981-15-3001-2

This Springer imprint is published by the registered company Springer Nature Singapore Pte Ltd.
The registered company address is: 152 Beach Road, #21-01/04 Gateway East, Singapore 189721, Singapore

Acknowledgments

I would like to thank Iris Cheng for her meticulous review of all the chapters in this volume. Her help was invaluable.

My sincere gratitude to all the contributing authors for providing such excellent material.

I would like to honor the memory of Dr. Jae Hyung Lee, who was unable to see this book in print. His academic and clinical contributions to our field will always be remembered.

Contents

About the Editor

Ivana K. Kim, MD is an Associate Professor of Ophthalmology at Harvard Medical School and serves as Co-Director of the Harvard Medical School Department of Ophthalmology Age-Related Macular Degeneration Center of Excellence, as well as Co-Director of the Ocular Melanoma Center at Massachusetts Eye and Ear. She graduated from Harvard Medical School and completed her ophthalmology residency and vitreoretinal fellowship at the Massachusetts Eye and Ear Infirmary. Her clinical practice includes surgical and medical retina, with a focus on age-related macular degeneration and uveal melanoma. She is actively involved in clinical trials for retinal diseases as well as translational research in AMD and ocular melanoma. She has published extensively and is a member of many prestigious societies including the American Ophthalmological Society, the Macula Society, the Retina Society, and the Club Jules Gonin.

Dry Age-Related Macular Degeneration

1

Vikram S. Makhijani, Cindy Ung, and Deeba Husain

Abbreviations

AMD	Age-related macular degeneration
BM	Bruch's membrane
CNV	Choroidal neovascularization
FA	Fluorescein angiography
FAF	Fundus autofluorescence
GA	Geographic atrophy
GWAS	Genome-wide association studies
LLD	Low luminance deficit
NIR	Near-infrared reflectance
OCT	Optical coherence tomography
PED	Pigment epithelium detachment
ROS	Reactive oxygen species
RPE	Retinal pigment epithelium
SDD	Subretinal drusenoid deposits
SD-OCT	Spectral-domain optical coherence tomography
SS-OCT	Swept-source optical coherence tomography

Introduction

Age-related macular degeneration (AMD) is the leading cause of blindness in the developed world in people over 50 years of age (Gehrs et al. 2006). Worldwide, age-related macular degeneration is projected to affect around 196 million people by 2020, increasing to 288 million in 2040 (Wong et al. 2014).

All AMD starts as dry AMD and drusen are the hallmark of the disease. The advanced form of the disease occurs in two forms: neovascular (exudative or wet) and nonneovascular (nonexudative or dry) forms. Geographic atrophy is the advanced dry form of age-related macular degeneration. Severe vision loss in up to 20% of legal blindness from AMD is due to the atrophic form (Sunness 1999).

AMD is a multifactorial complex disease, in which genetics as well as environmental risk factors influence its progression (Wong et al. 2014; Yonekawa and Kim 2014). Population-based studies have demonstrated that age is the most significant risk factor. In resource-rich countries, 10% of people over the age of 65 years and 25% over the age of 75 years have AMD (Smith et al. 2001). Additional risk factors include female sex, hypertension, hypercholesterolemia, cardiovascular disease, cigarette smoking, and positive family history (Ambati et al. 2013; Ferris et al. 2013). Smokers with more than 40 pack years have a twofold increased risk of losing vision from age-related macular degeneration (Khan et al. 2006). Racial origin is another important risk factor. The 10-year longitudinal Multi-Ethnic Study of Atherosclerosis (MESA) found a prevalence of AMD in the United States highest in whites (5.4%), followed by Asians (4.6%), Hispanics (4.2%) and African Americans (2.4%) (Fisher et al. 2016).

The genetic contribution to the development of AMD has been well-established with multiple risk loci identified through genome-wide association studies (GWAS) (Zhan et al. 2013; Ratnapriya et al. 2014; Fritsche et al. 2016). These studies have implicated genes such as ***CFH*** (Haines et al. 2005), ***C3*** (Yates et al. 2007), ***C2-CFB*** (Gold et al. 2006), a region on chromosome 10 with ***HTRA1/LOC387715/ARMS2*** (Dewan et al. 2006), ***TIMP3*** (Chen et al. 2010), ***VEGFA***, ***COL10A1*** (Yu et al. 2011), ***TNFRSF10A*** (Arakawa et al. 2011), and ***APOE*** (Zareparsi et al. 2004) with AMD. The largest AMD GWAS study to date examined more than 12 million variants in 16,144 patients and 17,832 controls (Fritsche et al. 2016). This study identified 52 independently associated common and rare variants distributed across 34 loci, 16 of which reached genome-wide significance.

V. S. Makhijani · C. Ung · D. Husain (✉)
Retina Service, Department of Ophthalmology, Massachusetts Eye and Ear, Harvard Medical School, Boston, MA, USA
e-mail: deeba_husain@meei.harvard.edu

I. K. Kim (ed.), *Macular Disorders*, Retina Atlas, https://doi.org/10.1007/978-981-15-3001-2_1

Pathogenesis

The first clinically detectable feature of AMD is the appearance of drusen, which are extracellular deposits that form in the RPE/Bruch's membrane complex (Hageman et al. 2001; Anderson et al. 2002; Chen et al. 2008). Drusen color varies from white to pale yellow to bright yellow. As drusen regress, they lose their coloration and may be associated with areas of RPE atrophy or depigmentation. Those individuals with drusen have been found to have functional impairment, such as with dark adaptation, and are at increased risk for developing vision loss and more advanced forms of AMD, such as geographic atrophy (GA) or choroidal neovascularization (CNV) (Bhutto and Lutty 2012; Laíns et al. 2017b).

The exact mechanism of AMD is not fully understood. The formation of drusen can be compared with extracellular lipid deposition in a vessel wall of the systemic circulation in atherosclerotic cardiovascular disease. Curcio et al. have formulated a compelling model for AMD pathogenesis, whereby the Bruch's membrane functions much like the endothelium in atherosclerosis (Curcio et al. 2011). RPE-secreted lipoproteins such as apolipoprotein B are a major source of lipids under the RPE where they are retained and eventually cleared through the choriocapillary endothelium. Lipoprotein particles begin to accumulate during adulthood and pathologic responses to these retained particles are thought to lead to AMD.

Oxidative stress has also been implicated in the occurrence of AMD. The photoreceptors in the retina are particularly susceptible to oxidative stress because of their exposure to light and high consumption of oxygen (Beatty et al. 2000). Risk factors such as smoking, hypercholesterolemia, and excessive light exposure can augment the generation of reactive oxygen species (ROS) and result in an imbalance between oxidative stress and the remodeling process. ROS causes severe damage to the lysosomal membrane of the RPE and leads to incomplete proteolytic digestion of ROS and photoreceptor outer membrane phagocytosis within the lysosomes of RPE cells (Arjamaa et al. 2009; Blasiak et al. 2014). Lipofuscin then accumulates within Bruch's membrane and the RPE and acts as a precursor for drusen formation (Arjamaa et al. 2009; Lin et al. 2013).

Clinical Features

Diagnosis of dry AMD in its early stages is made on the basis of characteristic anatomic features on a dilated fundus exam (Biomarkers Definitions Working Group et al. 2001; Husain et al. 2002; Klein et al. 2002). Less commonly, presenting symptoms such as difficulty with night vision, difficulty with dark adaptation, blurred near vision, metamorphopsia, or decreased contrast sensitivity may be perceived by the patient (Neely et al. 2017; Laíns et al. 2017b).

Drusen

Drusen appearance is important in diagnosis and classification of AMD. Drusen are the earliest clinical features of early to intermediate dry AMD (Fig. 1.1), and are historically classified ophthalmoscopically based on numerous parameters (Table 1.1) (van Leeuwen 2003). Current classification of AMD severity is based on classic fundus photography demonstrating these characteristics (Danis et al. 2013). Early dry AMD is defined by presence of small to medium drusen, while the appearance of extensive small to medium drusen or at least one large drusen indicates an intermediate stage (Fig. 1.2). Advanced AMD is defined by presence of neovascularization or center-involving geographic atrophy (Ferris et al. 2005, 2013).

The AREDS Research Group devised a classification scale based on nine steps of disease in order to characterize patterns and risk of progression (Tables 1.2, 1.3, and 1.4) (Age-Related Eye Disease Study Group 2005). This scale scores drusen based on area and, in combination with pigmentation alteration area, determines a step. Steps carry a 5-year risk of progression to advanced AMD ranging from less than 1% to about 50%. AREDS also devised a simplified scoring system to predict progression. In this system, risk factors are defined as presence of a large druse or presence of a pigmentary abnormality, and totaled for each eye. Five-year risk of progression to advanced AMD is 0.5% for 0 risk factors, 3% for 1, 12% for 2, 25% for 3, and 50% for 4 (Ferris et al. 2005).

Reticular Pseudodrusen

Subretinal drusenoid deposits (SDDs), or reticular pseudodrusen, are becoming increasingly recognized as anatomic features increasing the risk of AMD progression (Zweifel et al. 2010). SDDs, independent of classification of AMD, have been shown to correlate with decreases in visual function, such as dark adaptation (Sivaprasad et al. 2016; Laíns et al. 2017b). Unlike drusen, these drusenoid deposits are located within the RPE, generally are more anterior, and have different imaging characteristics. On autofluorescence, drusenoid deposits are seen as hypoautofluorescent dots if there is blocking of RPE, or hyperautofluorescent dots if there is overlying photoreceptor disruption (Fig. 1.3) (Zweifel et al. 2010). Near-infrared reflec-

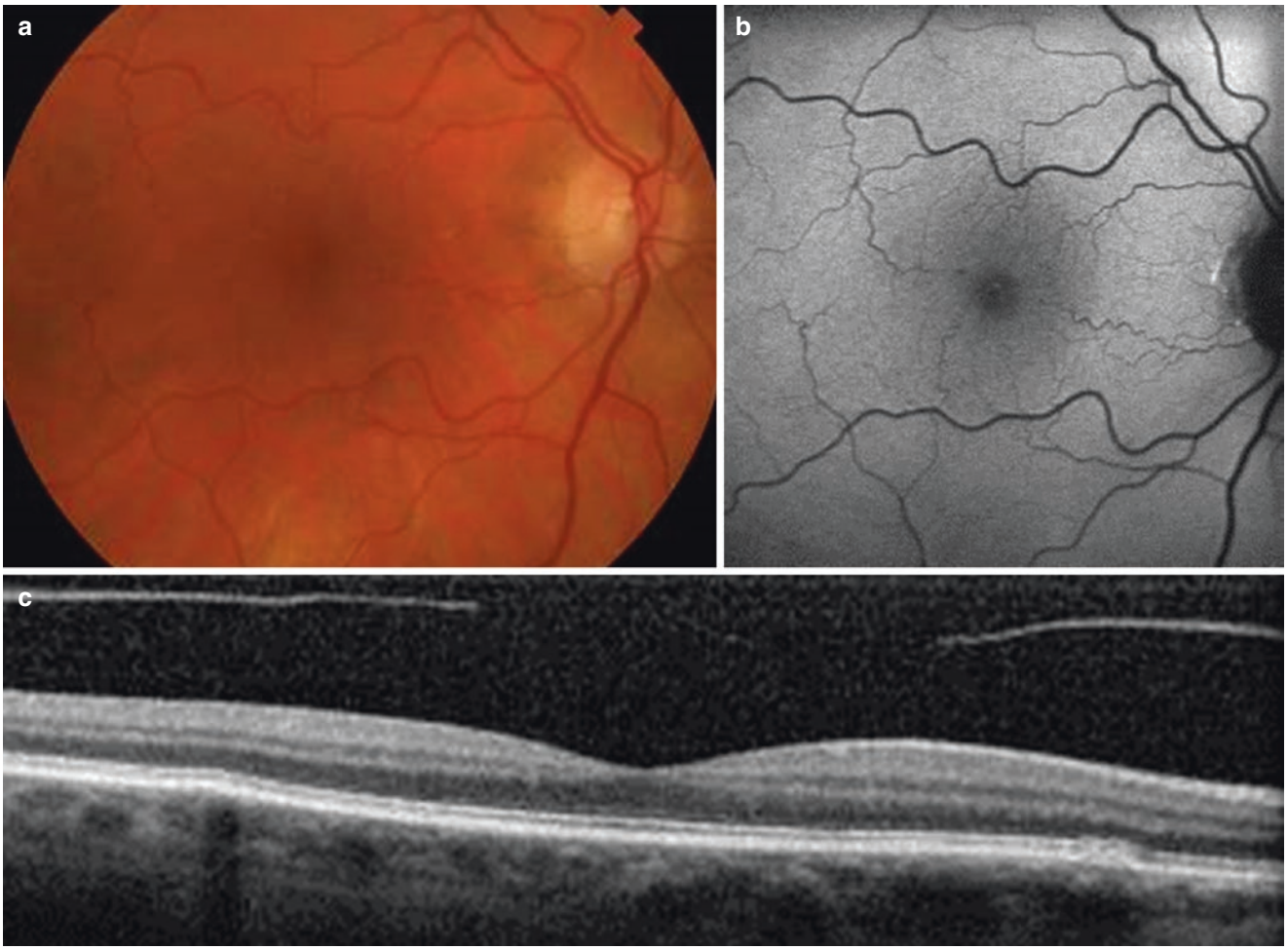

Fig. 1.1 Early AMD. (**a**) Color fundus photograph of an asymptomatic patient shows few small to medium scattered drusen. AREDS classification places this presentation at stage 1, given small drusen area and no pigmentary abnormalities or atrophy. By AREDS simplified classification, 0 risk factors carry a 0.5% 5-year risk of progression to advanced AMD. Drusen may not be as apparent on autofluorescence (**b**) or OCT (**c**)

Table 1.1 Anatomic characteristics of drusen

Number	
Size	Small: <63 μm Medium: 64–125 μm Large >125 μm
Location	Central, perivascular, peripheral
Density	Hard, soft
Confluence	Drusenoid PED
Modification	Calcification, cholesterolization, ossification

tance (NIR) shows varying reflective patterns that can be correlated with SD-OCT, which shows hyperreflective subretinal deposits between the RPE and ellipsoid zone (Fig. 1.3) (Schaal et al. 2017; Balaratnasingam et al. 2017; Sleiman et al. 2017). Classification schemes for pseudodrusen have been proposed based on SD-OCT anatomic features. With the advent of Swept Source-OCT, studies of the choroid have shown correlation between presence of SDDs and decreased choroidal thickness and volume (Laíns et al. 2017b, c).

Geographic Atrophy

AMD can progress to geographic atrophy, causing varying degrees of vision function loss. Atrophy can be of the RPE, retina, or choriocapillaris, in single or multiple patches, and at varying distance from the fovea. It is generally progressive at its margins, with corresponding gradual vision loss (Figs. 1.4 and 1.5) (Holz et al. 2007; Lujan et al. 2009; Fleckenstein et al. 2011). Progression has been demonstrated in areas of drusen regression, along with characteristic OCT findings, including tubulations (Fig. 1.6) (Lujan et al. 2009; Goldberg et al. 2013; Hariri et al. 2015). Autofluorescence of geographic atrophy demonstrates hypoautofluorescence, consistent with loss of

Fig. 1.2 Large drusen. Large soft confluent drusen are easily discernable on fundus examination or photograph (**a**). OCT (**b**) shows characteristic confluent subretinal changes

RPE. In progressors, it has been shown that areas of hyperautofluoresence present at the edges of atrophy can predict areas of growth of atrophy. Various patterns of autofluorescence at the edges of atrophy can be predictive of rate of growth. Patchy, banded, and diffuse trickling hyperautofluorescence at the edge of geographic atrophy have shown higher rates of progression than diffuse or focal patterns (Holz et al. 2007). Fluorescein angiography shows a hyperfluorescent window defect in the area of RPE atrophy (Yung et al. 2016). SD-OCT demonstrates attenuation or loss of RPE, photoreceptors, or thinning of the choriocapillaris (Lujan et al. 2009). OCT angiography further demonstrates choriocapillaris loss more pronounced than in intermediate AMD (Cicinelli et al. 2017).

Imaging in Dry AMD

Multimodal imaging has become increasingly useful in characterizing and defining features of drusen and drusenoid abnormalities in dry AMD (Yonekawa et al. 2015). As described, dilated fundus examination and color fundus photography had been the classic method of diagnosis and staging of AMD, with digital fundus photography shown to have the same reproducibility as film photography (Danis et al. 2013).

Fundus Autofluorescence

Fundus autofluorescence (FAF) detects a specific absorption-emission pattern of the fundus not always evident on examination or photography (Delori et al. 1995). Lipofuscin is the dominant retinal fluorophore at the wavelengths most useful for AMD autofluorescence (Yung et al. 2016). On autofluorescence, drusen demonstrate hyperautofluorescence due to the concentration of fluorescent accumulations including lipofuscin (Fig. 1.7) (Holz et al. 2015). Hypoautofluorescent areas may represent melanin or RPE atrophy. In the progression of AMD, geographic atrophy demonstrates hypoautofluorescence due to loss of RPE (Holz et al. 2007). Autofluorescence is useful in clinical practice to track changes in drusen or atrophic areas over time (Figs. 1.4 and 1.5).

Table 1.2 AREDS severity scale

Stage	Drusen area	Pigment area	Atrophy area
1	*	0	0
2	** *	0 >0	0 And/or +
3	***	0	0
4	**** **, *** *, **	0 >0 >0	0 And/or + ++
5	***** **** ***	0 >0 >0	0 And/or + ++
6	****** ***** ****	0 >0 >0	0 And/or + ++
7	****** *****	>0 >0	And/or + ++
8	***** Any	>0 >0	++ +++
9	-	-	Non-central GA

Drusen area			Atrophy area	
*	<C-1		+	>Q, <I-2
**	>C-1, <C-2		++	>I-2, <0.5DA
***	>C-2, <I-2		+++	>0.5DA
****	>I-2, <0-2			
*****	>0-2, <0.5DA			
******	>0.5DA			

Circle diameters and areas: *C-0*, 63 μm and 0.0017 DA; *C-1*, 125 μm and 0.0069 DA; *C-2*, 250 μm and 0.028 DA; *I-2*, 354 μm and 0.056 DA; *0-2*, 650 μm and 0.19 DA
DA disc area; *Q* questionable

Table 1.3 AREDS vs AREDS2 formulations

	AREDS	AREDS2
Vitamin C	500 mg	500 mg
Vitamin E	400 IU	400 IU
Beta-carotene	15 mg	–
Zinc	80 mg	80 mg
Cupric oxide	2 mg	2 mg
Lutein/zeaxanthin	–	10 mg/2 mg

Fluorescein Angiography

Fluorescein angiography (FA) is the gold standard for distinguishing conversion to wet AMD and is discussed further in the corresponding chapter. Fluorescein angiography in dry AMD can demonstrate variable hyperfluorescent staining of drusen, depending on the composition, size, and height of drusen (Fig. 1.7) (Delori et al. 1995; Yung et al. 2016). With geographic atrophy, FA demonstrates a window defect and the underlying choroidal vascular pattern.

Table 1.4 Current and investigational targets for dry AMD

Anti-oxidant	AREDS
	AREDS2
	Statins
Neuroprotection	Brimonidine
	CNTF
	CNTF (NT-501) implant
Inflammation	*Lampalizumab (anti-complement factor D)*
	Fluocinolone acetonide implant
	Glatiramer acetate
	C5: ARC1905
	Eculizumab
	POT-4 (Intravitreal C3 inhibition)
	a-beta: RN6G, GSK
Blood flow	*Vasodilator: alprostadil*
	MC-101
	Moxaverine (PDEI)
Lipofuscin (visual cycle)	*Fenretinide*
	Emixustat
Stem cell	hESC-RPE cells (human embryonic)
	hRPE cells (primary human)

Italics indicate failed or inactive investigations

Optical Coherence Tomography

Optical coherence tomography (OCT) has shed new light into anatomic characteristics and clinical analysis of drusen and AMD (Yonekawa et al. 2015). Anatomically, drusen are defined as deposits between Bruch's membrane and the RPE basement membrane (Fig. 1.2) (Balaratnasingam et al. 2017). This distinction is apparent on SD-OCT, and can help differentiate typical drusen from basal laminar drusen (Fleckenstein et al. 2011; Tan et al. 2017; Curcio et al. 2017). While drusen are usually visible on clinical examination, SD-OCT may detect early drusen (Fig. 1.1), or other related abnormalities such as outer retinal disruption, early geographic atrophy, or subretinal drusenoid deposits (Lujan et al. 2009). Recently, varying degrees of choriocapillaris abnormalities have been demonstrated with OCT angiography, while demonstrating normal retinal vascular architecture (Cicinelli et al. 2017). Swept source OCT (SS-OCT) is demonstrating new findings in decreased choroidal thickness and vessel volume in AMD and subretinal drusenoid deposits (Philip et al. 2016; Laíns et al. 2017c).

Management and Treatment

Functional Testing in Dry AMD

The focus of current management of dry AMD is aimed at prevention of and detection of disease progression to atrophy or development of the neovascular form of AMD. Standard clinical monitoring includes administration of Amsler grid testing, and imaging for detection of progression or development of subretinal or intraretinal fluid. Patient directions

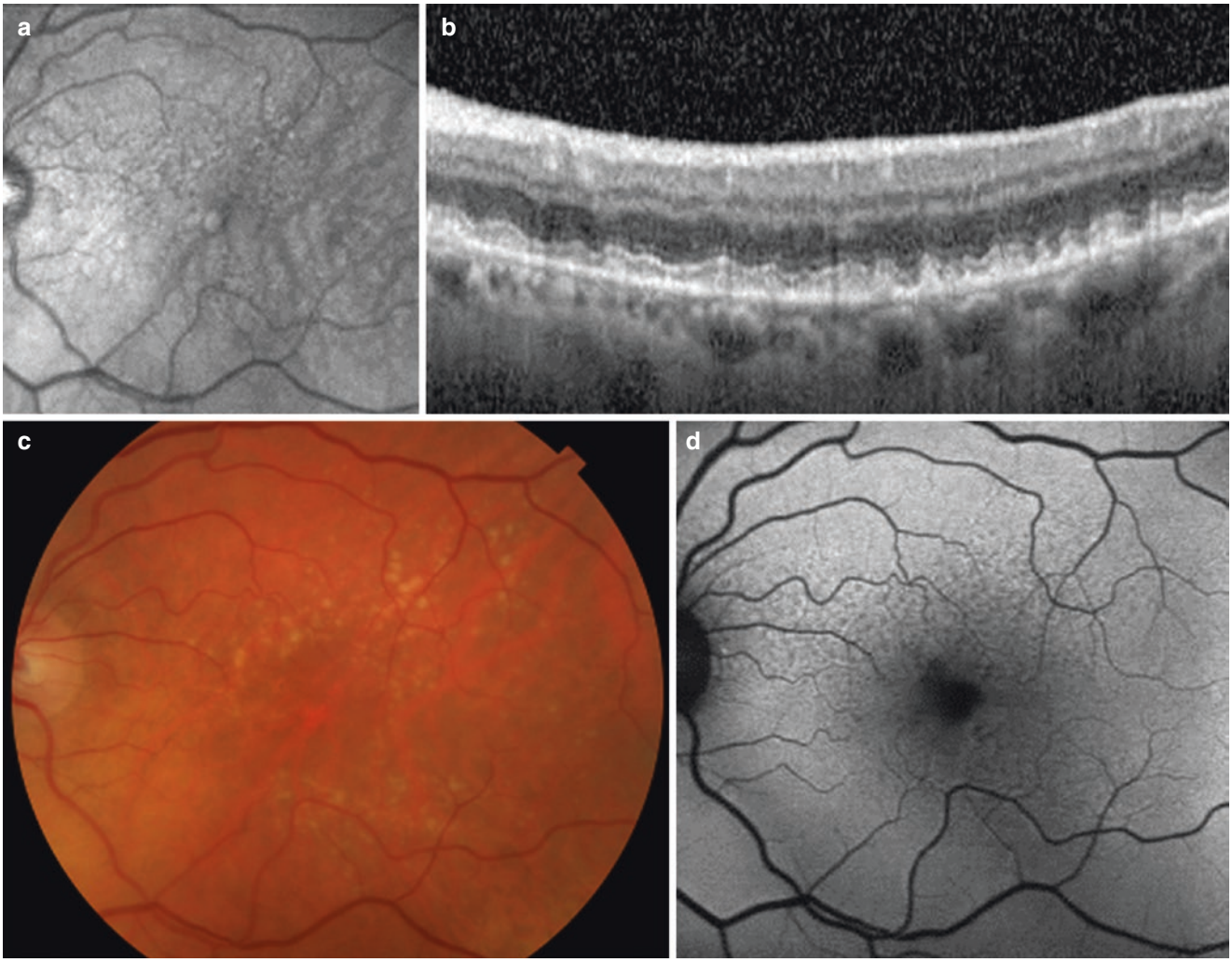

Fig. 1.3 Reticular pseudodrusen. Subretinal drusenoid deposits, or reticular pseudodrusen, can be seen on infrared reflectance imaging (**a**), but are best differentiated on OCT (**b**), which shows characteristic subretinal abnormalities. They may coexist in close proximity to drusen, and are less apparent on the fundus photograph (**c**) with prominent extensive drusen. Autofluorescence (**d**) shows scattered hypoautofluorescence outside of the areas of drusen

for home management between clinic visits include frequent Amsler grid testing (Hanus et al. 2016). Establishment of home monitoring protocols is allowing for more timely detection of disease progression. For example, the HOME study demonstrates the effectiveness of a home monitoring device for early detection of neovascularization between office visits (Chew et al. 2016).

The potential for functional measure testing in AMD with higher sensitivity than visual acuity is increasing with research in to low luminance, contrast sensitivity, dark adaptation, and microperimetry. Use of testing in low luminance, cone-specific contrast, and microperimetry for use in intermediate AMD diagnosis has been demonstrated to be feasible and reproducible (Chandramohan et al. 2016). Analysis of low luminance deficit (LLD), or the difference between best corrected visual acuity and low luminance visual acuity, demonstrates agreement with patients' subjective complaints in early AMD (Wu et al. 2016). Microperimetry has been shown to have promising sensitivity for functional measurement and correlation with structural changes (Biomarkers Definitions Working Group et al. 2001; Wu et al. 2014; Cassels et al. 2017). Dark adaptation has been correlated with diagnosis and staging of AMD and is being used increasingly in the management of AMD patients (Flamendorf et al. 2015).

Pharmacologic Therapy

Antioxidant multivitamins as established by the National Eye Institute's Age-Related Eye Disease Study 2 (AREDS2) are common practice for intermediate dry

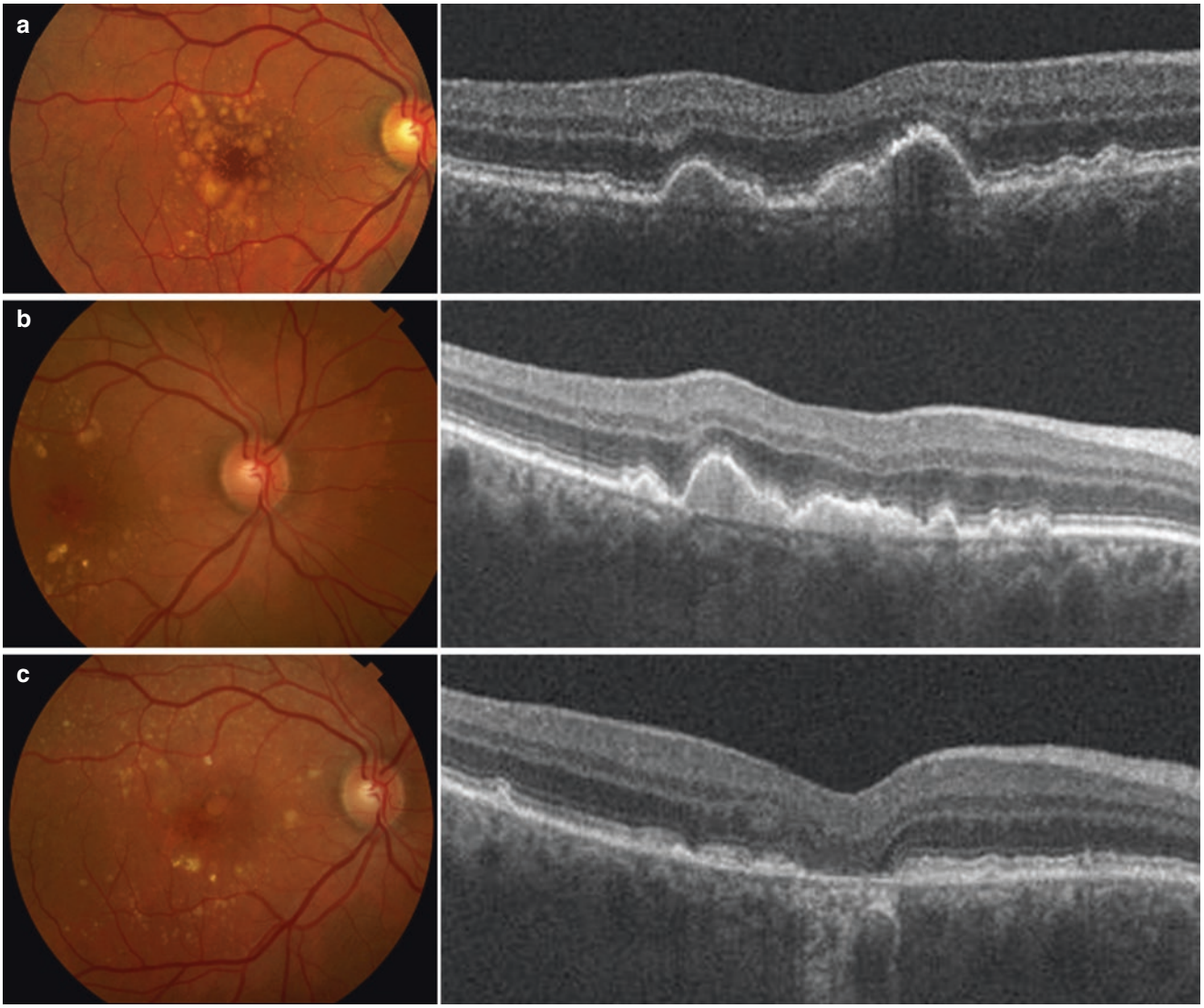

Fig. 1.4 Progression of AMD demonstrated with multimodal imaging over 8 years. Fundus photograph (**a**) shows extensive confluent high-risk drusen and drusenoid PED, which later progress (**b**) and then regress (**c**) with areas of atrophy. OCT shows RPE loss corresponding to the development of foveal geographic atrophy

AMD to reduce the risk of progression to late AMD (Ferris et al. 2005). The original AREDS formulation, vitamin C (500 mg), vitamin E (400 IU), beta-carotene (15 mg), zinc (80 mg), and cupric oxide (2 mg), reduced risk of progression by 25% (Age-Related Eye Disease Study Research Group 2001). AREDS2 determined that addition of lutein/zeaxanthin (10 mg/2 mg) in place of beta-carotene was also effective in reducing progression and eliminated the systemic risks of beta-carotene (Chew et al. 2014).

While there is not yet any standard therapy to reverse AMD severity, the study of high-dose oral statin use (atorvastatin 80 mg daily) to reverse large soft drusenoid deposits has resulted in promising results with associated gain in vision (Vavvas et al. 2016).

Ongoing Research to Find New Treatments

With the complex pathogenesis and multiple pathways affecting macular degeneration, various targets for reversal or slowing of disease progression have been proposed.

Drug Therapies

Currently, numerous studies are underway for various drugs affecting these pathways (Table 1.4). While the use of antioxidant supplementation has been well-established, further research is ongoing into optimizing formulations and delivery. Neuroprotective pathways are also under investigation in glaucoma research, and some drugs such as brimonidine with well-tested periocular safety profiles are being investigated for intraocular delivery (Sacconi et al. 2017).

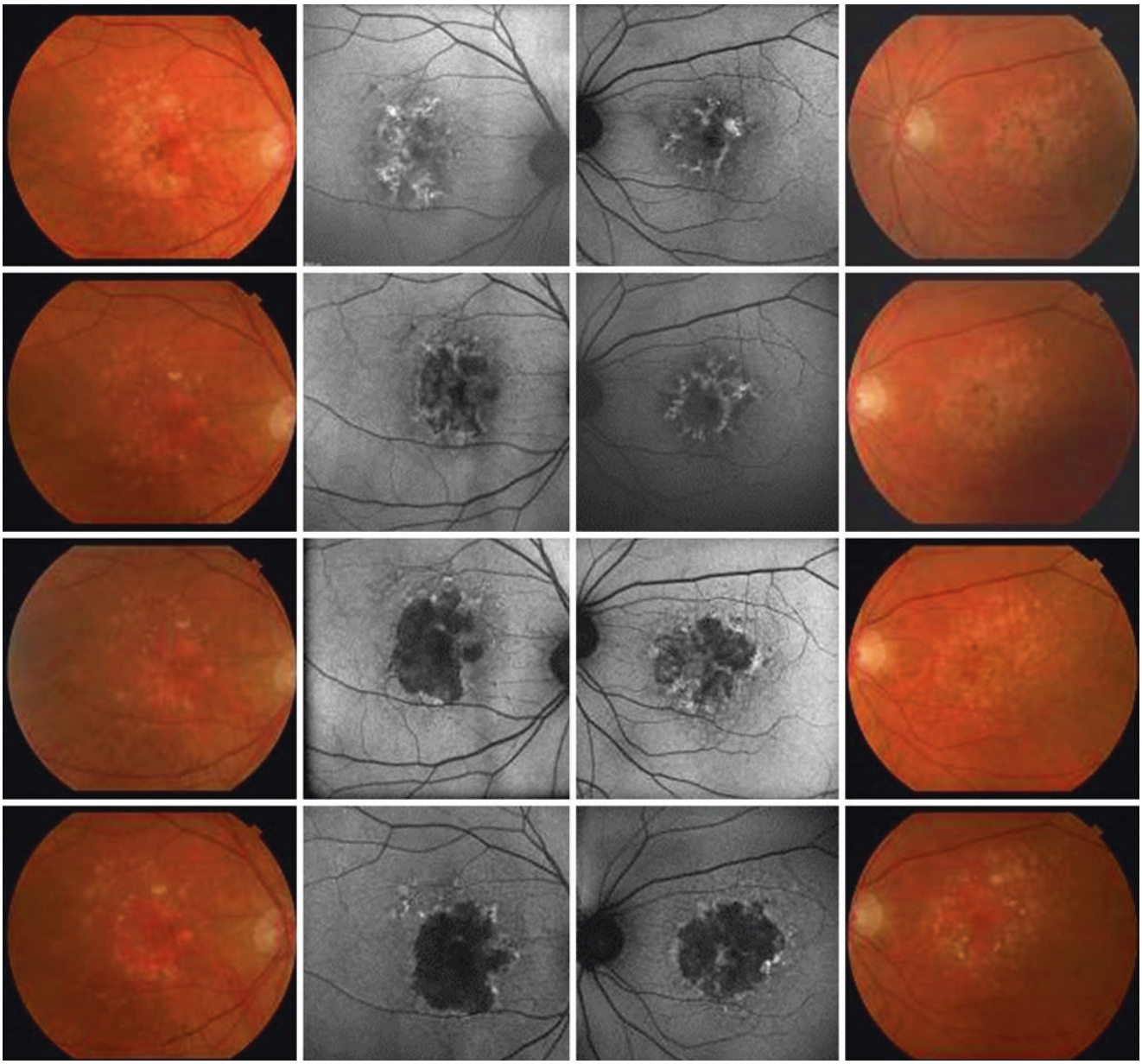

Fig. 1.5 Progressive enlargement of geographic atrophy in both eyes over time. Autofluorescence demonstrates expanding hypoautofluorescence and varying autofluorescent patterns at the margins of atrophy in successive imaging. Color fundus photographs show areas of drusen and pigment replaced by expanding atrophy

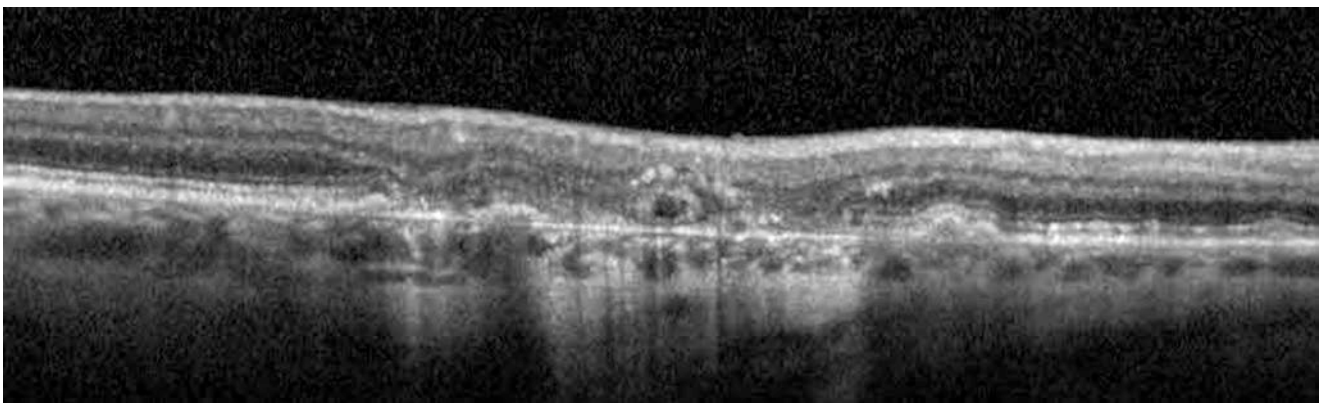

Fig. 1.6 OCT of outer retinal tubulations at the edge of progressive geographic atrophy

Inflammatory pathways are diverse in the pathogenesis of AMD Numerous clinical trials with complement-targeted agents have been performed. Phase 2 results of the MAHALO study for intravitreal lampalizumab (anti-complement factor D antibody fragment) showed 20% reduction in progression of atrophy versus controls, with a higher reduction for CFI risk-allele carriers (Yaspan et al. 2017). However, the Phase 3 trials failed to show treatment benefit (Holz et al. 2018).

Other target mechanisms, including enhancement of choroidal blood flow and visual cycle modulator molecules did not show any benefit in preventing progression of disease in clinical trials (Hanus et al. 2016). Investigation of metabolite biomarkers of disease may help achieve earlier diagnosis of AMD and identify further target therapeutic pathways (Laíns et al. 2017a).

Cell Therapies

The prospect of stem cell-derived RPE cells carries the potential of directly reversing cell loss and possibly functional loss in geographic atrophy (Sachdeva and Eliott 2016), although the

Fig. 1.7 Multimodal imaging of intermediate AMD demonstrating high-risk features while ruling out advanced AMD. Color fundus photographs (**a**) demonstrate numerous large confluent drusen and small areas of hyperpigmentation. Autofluorescence (**b**) demonstrates variable hyperautofluorescence in areas of drusen. Fluorescein angiography (**c**, **d**) shows variable staining of drusen in middle and late phases and no leakage or window defect. OCT (**e**) more definitively rules out RPE atrophy or Bruch's membrane defects in the volume area, but clearly shows high-risk drusenoid PEDs and pigment migration

Fig. 1.7 (continued)

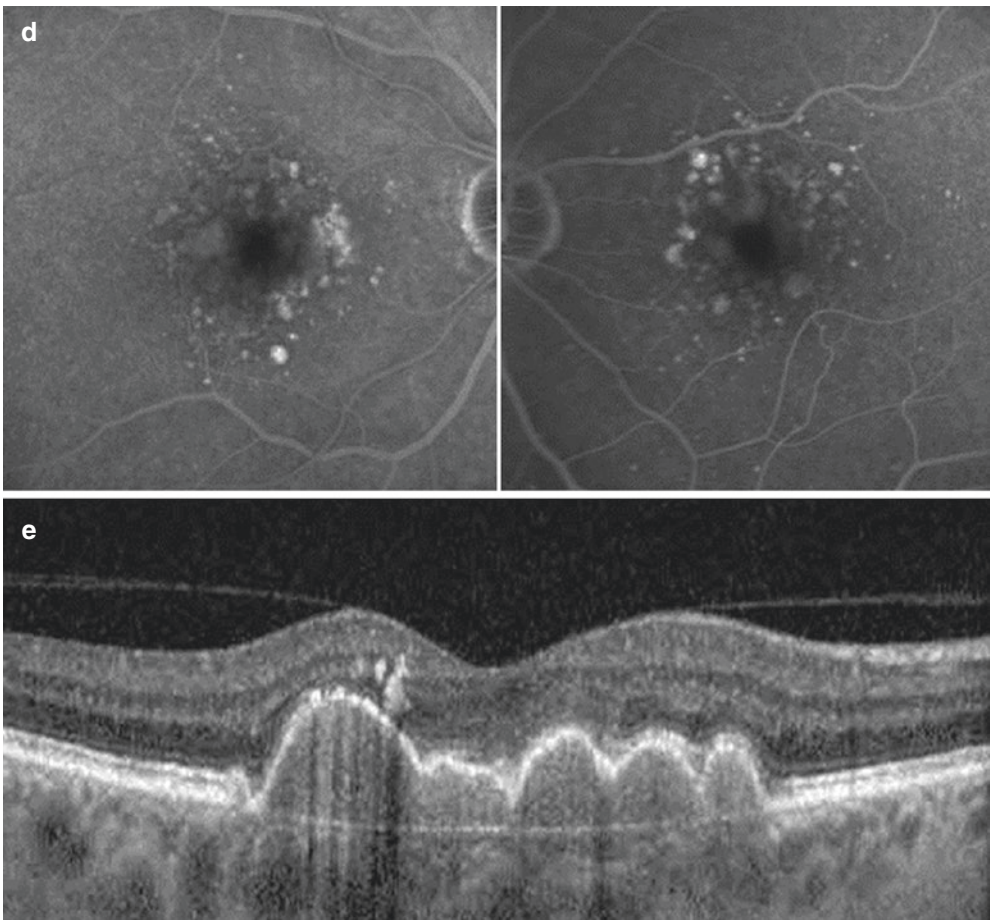

underlying degenerative impetus may persist. Recent phase 1/2 studies have demonstrated safety and tolerability of subretinal transplanted hESC-derived RPE cells (Schwartz et al. 2015, 2016). Along with further discovery in the pathophysiology, anatomic characterization, and genetics of dry AMD, the possibility of dry AMD as a treatable disease remains on the horizon.

References

Age-Related Eye Disease Study Group. The age-related eye disease study severity scale for age-related macular degeneration. Arch Ophthalmol. 2005;123:1484.

Age-Related Eye Disease Study Research Group. A randomized, placebo-controlled, clinical trial of high-dose supplementation with vitamins C and E, beta carotene, and zinc for age-related macular degeneration and vision loss: AREDS report no. 8. Arch Ophthalmol (Chicago, IL 1960). 2001;119:1417–36.

Ambati J, Atkinson JP, Gelfand BD. Immunology of age-related macular degeneration. Nat Rev Immunol. 2013;13:438–51.

Anderson DH, Mullins RF, Hageman GS, Johnson LV. A role for local inflammation in the formation of drusen in the aging eye. Am J Ophthalmol. 2002;134:411–31.

Arakawa S, Takahashi A, Ashikawa K, et al. Genome-wide association study identifies two susceptibility loci for exudative age-related macular degeneration in the Japanese population. Nat Genet. 2011;43:1001–4.

Arjamaa O, Nikinmaa M, Salminen A, Kaarniranta K. Regulatory role of HIF-1alpha in the pathogenesis of age-related macular degeneration (AMD). Ageing Res Rev. 2009;8:349–58.

Balaratnasingam C, Messinger JD, Sloan KR, et al. Histologic and optical coherence tomographic correlates in drusenoid pigment epithelium detachment in age-related macular degeneration. Ophthalmology. 2017;124:644–56.

Beatty S, Koh H, Phil M, et al. The role of oxidative stress in the pathogenesis of age-related macular degeneration. Surv Ophthalmol. 2000;45:115–34.

Bhutto I, Lutty G. Understanding age-related macular degeneration (AMD): relationships between the photoreceptor/retinal pigment epithelium/Bruch's membrane/choriocapillaris complex. Mol Asp Med. 2012;33:295–317.

Biomarkers Definitions Working Group. Biomarkers and surrogate endpoints: preferred definitions and conceptual framework. Clin Pharmacol Ther. 2001;69:89–95.

Blasiak J, Petrovski G, Vereb Z, et al. Oxidative stress, hypoxia, and autophagy in the neovascular processes of age-related macular degeneration. Biomed Res Int. 2014;2014:768026.

Cassels NK, Wild JM, Margrain TH, et al. The use of microperimetry in assessing visual function in age-related macular degeneration. Surv Ophthalmol. 2017;63:40–55.

Chandramohan A, Stinnett SS, Petrowski JT, et al. Visual function measures in early and intermediate age-related macular degeneration. Retina. 2016;36:1021–31.

Chen H, Liu B, Lukas TJ, Neufeld AH. The aged retinal pigment epithelium/choroid: a potential substratum for the pathogenesis of age-related macular degeneration. PLoS One. 2008;3:e2339.

Chen W, Stambolian D, Edwards AO, et al. Genetic variants near TIMP3 and high-density lipoprotein-associated loci influence susceptibility to age-related macular degeneration. Proc Natl Acad Sci U S A. 2010;107:7401–6.

Chew EY, Clemons TE, SanGiovanni JP, et al. Secondary analyses of the effects of lutein/zeaxanthin on age-related macular degeneration progression. JAMA Ophthalmol. 2014;132:142.

Chew EY, Clemons TE, Harrington M, et al. Effectiveness of different monitoring modalities in the detection of neovascular age-related macular degeneration. Retina. 2016;36:1542–7.

Cicinelli MV, Rabiolo A, Sacconi R, et al. Optical coherence tomography angiography in dry age-related macular degeneration. Surv Ophthalmol. 2017;63:236–44.

Curcio CA, Johnson M, Rudolf M, Huang JD. The oil spill in ageing Bruch membrane. Br J Ophthalmol. 2011;95:1638–45.

Curcio CA, Zanzottera EC, Ach T, et al. Activated retinal pigment epithelium, an optical coherence tomography biomarker for progression in age-related macular degeneration. Invest Ophthalmol Vis Sci. 2017;58:BIO211–26.

Danis RP, Domalpally A, Chew EY, et al. Methods and reproducibility of grading optimized digital color fundus photographs in the Age-Related Eye Disease Study 2 (AREDS2 Report Number 2). Invest Ophthalmol Vis Sci. 2013;54:4548–54.

Delori FC, Dorey CK, Staurenghi G, et al. In vivo fluorescence of the ocular fundus exhibits retinal pigment epithelium lipofuscin characteristics. Invest Ophthalmol Vis Sci. 1995;36:718–29.

Dewan A, Liu M, Hartman S, et al. HTRA1 promoter polymorphism in wet age-related macular degeneration. Science. 2006;314:989–92.

Ferris FL, Davis MD, Clemons TE, et al. A simplified severity scale for age-related macular degeneration: AREDS Report No. 18. Arch Ophthalmol (Chicago, IL 1960). 2005;123:1570–4.

Ferris FL, Wilkinson CP, Bird A, et al. Clinical classification of age-related macular degeneration. Ophthalmology. 2013;120:844–51.

Fisher DE, Klein BE, Wong TY, et al. Incidence of age-related macular degeneration in a multi-ethnic United States population: the multi-ethnic study of atherosclerosis. Ophthalmology. 2016;123:1297–308.

Flamendorf J, Agrón E, Wong WT, et al. Impairments in dark adaptation are associated with age-related macular degeneration severity and reticular pseudodrusen. Ophthalmology. 2015;122:2053–62.

Fleckenstein M, Schmitz-Valckenberg S, Martens C, et al. Fundus autofluorescence and spectral-domain optical coherence tomography characteristics in a rapidly progressing form of geographic atrophy. Invest Ophthalmol Vis Sci. 2011;52:3761–6.

Fritsche LG, Igl W, Bailey JN, et al. A large genome-wide association study of age-related macular degeneration highlights contributions of rare and common variants. Nat Genet. 2016;48:134–43.

Gehrs KM, Anderson DH, Johnson LV, Hageman GS. Age-related macular degeneration—emerging pathogenetic and therapeutic concepts. Ann Med. 2006;38:450–71.

Gold B, Merriam JE, Zernant J, et al. Variation in factor B (BF) and complement component 2 (C2) genes is associated with age-related macular degeneration. Nat Genet. 2006;38:458–62.

Goldberg NR, Greenberg JP, Laud K, et al. Outer retinal tubulation in degenerative retinal disorders. Retina. 2013;33:1871–6.

Hageman GS, Luthert PJ, Victor Chong NH, et al. An integrated hypothesis that considers drusen as biomarkers of immune-mediated processes at the RPE-Bruch's membrane interface in aging and age-related macular degeneration. Prog Retin Eye Res. 2001;20:705–32.

Haines JL, Hauser MA, Schmidt S, et al. Complement factor H variant increases the risk of age-related macular degeneration. Science. 2005;308:419–21.

Hanus J, Zhao F, Wang S. Current therapeutic developments in atrophic age-related macular degeneration. Br J Ophthalmol. 2016;100:122–7.

Hariri A, Nittala MG, Sadda SR. Outer retinal tubulation as a predictor of the enlargement amount of geographic atrophy in age-related macular degeneration. Ophthalmology. 2015;122:407–13.

Holz FG, Bindewald-Wittich A, Fleckenstein M, et al. Progression of geographic atrophy and impact of fundus autofluorescence patterns in age-related macular degeneration. Am J Ophthalmol. 2007;143:463–472.e2.

Holz FG, Steinberg JS, Göbel A, et al. Fundus autofluorescence imaging in dry AMD: 2014 Jules Gonin lecture of the Retina Research Foundation. Graefes Arch Clin Exp Ophthalmol. 2015;253:7–16.

Holz FG, Sadda SR, Busbee B, et al. Efficacy and safety of lampalizumab for geographic atrophy due to age-related macular degeneration. JAMA Ophthalmol. 2018;136(6):666.

Husain D, Ambati B, Adamis AP, Miller JW. Mechanisms of age-related macular degeneration. Ophthalmol Clin North Am. 2002;15:87–91.

Khan JC, Thurlby DA, Shahid H, et al. Smoking and age related macular degeneration: the number of pack years of cigarette smoking is a major determinant of risk for both geographic atrophy and choroidal neovascularisation. Br J Ophthalmol. 2006;90:75–80.

Klein R, Klein BE, Tomany SC, et al. Ten-year incidence and progression of age-related maculopathy: the Beaver Dam eye study1 1The authors have no proprietary interest in the products or devices mentioned herein. Ophthalmology. 2002;109:1767–79.

Laíns I, Kelly RS, Miller JB, et al. Human plasma metabolomics study across all stages of age-related macular degeneration identifies potential lipid biomarkers. Ophthalmology. 2017a;125:245–54.

Laíns I, Miller JWJB, Park DH, et al. Structural changes associated with delayed dark adaptation in age-related macular degeneration. Ophthalmology. 2017b;124:1340–52.

Laíns I, Wang J, Providência J, et al. Choroidal changes associated with subretinal drusenoid deposits in age-related macular degeneration using swept-source optical coherence tomography. Am J Ophthalmol. 2017c;180:55–63.

Lin CH, Li CH, Liao PL, et al. Silibinin inhibits VEGF secretion and age-related macular degeneration in a hypoxia-dependent manner through the PI-3 kinase/Akt/mTOR pathway. Br J Pharmacol. 2013;168:920–31.

Lujan BJ, Rosenfeld PJ, Gregori G, et al. Spectral domain optical coherence tomographic imaging of geographic atrophy. Ophthalmic Surg Lasers Imaging. 2009;40:96–101.

Neely DC, Bray KJ, Huisingh CE, et al. Prevalence of undiagnosed age-related macular degeneration in primary eye care. JAMA Ophthalmol. 2017;135:570.

Philip A-M, Gerendas BS, Zhang L, et al. Choroidal thickness maps from spectral domain and swept source optical coherence tomography: algorithmic versus ground truth annotation. Br J Ophthalmol. 2016;100:1372–6.

Ratnapriya R, Zhan X, Fariss RN, et al. Rare and common variants in extracellular matrix gene Fibrillin 2 (FBN2) are associated with macular degeneration. Hum Mol Genet. 2014;23:5827–37.

Sacconi R, Corbelli E, Querques L, et al. A review of current and future management of geographic atrophy. Ophthalmol Ther. 2017;6:69–77.

Sachdeva MM, Eliott D. Stem cell-based therapy for diseases of the retinal pigment epithelium: from bench to bedside. Semin Ophthalmol. 2016;31:25–9.

Schaal KB, Legarreta AD, Feuer WJ, et al. Comparison between wide-field En face swept-source OCT and conventional multimodal imaging for the detection of reticular pseudodrusen. Ophthalmology. 2017;124:205–14.

Schwartz SD, Regillo CD, Lam BL, et al. Human embryonic stem cell-derived retinal pigment epithelium in patients with age-related

macular degeneration and Stargardt's macular dystrophy: follow-up of two open-label phase 1/2 studies. Lancet. 2015;385:509–16.
Schwartz SD, Tan G, Hosseini H, et al. Subretinal transplantation of embryonic stem cell–derived retinal pigment epithelium for the treatment of macular degeneration: an assessment at 4 years. Invest Ophthalmol Vis Sci. 2016;57:ORSFc1.
Sivaprasad S, Bird A, Nitiahpapand R, et al. Perspectives on reticular pseudodrusen in age-related macular degeneration. Surv Ophthalmol. 2016;61:521–37.
Sleiman K, Veerappan M, Winter KP, et al. Optical coherence tomography predictors of risk for progression to non-neovascular atrophic age-related macular degeneration. Ophthalmology. 2017;124:1764–77.
Smith W, Assink J, Klein R, et al. Risk factors for age-related macular degeneration: pooled findings from three continents. Ophthalmology. 2001;108:697–704.
Sunness JS. The natural history of geographic atrophy, the advanced atrophic form of age-related macular degeneration. Mol Vis. 1999;5:25.
Tan ACS, Astroz P, Dansingani KK, et al. The evolution of the plateau, an optical coherence tomography signature seen in geographic atrophy. Invest Ophthalmol Vis Sci. 2017;58:2349.
van Leeuwen R. The risk and natural course of age-related maculopathy. Arch Ophthalmol. 2003;121:519.
Vavvas DG, Daniels AB, Kapsala ZG, et al. Regression of some high-risk features of age-related macular degeneration (AMD) in patients receiving intensive statin treatment. EBioMedicine. 2016;5:198–203.
Wong WL, Su X, Li X, et al. Global prevalence of age-related macular degeneration and disease burden projection for 2020 and 2040: a systematic review and meta-analysis. Lancet Glob Health. 2014;2:e106–16.
Wu Z, Ayton LN, Guymer RH, Luu CD. Low-luminance visual acuity and microperimetry in age-related macular degeneration. Ophthalmology. 2014;121:1612–9.
Wu Z, Guymer RH, Finger RP. Low luminance deficit and night vision symptoms in intermediate age-related macular degeneration. Br J Ophthalmol. 2016;100:395–8.
Yaspan BL, Williams DF, Holz FG, et al. Targeting factor D of the alternative complement pathway reduces geographic atrophy progression secondary to age-related macular degeneration. Sci Transl Med. 2017. https://doi.org/10.1126/scitranslmed.aaf1443.
Yates JR, Sepp T, Matharu BK, et al. Complement C3 variant and the risk of age-related macular degeneration. N Engl J Med. 2007;357:553–61.
Yonekawa Y, Kim IK. Clinical characteristics and current treatment of age-related macular degeneration. Cold Spring Harb Perspect Med. 2014;5:a017178.
Yonekawa Y, Miller JW, Kim IK. Age-related macular degeneration: advances in management and diagnosis. J Clin Med. 2015;4:343–59.
Yu Y, Bhangale TR, Fagerness J, et al. Common variants near FRK/COL10A1 and VEGFA are associated with advanced age-related macular degeneration. Hum Mol Genet. 2011;20:3699–709.
Yung M, Klufas MA, Sarraf D. Clinical applications of fundus autofluorescence in retinal disease. Int J Retina Vitreous. 2016;2:12.
Zareparsi S, Reddick AC, Branham KE, et al. Association of apolipoprotein E alleles with susceptibility to age-related macular degeneration in a large cohort from a single center. Invest Ophthalmol Vis Sci. 2004;45:1306–10.
Zhan X, Larson DE, Wang C, et al. Identification of a rare coding variant in complement 3 associated with age-related macular degeneration. Nat Genet. 2013;45:1375–9.
Zweifel SA, Spaide RF, Curcio CA, et al. Reticular pseudodrusen are subretinal drusenoid deposits. Ophthalmology. 2010;117:303–12.e1.

Neovascular AMD

2

Eric H. Souied and Francesca Amoroso

Abbreviations

BNV	Branching type 1 neovascular network
BVN	Branching vascular network
CNV	Choroidal neovascularization
CRA	Chorio-retinal anastomosis
ICGA	ICG angiography
NV	Neovascularization
OCRA	Occult choroidal retinal anastomosis
OCTA	OCT-Angiography
PCV	Polypoidal choroidal vasculopathy
PDT	Photodynamic therapy
PED	Pigment epithelium detachment
PRN	"Pro-Re-Nata"
RAP	Retinal angiomatous proliferation
RPE	Retinal pigment epithelium
SRD	Serous retinal detachment
SRF	Subretinal fluid
VEGF	Vascular endothelial growth factor
v-PED	Vascularized PED

Introduction

Neovascular AMD is defined by the presence of choroidal and/or intraretinal neovascularization with associated exudation, bleeding, and disciform scar (Ferris III et al. 1984). Choroidal neovascularization (CNV) is characterized by an abnormal growth of newly formed vessels within the macular area.

Different types of neovascular growth pattern have been described: pigment epithelial or type 1 choroidal neovascularization, preretinal pigment epithelial or type 2 choroidal neovascularization, and retinal angiomatous proliferation or type 3 neovascularization (NV) (Grossniklaus and Gass 1998; Yannuzzi et al. 2001; Freund et al. 2010; Cohen et al. 2007a, b; Jung et al. 2014).

Donald M. Gass described the histopathologic and fluorescein angiographic characteristics of CNV, defining as type 1 CNV the neovascularization proliferating under the retinal pigment epithelium (RPE) with less distinct margins and less actively proliferating than other types of neovascularization, with a poorly defined or "occult" CNV pattern on fluorescein angiography (FA) (Grossniklaus and Gass 1998).

Gass also described type 2 CNV as the neovascularization characterized by the active proliferation of the new vessels beneath the neurosensory retina, showing a well-defined or "classic" pattern of fluorescence on fluorescein angiography.

A third anatomic subtype of neovascularization in AMD has been described; type 3 neovascularization is characterized by the presence of an intraretinal neovascularization in conjunction with a compensatory proliferative response that is featured by perfusing arterioles, draining venules, and the eventual formation of anastomoses between the intraretinal proliferation and sub-RPE neovascularization.

The main feature of type 3 NV is the active proliferation within neurosensory retina; however, a concomitant choroidal component has been described (Yannuzzi et al. 2001; Freund et al. 2008).

Another form of neovascularization is polypoidal choroidal vasculopathy (PCV), which is considered a variant of type 1 neovascularization because it is located in the subpigment epithelial space. A branching type 1 neovascular network (BNV), similar to type 1 CNV with terminal aneurysmal changes (polyps), has been associated with PCV (Yannuzzi et al. 1990; Laude et al. 2010; Yannuzzi 1982). The frequency of neovascular subtypes in neovascular AMD in white patients is approximately 40% type 1, 9% type 2, 34% type 3, and 17% mixed (Jung et al. 2014; Cohen et al. 2007a).

E. H. Souied (✉) · F. Amoroso
Department of Ophthalmology, Centre Hospitalier Intercommunal de Créteil, Université de Paris Est Créteil, Créteil, France
e-mail: eric.souied@chicreteil.fr

I. K. Kim (ed.), *Macular Disorders*, Retina Atlas, https://doi.org/10.1007/978-981-15-3001-2_2

Classification and Diagnosis of Neovascular AMD: The Multimodal Imaging

Type 1 Neovascularization

Type 1 neovascularization originates from the choroid and extends under the RPE, with subsequent detachments of the RPE and overlying retina.

On fundus examination, type 1 CNV presents with moderate exudative signs.

The subretinal fluid (SRF) responsible for the functional syndrome is usually mild; retinal hemorrhages are rarely observed, although occult CNV can be complicated by extensive hematoma. Deep exudates are more common, whereas cystoid macular edema, unusual in the early form, is later formed. Finally, the precursors of AMD are present (drusen and abnormalities of the RPE).

On fluorescein angiography, type 1 CNV is poorly defined and inhomogeneous with early staining of the lesion, including hyperfluorescent pinpoints. On late phases of the angiographic sequence, the lesion increases in size, and leakage is observed. The precise limits of the neovascular lesion cannot be easily determined. The typical aspect of this CNV is the early hyperfluorescence on ICG angiography (ICGA), with the appearance of a "plaque" in late stages.

The SD-OCT shows increased central macular thickness (associated with RPE detachment), subretinal fluid, edema, and/or intraretinal cyst (Fig. 2.1). The SD-OCT examination shows, depending on the stage of evolution, the presence of an RPE elevation or pigment epithelium detachment (PED) (98% of cases). The elevation of the RPE is initially moderate, separated from the moderate reflectivity of Bruch's membrane by a hyporeflective space. The PED can, however, become very extensive. The presence of an occult CNV may be suspected due to an irregular, fragmented, or thickened appearance of the RPE. All exudative signs may be present: SRF, hyper-reflective points (Coscas et al. 2013), pre-epithelial exudation (Ores et al. 2014), and cystoid cells within the neurosensory retina.

On OCT-Angiography (OCTA), the type 1 neovascular lesion was compared to a "blossoming tree" or a "seafan pattern" to describe the typical aspect of the lesion: a central feeder vessel with neovessels radiating from the central trunk in both directions and on one side of the lesion. A more advanced lesion, called mature lesion, can harbor a tangled or a dead tree pattern (Fig. 2.2) (Kuehlewein et al. 2015).

Vascularized PED

Type 1 CNV, commonly described as a vascularized PED (v-PED), is a sign of hidden or "occult" neovascularization (Mrejen et al. 2013).

It generally appears as a well-circumscribed yellow-orange RPE bulge, showing late staining on fluorescein angiography. The SD-OCT typically shows heterogeneous sub-RPE signal and subretinal fluid (Fig. 2.3).

Vascularized PEDs may present a mixture of serous, drusenoid, and vascularized components. Fluorescein angiography reveals hyperfluorescent "pin-points" in late phases, whilst ICGA shows the early appearance of neovascular network with a late "plaque." SD-OCT reveals the elevation of the RPE, subretinal fluid, and exudation. The sub-RPE material may be heterogeneous, with serous, drusenoid, and vascular components.

Furthermore, vascularized PED variants have been described as:

- Multilayered PED (Rahimy et al. 2014)
- The "onion sign" (Pang et al. 2015)
- Retinal pigment epithelium tears/apertures (Querques et al. 2016)
- Wrinkled-PED (Lam et al. 2017)
- Quiescent type 1 (Querques et al. 2013c)

Type 2 Choroidal Neovascularization

Type 2 CNV, is called subretinal CNV or "well-defined CNV" because of its appearance on FA. Although it is less frequent than type 1 CNV, it is also known as classic CNV because it was the first pattern to be described on FA. Type 2 CNV originates from the choroidal circulation, penetrates through the pigmented epithelium, and extends into the subretinal space leading to bleeding and exudative features such as SRD and/or edema. This type of CNV actively proliferates below the neurosensory retina.

On fundus and color pictures, classic CNVs are not directly discernible in early stages, but result in discrete retinal thickening with a greyish-white retinal aspect. Exudative signs, the SRF, retinal or subretinal hemorrhages, lipied exudates, and intraretinal cystoid edema, are barely present (Grossniklaus and Gass 1998). PED is rare in pure visible pre-epithelial neovessels. The IR pictures reveal the presence of a multilayered structure. This structure appears as a complex with a dark central core surrounded by a whitish reflective ring, giving a halo-like shape (Semoun et al. 2009).

Fluorescein angiography typically shows an early staining of the lesion that appears as a *bicycle wheel* or an *umbrella pattern*. The classic CNV lesion is hyperfluorescent, commonly contrasting with a surrounding hypofluorescent ring. On late phase of the FA sequence, an intense leakage is observed associated with dye pooling in subretinal space in late stages. In some cases, the hyperfluorescence of the dye may decrease on late phase, corresponding to the "wash-out effect."

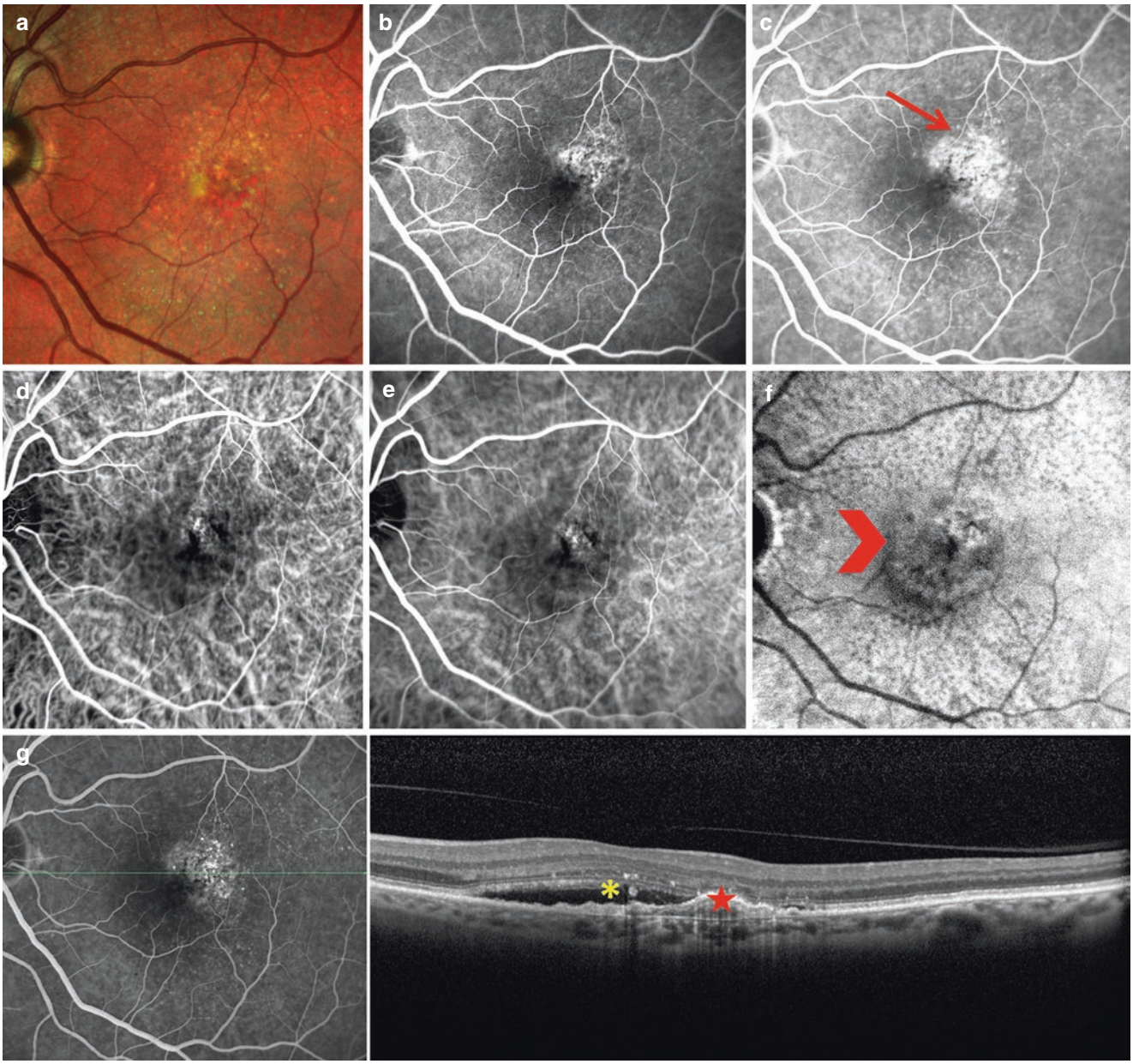

Fig. 2.1 Multimodal imaging of a patient with type 1 CNV. (**a**) Multicolor imaging shows the presence of a PED temporal to the fovea, reticular pseudodrusen at the posterior pole and the absence of exudates or hemorrhages; hyperfluorescent pinpoints in the early stages (**b**) persisting in late phases (arrow) (**c**) on fluorescein angiography; ICGA shows hypercyanescence of subretinal neovascularization in the early stages (**d**), persistence in the intermediate stages (**e**) and hypercyanescent "plaque" in late phases (arrowhead) (**f**); (**g**) SD-OCT showing the presence of a PED corresponding to the CNV (star), accompanied by subretinal fluid (asterisk)

Indocyanine green angiography reveals the early filling and the washout of the neovascular membrane in late stages (Grossniklaus and Gass 1998; Cohen et al. 2007a; Gelisken et al. 1998).

The OCT shows the typical hyperreflective fusiform lesion above the RPE, with or without visible effraction signs.

On SD-OCT, a serous retinal detachment can be seen, most often present on the edges of the fusiform lesion and the *grey hyperreflective subretinal exudation* (Ores et al. 2014), sign of neovascular lesion activity, as well as intraretinal cysts and serous detachment of neuroepithelium (Fig. 2.4).

Type 2 neovascularizations represent only 10% of neovascular AMD cases, but type 2 CNV is the most common lesion type in pathological myopia, angioid streaks, and multifocal choroiditis.

Several patterns of type 2 neovascularization have been described on OCTA, with a constant high flow appearance present both in the outer retinal segmentation and in the

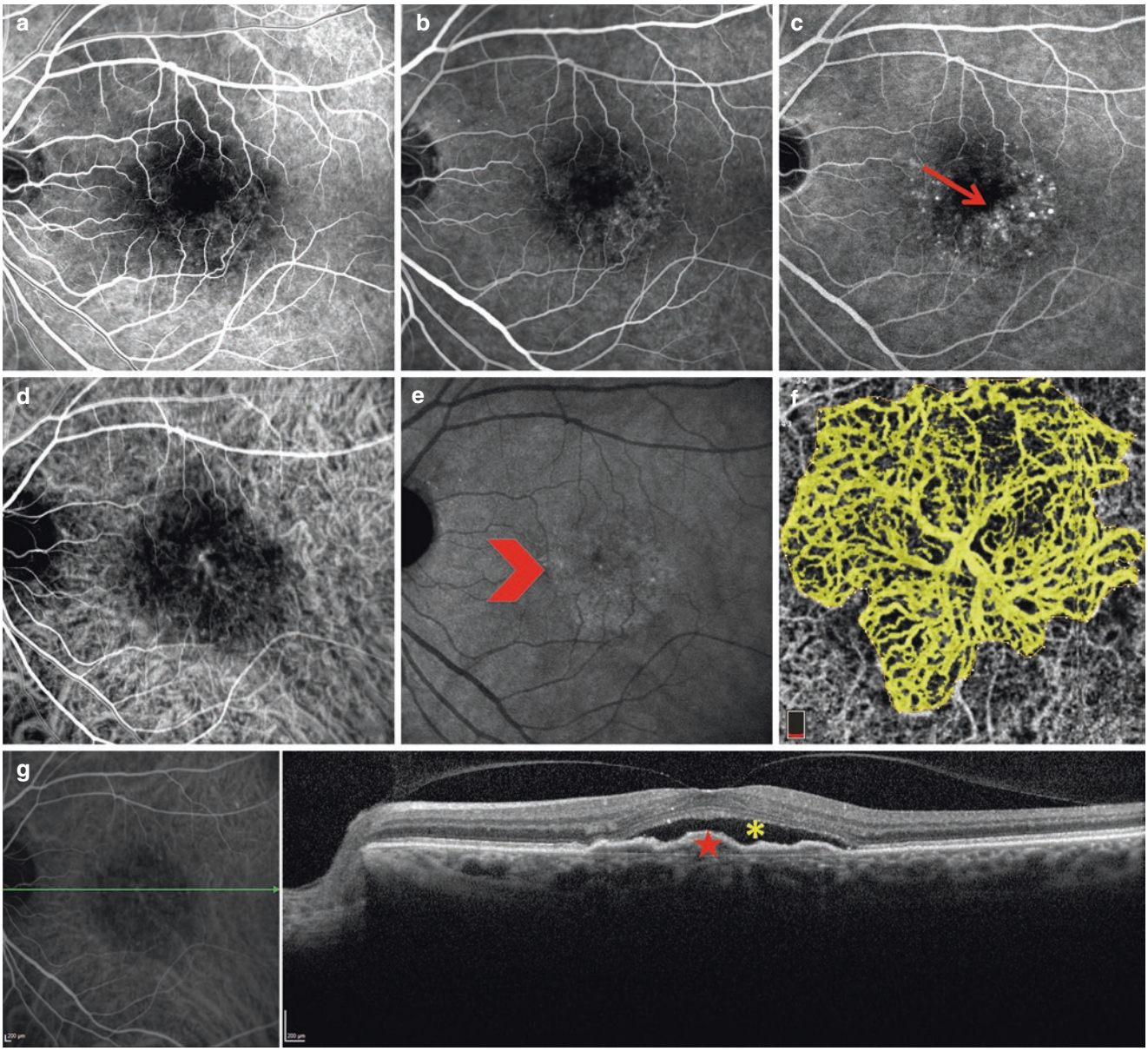

Fig. 2.2 Multimodal imaging of a patient with type 1 CNV: (**a**) hyperfluorescent pinpoints appearing in early phases (**b**) persisting in late stages (arrow) (**c**) on fluorescein angiography; ICG shows the hypercyanescence of subretinal neovessels in early stages (**d**) and the appearance of the "plaque" in late phases (arrowhead) (**e**); (**f**) OCTA 3 × 3 scan highlights a large neovascular membrane, characterized by a central trunk with small, high-flowing vessels branching in all directions. The image is almost overlapping with the ICGA; (**g**) SD-OCT shows the PED (star), accompanied by suburetinal fluid (asterisk)

choriocapillaris segmentation. OCTA showed a 100% sensitivity in the detection of type 2 CNVs (El Ameen et al. 2015).

Based on the different morphological aspects, two types of classic neovascularization are distinguished:

1. *Medusa-shaped lesion*, defined as a compact zone of small new blood vessels with minimal hypodense structure inside; the lesions are typically connected to a thicker main branch, which seem continuous from the outer retina into the more profound choroidal layers.
2. *Glomerulus-shaped lesion*, defined per comparison with the kidney glomerulus, harboring globular structures of entwined vessels that are separated by hypodense spaces.

Generally, the neovascular complex is surrounded by a dark zone located at choriocapillaris level, defined *"dark halo."* This aspect would correspond to a phenomenon of "vascular stealing" by the lesion against the surrounding choroid (Fig. 2.5).

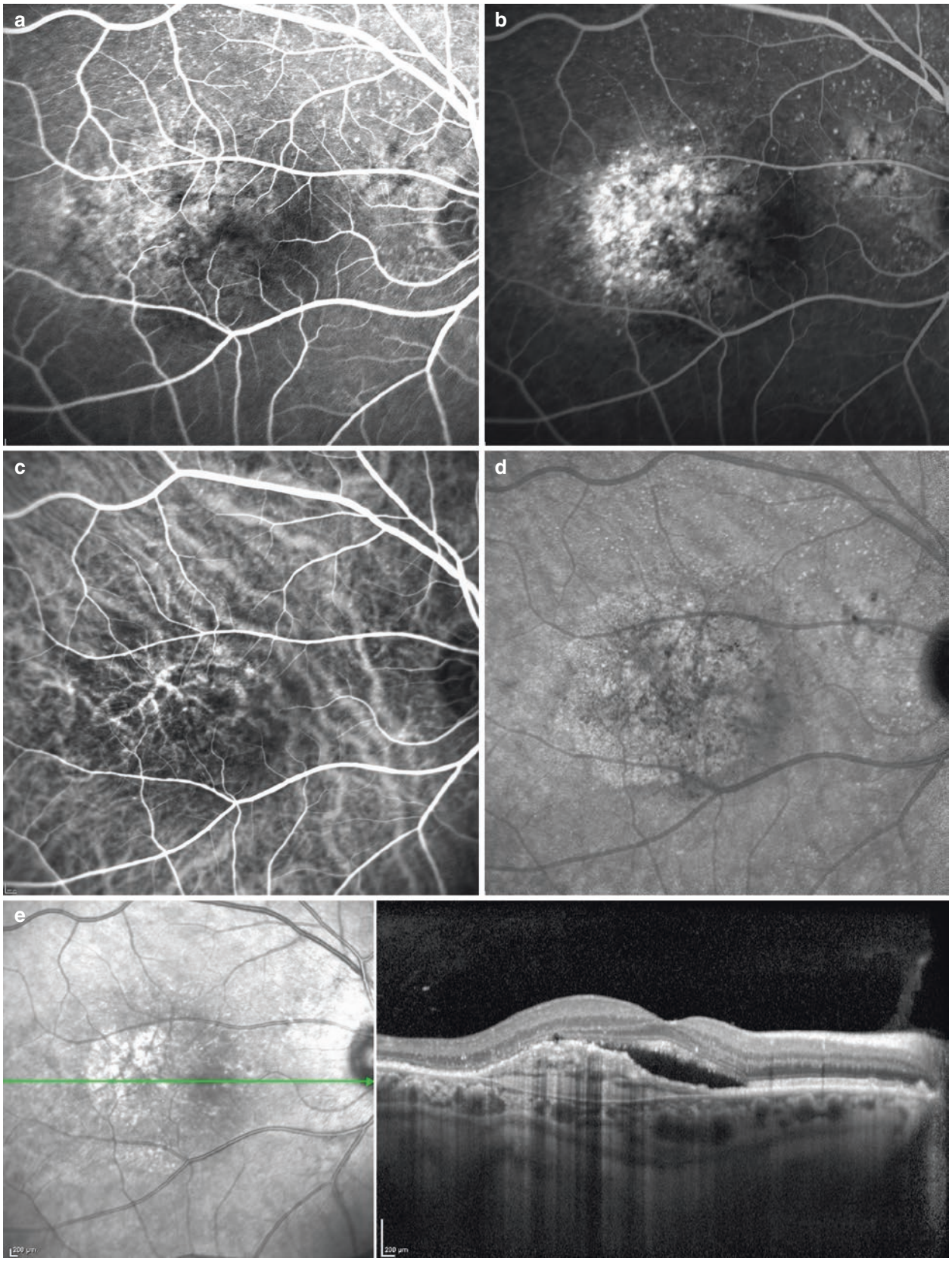

Fig. 2.3 Example of a patient with vascularized PED. (**a**) Fluorescein angiography reveals minimal stippled and irregular hyperfluorescence in the early phase and staining of the fibrovascular PED with the appearance of the characteristic pin-points in the later phases (**b**), consisting of an occult choroidal neovascular membrane; (**c**) indocyanine green angiography demonstrates a clear delineation of the neovascular complex in the early phase, revealing a well-defined area of hyperfluorescence, referred to as a "plaque," in the late phase (**d**); (**e**) SD-OCT shows an elevation of the RPE with sub-RPE heterogeneous signals consistent with a vascularized PED

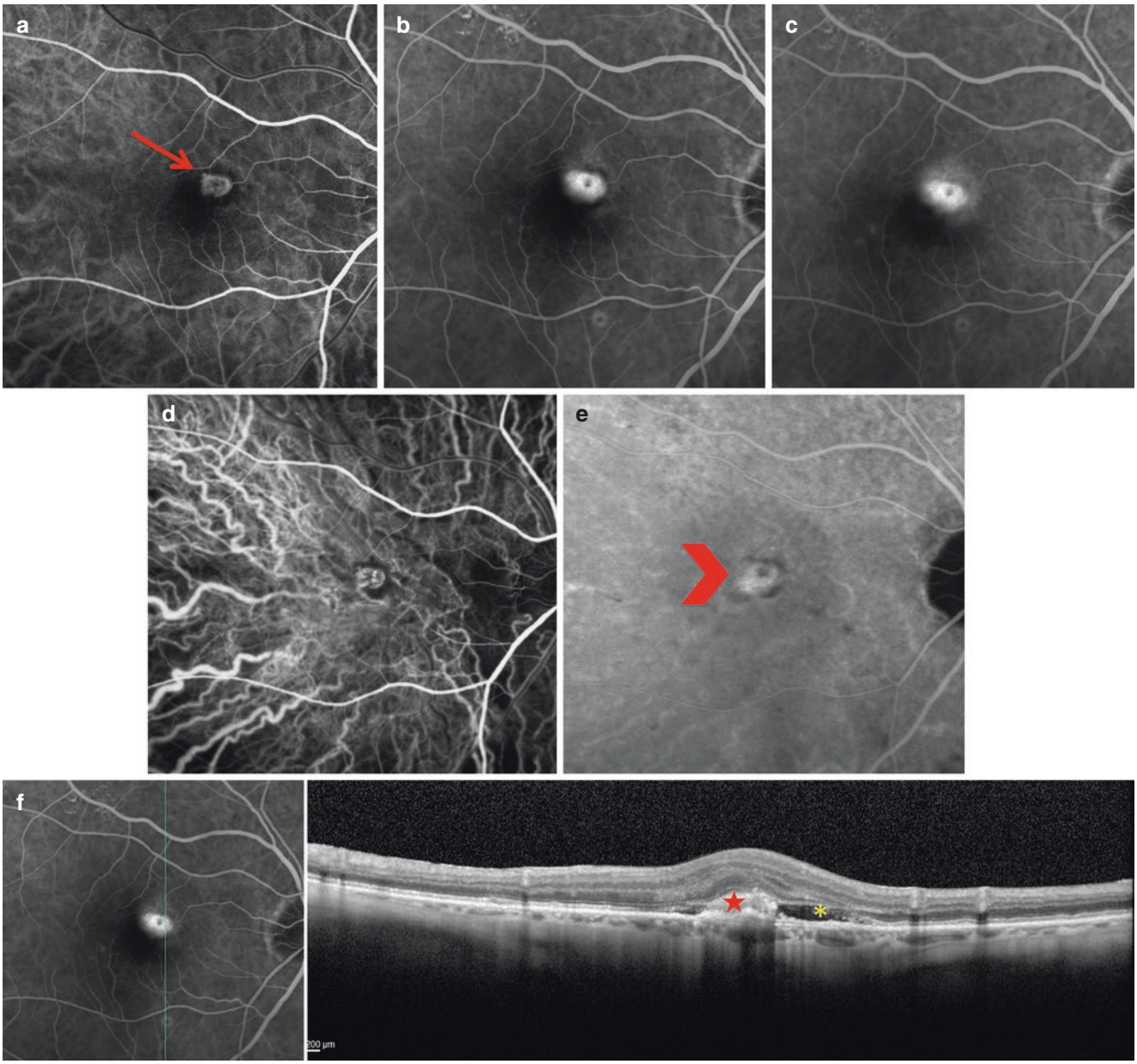

Fig. 2.4 Multimodal imaging of a patient with type 2 CNV in an exudative AMD patient. Fluorescein angiography shows, in early stages (**a**), the rapid filling of the neovascular membrane (arrow) which increases in intermediate stages (**b**) with leakage in late stages (**c**); indocyanine green angiography shows the filling of the neovascular membrane in early phases (**d**), with slight diffusion in late phases (arrow head) (**e**); (**f**) SD-OCT reveals the presence of a neovascular lesion, localized above the RPE (star), accompanied by serous detachment of neuroepithelium (asterisk) and subretinal exudation. Note the absence of drusen in this peculiar case

Mixed-Type Neovascularization

Most choroidal neovascularization secondary to AMD consists of a combination of type 1 and type 2 neovascularizations, also called predominantly "occult" or "classic" neovascularizations. If most new vessels are of type 1, lesion is defined as predominantly type 1 neovascularization or "minimally classic"; if, on the contrary, the lesion is predominantly of type 2, it is defined as "predominantly classic."

Type 3 Neovascularization

The term "type 3 Neovascularization" was introduced by Freund in 2008 (Freund et al. 2008).

The origin of type 3 neovascularization remains debated as to whether it arises from the retinal circulation or the choroidal circulation. Several anatomical findings correspond-

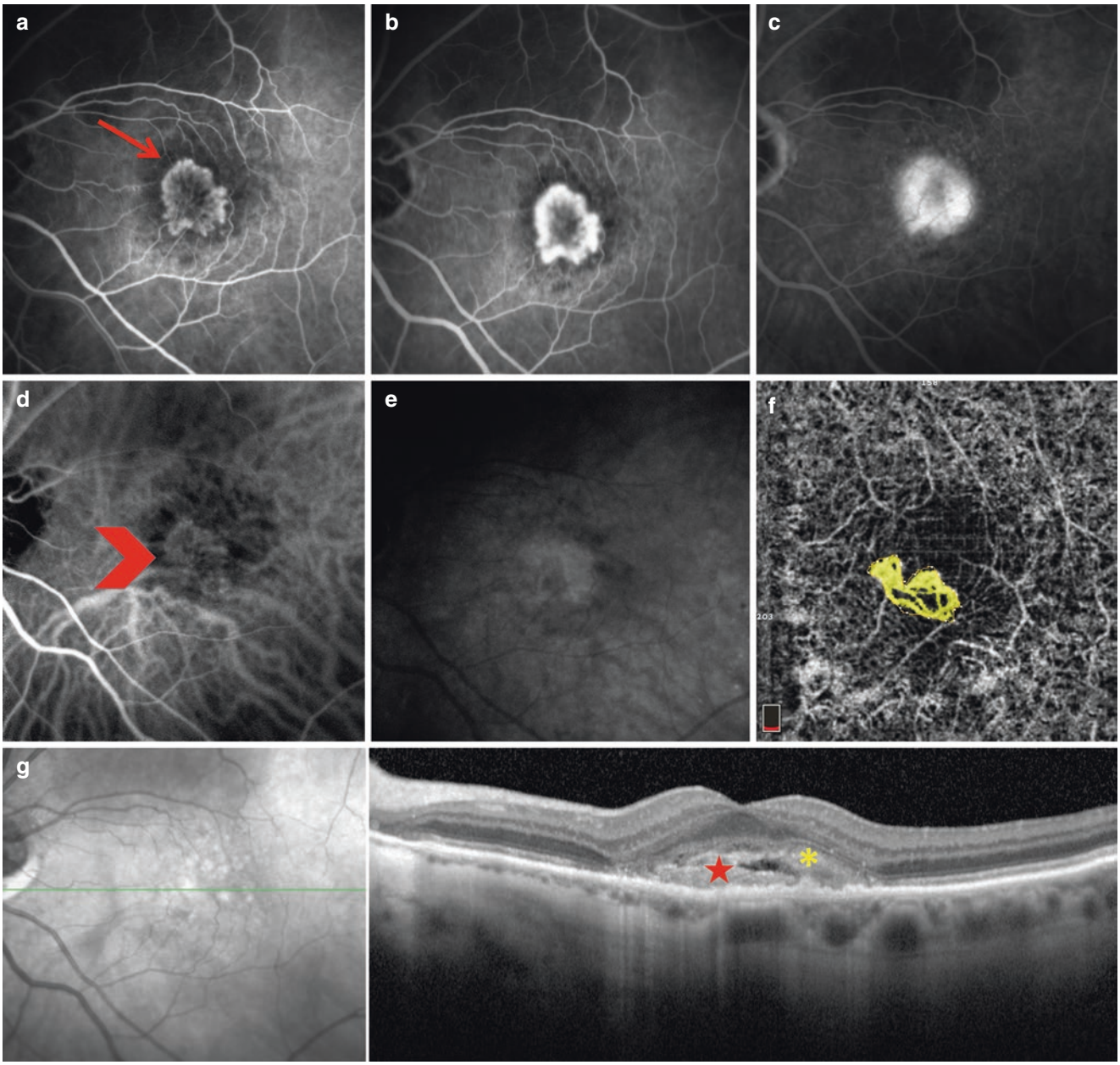

Fig. 2.5 Multimodal imaging of a patient with type 2 CNV. Fluorescein angiography shows, in early stages (**a**), the rapid filling of the neovascular membrane (arrow) which increases in intermediate stages (**b**) with leakage in late stages (**c**); indocyanine green angiography shows the filling of the neovascular membrane in early phases (arrow head) (**d**), with slight diffusion in late phases (**e**); (**f**) OCTA 3 × 3 (OptoVue) shows a high flow neovascular membrane in choriocapillaris segmentation; (**g**) SD-OCT shows the preepithelial neovascular lesion (star), accompanied by subretinal exudation (yellow asterisk) and a serous detachment of neuroepithelium

ing to type 3 NV have been described in the past: Hartnett, in 1992, defined the type 3 as "Abnormal deep retinal vascular complexes"; Kuhn, in 1995, described the "Chorio-Retinal Anastomosis" (CRA); Yannuzzi, in 2001, coined the term "Retinal Angiomatous Proliferation" (RAP); and Gass, in 2003, defined the "Occult choroidal retinal anastomosis" (OCRA).

Yannuzzi proposed three variants in the vasogenic process (Yannuzzi et al. 2008):

1. Initial focal retinal proliferation and progression
2. Initial focal choroidal proliferation and progression
3. Focal retinal proliferation with preexisting or simultaneous choroidal proliferation

More recent papers defined type 3 neovascularization as intraretinal neovascularization (Freund et al. 2008).

Drusenoid PED, intraretinal pigment migration, and focal outer retinal atrophy usually precede the development of type 3 NV. It has been demonstrated that drusenoid PED and focal photoreceptor and RPE loss precede type 3 neovascularization at the future site of lesion development, generating outer retinal atrophy, and ultimately allowing the deep capillary plexus to approach the RPE/sub-RPE space. The result of the increased vascular endothelial growth factor at this level may explain why sometimes type 3 neovascularization develops in close contact with the RPE/sub-RPE content (Querques et al. 2013a, b, c). Interestingly, it was recently demonstrated that although in the presence of a drusenoid PED, the exaggerated distance between the choroid and the photoreceptors drives this hypoxic response (Nagiel et al. 2015). In the absence of a PED, localized vascular endothelial growth factor production may arise from choroidal hypoperfusion.

In contrast to type 1 or type 2 NV, type 3 NV is commonly associated with intraretinal edema and is rarely associated with subretinal fluid.

On fundus examination, a small, deep, juxta-foveal intraretinal hemorrhage typically appears. The CRA is manifested by the sudden interruption of a retinal vessel whose diameter improves at 90° toward the choroid. Type 3 NVs are typically associated with the presence of reticular pseudodrusen at the posterior pole (Cohen et al. 2007b; Zweifel et al. 2010).

Fluorescein angiography usually reveals a hyperfluorescent hot-spot, localized at the termination of a retinal capillary branch. The lesion is frequently associated with an adjacent small hypofluorescence due to the masking effect of a punctuate hemorrhage. On late phases of the FA, the lesion is barely visible compared to the persisting hyperfluorescence corresponding to the "hot-spot," frequently accompanied by a cystoid macular edema in advanced type 3. ICGA shows the appearance of the feeder vessel in early stages appearing as a hyperfluorescent hot-spot that becomes more visible in late phases. The type 3 NV can sometimes be associated with a plaque on late phases, signaling the co-existence of a type 1 lesion. SD-OCT generally shows the intraretinal neovascular network, accompanied by cystoid edema and minimal subretinal fluid (Fig. 2.6).

An SD-OCT classification describing the evolution of type 3 NV in 3 phases has been proposed (Querques et al. 2010, 2013b, 2015):

- Phase 1 or *erosion sign*: appearance of early neovascularization from the choroid (characterized by a point of focal hyperfluorescence in angiography) which erodes the basement membrane of the RPE without breaking it.
- Phase 2 or *flap sign*: neovascularization infiltrates the outer layers of the retina forming an early type 3 (characterized by angiography by a hot-spot without serosanguinous PED).
- Phase 3 or *kissing sign*: infiltration of neovascularization in the inner layers of the retina and formation of a complete type 3 (characterized in angiography by a hot-spot associated with a serosanguinous PED).

Moreover, the choroidal thickness is typically more reduced in type 3 NV compared to type 1 and 2 CNV (Kim et al. 2013).

The early detection and treatment of type 3 NV is crucial not only because of the potential for rapid vision loss but also for a major regression of neovascular lesions following early anti-VEGF (Vascular Endothelial Growth Factor) therapy.

These neovascular lesions present a high rate of fellow eye involvement (about 100% by 3 years) (Gross et al. 2005).

Type 3 neovascularization, as described by Miere et al. (2015a, b), is characterized on OCTA by the presence of a retinal-retinal anastomosis emerging from the deep capillary plexus that forms a high-flow vascular network, called a "tuft," at the outer retina level, projecting at the sub-RPE space. Typically, at choriocapillaris segmentation, type 3 NV appears as a small high-flow lesion, defined *"clew-like,"* variously associated with the underlying choroidal vascularization by small interconnecting vessels (Fig. 2.7).

Polypoidal Choroidal Vasculopathy

Yannuzzi firstly described (Yannuzzi 1982) polypoidal choroidal vasculopathy (PCV) as an acquired, abnormal choroidal vasculopathy, distinct from typical CNV (Yannuzzi et al. 1990; Laude et al. 2010).

Originally described as a distinct entity occurring predominantly in African-American and Asian individuals between 50 and 65 years of age, PCV is actually considered as a form of type 1 neovascularization because the polyps appear to originate from neovascular tissue above the Bruch's membrane and is frequently associated with a branching vascular network. PCV is associated with choroidal abnormalities such as increased thickness, hyperpermeability, and pachyvessels.

PCV is characterized by single or multiple polypoidal vascular dilatations, accompanied by a type 1 CNV, and a "choroidal branching vascular network" (BVN), as observed on indocyanine green angiography (Yannuzzi et al. 1990; Laude et al. 2010; Yannuzzi 1982; Ciardella et al. 2004; Spaide et al. 1995).

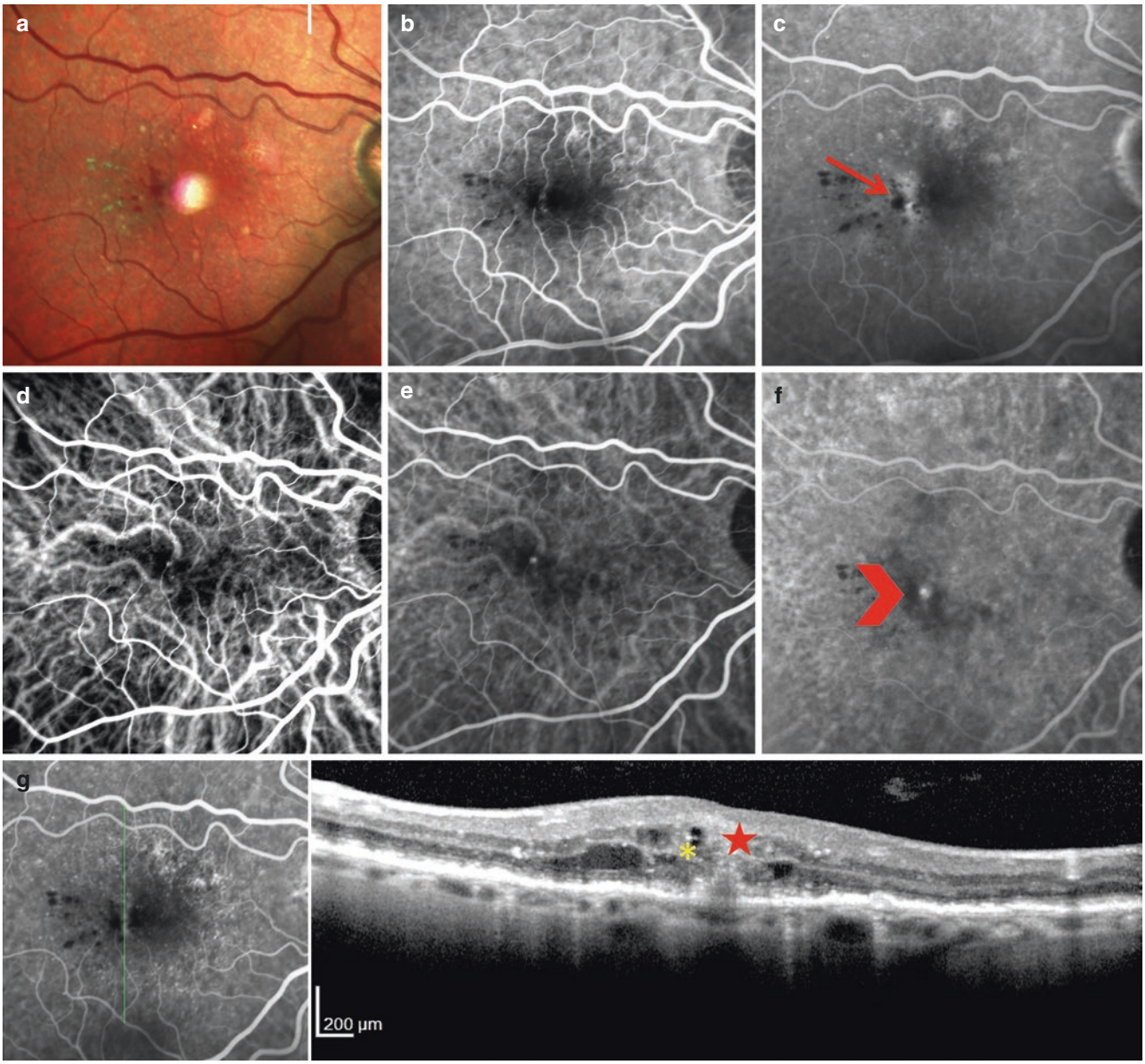

Fig. 2.6 Multimodal imaging of a patient with type 3 neovascularization: (**a**) Multicolor imaging shows the presence of small retinal hemorrhages at the fovea, accompanied by hard exudates, and reticular pseudodrusen wounds to the posterior pole; fluorescein angiography shows early hyperfluorescence (**b**), with late diffusion (arrow) (**c**); ICGA shows the appearance of the feeder vessel in early stages (**d**) and the typical "hot-spot" (arrowhead) persisting in late phases (**e**, **f**); (**g**) SD-OCT shows the "kissing sign" (star), accompanied by cystoid edema (asterisk) and small, hyper-reflective spots

On SD-OCT, the polypoidal dilations appear as dome-like elevations of RPE with moderate internal reflectivity (Sa et al. 2005; Iijima et al. 1999; Otsuji et al. 2000; De Salvo et al. 2014).

The branching neovascular network presents as two highly reflective lines ("double layer sign") (Sato et al. 2007).

Srour et al. (2016) recently showed the OCTA features of PCV. The authors demonstrated that OCTA could visualize different structures in PCV. On the choriocapillaris segmentation, OCTA constantly showed the BVN, appearing as a hyperflow lesion, and polypoidal lesions, appearing either as a hyperflow round structure surrounded by a hypointense halo, or as a hypoflow round structure (Fig. 2.8).

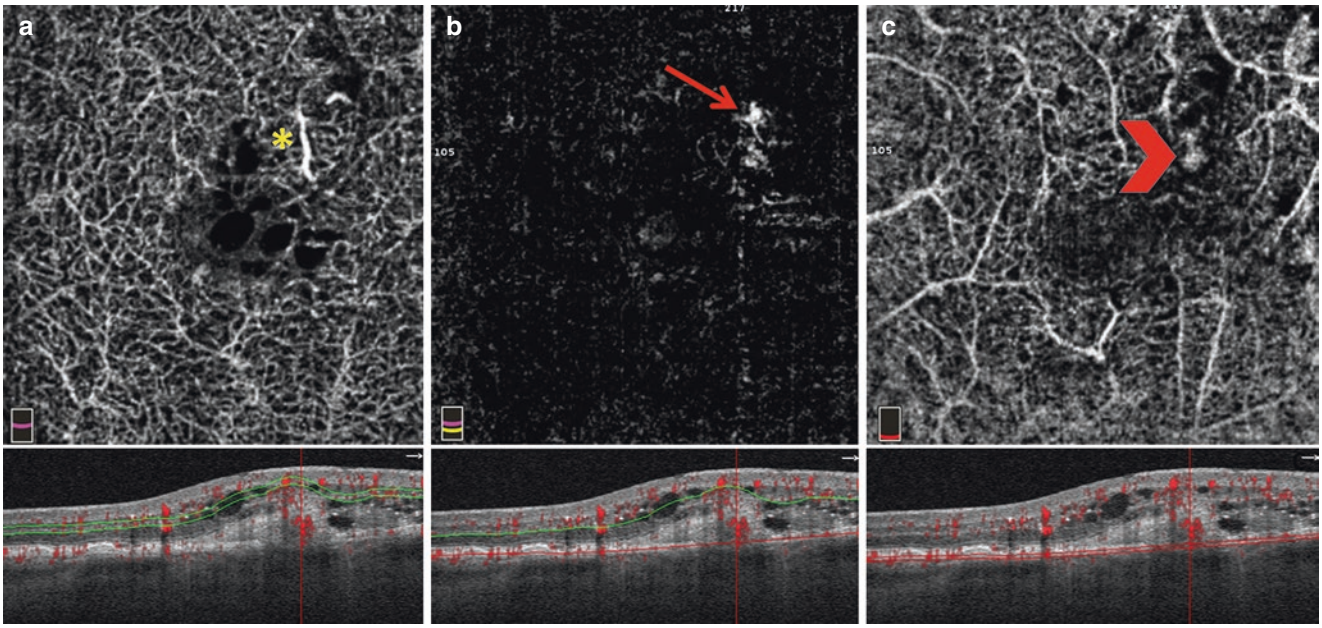

Fig. 2.7 OCTA of a patient with type 3 neovascularization. 3 × 3 OCTA scans (OptoVue) with correspondent B-scans. (**a**) The deep capillary plexus segmentation shows a small, high-flow vessel that deepens in the external retinal layers (asterisk); (**b**) high-flow "tuft-shaped" lesion (arrow) at outer retina segmentation; (**c**) choriocapillaris segmentation shows the presence of the characteristic "clew-like lesion" (arrow head) apparently connected with the "tuft"

In most cases the polypoidal lesions appeared as hypoflow round structures; this absence of signal does not mean that there is no blood flow, but rather that blood flow is not within the level of detection of the OCTA device.

The non-visualization of the vascular structure may be due to an increased (turbulent flow) or decreased flow within the polyps.

Subretinal Fibrosis

Neovascular lesions resemble a dynamic wound healing process characterized by inflammation, angiogenesis, and fibrosis (Schlingemann 2004).

The subretinal fibrosis is the result of neovascular tissue remodeling, a sign of advanced neovascular lesions, repeated bleeding, macrophagic invasion, and healing.

Several studies have shown the risk of evolution toward macular atrophy and/or subretinal fibrosis of the treated CNV (Bloch et al. 2013; Channa et al. 2015; Toth et al. 2015; Rosenfeld et al. 2011; Cohen et al. 2012).

Nevertheless, subretinal fibrosis may also occur as the consequence of repeated subfoveal hemorrhages (Hwang et al. 2011).

On fundus examination, subretinal fibrosis appears as a well-demarcated, elevated mound of yellowish-white tissue (Fig. 2.9).

Multicolor imaging may help in the diagnosis showing a white/green dome-shaped elevation at the posterior pole.

Fluorescein angiography generally reveals early and intense staining of the dye in late phases of the sequence. SD-OCT shows subretinal hyperreflective lesions, of variable size and location, with possible loss of adjacent retinal pigment epithelium and ellipsoid zone. In the absence of associated exudative component, no leakage is visible.

As showed by Miere et al. (2015b) the OCTA allowed the visualization and analysis of subretinal fibrosis (Fig. 2.10).

A complete lack of signal, possibly blocked by the fibrous scar, generating a complete masking effect of the lesion, was the only discernible feature on OCTA images for 3 out of 49 patients (6.2% of the whole study population).

The authors described three different neovascularization phenotypes inside the fibroglial scar: pruned vascular tree pattern (53.1%), tangled network pattern (28.6%), and/or vascular loop (51.0%). Two features, "large flow void" and a "dark halo," have been associated with subretinal fibrosis, presenting as an obscure zone surrounding the neovascular network. Pruned vascular tree pattern was characterized by an irregular, filamentous flow inside the neovascular network on the OCTA scans, comprising only important vessels, with thinner capillaries not visible. In all cases of pruned vascular tree, a large central feeder vessel was detected. Tangled network was characterized by an abnormal, high flow,

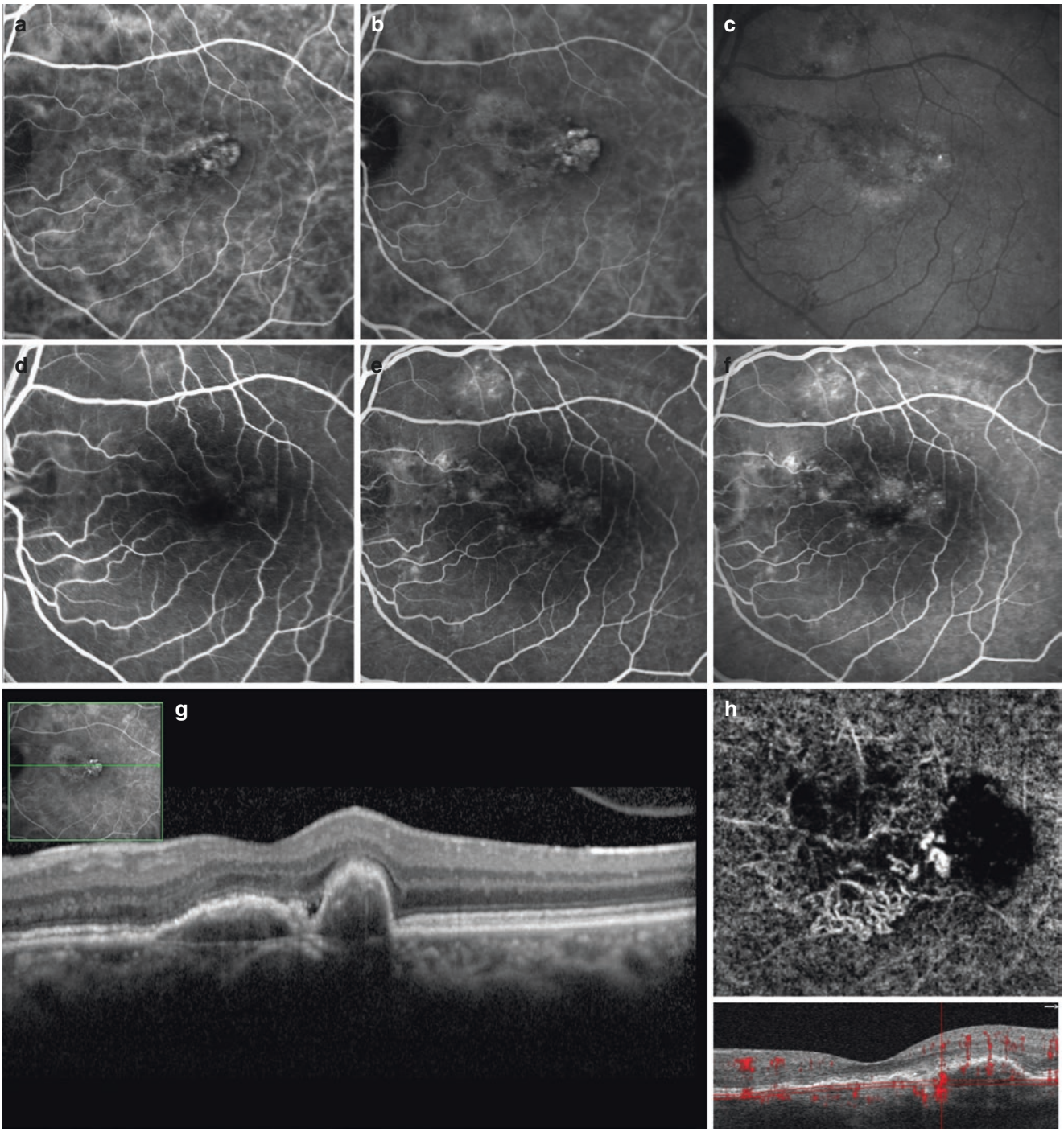

Fig. 2.8 Multimodal imaging of a patient with polypoidal choroidal vasculopathy: (**a**) ICGA shows the early filling of polypoidal lesions and the BVN, persisting in the intermediate phases (**b**) and the wash-out in late phases (**c**); fluorescein angiography shows an inhomogeneous hyperfluorescence during all the angiographic sequence (**d**–**f**); SD-OCT shows the polypoidal lesions accompanied by the BVN (**g**); OCTA 3 × 3 scan shows two different high-flow lesions, corresponding to the polyps, and a hypodense lesion corresponding to the PED and the high-flow BVN (**h**)

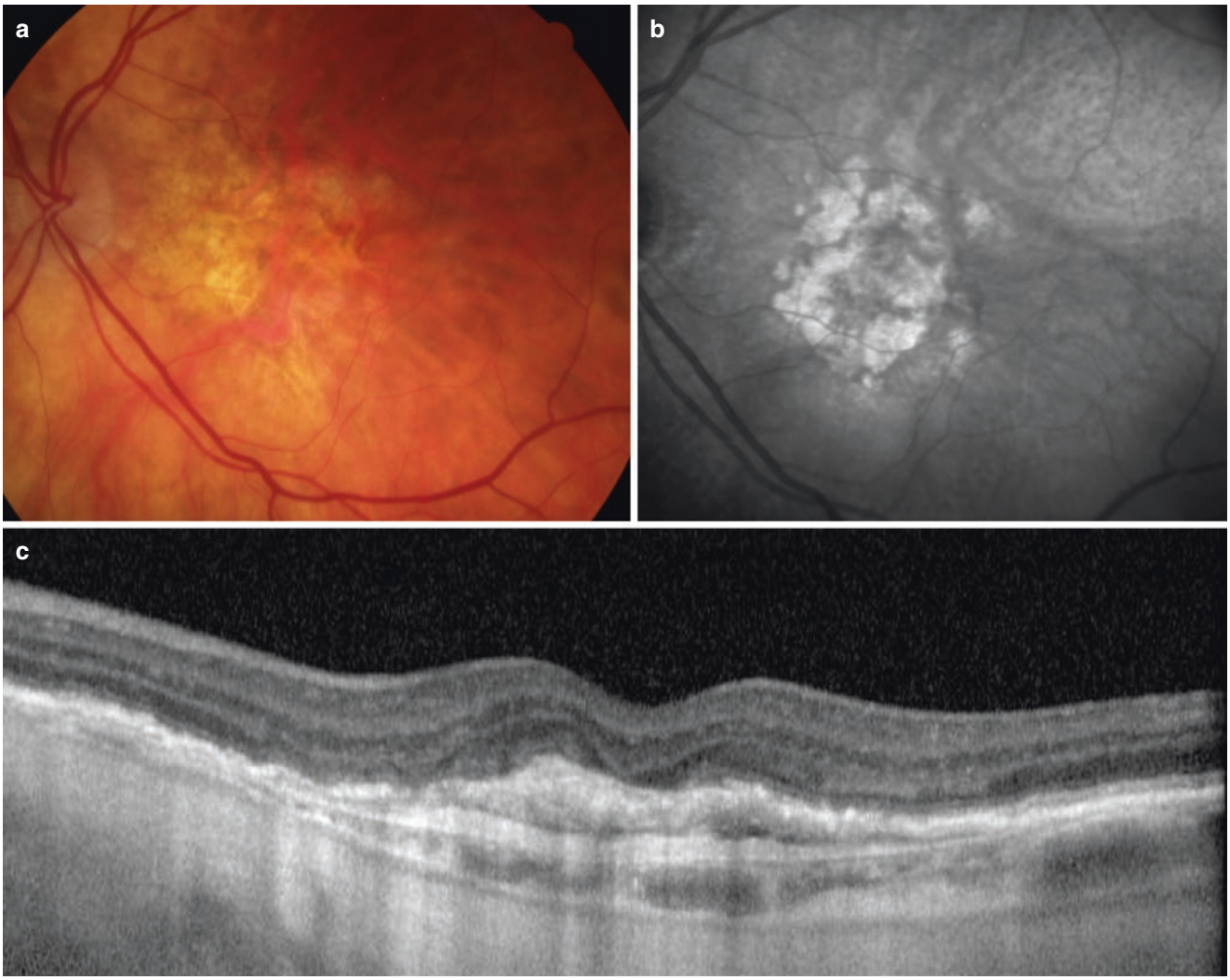

Fig. 2.9 Multimodal imaging of a patient with subretinal fibrosis. (**a**) Color fundus photo showing well-demarcated, elevated mound of yellowish-white tissue; (**b**) Infrared imaging reveals a greyish-white aspect of subretinal fibrosis; (**c**) SD-OCT shows the homogeneous hyperreflective lesion located in subretinal space

frequently interlacing vascular network in the automatic segmentation zone corresponding to the fibrotic scar on the B-scan image. Vascular loop was defined as a high flow with a convoluted network on the OCTA scans.

Management: Anti-VEGF Therapy

The anti-VEGFs have become the gold standard for the treatment of neovascular AMD. Laser photocoagulation and photodynamic therapy (PDT) are no longer the first-line treatments of CNV complicating AMD. VEGF is secreted by RPE cells, causing endothelial cell proliferation and vascular permeability increase. VEGF has a pivotal role in neovascular AMD. The cascade of VEGF-induced angiogenesis could be stopped at different stages; this fact has led to the development of several VEGF targeting molecules.

There are four therapeutic molecules targeting the VEGF for the treatment of neovascular AMD.

The Anti-VEGFs

Pegaptanib (Macugen®)

Pegagtanib was the first molecule that showed an effectiveness in neovascular AMD. Its effectiveness was partial by showing less loss of visual acuity compared to the control group. Its use has decreased considerably since the availability of the new anti-VEGFs.

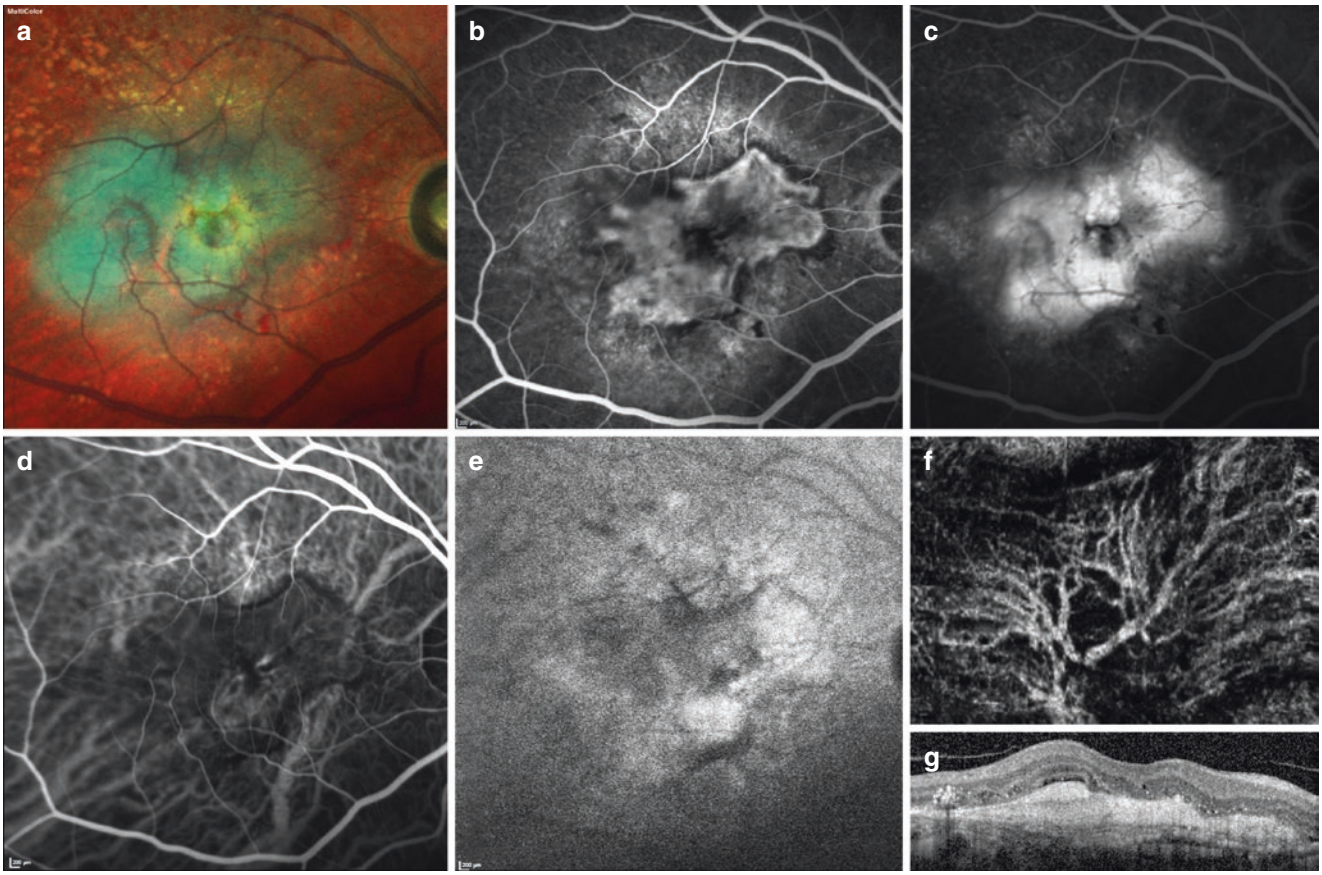

Fig. 2.10 Multimodal imaging of a patient with subretinal fibrosis. (**a**) Multicolor imaging shows a yellowish-green elevated lesion, involving the macula and extending at the posterior pole. Fluorescein angiography reveals the staining of the lesion (**b**) with no leakage in late stages (**c**); ICGA shows rapid filling of neovascular network (**d**) and late hyperfluorescence (**e**). Note the hypofluorescent borders of the lesion, corresponding to the neovascular tissue retraction, during all the angiographic sequence; (**f**) OCTA scan in the outer retina segmentation reveals the large central feeder vessel, few emergent collateral branches, along with the absence of flow between the large branches; (**g**) SD-OCT showing subretinal hyperreflective lesion with loss of adjacent retinal pigment epithelium and ellipsoid zone

Bevacizumab (Avastin®) and Ranibizumab (Lucentis®)

Bevacizumab is a full-length humanized monoclonal antibody directed against VEGF-A.

Ranibizumab is an Fab fragment of an anti-VEGF humanized monoclonal antibody.

This low molecular weight molecule consists of a non-binding sequence of human origin (decreasing the antigenicity of this molecule) and contains a high-affinity sequence for VEGF-A.

The efficacy of bevacizumab has been demonstrated in several large studies (CATT and GEFAL) (CATT Research Group et al. 2011; Kodjikian et al. 2013).

The effectiveness of ranibizumab in monthly injections has been clearly demonstrated in several randomized controlled trials. The pivotal studies that led to its use were MARINA (gain of 6.6 letters ETDRS at 24 months) (Rosenfeld et al. 2006) and ANCHOR (gain of 11.3 letters at 1 year, a difference of 20.8 letters compared to the group PDT) (Brown et al. 2009).

Regarding the use of the two molecules (ranibizumab and bevacizumab), the studies show no significant difference in efficacy between the two treatments (CATT, GEFAL, IVAN) (CATT Research Group et al. 2011; Kodjikian et al. 2013; IVAN Study Investigators et al. 2012).

Aflibercept (Eylea®)

Aflibercept is a recombinant fusion protein: VEGF-Trap. The evaluation of its efficacy in the treatment of exudative AMD is based on the two pivotal studies VIEW1 and VIEW2 of non-inferiority compared to ranibizumab (Heier et al. 2012). The results showed similar efficacy and safety between the two molecules at 52 and 96 weeks (7.9 letters gain in the ranibizumab monthly group and 7.6 letters in the aflibercept group).

Therapeutic Protocols

Fixed Protocols

Fixed protocols are the first therapeutic protocols proposed in anti-VEGF, with strict monthly protocols (Rosenfeld et al. 2006) where patients routinely receive a monthly injection, regardless of the neovascular activity.

The PIER study attempted to reduce the rate of routine injections to quarterly injections (fixed regimen of three IVT ranibizumab followed by quarterly injections), but it scored lower than the previous two pivotals (Regillo et al. 2008).

The strict bi-monthly protocol ("Q8") consists of a systematic administration every 2 months, after the first phase of 3 monthly injections.

This type of protocol has the advantage of regularity and continuous intra-vitreous antiangiogenic coverage.

However, the fixed and repeated nature of these so-called "proactive" protocols may place many patients in the potential position of treatment, with a theoretical increase in the risk of endophthalmitis.

Indeed, several studies have shown that a proportion of patients did not require a new injection after the induction phase in the first year (20% in the SUSTAIN study) (Holz et al. 2011). Finally, repeated injections of anti-VEGF may induce a potential risk for chorioretinal atrophy.

Protocols on Demand

The PrONTO study evaluated patients' therapeutic retreatment strategy (ranibizumab) based on the results of monthly clinical examination and OCT data, following an induction phase of 3 monthly intravitreal injections.

This protocol appears to be as effective as a functionally stable monthly regimen with a lower IVT number (Lalwani et al. 2009) finding a visual acuity gain of 9.3 letters at 1 year, with 5.6 injections (versus 12 in MARINA and ANCHOR studies).

This is a "Pro-Re-Nata" (PRN) treatment regimen that was quickly adopted. Subsequently, other studies have confirmed the equivalence of this protocol to fixed monthly schedules in terms of visual gain. There are some adjustments to this PRN protocol: when it includes a series of successive systematic injections, it is called reinforced PRN, and when an injection is programmed systematically at regular intervals, whatever the exudative activity, the PRN is called "cappé."

Evolutionary Protocols

A third strategy has been proposed: the "Treat and Extend" which aims to reduce the number of visits while maintaining the gain in visual acuity.

It consists of reviewing the patients after the induction phase of three IVT (Spaide 2007): in case of persistence of the exudation, the patients are treated and reviewed again at 4 weeks. In case of absence of exudation, they will still be treated ("Treat") but the time of the next control will be extended ("Extend"). Monitoring can therefore be progressively spaced.

Thus, schematically, the patient will be treated at each visit and the interval is gradually increased by 2 weeks in the absence of exudation up to a maximum of 12 weeks. On the other hand, in the presence of exudation, the interval is reduced by 2 weeks to a minimum of 4 weeks. This approach has the advantage of a gradual individualization of the treatment but also presents obvious risks of over or under treatment.

Recently, a new protocol has been described: the "Observe and Plan" protocol (Mantel et al. 2014). It is based on the principle that the exudative reactivation delay after the induction phase will condition future recurrence intervals.

Thus, patients will receive a series of three systematic IVT followed by a monthly observation period "Observe" which will determine the interval between the third injection and the appearance of exudative signs on OCT, and this interval will be decreased by 2 weeks.

From here, a fixed individual treatment "Plan" of three new injections whose achievement interval was set during the observation period is realized.

Then, at the end of this new series of IVT if neovascular activity persists, the interval is further reduced by 2 weeks for the following three systematic IVT, otherwise, the interval is increased by 2 weeks and so after.

This protocol reduces the number of total visits over the year but also presents a risk for over-treatment.

There is currently no consensus on the strategy to follow when monitoring patients. It is important to individualize the therapeutic protocol according to the profile of recurrence of the patient after an observation phase.

References

Bloch SB, Lund-Andersen H, Sander B, Larsen M. Subfoveal fibrosis in eyes with neovascular age-related macular degeneration treated with intravitreal ranibizumab. Am J Ophthalmol. 2013;156:116–24.

Brown DM, Michels M, Kaiser PK, et al. Ranibizumab versus verteporfin photodynamic therapy for neovascular age-related macular degeneration: two-year results of the ANCHOR study. Ophthalmology. 2009;116:57–65.e5.

CATT Research Group, Martin DF, Maguire MG, Ying G, et al. Ranibizumab and bevacizumab for neovascular age-related macular degeneration. N Engl J Med. 2011;364:1897–908.

Channa R, Sophie R, Bagheri S, et al. Regression of choroidal neovascularization results in macular atrophy in anti-vascular endothelial growth factor-treated eyes. Am J Ophthalmol. 2015;159:9–19.

Ciardella AP, Donsoff IM, Huang SJ, et al. Polypoidal choroidal vasculopathy. Surv Ophthalmol. 2004;49:25–37.

Cohen SY, Creuzot-Garcher C, Darmon J, et al. Types of choroidal neovascularization in newly diagnosed exudative age-related macular degeneration. Br J Ophthalmol. 2007a;91:1173–6.

Cohen SY, Dubois L, Tadayoni R, et al. Prevalence of reticular pseudodrusen in age-related macular degeneration with newly diagnosed choroidal neovascularisation. Br J Ophthalmol. 2007b;91:354–9.

Cohen SY, Oubraham H, Uzzan J, et al. Causes of unsuccessful ranibizumab treatment in exudative age-related macular degeneration in clinical settings. Retina. 2012;32:1480–5.

Coscas G, De Benedetto U, Coscas F, et al. Hyperreflective dots: a new spectral-domain optical coherence tomography entity for follow-up and prognosis in exudative age-related macular degeneration. Int J Ophthalmol. 2013;229:32–7.

De Salvo G, Vaz-Pereira S, Keane PA, et al. Sensitivity and specificity of spectral-domain optical coherence tomography in detecting idiopathic polypoidal choroidal vasculopathy. Am J Ophthalmol. 2014;158:1228–38.e1.

El Ameen A, Cohen SY, Semoun O, et al. Type 2 neovascularization secondary to age-related macular degeneration imaged by optical coherence tomography angiography. Retina. 2015;35:2212–8.

Ferris FL III, Fine SL, Hyman L. Age related macular degeneration and blindness due to neovascular maculopathy. Arch Ophthalmol. 1984;102:1640–2.

Freund B, Ho I-V, Barbazetto I, et al. Type 3 neovascularization. The expanded spectrum of retinal angiomatous proliferation. Retina. 2008;28:201–11.

Freund KB, Zweifel SA, Engelbert M. Do we need a new classification for choroidal neovascularization in age-related macular degeneration? Retina. 2010;30:1333–49.

Gass JDM, Agarwal A, Lavina AM, et al. Focal inner retinal hemorrhages in patients with drusen: an early sign of occult choroidal anastomosis. Retina. 2003;23:241–51.

Gelisken F, Inhoffen W, Schneider U, et al. Indocyanine green angiography in classic choroidal neovascularization. Jpn J Ophthalmol. 1998;42:300–3.

Gross NE, Aizman A, Brucker A, Klancnik JM Jr, Yannuzzi LA. Nature and risk of neovascularization in the fellow eye of patients with unilateral retinal angiomatous proliferation. Retina. 2005;25:713–8.

Grossniklaus HE, Gass JD. Clinicopathologic correlations of surgically excised type 1 and type 2 submacular choroidal neovascular membranes. Am J Ophthalmol. 1998;126:59–69.

Hartnett ME, Weiter JJ, Gardts A, Jalkh AE. Classification of retinal pigment epithelial detachments associated with drusen. Graefes Arch Clin Exp Ophthalmol. 1992;230:11–9.

Heier JS, Brown DM, Chong V, et al. Intravitreal aflibercept (VEGF trap-eye) in wet age-related macular degeneration. Ophthalmology. 2012;119:2537–48.

Holz FG, Amoaku W, Donate J, et al. Safety and efficacy of a flexible dosing regimen of ranibizumab in neovascular age-related macular degeneration: the SUSTAIN study. Ophthalmology. 2011;118:663–71.

Hwang JC, Del Priore LV, Freund KB, et al. Development of subretinal fibrosis after anti-VEGF treatment in neovascular age-related macular degeneration. Ophthalmic Surg Lasers Imaging. 2011;42:6–11.

Iijima H, Imai M, Gohdo T, et al. Optical coherence tomography of idiopathic polypoidal choroidal vasculopathy. Am J Ophthalmol. 1999;127:301–5.

IVAN Study Investigators, Chakravarthy U, Harding SP, Rogers CA, et al. Ranibizumab versus bevacizumab to treat neovascular age-related macular degeneration: one-year findings from the IVAN randomized trial. Ophthalmology. 2012;119:1399–411.

Jung JJ, Chen CY, Mrejen S, et al. The incidence of neovascular subtypes in newly diagnosed neovascular age-related macular degeneration. Am J Ophthalmol. 2014;158:769–79.

Kim JH, Kim JR, Kang SJ, Ha HS. Thinner choroid and greater drusen extent in retinal angiomatous proliferation than in typical exudative age-related macular degeneration. Am J Ophthalmol. 2013;155(743–9):749.

Kodjikian L, Souied EH, Mimoun G, et al. Ranibizumab versus bevacizumab for neovascular age-related macular degeneration: results from the GEFAL noninferiority randomized trial. Ophthalmology. 2013;120:2300–9.

Kuehlewein L, Bansal M, Lenis LT, et al. Optical coherence tomography angiography of type 1 neovascularization in age-related macular degeneration. Am J Ophthalmol. 2015;160:739–48.

Kuhn D, Meunier I, Soubrane G, Coscas G. Imaging of chorioretinal anastomoses in vascularized retinal pigment epithelium detachments. Arch Ophthalmol. 1995;113:1392–8.

Lalwani GA, Rosenfeld PJ, Fung AE, et al. A variable-dosing regimen with intravitreal ranibizumab for neovascular age-related macular degeneration: year 2 of the PrONTO Study. Am J Ophthalmol. 2009;148:43–58.e1.

Lam D, Semoun O, Blanco-Garavito R, et al. Wrinkled vascularized retinal pigment epithelium detachment prognosis after intravitreal anti-VEGF therapy. Retina. 2017;38:1100–9.

Laude A, Cackett PD, Vithana EN, et al. Polypoidal choroidal vasculopathy and neovascular age-related macular degeneration: same or different disease? Prog Retin Eye Res. 2010;29:19–29.

Mantel I, Niderprim S-A, Gianniou C, et al. Reducing the clinical burden of ranibizumab treatment for neovascular age-related macular degeneration using an individually planned regimen. Br J Ophthalmol. 2014;98:1192–6.

Miere A, Querques G, Semoun O, et al. Optical coherence tomography angiography in early type 3 neovascularization. Retina. 2015a;35:2236–41.

Miere A, Semoun O, Cohen SY, et al. Optical coherence tomography angiography features of subretinal fibrosis in age-related macular degeneration. Retina. 2015b;35:2275–84.

Mrejen S, Sarraf D, Mukkamala SK, Freund KB. Multimodal imaging of pigment epithelial detachment: a guide to evaluation. Retina. 2013;33:1735–62.

Nagiel A, Sarraf D, Sadda SR, et al. Type 3 neovascularization: evolution, association with pigment epithelial detachment, and treatment response as revealed by spectral domain optical coherence tomography. Retina. 2015;35:638–47.

Ores R, Puche N, Querques G, et al. Gray hyper-reflective subretinal exudative lesions in exudative age-related macular degeneration. Am J Ophthalmol. 2014;158:354–61.

Otsuji T, Takahashi K, Fukushima I, et al. Optical coherence tomographic findings of idiopathic polypoidal choroidal vasculopathy. Ophthalmic Surg Lasers. 2000;31:210–4.

Pang CE, Messinger JD, Zanzottera EC, et al. The Onion Sign in neovascular age-related macular degeneration represents cholesterol crystals. Ophthalmology. 2015;122:2316–26.

Querques G, Atmani K, Berboucha E, et al. Angiographic analysis of retinal-choroidal anastomosis by confocal scanning laser ophthalmoscopy technology and corresponding (eye-tracked) spectral-domain optical coherence tomography. Retina. 2010;30:222–34.

Querques G, Querques L, Forte R, et al. Precursors of type 3 neovascularization: a multimodal imaging analysis. Retina. 2013a;33:1241–8.

Querques G, Souied EH, Freund KB. Multimodal imaging of early stage 1 type 3 neovascularization with simultaneous eye-tracked spectral-domain optical coherence tomography and high-speed real-time angiography. Retina. 2013b;33:1881–7.

Querques G, Srour M, Massmaba N, et al. Functional characterization and multimodal imaging of treatment-naive "quiescent" choroidal neovascularization. Invest Ophthalmol Vis Sci. 2013c;54:6886–92.

Querques G, Souied EH, Freund KB. How has high-resolution multimodal imaging refined our understanding of the vasogenic process in type 3 neovascularization? Retina. 2015;35:603–13.

Querques G, Capuano V, Costanzo E, et al. Retinal pigment epithelium aperture: a previously unreported finding in the evolution of avascular pigment epithelium detachment. Retina. 2016;36(Suppl 1):S65–72.

Rahimy E, Freund KB, Larsen M. Multilayered pigment epithelial detachment in neovascular age-related macular degeneration. Retina. 2014;34:1289–95.

Regillo CD, Brown DM, Abraham P, et al. Randomized, double-masked, sham-controlled trial of ranibizumab for neovascular age-related macular degeneration: PIER Study year 1. Am J Ophthalmol. 2008;145:239–48.

Rosenfeld PJ, Brown DM, Heier JS, et al. Ranibizumab for neovascular age-related macular degeneration. N Engl J Med. 2006;355:1419–31.

Rosenfeld PJ, Shapiro H, Tuomi L, et al. Characteristics of patients losing vision after 2 years of monthly dosing in the phase III ranibizumab clinical trials. Ophthalmology. 2011;118:523–30.

Sa HS, Cho HY, Kang SW. Optical coherence tomography of idiopathic polypoidal choroidal vasculopathy. Korean J Ophthalmol. 2005;19:275–80.

Sato T, Kishi S, Watanabe G, et al. Tomographic features of branching vascular networks in polypoidal choroidal vasculopathy. Retina. 2007;27:589–94.

Schlingemann RO. Role of growth factors and the wound healing response in age-related macular degeneration. Graefes Arch Clin Exp Ophthalmol. 2004;242:91–101.

Semoun O, Guigui B, Tick S, et al. Infrared features of classic choroidal neovascularization in exudative age related macular degeneration. Br J Ophthalmol. 2009;93:182–5.

Spaide R. Ranibizumab according to need: a treatment for age-related macular degeneration. Am J Ophthalmol. 2007;143:679–80.

Spaide RF, Yannuzzi LA, Slakter JS, et al. Indocyanine green videoangiography of idiopathic polypoidal choroidal vasculopathy. Retina. 1995;15:100–10.

Srour M, Querques G, Semoun O, et al. Optical coherence tomography angiography characteristics of polypoidal choroidal vasculopathy. Br J Ophthalmol. 2016;100(11):1489–93.

Toth LA, Stevenson M, Chakravarthy U. Anti-vascular endothelial growth factor therapy for neovascular age-related macular: outcomes in eyes with poor initial vision. Retina. 2015;35:1957–63.

Yannuzzi LA. Idiopathic polypoidal choroidal vasculopathy. Presented at The Macula Society Meeting. Miami; 1982.

Yannuzzi LA, Sorenson J, Spaide RF, et al. Idiopathic polypoidal choroidal vasculopathy (IPCV). Retina. 1990;10:1–8.

Yannuzzi LA, Negrão S, Iida T, et al. Retinal angiomatous proliferation in age-related macular degeneration. Retina. 2001;21:416–34.

Yannuzzi LA, Freund KB, Takahashi BS. Review of retinal angiomatous proliferation or type 3 neovascularization. Retina. 2008;28:375–84.

Zweifel SA, Spaide RF, Curcio CA, Malek G, Imamura Y. Reticular pseudodrusen are subretinal drusenoid deposits. Ophthalmology. 2010;117:303–12.e1.

Polypoidal Choroidal Vasculopathy

3

Jonathan C. H. Cheung, Danny S. C. Ng, and Timothy Y. Y. Lai

Abbreviations

AF	Autofluorescence
AMD	Age-related macular degeneration
BVN	Branching vascular network
CNV	Choroidal neovascularization
CSC	Central serous chorioretinopathy
FA	Fluorescein angiography
FAF	Fundus autofluorescence
FCE	Focal choroidal excavation
ICGA	Indocyanine green angiography
MMP	Matrix metalloproteinase
OCTA	Optical coherence tomography angiography
PCV	Polypoidal choroidal vasculopathy
PED	Pigment epithelial detachment
PRN	Pro re nata
RPE	Retinal pigment epithelium
SD-OCT	Spectral-domain optical coherence tomography
VA	Visual acuity
VEGF	Vascular endothelial growth factor
vPDT	Verteporfin photodynamic therapy

Introduction

Polypoidal choroidal vasculopathy (PCV) is a serosanguinous maculopathy more frequently affecting Asian populations (Cheung et al. 2018). It was first described in the 1980s and is characterized by the presence of polyp-like aneurysmal subretinal vascular lesions which are best visualized using indocyanine green angiography (ICGA) (Yannuzzi et al. 1990). PCV is generally considered a subtype of age-related macular degeneration (AMD) as they share many common clinical features and risk factors (Wong et al. 2016). Yet, more recent evidence has demonstrated some significant disparities between PCV and typical AMD, particularly in their clinical course and response to treatment. Clinicians and researchers are now therefore considering PCV as a separate disease entity in its own right or as a variant of type 1 (sub-retinal pigment epithelial) choroidal neovascularization (CNV).

Epidemiology of PCV

The definition and epidemiology of PCV is constantly evolving as newer imaging techniques become available. With the presumption that PCV is a subtype of neovascular AMD, epidemiological data of PCV have largely been derived from studies on AMD. Interestingly, PCV appears to have different epidemiological profiles among various racial groups. The prevalence of PCV in the general East Asian population is estimated to be 0.3% (Li et al. 2014), and the prevalence of PCV among the presumed AMD population is estimated to be 20–60% in Asians and 8–13% in Caucasians respectively (Li et al. 2014; Sho et al. 2003; Wen et al. 2004; Liu et al. 2007; Maruko et al. 2007; Byeon et al. 2008; Chang and Wu 2009; Mori et al. 2010; Coscas et al. 2014; Cheung et al. 2014; Ciardella et al. 2004). In Asians, PCV typically is a unilateral disease with a male preponderance (Honda et al. 2014), whereas in white and black patients, it tends to involve both eyes and occurs predominantly in females (Lafaut et al. 2000).

Risk Factors of PCV

PCV shares several but not all risk factors with AMD (Kikuchi et al. 2007; Zeng et al. 2013; Zhao et al. 2015; Cheng et al. 2014) (Table 3.1). A number of studies have

J. C. H. Cheung · D. S. C. Ng
Department of Ophthalmology and Visual Sciences, The Chinese University of Hong Kong, Kowloon, Hong Kong

T. Y. Y. Lai (✉)
2010 Retina and Macula Centre, Kowloon, Hong Kong

Department of Ophthalmology and Visual Sciences, The Chinese University of Hong Kong, 3/F Hong Kong Eye Hospital, Kowloon, Hong Kong
e-mail: tyylai@cuhk.edu.hk

I. K. Kim (ed.), *Macular Disorders*, Retina Atlas, https://doi.org/10.1007/978-981-15-3001-2_3

Table 3.1 Risk factors for the development of PCV

Smoking
Diabetes mellitus
End-stage renal failure
Inflammatory markers, e.g., *C-reactive protein*, interleukin-1B
Homocysteine
MMP-2, MMP-9
Serum VEGF level

MMP matrix metalloproteinase, *VEGF* vascular endothelial growth factor, bold text: risk factors shared with AMD, *italic* text: risk factors more strongly correlate with AMD

evaluated the genetics of PCV, and associations between PCV and several gene loci involved in the inflammation, lipid metabolism, and complement pathways have been identified (Sakurada et al. 2013; Ma et al. 2015). Some of the single nucleotide polymorphisms including *ARMS2*, *HTRA1*, and *SERPING1* genes have been found to predict the treatment response and outcomes (Ma et al. 2015) (see section "Natural History of PCV").

Etiology and Pathogenesis of PCV

The polypoidal lesions in PCV originate from an abnormal CNV, likely as a consequence of local ischemia or inflammatory responses (Okubo et al. 2002). Angiogenic factors like vascular endothelial growth factor (VEGF) have been implicated in the development of PCV since elevated levels of VEGF have been found in eyes with PCV (Lee et al. 2013; Tong et al. 2006). The aberrant, dilated choroidal vessels interconnect into a branching vascular network (BVN), and aneurysmal dilatations may arise at the outer border of the BVN to form the characteristic polyps (Sato et al. 2007; Okubo et al. 2002; Yannuzzi et al. 1990). These aberrant BVN and polyps can cause exudation, breaching the retinal pigment epithelium (RPE), and may rupture to cause hemorrhage.

The choroid in PCV is commonly found to be hyperpermeable and thickened (Chung et al. 2011). These features of choroidal hyperpermeability and thickening have also been found in other macular diseases including central serous chorioretinopathy (CSC), pachychoroid pigment epitheliopathy, and pachychoroid neovasculopathy, which are now collectively called pachychoroid eye diseases (Balaratnasingam et al. 2016; Gallego-Pinazo et al. 2014).

Clinical and Imaging Features of PCV

PCV might sometimes be clinically indistinguishable from neovascular AMD because on fundus examination, they share a number of common clinical features, such as subretinal exudate or hemorrhage, serous or hemorrhagic pigment epithelial detachment (PED), and RPE atrophy (Tsujikawa et al. 2007) (Figs. 3.1, 3.2, and 3.3). Importantly, eyes with PCV often lack the typical signs of AMD like soft drusen, pigmentary changes, and geographic atrophy (Yannuzzi et al. 1990, 1997; Sho et al. 2003; Balaratnasingam et al. 2016). The polypoidal lesions can sometimes be seen on fundus examination as protruding subretinal orange-red nodules in the macular or peripapillary areas.

At present, ICGA is the gold standard for diagnosing PCV. Although PCV demonstrates certain characteristic features when assessed by other imaging modalities, ICGA remains singularly important for reaching a definitive diagnosis. Nevertheless, accurately diagnosing PCV might be a

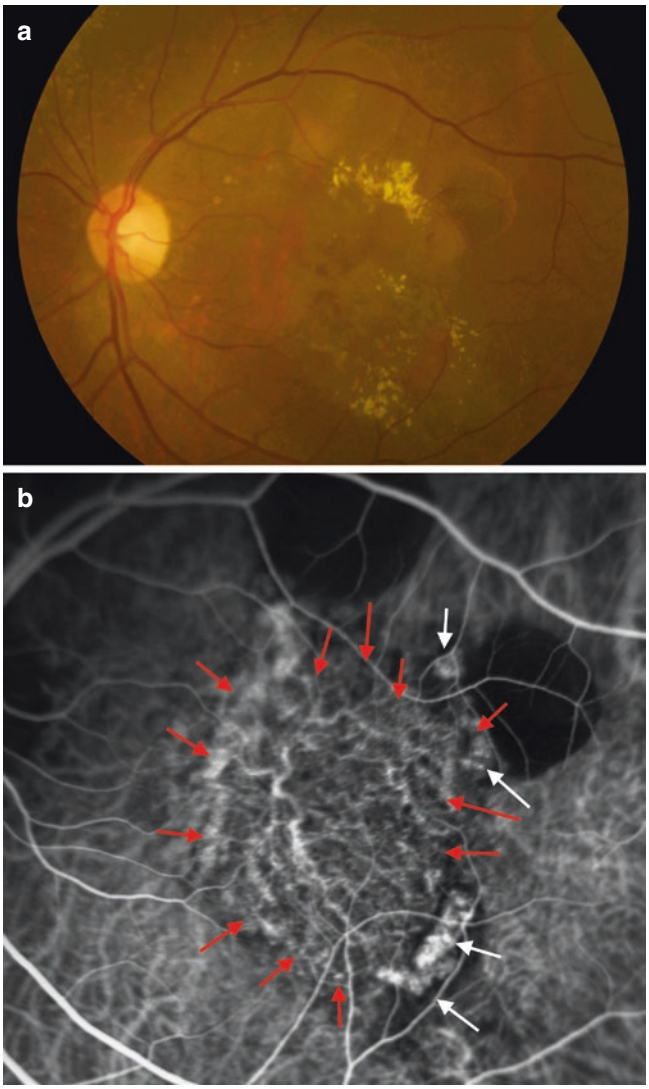

Fig. 3.1 (**a**) Left eye fundus photograph with polypoidal choroidal vasculopathy showing serosanginous pigment epithelial detachments, macular hemorrhage, and hard exudate. (**b**) Early phase indocyanine green angiography of the eye showing multiple polyps (white arrows) causing nodular hyperfluorescence and area of hyperfluorescence due to branching vascular network (red arrows)

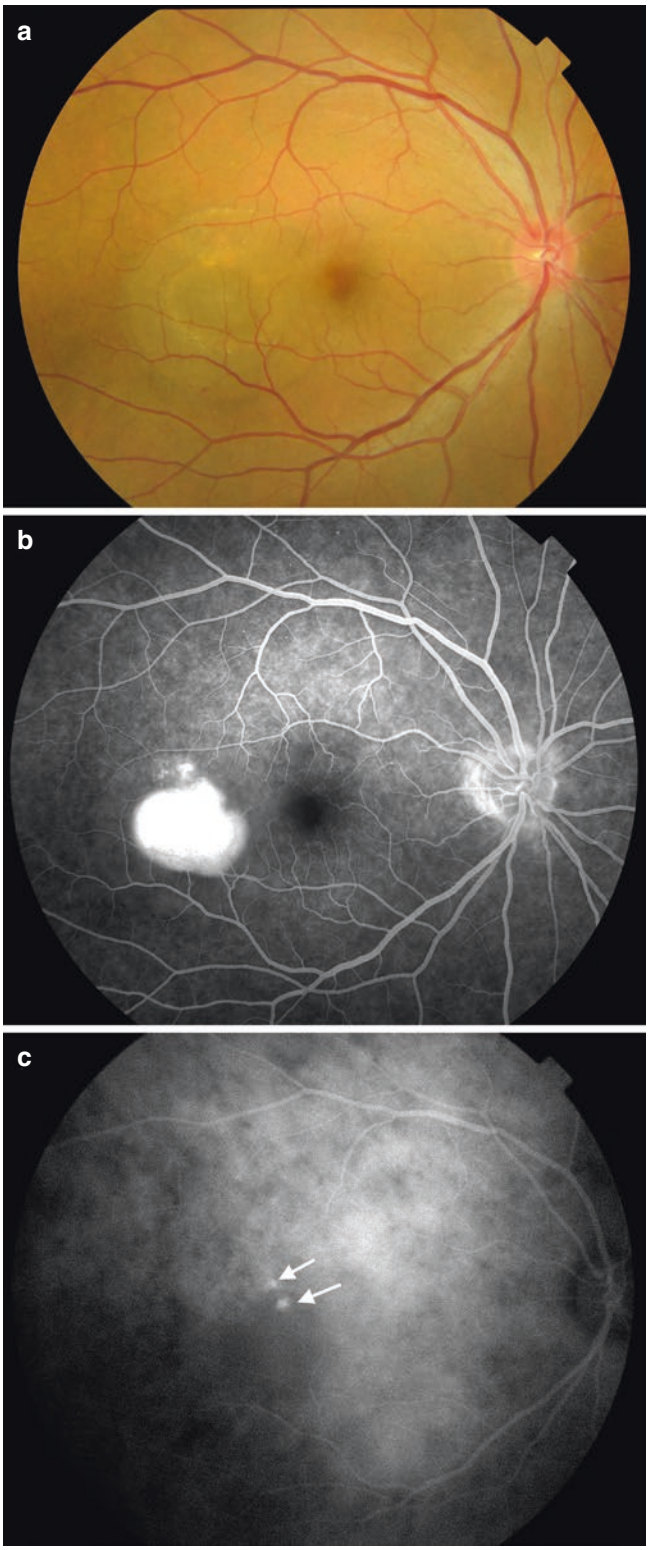

Fig. 3.2 (**a**) Right eye fundus photograph showing serous pigment epithelial detachment with serous macular detachment. (**b**) Mid-phase fluorescein angiography of the eye showing pooling of dye due to serous pigment epithelial detachment. (**c**) Early phase indocyanine green angiography of the eye showing nodular hyperfluorescence due to multiple polyps (white arrows) and an area of hypofluorescence due to serous pigment epithelial detachment

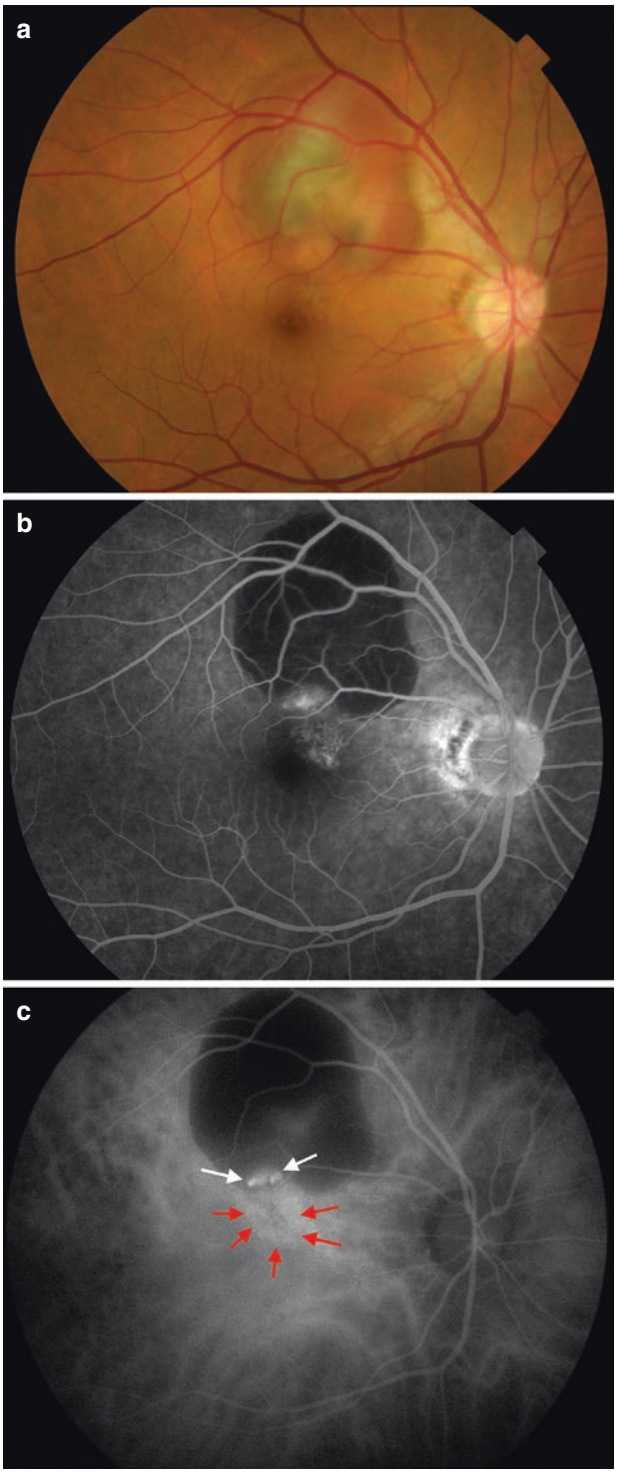

Fig. 3.3 (**a**) Right eye fundus photograph with polypoidal choroidal vasculopathy showing right eye hemorrhagic pigment epithelial detachment involving the superior macula. (**b**) Mid phase fluorescein angiography of the eye showing blocked fluorescence due to hemorrhagic pigment epithelial detachment and hyperfluorescence lesion at the inferior edge of the pigment epithelial detachment. (**c**) Early phase indocyanine green angiography of the eye showing two nodular hyperfluorescent spots due to polyps (white arrows) at the inferior edge of the pigment epithelial detachment and an area of hyperfluorescence due to branching vascular network (red arrows)

challenge even for the experienced due to similarities of PCV with typical neovascular AMD. On some occasions, the polypoidal lesions might be invisible in the early stage of the disease process and therefore repeated imaging is sometimes needed to diagnose PCV.

Indocyanine Green Angiography

ICGA is the gold standard investigation in the diagnosis of PCV. The polypoidal lesions appear as focal hyperfluorescent nodules which may have a hypofluorescent halo, which can be pulsatile and can be clustered in various configurations (Koh et al. 2012; Spaide et al. 1995; Tan et al. 2015) (Figs. 3.1, 3.2 and 3.3). BVN can also be seen as interconnecting subretinal vessels (Tan et al. 2015). With the need of recruiting PCV patients for multicentered clinical trials, the EVEREST Study Group has established a set of criteria for the diagnosis of PCV and this has been widely utilized by many investigators worldwide. The EVEREST Study diagnostic criteria require the presence of focal hyperfluorescent lesions appearing within the first 6 min on ICGA plus at least one of the following additional features: BVN on ICGA, pulsatile polyp on dynamic ICGA, nodular appearance of the polyps on stereoscopic viewing, presence of hypofluorescent halo, orange subretinal nodule on color fundus photography, and/or associated massive hemorrhage (Koh et al. 2012) (Fig. 3.4).

Spectral-Domain Optical Coherence Tomography

Although unable to replace ICGA in the diagnosis of PCV, spectral-domain optical coherence tomography (SD-OCT) has been found to have reasonable concordance with ICGA for diagnosing PCV (Chang et al. 2016; De Salvo et al. 2014), making it a useful screening tool, especially in places where ICGA is not readily available. The polyps on SD-OCT can appear as sharply peaked elevation of the RPE (PED peak or thumb-like protrusion) (Fig. 3.5) (Iijima et al. 1999, 2000). There is often a notch seen in the margin of a PED, representing the site of the polypoidal lesion (Tsujikawa et al. 2007). The separation between the RPE and Bruch's membrane caused by the BVN produces two distinct hyperreflective lines on SD-OCT, known as the double-layer sign (Sato et al. 2007; Kim et al. 2013). Eyes with PCV have SD-OCT findings in common with other pachychoroid diseases, namely, thickened choroid, presence of dilated large choroidal vessels (pachyvessels) obliterating the choriocapillaris and Sattler layer, and some eyes might also have localized choroidal pitting known as focal choroidal excavation (FCE) (Balaratnasingam et al. 2016; Gallego-Pinazo et al. 2014; Dansingani et al. 2016).

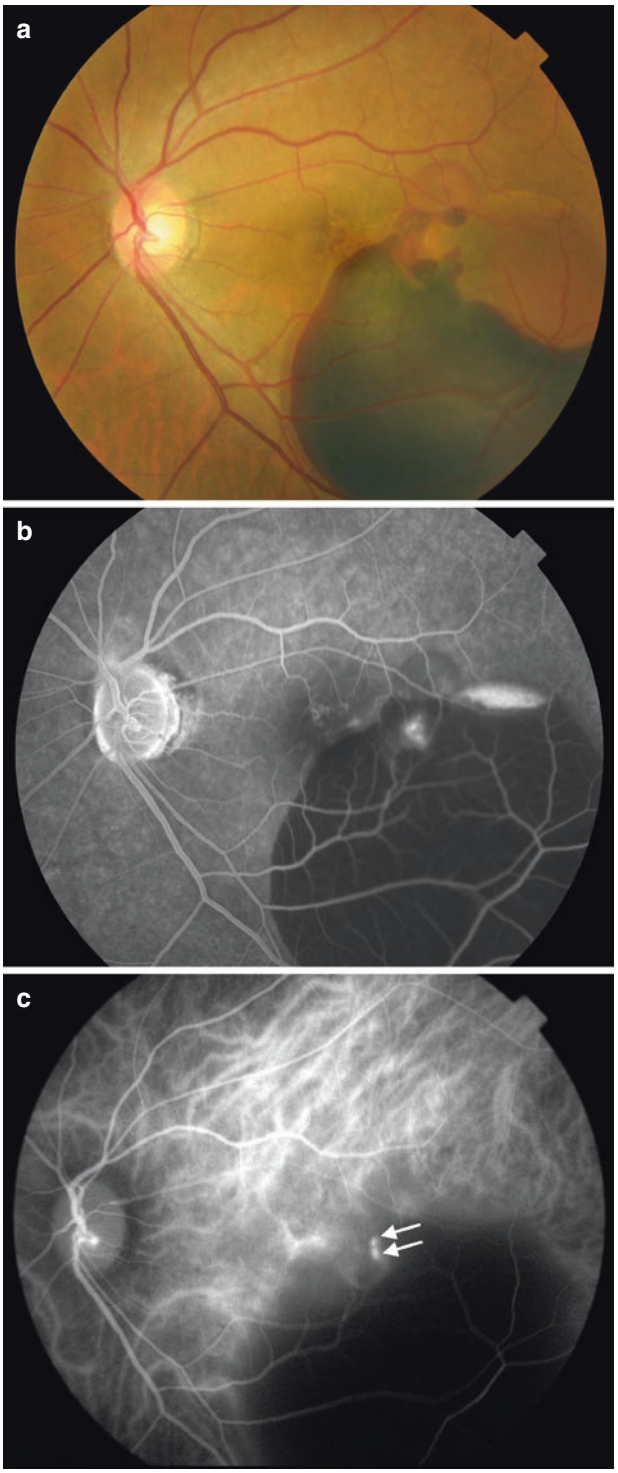

Fig. 3.4 (**a**) Left eye fundus photograph with polypoidal choroidal vasculopathy showing left eye hemorrhagic pigment epithelial detachments with massive subretinal hemorrhage involving inferiotemporal macula. (**b**) Mid phase fluorescein angiography of the eye showing blocked fluorescence due to hemorrhagic pigment epithelial detachment and subretinal hemorrhage. Hyperfluorescence can be seen at the superior edge of the pigment epithelial detachment and at the possible polyps. (**c**) Early phase indocyanine green angiography of the eye showing two nodular hyperfluorescent spots due to polyps (white arrows) at the superior edge of the subretinal hemorrhage

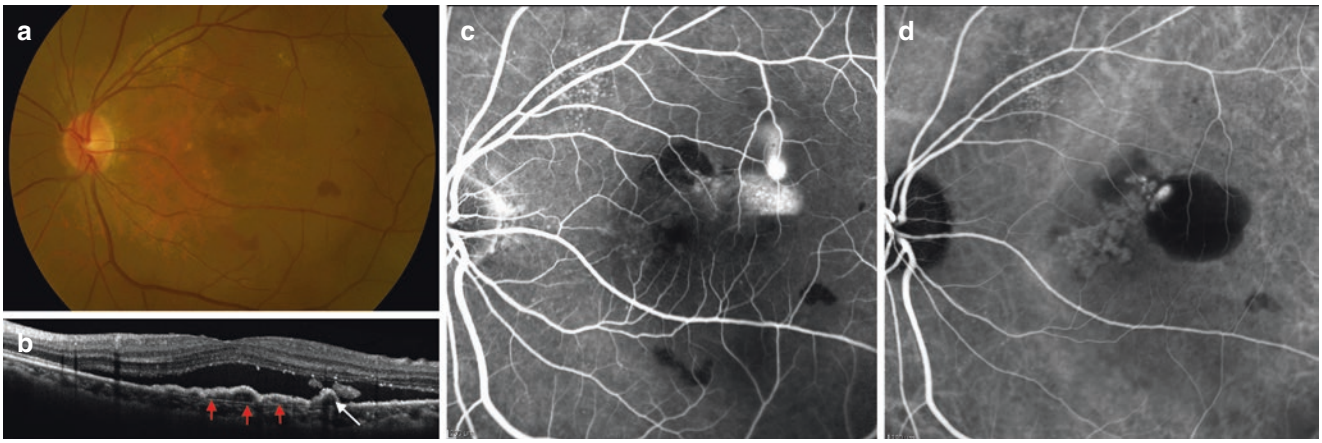

Fig. 3.5 (**a**) Left eye fundus photograph with polypoidal choroidal vasculopathy showing left eye serous macular hemorrhage with pigment epithelial detachment and patches of subretinal hemorrhage. (**b**) Spectral-domain optical coherence tomography showing serous macular detachment with thumb-like protrusion due to polyp (white arrow) and double-layer sign due to branching vascular network (red arrows). (**c**) Mid phase fluorescein angiography of the eye showing blocked fluorescence due to subretinal hemorrhages and smoke stalk leakage superior to the pigment epithelial detachment. (**d**) Early phase indocyanine green angiography of the eye showing two nodular hyperfluorescent spots due to polyps with branching vascular network at the notch of the pigment epithelial detachment

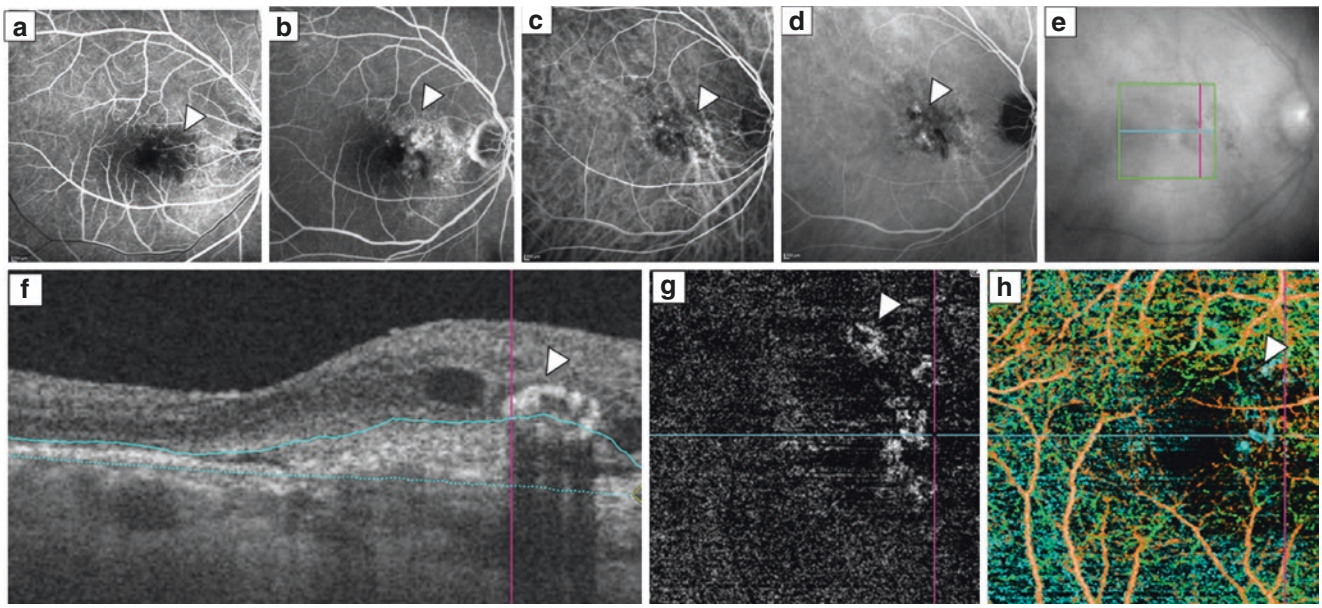

Fig. 3.6 Right eye of a patient with polypoidal choroidal vasculopathy associated with serous pigment epithelial detachment (PED). (**a**) Early phase fluorescein angiography (FA) revealed hyperfluorescence (arrow head). (**b**) Late phase FA photo was graded as transmission defect without obvious leakage. (**c**) Early and (**d**) late phase indocyanine green angiography (ICGA) showed a cluster subretinal focal hyperfluorescence from polypoidal lesion (arrow head). (**e**) The 3 × 3 mm en face optical coherence tomography angiography (OCTA) scan area (green box) and cross hairs (purple and blue lines) overlay on the black and white fundus photo. (**f**) The segmentation slab (blue lines) was placed according to the outline of the PED on OCT B-scan. The thumb-like protrusion attached just below the retinal pigment epithelium represented a polyp. (**g**) En face OCTA revealed flow signal from a branching vascular network in the outer retina. The roundish flow signal (arrow head) indicated the polyps. (**h**) The projection resolved en face OCTA coded the polyps (arrow head) and branching vascular network in blue color

Optical Coherence Tomography Angiography

Optical coherence tomography angiography (OCTA) is an emerging non-invasive technique for imaging retinal and choroidal vasculature by detecting flow within the blood vessels without the use of dye. Localized increase in flow signal can be seen at the site of the polyps and BVN (Fig. 3.6). Despite having this advantage over ICGA, OCTA cannot substitute ICGA at present due to its incomplete PCV detection rate (Inoue et al. 2015).

Fluorescein Angiography

Despite its value for diagnosing CNV in neovascular AMD, fluorescein angiography (FA) is not essential for the diagnosis of PCV because FA does not visualize the choroidal vasculature well, as the polyps are not clearly delineated while the size of the BVN is often exaggerated (Cheung et al. 2018). It has been suggested that FA does not seem to provide much additional diagnostic information on PCV when other imaging modalities are available (Chaikitmongkol et al. 2018). Nonetheless, FA is still useful to assess the development of CNV in some cases of PCV, especially in long-standing cases.

Fundus Autofluorescence

Fundus autofluorescence (FAF) is a non-invasive investigation which can detect the disruption of RPE metabolism and function. In PCV, the polyps most often appear as confluent hypo-autofluorescence (AF) surrounded by a hyper-AF ring. However, it may less commonly display other patterns or even the opposite pattern, i.e., hyper-AF with circumferential hypo-AF. BVN primarily manifests as granular hypo-AF (Oztas et al. 2016; Zhao et al. 2018; Yamagishi et al. 2012). Early reports suggest that these appearances may change as the disease progresses or regresses with treatment (Suzuki et al. 2013; Yamagishi et al. 2014).

Natural History of PCV

PCV can cause exudative or hemorrhagic complications similar to neovascular AMD (Uyama et al. 2002). However, PCV was believed to have a more favorable outcome compared to neovascular AMD, which may be partly due to the lower frequency of fibrotic scar formation (Yannuzzi et al. 1997). PCV demonstrates significant heterogeneity in terms of its natural history and prognosis. In half of the patients, PCV is relatively self-limiting, or even may spontaneously improve without treatment, whereas in the other half, the disease can relapse and progress despite active treatment, resulting in significant visual loss (Cheung et al. 2015). This led to investigators further classifying PCV into potential subtypes with different clinical courses and features according to choroidal vascular abnormalities in ICGA, as well as the degree of complexity of the vascular lesions (Yuzawa et al. 2005; Tan et al. 2014). The presence of such vascular lesions was found to be associated with *ARMS2* gene polymorphism, which may in part explain the observed phenotypic differences (Tanaka et al. 2011). The "grape cluster" pattern in particular is a negative prognostic factor (Uyama et al. 2002).

Treatment of PCV

Several treatment options have been used in the treatment of PCV, including verteporfin photodynamic therapy (vPDT), intravitreal anti-VEGF therapy, thermal laser photocoagulation, and combination therapy. The choice of treatment depends on the individual patient's clinical characteristics, patients' and doctors' preferences, and the availability of the treatment.

Verteporfin Photodynamic Therapy for PCV

Monotherapy using verteporfin photodynamic therapy (vPDT) has been the most widely used treatment for PCV prior to the availability of anti-VEGF therapy. The primary effect of vPDT is to cause polyp closure thereby reducing the exudation from the polyp (Kokame 2014). Paradoxically, the initial visual acuity (VA) improvement following vPDT monotherapy failed to last longer than 3 years (Wong et al. 2015). One hypothesis is that the collateral damage caused by vPDT accrues over time and will ultimately be detrimental to the choriocapillaris, RPE, and photoreceptors, resulting in macular atrophy. Furthermore, vPDT seems to be rather ineffective against leakage from BVN (Wakabayashi et al. 2008). The rare complications of massive subretinal hemorrhage, RPE tear, and choroidal ischemia also have hindered the use of vPDT in eyes with relatively good visual acuity or large lesions involving the fovea (Oishi et al. 2013).

Anti-VEGF Therapy for PCV

Initial reports in the use of anti-VEGF therapy for PCV showed that PCV might be more resistant to treatment as compared to typical CNV due to neovascular AMD (Cho et al. 2009; Hatz and Prunte 2014). Some patients only received their revised diagnosis of PCV after they have failed to respond to multiple anti-VEGF injections as typical neovascular AMD patients. Nonetheless, early studies showed that anti-VEGF therapy can improve VA and reduce subretinal fluid and hemorrhage (Gomi et al. 2008; Lai et al. 2008; Kokame et al. 2014; Oishi et al. 2014). The EVEREST study showed that anti-VEGF monotherapy with ranibizumab may even outperform vPDT monotherapy in terms of VA gain, albeit considerably less effective in causing polyp regression (Koh et al. 2012). Different treatment schedules with fixed or pro re nata (PRN) dosing regimens have been looked at, but no significant difference was detected (Inoue et al. 2016). From cross-study results, the efficacy of ranibizumab and bevacizumab as monotherapy appeared to be comparable (Cho et al. 2012). Aflibercept, on the other hand, may have

better polyp closure rates (Yamamoto et al. 2015), but these results are yet to be confirmed by formal prospective head-to-head studies.

Combination Therapy for PCV

There appears to be a slight disparity between the angiographic and functional response following treatment of PCV: vPDT appears to perform better anatomically by causing polyp closure; whereas anti-VEGF therapy brings about better VA improvement and reduce leakage but has a weaker effect on polyp closure. The EVEREST II study showed that the combination of ranibizumab and vPDT resulted in better VA gain, polyp regression rate, and lower number of injections compared with ranibizumab monotherapy (Koh et al. 2017). Deferring vPDT may expose fewer patients to the potential risks of vPDT but the FUJISAN study showed that patients who had deferred PDT in combination with ranibizumab may require more additional ranibizumab injections after the initial 3 months (Gomi et al. 2015). However, the PLANET study found that deferred rescue PDT therapy did not have any additional benefits compared to aflibercept monotherapy with a fixed dosing interval (Lee et al. 2018).

Thermal Focal Laser Photocoagulation

Thermal focal laser is generally no longer performed as a first-line therapy due to its high recurrence rate (Yuzawa et al. 2003). Its use is usually limited to treating extrafoveal lesions because of the potential in causing damage and scarring of the retina and RPE (Gemmy Cheung et al. 2013). However, the selective use of thermal laser may be applied in conjunction with PDT or anti-VEGF for recurrent PCV (Jeon et al. 2013).

Management Algorithm of PCV

There is yet a standard treatment algorithm set by any guidelines. Still, there are several principles in which most experts agree upon. First of all, both anti-VEGF monotherapy and combination with vPDT are reasonable first-line therapy according to current evidence. Any relative contraindications of vPDT, such as good baseline VA or uncertainty over the diagnosis of PCV, may make anti-VEGF therapy more preferable as the first-line therapy. Regardless of the initial treatment modality, close follow-up is paramount to monitoring the treatment response due to the high recurrence rate of PCV. Thermal focal laser photocoagulation may have a role in treating extrafoveal disease. Recurrent PCV may require anti-VEGF plus selective vPDT or laser therapy.

References

Balaratnasingam C, Lee WK, Koizumi H, et al. Polypoidal choroidal vasculopathy: a distinct disease or manifestation of many? Retina. 2016;36:1–8.

Byeon SH, Lee SC, Oh HS, et al. Incidence and clinical patterns of polypoidal choroidal vasculopathy in Korean patients. Jpn J Ophthalmol. 2008;52:57–62.

Chaikitmongkol V, Khunsongkiet P, Patikulsila D, et al. Color fundus photography, optical coherence tomography, and fluorescein angiography in diagnosing polypoidal choroidal vasculopathy. Am J Ophthalmol. 2018;192:77–83.

Chang YC, Wu WC. Polypoidal choroidal vasculopathy in Taiwanese patients. Ophthalmic Surg Lasers Imaging. 2009;40:576–81.

Chang YS, Kim JH, Kim JW, et al. Optical coherence tomography-based diagnosis of polypoidal choroidal vasculopathy in Korean Patients. Korean J Ophthalmol. 2016;30:198–205.

Cheng HC, Liu JH, Lee SM. Hyperhomocysteinemia in patients with polypoidal choroidal vasculopathy: a case control study. PLoS One. 2014;9:e110818.

Cheung CM, Li X, Cheng CY, et al. Prevalence, racial variations, and risk factors of age-related macular degeneration in Singaporean Chinese, Indians, and Malays. Ophthalmology. 2014;121:1598–603.

Cheung CM, Yang E, Lee WK, et al. The natural history of polypoidal choroidal vasculopathy: a multi-center series of untreated Asian patients. Graefes Arch Clin Exp Ophthalmol. 2015;253:2075–85.

Cheung CMG, Lai TYY, Ruamviboonsuk P, et al. Polypoidal choroidal vasculopathy: definition, pathogenesis, diagnosis, and management. Ophthalmology. 2018;125:708–24.

Cho M, Barbazetto IA, Freund KB. Refractory neovascular age-related macular degeneration secondary to polypoidal choroidal vasculopathy. Am J Ophthalmol. 2009;148:70–8.e1.

Cho HJ, Baek JS, Lee DW, et al. Short-term effectiveness of intravitreal bevacizumab vs. ranibizumab injections for patients with polypoidal choroidal vasculopathy. Korean J Ophthalmol. 2012;26:157–62.

Chung SE, Kang SW, Lee JH, et al. Choroidal thickness in polypoidal choroidal vasculopathy and exudative age-related macular degeneration. Ophthalmology. 2011;118:840–5.

Ciardella AP, Donsoff IM, Huang SJ, et al. Polypoidal choroidal vasculopathy. Surv Ophthalmol. 2004;49:25–37.

Coscas G, Yamashiro K, Coscas F, et al. Comparison of exudative age-related macular degeneration subtypes in Japanese and French Patients: multicenter diagnosis with multimodal imaging. Am J Ophthalmol. 2014;158:309–318e2.

Dansingani KK, Balaratnasingam C, Naysan J, et al. En face imaging of pachychoroid spectrum disorders with swept-source optical coherence tomography. Retina. 2016;36:499–516.

De Salvo G, Vaz-Pereira S, Keane PA, et al. Sensitivity and specificity of spectral-domain optical coherence tomography in detecting idiopathic polypoidal choroidal vasculopathy. Am J Ophthalmol. 2014;158:1228–38.e1.

Gallego-Pinazo R, Dolz-Marco R, Gomez-Ulla F, et al. Pachychoroid diseases of the macula. Med Hypothesis Discov Innov Ophthalmol. 2014;3:111–5.

Gemmy Cheung CM, Yeo I, Li X, et al. Argon laser with and without anti-vascular endothelial growth factor therapy for extrafoveal polypoidal choroidal vasculopathy. Am J Ophthalmol. 2013;155:295–304.

Gomi F, Sawa M, Sakaguchi H, et al. Efficacy of intravitreal bevacizumab for polypoidal choroidal vasculopathy. Br J Ophthalmol. 2008;92:70–3.

Gomi F, Oshima Y, Mori R, et al. Initial versus delayed photodynamic therapy in combination with ranibizumab for treament of polypoidal choroidal vasculopathy: the Fujisan Study. Retina. 2015;35:1569–76.

Hatz K, Prunte C. Polypoidal choroidal vasculopathy in Caucasian patients with presumed neovascular age-related macular degeneration and poor ranibizumab response. Br J Ophthalmol. 2014;98:188–94.

Honda S, Matsumiya W, Negi A. Polypoidal choroidal vasculopathy: clinical features and genetic predisposition. Ophthalmologica. 2014;231:59–74.

Iijima H, Imai M, Gohdo T, et al. Optical coherence tomography of idiopathic polypoidal choroidal vasculopathy. Am J Ophthalmol. 1999;127:301–5.

Iijima H, Iida T, Imai M, et al. Optical coherence tomography of orange-red subretinal lesions in eyes with idiopathic polypoidal choroidal vasculopathy. Am J Ophthalmol. 2000;129:21–6.

Inoue M, Balaratnasingam C, Freund KB. Optical coherence tomography angiography of polypoidal choroidal vasculopathy and polypoidal choroidal neovascularization. Retina. 2015;35:2265–74.

Inoue M, Yamane S, Taoka R, et al. Aflibercept for polypoidal choroidal vasculopathy: as needed versus fixed interval dosing. Retina. 2016;36:1527–34.

Jeon S, Lee WK, Kim KS. Adjusted retreatment of polypoidal choroidal vasculopathy after combination therapy: results at 3 years. Retina. 2013;33:1193–200.

Kikuchi M, Nakamura M, Ishikawa K, et al. Elevated C-reactive protein levels in patients with polypoidal choroidal vasculopathy and patients with neovascular age-related macular degeneration. Ophthalmology. 2007;114:1722–7.

Kim JH, Kang SW, Kim TH, et al. Structure of polypoidal choroidal vasculopathy studied by colocalization between tomographic and angiographic lesions. Am J Ophthalmol. 2013;156:974–80.

Koh A, Lee WK, Chen LJ, et al. EVEREST study: efficacy and safety of verteporfin photodynamic therapy in combination with ranibizumab or alone versus ranibizumab monotherapy in patients with symptomatic macular polypoidal choroidal vasculopathy. Retina. 2012;32:1453–64.

Koh A, Lai TYY, Takahashi K, et al. Efficacy and safety of ranibizumab with or without verteporfin photodynamic therapy for polypoidal choroidal vasculopathy: a randomized clinical trial. JAMA Ophthalmol. 2017;135:1206–13.

Kokame GT. Prospective evaluation of subretinal vessel location in polypoidal choroidal vasculopathy (PCV) and response of hemorrhagic and exudative PCV to high-dose antiangiogenic therapy (an American Ophthalmological Society thesis). Trans Am Ophthalmol Soc. 2014;112:74–93.

Kokame GT, Yeung L, Teramoto K, et al. Polypoidal choroidal vasculopathy exudation and hemorrhage: results of monthly ranibizumab therapy at one year. Ophthalmologica. 2014;231:94–102.

Lafaut BA, Leys AM, Snyers B, et al. Polypoidal choroidal vasculopathy in Caucasians. Graefes Arch Clin Exp Ophthalmol. 2000;238:752–9.

Lai TY, Chan WM, Liu DT, et al. Intravitreal bevacizumab (Avastin) with or without photodynamic therapy for the treatment of polypoidal choroidal vasculopathy. Br J Ophthalmol. 2008;92:661–6.

Lee MY, Lee WK, Baek J, et al. Photodynamic therapy versus combination therapy in polypoidal choroidal vasculopathy: changes of aqueous vascular endothelial growth factor. Am J Ophthalmol. 2013;156:343–8.

Lee WK, Iida T, Ogura Y, et al. Efficacy and safety of intravitreal aflibercept for polypoidal choroidal vasculopathy in the PLANET Study: a randomized clinical trial. JAMA Ophthalmol. 2018;136:786–93.

Li Y, You QS, Wei WB, et al. Polypoidal choroidal vasculopathy in adult chinese: the Beijing Eye Study. Ophthalmology. 2014;121:2290–1.

Liu Y, Wen F, Huang S, et al. Subtype lesions of neovascular age-related macular degeneration in Chinese patients. Graefes Arch Clin Exp Ophthalmol. 2007;245:1441–5.

Ma L, Li Z, Liu K, et al. Association of genetic variants with polypoidal choroidal vasculopathy: a systematic review and updated meta-analysis. Ophthalmology. 2015;122:1854–65.

Maruko I, Iida T, Saito M, et al. Clinical characteristics of exudative age-related macular degeneration in Japanese patients. Am J Ophthalmol. 2007;144:15–22.

Mori K, Horie-Inoue K, Gehlbach PL, et al. Phenotype and genotype characteristics of age-related macular degeneration in a Japanese population. Ophthalmology. 2010;117:928–38.

Oishi A, Kojima H, Mandai M, et al. Comparison of the effect of ranibizumab and verteporfin for polypoidal choroidal vasculopathy: 12-month LAPTOP study results. Am J Ophthalmol. 2013;156:644–51.

Oishi A, Miyamoto N, Mandai M, et al. LAPTOP study: a 24-month trial of verteporfin versus ranibizumab for polypoidal choroidal vasculopathy. Ophthalmology. 2014;121:1151–2.

Okubo A, Sameshima M, Uemura A, et al. Clinicopathological correlation of polypoidal choroidal vasculopathy revealed by ultrastructural study. Br J Ophthalmol. 2002;86:1093–8.

Oztas Z, Mentes J, Nalcaci S, et al. Characteristics of fundus autofluorescence in active polypoidal choroidal vasculopathy. Turk J Ophthalmol. 2016;46:165–8.

Sakurada Y, Yoneyama S, Imasawa M, et al. Systemic risk factors associated with polypoidal choroidal vasculopathy and neovascular age-related macular degeneration. Retina. 2013;33:841–5.

Sato T, Kishi S, Watanabe G, et al. Tomographic features of branching vascular networks in polypoidal choroidal vasculopathy. Retina. 2007;27:589–94.

Sho K, Takahashi K, Yamada H, et al. Polypoidal choroidal vasculopathy: incidence, demographic features, and clinical characteristics. Arch Ophthalmol. 2003;121:1392–6.

Spaide RF, Yannuzzi LA, Slakter JS, et al. Indocyanine green videoangiography of idiopathic polypoidal choroidal vasculopathy. Retina. 1995;15:100–10.

Suzuki M, Gomi F, Sawa M, et al. Changes in fundus autofluorescence in polypoidal choroidal vasculopathy during 3 years of follow-up. Graefes Arch Clin Exp Ophthalmol. 2013;251:2331–7.

Tan CS, Ngo WK, Lim LW, et al. A novel classification of the vascular patterns of polypoidal choroidal vasculopathy and its relation to clinical outcomes. Br J Ophthalmol. 2014;98:1528–33.

Tan CS, Ngo WK, Chen JP, et al. EVEREST study report 2: imaging and grading protocol, and baseline characteristics of a randomised controlled trial of polypoidal choroidal vasculopathy. Br J Ophthalmol. 2015;99:624–8.

Tanaka K, Nakayama T, Mori R, et al. Associations of complement factor H (CFH) and age-related maculopathy susceptibility 2 (ARMS2) genotypes with subtypes of polypoidal choroidal vasculopathy. Invest Ophthalmol Vis Sci. 2011;52:7441–4.

Tong JP, Chan WM, Liu DT, et al. Aqueous humor levels of vascular endothelial growth factor and pigment epithelium-derived factor in polypoidal choroidal vasculopathy and choroidal neovascularization. Am J Ophthalmol. 2006;141:456–62.

Tsujikawa A, Sasahara M, Otani A, et al. Pigment epithelial detachment in polypoidal choroidal vasculopathy. Am J Ophthalmol. 2007;143:102–11.

Uyama M, Wada M, Nagai Y, et al. Polypoidal choroidal vasculopathy: natural history. Am J Ophthalmol. 2002;133:639–48.

Wakabayashi T, Gomi F, Sawa M, et al. Marked vascular changes of polypoidal choroidal vasculopathy after photodynamic therapy. Br J Ophthalmol. 2008;92:936–40.

Wen F, Chen C, Wu D, et al. Polypoidal choroidal vasculopathy in elderly Chinese patients. Graefes Arch Clin Exp Ophthalmol. 2004;242:625–9.

Wong CW, Cheung CM, Mathur R, et al. Three-year results of polypoidal choroidal vasculopathy treated with photodynamic therapy: retrospective study and systematic review. Retina. 2015;35:1577–93.

Wong CW, Yanagi Y, Lee WK, et al. Age-related macular degeneration and polypoidal choroidal vasculopathy in Asians. Prog Retin Eye Res. 2016;53:107–39.

Yamagishi T, Koizumi H, Yamazaki T, et al. Fundus autofluorescence in polypoidal choroidal vasculopathy. Ophthalmology. 2012;119:1650–7.

Yamagishi T, Koizumi H, Yamazaki T, et al. Changes in fundus autofluorescence after treatments for polypoidal choroidal vasculopathy. Br J Ophthalmol. 2014;98:780–4.

Yamamoto A, Okada AA, Kano M, et al. One-Year results of intravitreal aflibercept for polypoidal choroidal vasculopathy. Ophthalmology. 2015;122:1866–72.

Yannuzzi LA, Sorenson J, Spaide RF, et al. Idiopathic polypoidal choroidal vasculopathy (IPCV). Retina. 1990;10:1–8.

Yannuzzi LA, Ciardella A, Spaide RF, et al. The expanding clinical spectrum of idiopathic polypoidal choroidal vasculopathy. Arch Ophthalmol. 1997;115:478–85.

Yuzawa M, Mori R, Haruyama M. A study of laser photocoagulation for polypoidal choroidal vasculopathy. Jpn J Ophthalmol. 2003;47:379–84.

Yuzawa M, Mori R, Kawamura A. The origins of polypoidal choroidal vasculopathy. Br J Ophthalmol. 2005;89:602–27.

Zeng R, Wen F, Zhang X, et al. Serum levels of matrix metalloproteinase 2 and matrix metalloproteinase 9 elevated in polypoidal choroidal vasculopathy but not in age-related macular degeneration. Mol Vis. 2013;19:729–36.

Zhao M, Bai Y, Xie W, et al. Interleukin-1beta level is increased in vitreous of patients with neovascular age-related macular degeneration (nAMD) and polypoidal choroidal vasculopathy (PCV). PLoS One. 2015;10:e0125150.

Zhao X, Xia S, Chen Y. Characteristic appearances of fundus autofluorescence in treatment-naive and active polypoidal choroidal vasculopathy: a retrospective study of 170 patients. Graefes Arch Clin Exp Ophthalmol. 2018;256:1101–10.

Central Serous Chorioretinopathy/ Pachychoroid Eye Diseases

4

Jae Hyung Lee and Won Ki Lee

Abbreviations

AMD	Age-related macular degeneration
CNV	Choroidal neovascularization
CSC	Central serous chorioretinopathy
FA	Fluorescein angiography
FAF	Fundus autofluorescence
ICGA	Indocyanine green angiography
OCT	Optical coherence tomography
PDT	Photodynamic therapy
PED	Pigment epithelial detachment
PPE	Pachychoroid pigment epitheliopathy
PPS	"Peripapillary pachychoroid syndrome"
RPE	Retinal pigment epithelial
VEGF	Vascular endothelial growth factor

Central Serous Chorioretinopathy

Introduction

Central serous chorioretinopathy (CSC) is a chorioretinal disorder characterized by serous detachment of the neurosensory retina, associated with serous retinal pigment epithelial (RPE) detachment, angiographic leakage at the level of the RPE, and choriodal hyperpermeability (Nicholson et al. 2013). It is usually idiopathic but might also be secondary to high levels of endogenous or exogenous corticosteroids. CSC typically affects young to middle-aged men, and the lesion is usually located at the posterior pole (Kitzmann et al. 2008). CSC can be classified according to its clinical course: acute or chronic (persisting for more than 3–6 months). Acute CSC usually resolves spontaneously within 2–3 months with good visual prognosis. However, some patients with chronic CSC may suffer from persistent or recurrent serous macular detachment with subsequent progressive visual loss (Gilbert et al. 1984).

Pathogenesis

The pathophysiology of CSC is poorly understood. It was initially suggested that CSC results from the dysfunction of RPE ion pumping, with a reverse in fluid movement in a chorioretinal direction (Spitznas 1986). Later, the pathogenesis of CSC was proposed to be choroidal vascular hyperpermeability, with and without associated active pigment epithelial leaks or pigment epithelial detachment (PED) (Guyer et al. 1994). It has been widely accepted that choroidal hyperpermeability causes serous detachments of the RPE, which can induce a rip or decompensation of the RPE. This subsequently causes RPE leakage, leading to diffusion of water, electrolytes, and proteins to neurosensory retinal space. The cause of the choroidal abnormality is still unknown, and changes of the autoregulation in the choroidal blood flow or localized lobular choroidal ischemia have been suggested as a possible cause (Tittl et al. 2005; Prunte and Flammer 1996).

The risk factors for CSC include the use of corticosteroid medication, psychological stress and type A personality, hypertension, gastroesophageal reflux disease, pregnancy, and the use of psychotropic medication (Yannuzzi 1987; Tittl et al. 1999; Liew et al. 2013). The use of corticosteroid medication is the most widely accepted risk factor, and the use of both systemic and local glucocorticoids has been implicated in CSC (Carvalho-Recchia et al. 2002). The proposed mechanisms to explain this association are induction of choroidal vasoconstriction by reducing nitric oxide production, direct increase in the permeability of the blood vessels, and RPE cell tight junction damage (Smith 1984; Liew et al. 2013). Corticosteroids can

J. H. Lee
Department of Ophthalmology, Seoul St. Mary's Hospital, College of Medicine, Catholic University of Korea, Seoul, South Korea

W. K. Lee (✉)
Department of Ophthalmology, Nune Eye Hospital, Seoul, South Korea

I. K. Kim (ed.), *Macular Disorders*, Retina Atlas, https://doi.org/10.1007/978-981-15-3001-2_4

also reverse the polarity of RPE cells, which causes them to pump ions into the subretinal space (Bastl 1987; Sandle and McGlone 1987).

Clinical Features

On fundus examination, acute CSC typically shows a well-demarcated oval-shaped area of neurosensory retinal detachment in the posterior pole (Fig. 4.1). Serous PED can also occur together or independently. In chronic recurrent cases, RPE changes and atrophy may develop and an atrophic RPE tract connecting the macula to the inferior detachment might be seen. Bullous neurosensory detachments can be noted in atypical CSC cases, which are usually located inferiorly as the subretinal fluid drains down from the macula by gravity (Yannuzzi et al. 1984; Gass and Little 1995) (Fig. 4.2).

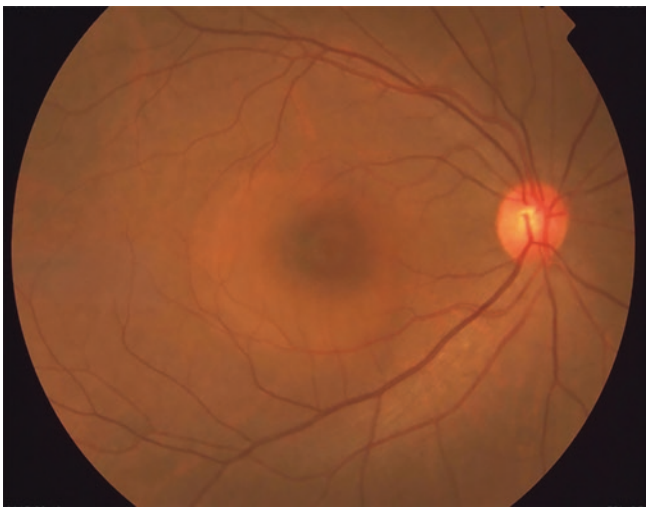

Fig. 4.1 Color fundus photograph shows round neurosensory retinal detachment at the posterior pole

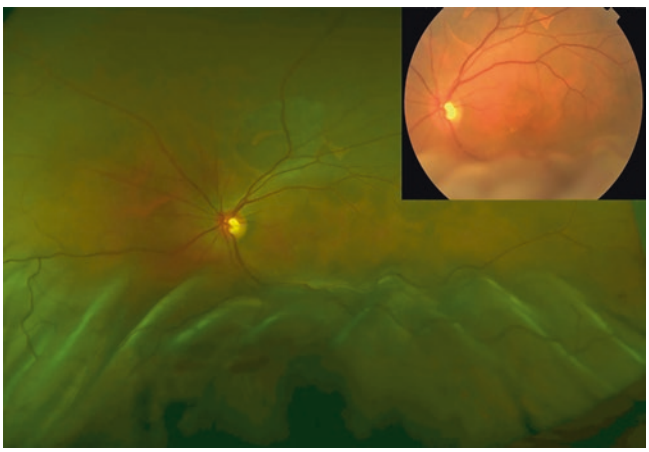

Fig. 4.2 Wide color fundus photograph shows serous pigment epithelial detachment at the posterior pole and bullous neurosensory detachment involving the inferior half of the retina

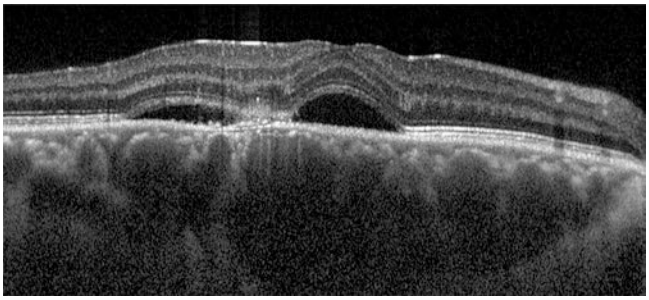

Fig. 4.3 Enhanced-depth imaging optical coherence tomography shows increased choroidal thickness (measured subfoveally at 650 μm), a retinal pigment epithelial elevation, and a hyper-reflective flow within the subretinal fluid. Beneath the retinal pigment epithelial elevation, the choroidal vessels are more dilated, and the choriocapillaris is thinner than in the adjacent area

Optical coherence tomography (OCT) is the primary modality for the diagnosis and follow-up of CSC. Recently, enhanced-depth imaging and swept-source technologies have allowed full-depth visualization of the choroid, improving the morphological analysis of choroidal vessels. Compared to healthy subjects, increased choroidal thickness has been reported in both affected and fellow eyes of CSC patients (Kuroda et al. 2013; Maruko et al. 2011). Increased choroidal thickness can result from focal or diffuse dilatation of large choroidal vessels, which are commonly co-localized within areas of choroidal vascular hyperpermeability on indocyanine green angiography (ICGA) (Jirarattanasopa et al. 2012; Yang et al. 2013). Attenuation of the inner choroidal layer or RPE elevations are also frequently observed above dilated choroidal vessels (Fig. 4.3). Elongation of photoreceptor outer segments in the area of serous retinal detachment, which is attributable to the lack of phagocytosis by the RPE, is a frequent OCT finding in CSC (Matsumoto et al. 2008).

Fluorescein angiography (FA) in acute CSC typically shows one of the two different types of leakage patterns: ink blot or smoke stack (Fig. 4.4). Smoke stack appearance is less common and only appears in about 10–15% of patients with acute CSC (Bujarborua et al. 2010). PED manifests on FA as the pooling of dye in the sub-RPE space. Chronic CSC may show an RPE window defect due to RPE atrophy. In atypical CSC cases, multiple sites of leakage can be noted (Fig. 4.5).

In CSC, ICGA provides an insight into choroidal changes contributing to the disease process and essential data to distinguish complex chronic cases with accompanying choroidal neovascularization (CNV). ICGA typically exhibits abnormally dilated choroidal vasculature in the early phase and choroidal hyperpermeability in the mid- to late phase (Spaide et al. 1996) (Fig. 4.6). Delayed initial filling of arteries and choriocapillaris in the early phase and hypofluorescent areas persisting in mid- and late phases can also be seen, which

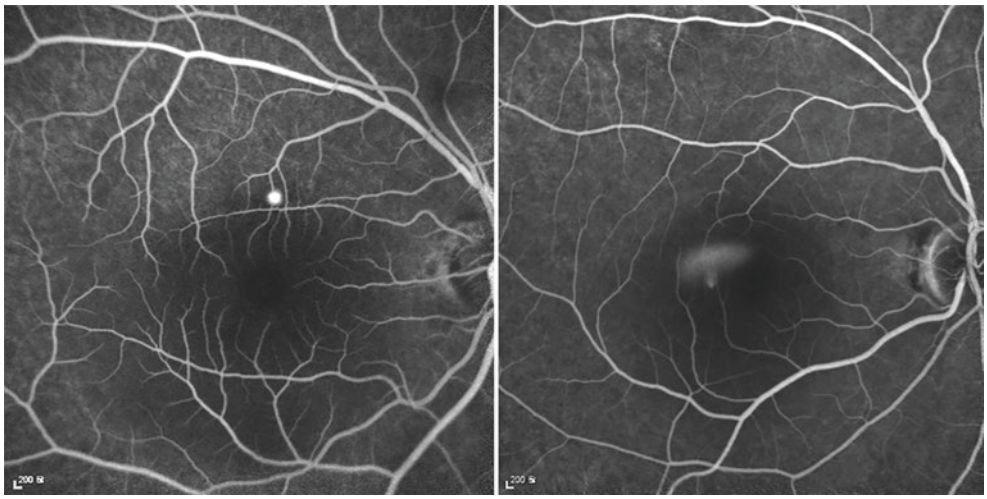

Fig. 4.4 Fundus fluorescein angiography of acute central serous chorioretinopathy shows leakage with an ink blot appearance (left) and a smoke stack appearance (right)

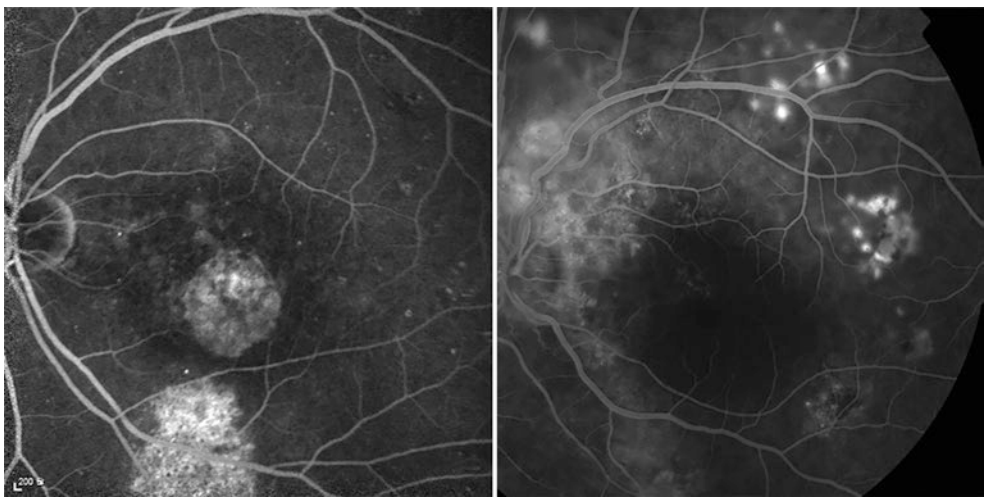

Fig. 4.5 Fundus fluorescein angiography of chronic central serous chorioretinopathy shows a window defect due to retinal pigment epithelial atrophy (left) and multiple pin-point leakages (right)

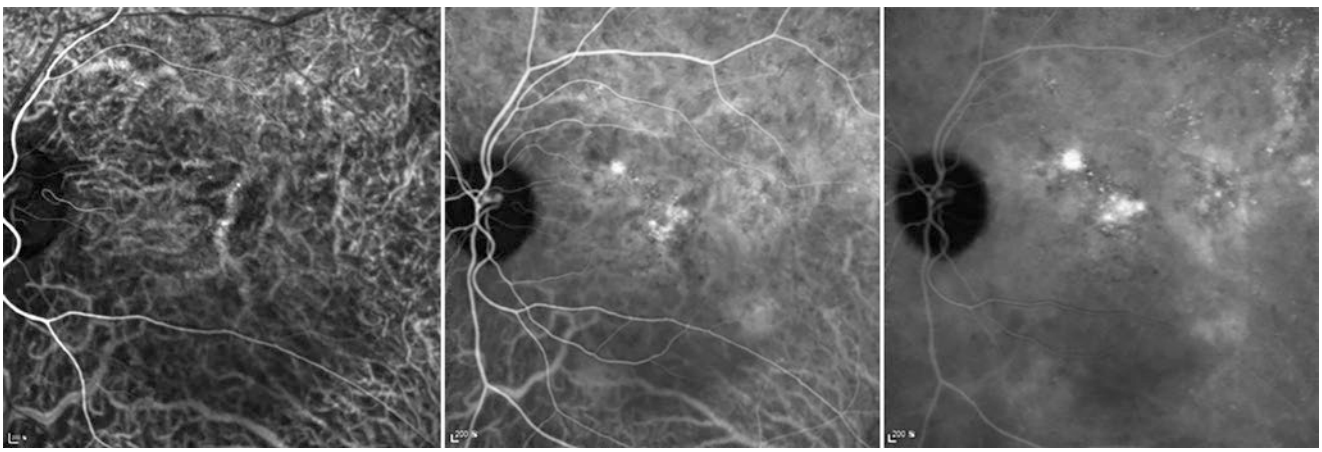

Fig. 4.6 Indocyanine green angiography shows delayed initial filling of arteries and choriocapillaris in the early phase (left), and areas of hyperfluorescence in the mid-phase (middle) which persist through the lase phase (right)

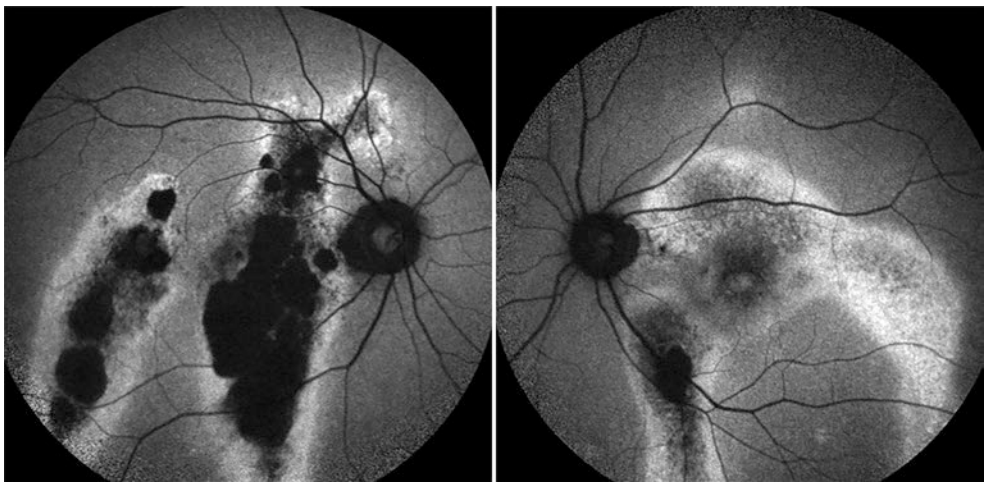

Fig. 4.7 Fundus autofluorescence imaging of chronic central serous chorioretinopathy shows hypo-autofluorescent gravitational tracks in both eyes, and areas of hyperfluorescence in the left eye

may be one of the mechanisms that lead to choroidal venous dilation and congestion (Prunte and Flammer 1996; Kitaya et al. 2003). In more than half of the asymptomatic fellow eyes, choroidal changes similar to those of affected eyes were observed on ICGA (Iida et al. 1999).

During the acute phase of the disease, fundus autofluorescence (FAF) typically shows hypofluorescence over the area of neurosensory detachment due to blockage by subretinal fluid. It may either return to normal, or be progressively replaced by hyperfluorescence (Framme et al. 2005). The accumulation of non-shed fluorophore in elongated outer segments or the loss of photoreceptor outer segments may explain the subsequent increase in FAF (Iacono et al. 2015; Matsumoto et al. 2011). In chronic CSC, multiple oblong descending tracks of decreased FAF surrounded by a thin contour of increased FAF can be noted, often originating from the optic disc and the macula (Fig. 4.7).

Management

There is no consensus about the most suitable treatment and the optimal timing for intervention in CSC. Regarding the favorable natural course of the disease, observation can be the appropriate first-line approach in acute CSC. However, intervention can be considered in the following indications: persistent submacular fluid for over 4–6 months, history of multiple recurrences, diffuse RPE atrophy, reduced visual acuity, and cases requiring rapid recovery (Nicholson et al. 2013).

Medical Therapy: Mineralocorticoid Receptor Antagonists

The association between CSC and elevated systemic cortisol level has been well documented, and steroid antagonists have been investigated as treatments for CSC. The mineralocorticoid antagonists, spironolactone and eplerenone, have been introduced as a systemic treatment option for CSC by reducing steroid levels. Although short-term anatomical and visual benefits were demonstrated in several retrospective and a few prospective studies (Daruich et al. 2016; Bousquet et al. 2015), most were limited by their retrospective and non-randomized designs, small sample sizes, and relatively short follow-up periods. Ongoing and future studies are needed to elucidate the role of mineralocorticoid antagonists in the treatment of CSC.

Medical Therapy: Anti-vascular Endothelial Growth Factor Agents

Although CSC is not associated with increased vascular endothelial growth factor (VEGF) ocular levels (Shin and Lim 2011), anti-VEGF therapy has been used based on the expectation of reducing the choroidal hyperpermeability (Chung et al. 2013). A few case series reported beneficial effects of anti-VEGF treatment in chronic or recurrent cases (Artunay et al. 2010; Pitcher et al. 2015). However, based on the meta-analysis of comparative studies including acute and chronic CSC, no significant difference was observed between anti-VEGF treatment and observation in visual and anatomical outcomes (Ji et al. 2017; Chung et al. 2013).

Conventional Laser Photocoagulation

Traditionally, the use of thermal laser photocoagulation has been attempted to seal the RPE leakage points, although it is not expected to act on choroidal congestion and hyperpermeability. Several studies have compared laser photocoagulation to observation and reported that it may not affect the final functional outcomes or the rate of recurrence (Burumcek et al. 1997). Also, significant adverse effects such as permanent scotoma, enlargement of RPE scarring, and secondary laser-induced CNV formation have been reported (Robertson and Ilstrup 1983). However, laser photocoagulation may still have a role in the management of CSC with a discrete, solitary extrafoveal leaking point.

Subthreshold Laser Therapy

In subthreshold laser therapy, RPE cells are selectively destroyed by exploding melanosomes with microsecond or nanosecond pulses, while photoreceptors and Bruch membrane are spared (Roider et al. 1993). The RPE cells in the surrounding areas then stretch, migrate, and proliferate to refill the damage zone. It is assumed that this process improves the cellular tight junctions and pumping functions of RPE cells (Flaxel et al. 2007; Paulus et al. 2011). This may theoretically reduce the risk of structural and functional retinal damage while retaining the therapeutic efficacy of conventional laser treatment. Several retrospective, prospective case series and small randomized clinical trials have demonstrated the safety and short-term efficacy of subthreshold laser therapy in patients with chronic and possibly acute CSC (Scholz et al. 2015; Kretz et al. 2015). Because of wide variations in study designs and laser protocols, further prospective, randomized, and controlled studies should be performed to fully substantiate the observed treatment efficacy and safety of subthreshold laser therapy.

Photodynamic Therapy

Photodynamic therapy (PDT) is proposed to work through vascular remodeling of the choroid which leads to decreased choroidal volume, permeability, and leakage of fluid. At the beginning, several studies reported that ICGA-guided PDT with standard parameters and standard dose of verteporfin led to anatomic and functional improvement in CSC (Yannuzzi et al. 2003; Battaglia Parodi et al. 2003). However, complications appeared in some cases subsequently, including RPE atrophy, choriocapillaris ischemia, and secondary CNV (Chan et al. 2003). In an attempt to enhance the efficacy of PDT in treating CSC while minimizing its side effects, distinct strategies modifying the route of administration, timing of laser exposure, and reduction in fluence and verteporfin dose have been tried. Both half-dose verteporfin (3.0 mg/m^2) and half-fluence (25 J/cm^2) PDT achieved resolution of subretinal fluid and visual improvement. Also, these safety-enhanced PDT protocols could significantly decrease the hypoxic damage to physiologic choroid caused by conventional PDT (Reibaldi et al. 2010; Shin et al. 2011). In several meta-analyses, PDT was superior with respect to absorption of subretinal fluid compared to laser photocoagulation and intravitreal injection of anti-VEGF drugs (Ma et al. 2014; Lu et al. 2016). Also, a randomized, controlled trial demonstrated the superiority of half-fluence PDT compared with intravitreal ranibizumab in the treatment of chronic CSC (Bae et al. 2014). Therefore, based on the evidence to date, PDT stands out as the most promising therapy among all treatment options in treating both acute and chronic CSC patients.

Pachychoroid Eye Diseases

The term pachychoroid was initially introduced into the literature in 2013 to describe retinal pigment epitheliopathy in patients with choroidal findings resembling those of central serous chorioretinopathy (Warrow et al. 2013). It was originally conceived to reflect choroidal congestion and choroidal hyperpermeability manifested by choroidal thickening on OCT. However, there is no consensus on the definition of thick choroid. Subfoveal choroidal thickness can be influenced by physiologic and ocular factors including age, sex, and axial length, and the normative value has not been determined (Barteselli et al. 2012). Also, it is possible for an eye with normal choroidal thickness to be defined as pachychoroid when the increased luminal volume secondary to choroidal vessel dilation is offset by the reduction in tissue volume from the stroma. Indeed, further investigations have broadened its original description to emphasize additional qualitative features. These features include diffuse or focal choroidal thickening that is localized within the disease focus and attributable to pathologically dilated Haller's veins (termed "pachyvessels") (Lee et al. 2016a, b; Balaratnasingam et al. 2016). Choriocapillaris and Sattler layers overlying pachyvessels become attenuated focally, and close approximation of pachyvessels and the Bruch-RPE complex may lead to pathologic pachychoroid-driven process. Currently, the concept of pachychoroid includes not only the anatomical increase of choroidal thickness, but has evolved into structural and functional changes of the choroid.

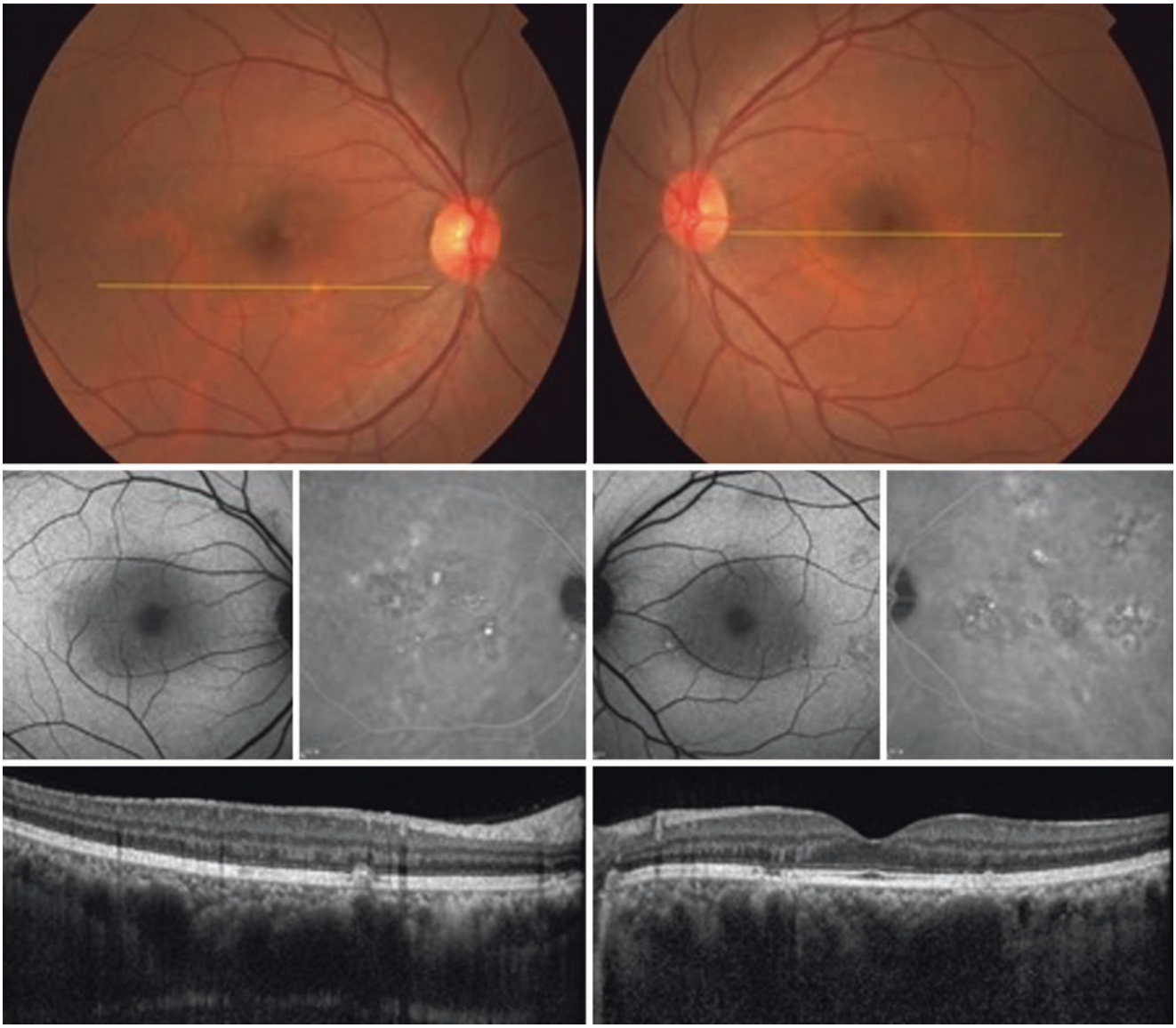

Fig. 4.8 Multimodal imaging of pachychoroid pigment epitheliopathy. Color fundus photographs of both eyes show pigmentary changes without drusen. Fundus autofluorescence imaging reveal hyper- and hypoautofluorescent changes in the posterior poles, and indocyanine green angiography in the mid- to late phase shows choroidal hyperpermeability. Enhanced depth imaging optical coherence tomography reveals retinal pigment epithelial elevation inferonasal to the fovea in the right eye. Disruption of ellipsoid zone and shallow pigment epithelial detachment temporal are seen in the left eye. Note the thickened choroid with dilated choroidal vessels under the RPE changes

Pachychoroid Pigment Epitheliopathy

Pachychoroid pigment epitheliopathy (PPE) is a novel clinical entity first described in 2013 that is characterized by a range of RPE abnormalities and pigmentary changes overlying the areas of choroidal thickening (Warrow et al. 2013). These patients exhibit reduced fundus tessellation at the posterior pole on ophthalmoscopy, choroidal hyperpermeability on ICGA, and relatively thick subfoveal choroid and Haller's layer vessel dilation on enhanced depth imaging OCT, particularly at the sites of RPE abnormalities (Fig. 4.8). FAF abnormalities are also noted at the sites corresponding to RPE disturbances. Although these features are similar to that of CSC, these patients had no findings or history indicative of subretinal fluid. Therefore, PPE was described as a possible precursor, or forme fruste, of CSC. Since none of the patients developed clinically evident subretinal fluid, choroidal vascular hyperpermeability and/or choroidal thickening alone may be the cause of pigment epitheliopathy.

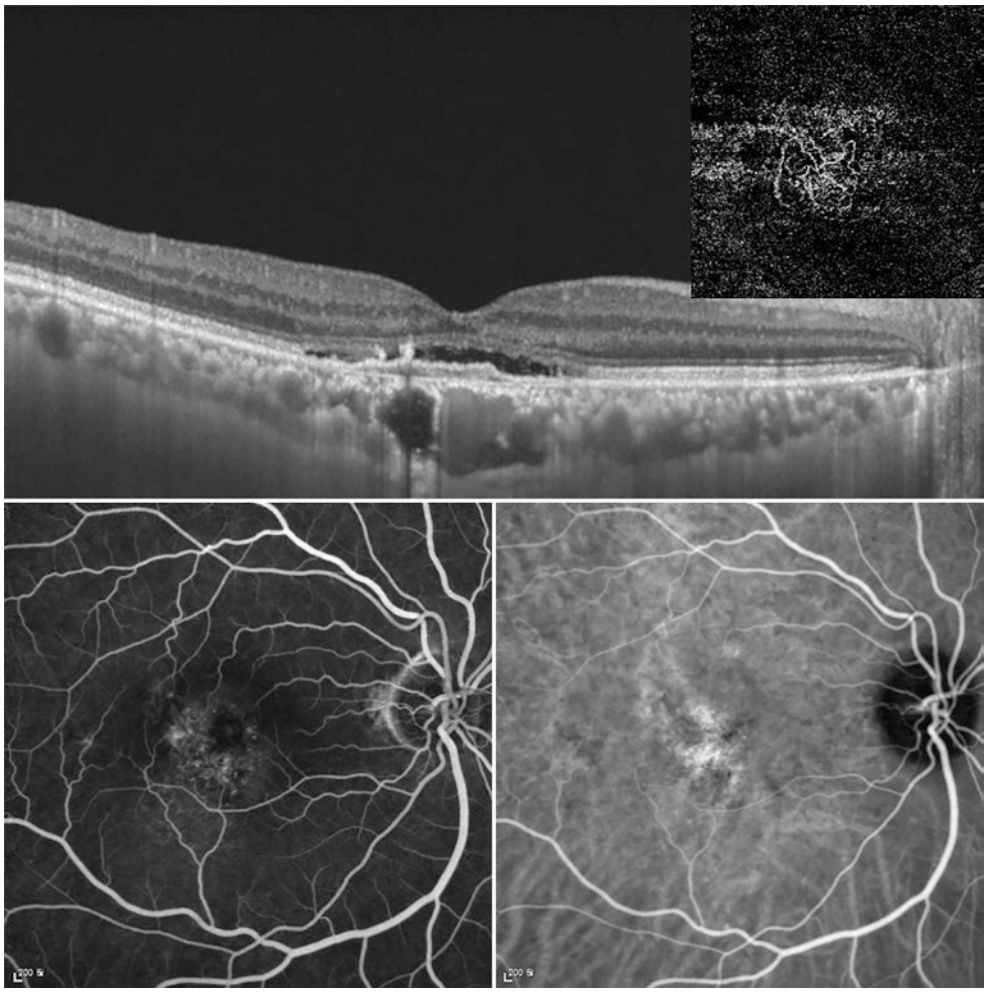

Fig. 4.9 Multimodal imaging of pachychoroid neovasculopathy. Swept-source optical coherence tomography and optical coherence tomography angiography show type 1 neovascularization above the dilated Haller's vessels. Fluorescein angiography shows occult choroidal neovascularization with diffuse leakage, and indocyanine green angiography in the early to mid-phase reveals hyperfluorescent plaque without polypoidal lesions

Pachychoroid Neovasculopathy

The term "pachychoroid neovasculopathy" has been introduced to describe type 1 neovascularization associated with choroidal thickening and/or dilated Haller's vessels in the absence of characteristic age-related macular degeneration features such as drusen (Pang and Freund 2015) (Fig. 4.9). The proposed mechanism for the development of pachychoroid neovasculopathy is the mechanical stress and/or ischemic insult induced by dilated Haller vessels to the overlying RPE-Bruch membrane-choriocapillaris complex, leading to the expression of angiogenic factors. It can develop after long-standing CSC, but it can also develop without antecedent neurosensory detachment attributable to CSC (Fung et al. 2012). It was hypothesized that pachychoroid neovasculopathy is associated with PCV and that pachychoroid neovasculopathy can ultimately progress to the development of polypoidal lesions. Eventually, a pachychoroid-related spectrum of diseases including PPE-CSC-pachychoroid neovasculopathy-PCV has been proposed. The frequency of pachychoroid neovasculopathy among neovascular age-related macular degeneration (AMD) is not reported yet, but it is considered to comprise a significant portion of lesions which were classified as exudative AMD in Asians previously (Wong et al. 2016). OCT angiography can be useful in detecting the CNV complex within irregular PEDs in chronic CSC, particularly where FA, ICGA, and OCT reveal inconclusive results (Hage et al. 2015). The treatment response to anti-VEGF injection is not fully understood in pachychoroid neovasculopathy. Since aflibercept showed greater effects on the choroid and was superior to ranibizumab in achieving remission of exudation in eyes with choroidal hyperpermeability (Hata et al. 2014; Koizumi et al. 2015), it may also have advantages in treating pachychoroid neovasculopathy. In cases refractory to anti-VEGF injection, adjunctive PDT was reported to be effective in the resolution of the exudation and stabilization/improvement of vision (Lee and Lee 2016).

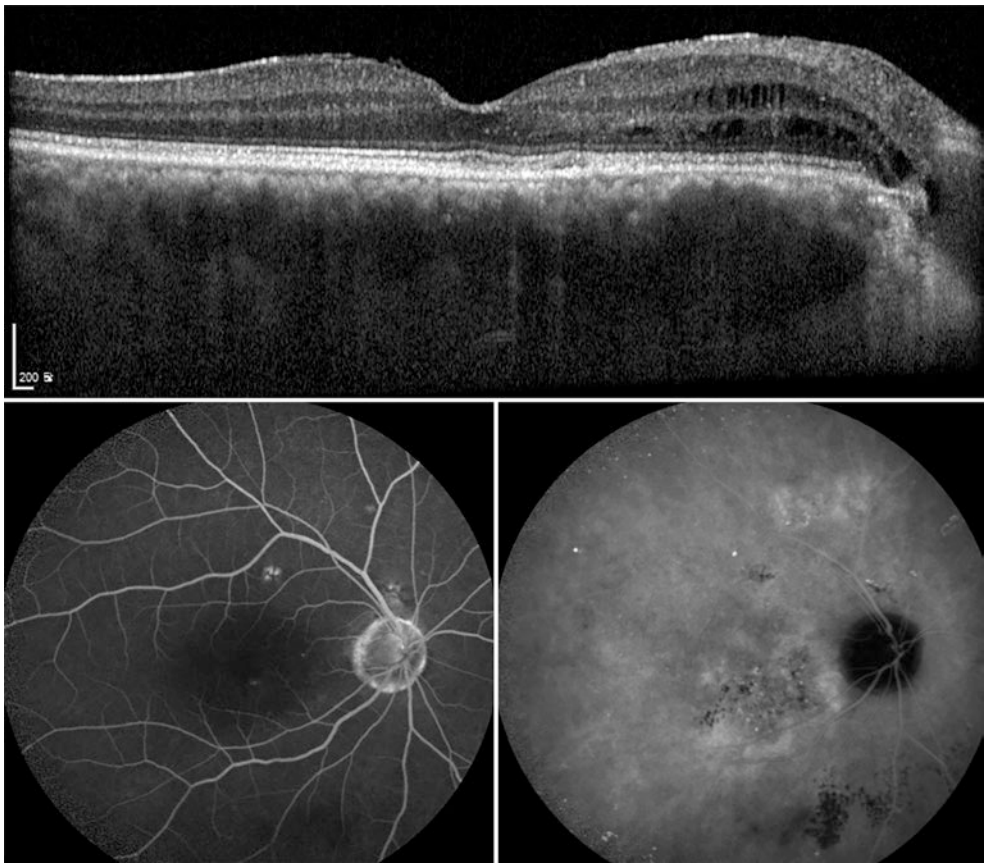

Fig. 4.10 Multimodal imaging of peripapillary pachychoroid syndrome. Enhanced-depth imaging optical coherence tomography shows intraretinal fluid in the nasal macula extending from the temporal optic disc margin in which atrophy of the retinal pigment epithelium, ellipsoid zone, and external limiting membrane is noted. Fluorescein angiography demonstrates the peripapillary hyperfluorescent ring without significant leakage. Indocyanine green angiography exhibits choroidal hyperpermeability at the papillomacular area

Peripapillary Pachychoroid Syndrome

The term "peripapillary pachychoroid syndrome" (PPS) has been suggested to describe eyes that exhibit peripapillary choroidal thickening and intraretinal and/or subretinal fluid in the nasal macular region extending from the temporal margin of the optic disc (Phasukkijwatana et al. 2018). The nasal macular choroid tends to be thicker than the temporal macular choroid, and dilated large choroidal vessels are more prominent in the nasal areas versus the temporal areas (Fig. 4.10). Intraretinal and/or subretinal fluid can also be seen on the nasal side of the nerve. FA usually illustrates minimal or no leakage, and mild late fluorescein disc leakage can be identified in some cases. Dilated Haller's vessels on OCT and choroidal hyperpermeability are frequently noted, and eyes with PPS can exhibit overlapping findings with CSC, such as serous PED and gravitational tracks. The reason why the choroid is congested preferentially in the peripapillary region and the mechanism of intraretinal fluid extension from the disc margin are unclear. Acquired lamina cribrosa defects or disinsertion have been noted in a certain portion of PPS eyes and have been suggested as a potential source of fluid entrance (Lee et al. 2016a, b). Alternatively, atrophy of RPE and external limiting membrane in the peripapillary region may allow fluid from congested choroid to enter the retina (Pautler and Browning 2015).

References

Artunay O, Yuzbasioglu E, Rasier R, et al. Intravitreal bevacizumab in treatment of idiopathic persistent central serous chorioretinopathy: a prospective, controlled clinical study. Curr Eye Res. 2010;35:91–8.

Bae SH, Heo J, Kim C, et al. Low-fluence photodynamic therapy versus ranibizumab for chronic central serous chorioretinopathy: one-year results of a randomized trial. Ophthalmology. 2014;121:558–65.

Balaratnasingam C, Lee WK, Koizumi H, et al. Polypoidal choroidal vasculopathy: a distinct disease or manifestation of many? Retina. 2016;36:1–8.

Barteselli G, Chhablani J, El-Emam S, et al. Choroidal volume variations with age, axial length, and sex in healthy subjects: a three-dimensional analysis. Ophthalmology. 2012;119:2572–8.

Bastl CP. Regulation of cation transport by low doses of glucocorticoids in in vivo adrenalectomized rat colon. J Clin Invest. 1987;80:348–56.

Battaglia Parodi M, Da Pozzo S, Ravalico G. Photodynamic therapy in chronic central serous chorioretinopathy. Retina. 2003;23:235–7.

Bousquet E, Beydoun T, Rothschild PR, et al. Spironolactone for non-resolving central serous chorioretinopathy: a randomized controlled crossover study. Retina. 2015;35:2505–15.

Bujarborua D, Nagpal PN, Deka M. Smokestack leak in central serous chorioretinopathy. Graefes Arch Clin Exp Ophthalmol. 2010;248:339–51.

Burumcek E, Mudun A, Karacorlu S, Arslan MO. Laser photocoagulation for persistent central serous retinopathy: results of long-term follow-up. Ophthalmology. 1997;104:616–22.

Carvalho-Recchia CA, Yannuzzi LA, Negrao S, et al. Corticosteroids and central serous chorioretinopathy. Ophthalmology. 2002;109:1834–7.

Chan WM, Lam DS, Lai TY, et al. Choroidal vascular remodelling in central serous chorioretinopathy after indocyanine green guided

photodynamic therapy with verteporfin: a novel treatment at the primary disease level. Br J Ophthalmol. 2003;87:1453–8.
Chung YR, Seo EJ, Lew HM, Lee KH. Lack of positive effect of intravitreal bevacizumab in central serous chorioretinopathy: meta-analysis and review. Eye (Lond). 2013;27:1339–46.
Daruich A, Matet A, Dirani A, et al. Oral mineralocorticoid-receptor antagonists: real-life experience in clinical subtypes of nonresolving central serous chorioretinopathy with chronic epitheliopathy. Transl Vis Sci Technol. 2016;5:2.
Flaxel C, Bradle J, Acott T, Samples JR. Retinal pigment epithelium produces matrix metalloproteinases after laser treatment. Retina. 2007;27:629–34.
Framme C, Walter A, Gabler B, et al. Fundus autofluorescence in acute and chronic-recurrent central serous chorioretinopathy. Acta Ophthalmol Scand. 2005;83:161–7.
Fung AT, Yannuzzi LA, Freund KB. Type 1 (sub-retinal pigment epithelial) neovascularization in central serous chorioretinopathy masquerading as neovascular age-related macular degeneration. Retina. 2012;32:1829–37.
Gass JD, Little H. Bilateral bullous exudative retinal detachment complicating idiopathic central serous chorioretinopathy during systemic corticosteroid therapy. Ophthalmology. 1995;102:737–47.
Gilbert CM, Owens SL, Smith PD, Fine SL. Long-term follow-up of central serous chorioretinopathy. Br J Ophthalmol. 1984;68:815–20.
Guyer DR, Yannuzzi LA, Slakter JS, et al. Digital indocyanine green videoangiography of central serous chorioretinopathy. Arch Ophthalmol. 1994;112:1057–62.
Hage R, Mrejen S, Krivosic V, et al. Flat irregular retinal pigment epithelium detachments in chronic central serous chorioretinopathy and choroidal neovascularization. Am J Ophthalmol. 2015;159:890–903.
Hata M, Oishi A, Tsujikawa A, et al. Efficacy of intravitreal injection of aflibercept in neovascular age-related macular degeneration with or without choroidal vascular hyperpermeability. Invest Ophthalmol Vis Sci. 2014;55:7874–80.
Iacono P, Battaglia PM, Papayannis A, et al. Acute central serous chorioretinopathy: a correlation study between fundus autofluorescence and spectral-domain OCT. Graefes Arch Clin Exp Ophthalmol. 2015;253:1889–97.
Iida T, Kishi S, Hagimura N, Shimizu K. Persistent and bilateral choroidal vascular abnormalities in central serous chorioretinopathy. Retina. 1999;19:508–12.
Ji S, Wei Y, Chen J, Tang S. Clinical efficacy of anti-VEGF medications for central serous chorioretinopathy: a meta-analysis. Int J Clin Pharm. 2017;39:514–21.
Jirarattanasopa P, Ooto S, Tsujikawa A, et al. Assessment of macular choroidal thickness by optical coherence tomography and angiographic changes in central serous chorioretinopathy. Ophthalmology. 2012;119:1666–78.
Kitaya N, Nagaoka T, Hikichi T, et al. Features of abnormal choroidal circulation in central serous chorioretinopathy. Br J Ophthalmol. 2003;87:709–12.
Kitzmann AS, Pulido JS, Diehl NN, et al. The incidence of central serous chorioretinopathy in Olmsted County, Minnesota, 1980-2002. Ophthalmology. 2008;115:169–73.
Koizumi H, Kano M, Yamamoto A, et al. Short-term changes in choroidal thickness after aflibercept therapy for neovascular age-related macular degeneration. Am J Ophthalmol. 2015;159:627–33.
Kretz FT, Beger I, Koch F, et al. Randomized clinical trial to compare micropulse photocoagulation versus half-dose verteporfin photodynamic therapy in the treatment of central serous chorioretinopathy. Ophthalmic Surg Lasers Imaging Retina. 2015;46:837–43.
Kuroda S, Ikuno Y, Yasuno Y, et al. Choroidal thickness in central serous chorioretinopathy. Retina. 2013;33:302–8.
Lee JH, Lee WK. One-year results of adjunctive photodynamic therapy for type 1 neovascularization associated with thickened choroid. Retina. 2016;36:889–95.
Lee WK, Baek J, Dansingani KK, et al. Choroidal morphology in eyes with polypoidal choroidal vasculopathy and normal or subnormal subfoveal choroidal thickness. Retina. 2016a;36(Suppl 1): S73–s82.
Lee JH, Park HY, Baek J, Lee WK. Alterations of the lamina cribrosa are associated with peripapillary retinoschisis in glaucoma and pachychoroid spectrum disease. Ophthalmology. 2016b;123: 2066–76.
Liew G, Quin G, Gillies M, Fraser-Bell S. Central serous chorioretinopathy: a review of epidemiology and pathophysiology. Clin Exp Ophthalmol. 2013;41:201–14.
Lu HQ, Wang EQ, Zhang T, Chen YX. Photodynamic therapy and anti-vascular endothelial growth factor for acute central serous chorioretinopathy: a systematic review and meta-analysis. Eye (Lond). 2016;30:15–22.
Ma J, Meng N, Xu X, et al. System review and meta-analysis on photodynamic therapy in central serous chorioretinopathy. Acta Ophthalmol. 2014;92:e594–601.
Maruko I, Iida T, Sugano Y, et al. Subfoveal choroidal thickness in fellow eyes of patients with central serous chorioretinopathy. Retina. 2011;31:1603–8.
Matsumoto H, Kishi S, Otani T, Sato T. Elongation of photoreceptor outer segment in central serous chorioretinopathy. Am J Ophthalmol. 2008;145:162–8.
Matsumoto H, Kishi S, Sato T, Mukai R. Fundus autofluorescence of elongated photoreceptor outer segments in central serous chorioretinopathy. Am J Ophthalmol. 2011;151:617–23.
Nicholson B, Noble J, Forooghian F, Meyerle C. Central serous chorioretinopathy: update on pathophysiology and treatment. Surv Ophthalmol. 2013;58:103–26.
Pang CE, Freund KB. Pachychoroid neovasculopathy. Retina. 2015;35:1–9.
Paulus YM, Jain A, Nomoto H, et al. Selective retinal therapy with microsecond exposures using a continuous line scanning laser. Retina. 2011;31:380–8.
Pautler SE, Browning DJ. Isolated posterior uveal effusion: expanding the spectrum of the uveal effusion syndrome. Clin Ophthalmol. 2015;9:3–49.
Phasukkijwatana N, Freund KB, Dolz-Marco R, et al. Peripapillary pachychoroid syndrome. Retina. 2018;38:1652–67.
Pitcher JD 3rd, Witkin AJ, DeCroos FC, Ho AC. A prospective pilot study of intravitreal aflibercept for the treatment of chronic central serous chorioretinopathy: the CONTAIN study. Br J Ophthalmol. 2015;99:848–52.
Prunte C, Flammer J. Choroidal capillary and venous congestion in central serous chorioretinopathy. Am J Ophthalmol. 1996;121:26–34.
Reibaldi M, Cardascia N, Longo A, et al. Standard-fluence versus low-fluence photodynamic therapy in chronic central serous chorioretinopathy: a nonrandomized clinical trial. Am J Ophthalmol. 2010;149:307–15.
Robertson DM, Ilstrup D. Direct, indirect, and sham laser photocoagulation in the management of central serous chorioretinopathy. Am J Ophthalmol. 1983;95:457–66.
Roider J, Hillenkamp F, Flotte T, Birngruber R. Microphotocoagulation: selective effects of repetitive short laser pulses. Proc Natl Acad Sci U S A. 1993;90:8643–7.
Sandle GI, McGlone F. Acute effects of dexamethasone on cation transport in colonic epithelium. Gut. 1987;28:701–6.
Scholz P, Ersoy L, Boon CJ, Fauser S. Subthreshold micropulse laser (577 nm) treatment in chronic central serous chorioretinopathy. Ophthalmologica. 2015;234:189–94.
Shin MC, Lim JW. Concentration of cytokines in the aqueous humor of patients with central serous chorioretinopathy. Retina. 2011;31:1937–43.
Shin JY, Woo SJ, Yu HG, Park KH. Comparison of efficacy and safety between half-fluence and full-fluence photodynamic therapy for chronic central serous chorioretinopathy. Retina. 2011;31:119–26.

Smith TJ. Dexamethasone regulation of glycosaminoglycan synthesis in cultured human skin fibroblasts. Similar effects of glucocorticoid and thyroid hormones. J Clin Invest. 1984;74:2157–63.

Spaide RF, Hall L, Haas A, et al. Indocyanine green videoangiography of older patients with central serous chorioretinopathy. Retina. 1996;16:203–13.

Spitznas M. Pathogenesis of central serous retinopathy: a new working hypothesis. Graefes Arch Clin Exp Ophthalmol. 1986;224:321–4.

Tittl MK, Spaide RF, Wong D, et al. Systemic findings associated with central serous chorioretinopathy. Am J Ophthalmol. 1999;128:63–8.

Tittl M, Maar N, Polska E, et al. Choroidal hemodynamic changes during isometric exercise in patients with inactive central serous chorioretinopathy. Invest Ophthalmol Vis Sci. 2005;46:4717–21.

Warrow DJ, Hoang QV, Freund KB. Pachychoroid pigment epitheliopathy. Retina. 2013;33:1659–72.

Wong CW, Yanagi Y, Lee WK, et al. Age-related macular degeneration and polypoidal choroidal vasculopathy in Asians. Prog Retin Eye Res. 2016;53:107–39.

Yang L, Jonas JB, Wei W. Optical coherence tomography-assisted enhanced depth imaging of central serous chorioretinopathy. Invest Ophthalmol Vis Sci. 2013;54:4659–65.

Yannuzzi LA. Type-A behavior and central serous chorioretinopathy. Retina. 1987;7:11–131.

Yannuzzi LA, Shakin JL, Fisher YL, Altomonte MA. Peripheral retinal detachments and retinal pigment epithelial atrophic tracts secondary to central serous pigment epitheliopathy. Ophthalmology. 1984;91:1554–72.

Yannuzzi LA, Slakter JS, Gross NE, et al. Indocyanine green angiography-guided photodynamic therapy for treatment of chronic central serous chorioretinopathy: a pilot study. Retina. 2003;23:288–98.

Myopic Maculopathy Due to Pathologic Myopia

5

Kyoko Ohno-Matsui

Abbreviations

BCVA	Best-corrected visual acuity
BM	Bruch's membrane
CNV	Choroidal neovascularization
HM	High myopia
META-PM	Meta-analyses of pathologic myopia
MTM	Myopic traction maculopathy
OCT	Optical coherence tomography
PDCA	Peripapillary diffuse choroidal atrophy
PM	Pathologic myopia

Introduction

Complications from pathologic myopia (PM) are a major cause of the loss of the best-corrected visual acuity (BCVA), especially in East Asia (Asakuma et al. 2012; Xu et al. 2006; Liang et al. 2008; Chang et al. 2013; Morgan et al. 2012; Wong and Saw 2016). The loss of BCVA in addition to decrease in uncorrected visual acuity is a major feature of PM due to its specific complications. Complications of PM develop mainly in the macula and in the optic nerve area. The deformity of the globe, including posterior staphyloma, may facilitate the development of these pathologies.

Definition of Pathologic Myopia

The definition of "PM" has not been standardized among studies; other terms like "high myopia (HM)" have been used similarly. However, "HM" means a high degree of myopia and does not always include the presence of complications causing the BCVA decrease.

Excessive elongation of the globe and posterior staphyloma are believed to be important factors in the development of posterior fundus lesions in PM (Curtin 1977; Steidl and Pruett 1997; Spaide 2014; Moriyama et al. 2011; Ohno-Matsui et al. 2012). However, refractive error or axial length alone often does not adequately reflect "pathologic myopia." Posterior staphyloma, which is a hallmark lesion of pathologic myopia, can occur also in non-highly myopic eyes (Curtin and Karlin 1970; Wang et al. 2016). Recently, an international panel of researchers in myopia reviewed previously published studies and classifications and proposed a simplified, uniform classification system for PM for use in future studies (Ohno-Matsui et al. 2015a, b). In this META-PM (meta-analyses of pathologic myopia) study classification, PM was defined as eyes having chorioretinal atrophy equal to or more severe than diffuse atrophy or as eyes having posterior staphyloma (Ohno-Matsui et al. 2016a, b; Ohno-Matsui 2017).

Complications of PM

Myopic Maculopathy

Curtin and Karlin first proposed a definition of myopic maculopathy that included the features of chorioretinal atrophy, central pigment spot, lacquer cracks, posterior staphyloma, and optic disc changes in 1970 (Curtin and Karlin 1970). Later, Tokoro updated the classification of myopic macular lesions into four categories: (1) tessellated fundus, (2) diffuse chorioretinal atrophy, (3) patchy chorioretinal atrophy, and (4) macular hemorrhage (Tokoro 1998).

Recently, an international panel of researchers in myopia reviewed previously published studies and classifications and proposed a simplified, uniform classification system for pathologic myopia for use in future studies (Ohno-Matsui et al. 2015a, b). In this simplified system (META-PM clas-

K. Ohno-Matsui (✉)
Tokyo Medical and Dental University, Tokyo, Japan
e-mail: k.ohno.oph@tmd.ac.jp

I. K. Kim (ed.), *Macular Disorders*, Retina Atlas, https://doi.org/10.1007/978-981-15-3001-2_5

Table 5.1 Summary of the classification of myopic maculopathy according to META-PM study

META-PM classification	Myopic retinal changes	Fundus appearance
Category 0	No myopic retinal changes	
Category 1	Tessellated fundus	Well-defined choroidal vessels can be observed clearly around the fovea and arcade vessels
Category 2	Diffuse chorioretinal atrophy	The posterior pole appears yellowish white, extent of which is variable
Category 3	Patchy chorioretinal atrophy	Well-defined, grayish white lesions, size variable between 1 and several choroidal lobules
Category 4	Macular atrophy	Well-defined, round chorioretinal atrophic lesion that is grayish white or whitish around a regressed fibrovascular membrane that enlarges with time. Generally, macular atrophy is centered on the central fovea and has a round shape
+ Lc	Lacquer cracks	Yellowish thick linear pattern
+ CNV	Choroidal neovascularization	Active CNV should be accompanied by exudative activity or hemorrhage. Serous retinal detachments can be present
+ Fs	Fuchs spot	Pigmented spot representing the dry fibrovascular scar of myopic CNV
–	Posterior staphyloma	Local bulging of the sclera at the posterior pole that has a radius of less than the surrounding curvature of the wall of the eye

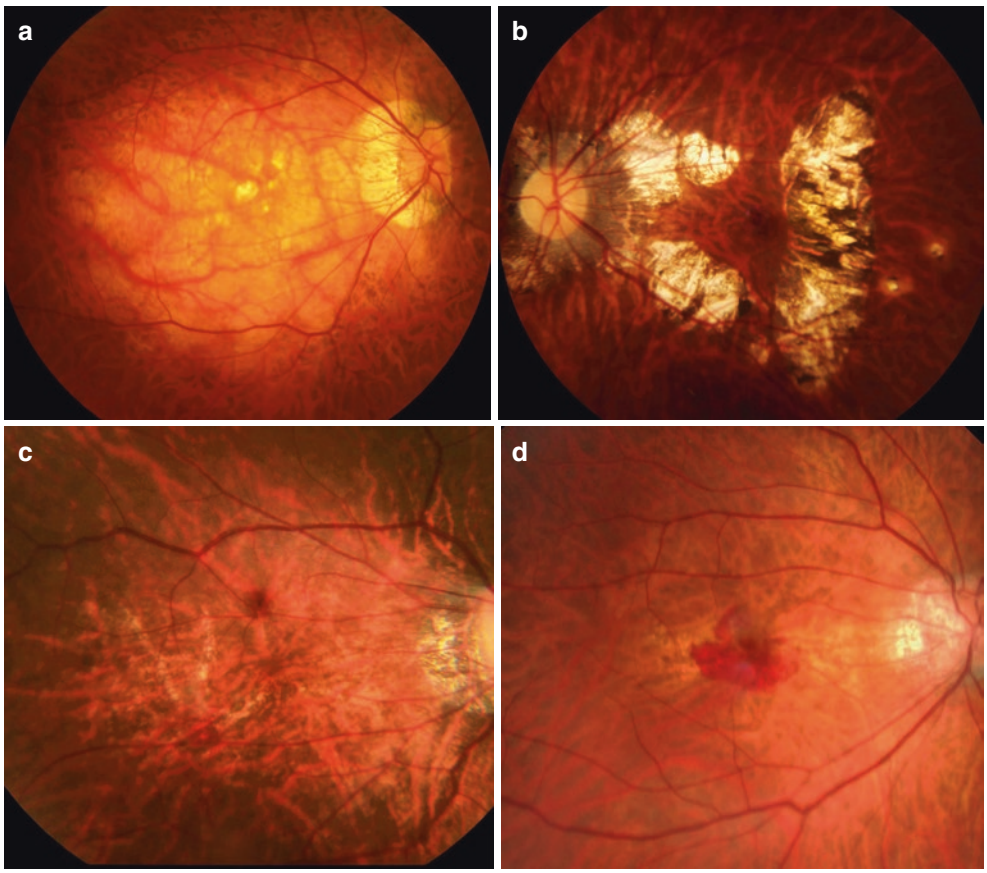

Fig. 5.1 Maculopathy due to pathologic myopia. (**a**) Diffuse atrophy is observed as a yellowish, ill-defined lesion in the posterior fundus. (**b**) Patchy atrophy. Areas of patchy atrophy are observed as whitish, well-defined lesions lower to the macula. (**c**) Lacquer cracks are observed as yellowish, linear lesions. (**d**) Myopic choroidal neovascularization (myopic CNV). Myopic CNV in this case is observed as grayish fibrovascular membrane. Subretinal bleeding is observed around the CNV

sification; Table 5.1), myopic maculopathy lesions are categorized into five categories from "no myopic retinal lesions" (Category 0), "tessellated fundus only" (Category 1), "diffuse chorioretinal atrophy" (Category 2; Fig. 5.1a), "patchy chorioretinal atrophy" (Category 3; Fig. 5.1b), to "macular atrophy" (Category 4). Three additional features were added to these categories and were included as "plus signs": (1) lacquer cracks (Fig. 5.1c), (2) myopic CNV (Fig. 5.1d), and (3) Fuchs spot. The reason for separately defining these "plus signs" is that these three lesions have been shown to be strongly associated with central vision loss, but they do not fit into any particular category and may develop from, or coexist, in eyes with any of the myopic maculopathy categories described above. Based on this new classification, pathologic myopia is defined as myopic maculopathy category 2 or above, or presence of "plus" sign, or the presence of posterior staphyloma (Ohno-Matsui et al. 2016a, b; Verkicharla et al. 2015).

Currently, an update of the META-PM classification is proposed based on our recent longer follow-up study (>10 years). Longer follow-up data showed that the progression from C3 to C4 is uncommon, and most macular

atrophy (C4) is myopic CNV-related. In addition, a Fuchs spot is a pigmented scar of myopic CNV. Not all scarring from myopic CNV shows an increased pigmentation. Thus, it might be better not to separately identify Fuchs spot, but rather to designate active phase and scar phase together under the category of myopic CNV. Finally, the lesions from C2 through C4 are specific to PM, whereas C1 is seen even in mild myopia and C0 is just normal fundus. Thus, new classification is expected to include only the lesions specific to PM (thus, C2, C3, C4, lacquer cracks, myopic CNV) and would be better named "PM maculopathy."

Features of Each Lesion of PM Maculopathy

Diffuse Atrophy

Diffuse chorioretinal atrophy is observed as ill-defined yellowish lesions in the posterior fundus of highly myopic eyes (Fig. 5.1a). The main feature of diffuse atrophy is a marked thinning (almost absence) of choroid. Optical coherence tomography (OCT) shows a marked thinning of the choroid in the area of diffuse atrophy (Fig. 5.2). In most of the cases, the choroid is almost absent except for sporadic large choroidal vessels. The presence of outer retina and RPE even in areas where most of the choroid is gone might explain relatively preserved vision in eyes with diffuse atrophy. Although the choroid becomes thinned in eyes with tessellated fundus, the degree of choroidal thinning is much more serious in eyes with diffuse atrophy, and such disproportionate thinning of choroid compared to the surrounding tissue (RPE, outer retina, and sclera) might be a key phenomenon in diffuse atrophy.

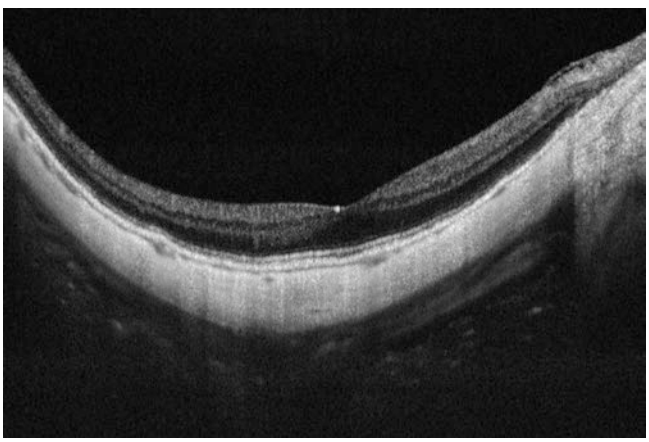

Fig. 5.2 Extreme thinning of choroid in an eye with diffuse atrophy shown by optical coherence tomography (OCT). OCT image of eyes with diffuse atrophy shows almost absence of choroid between retina and sclera

Recently, in a retrospective study of myopic children with at least 20 years of follow-up, Yokoi et al. reported that 83% of adults with PM had peripapillary diffuse choroidal atrophy (PDCA) in childhood (Yokoi et al. 2016). OCT showed that PDCA was an abrupt and focal loss of peripapillary choroid (Yokoi et al. 2017).

Patchy Atrophy

Patchy chorioretinal atrophy is observed as a grayish-white, well-defined atrophy (Figs. 5.1b and 5.3) (Tokoro 1998). Due to an absence of RPE and most of the choroid, the sclera can be observed through transparent retinal tissue, which is considered to show white color. By using a recent imaging technology, swept-source OCT, Ohno-Matsui et al. (2016a, b) recently reported that patchy atrophy was not simply a patch of chorioretinal atrophy but it was a hole in

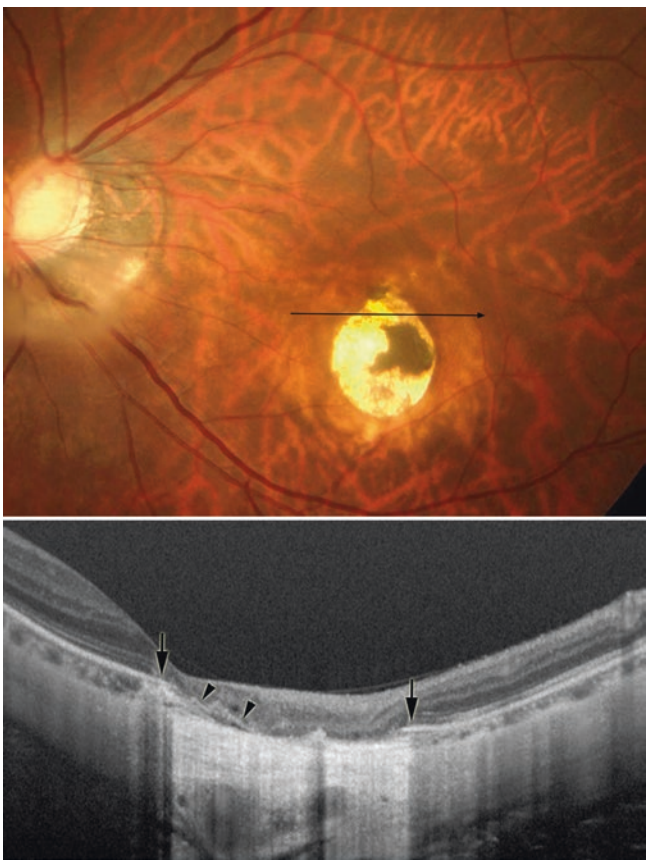

Fig. 5.3 Bruch's membrane defects in the area of patchy atrophy. **Top**. Fundus of a left eye shows an area of patchy atrophy. Long narrow arrow indicates a scanned line examined by OCT. **Bottom**. A horizontal OCT section across the area of patchy atrophy shows the end of retinal pigment epithelium (black arrows). Increased light penetrance is observed in the area defective of RPE. The remnants of Bruch's membrane are observed near the edge of the Bruch's membrane defect (arrowheads) are jagged. In an area defective of Bruch's membrane, almost the entire choroid is missing and the inner retina is in direct contact with the sclera. (Reproduced with permission from Elsevier. License number is 4786210056925)

Bruch's membrane (BM) (Fig. 5.3, cited with permission). In the area of patchy atrophy without BM, most of the thickness of choroid, RPE, and outer retina are lost and the inner retina directly sits on the sclera. This differs from the finding that the RPE and outer retina are preserved in most of the eyes with diffuse atrophy, although it is not certain if the remaining photoreceptors and RPE function normally in those eyes.

Lacquer Cracks

Lacquer cracks are fine, irregular, yellow lines, often branching and crisscrossing, seen in the posterior fundus of highly myopic eyes (Fig. 5.1d). Curtin and Karlin reported that lacquer cracks were found in 4.3% of highly myopic eyes (Curtin and Karlin 1970). Histologically, the lacquer cracks represent healed mechanical fissures in the RPE-Bruch's membrane-choriocapillaris complex (Grossniklaus and Green 1992).

Lacquer cracks can develop at a relatively early age in highly myopic patients (e.g., in the 30s). Tokoro reported that the frequency of lacquer cracks was low in patients younger than age 20 and in the elderly, but increases around ages 40 and 60 years (Tokoro 1998). The frequency distribution of lacquer cracks showed two peaks in the age between 35 and 39 years and the age between 55 and 59 years.

Lacquer cracks might be a unique lesion among the various lesions of myopic maculopathy, because they seem to be caused almost purely by mechanical expansion of the globe and are not much influenced by aging. In OCT examinations, lacquer cracks are observed as an increased light penetration into deep tissues with RPE discontinuity. The most recent technology, OCT angiography, can clearly demonstrate the crack in the choriocapillaris.

Myopic CNV and CNV-Related Macular Atrophy

Myopic CNV (Fig. 5.1c) is a major sight-threatening complication of pathologic myopia. It is the most common cause of CNV in individuals aged below 50 years, and the second most common cause of CNV overall (Cohen et al. 1996; Neelam et al. 2012). Myopic CNV tends to be small and thus about 20% of them are extra-foveal (Yoshida et al. 2003). Most of them are type II CNV, above the RPE. In natural course as well as after treatment, myopic CNV goes through three phases: active phase, scar phase, and atrophic phase (also known as myopic CNV-related macular atrophy) (Fig. 5.4).

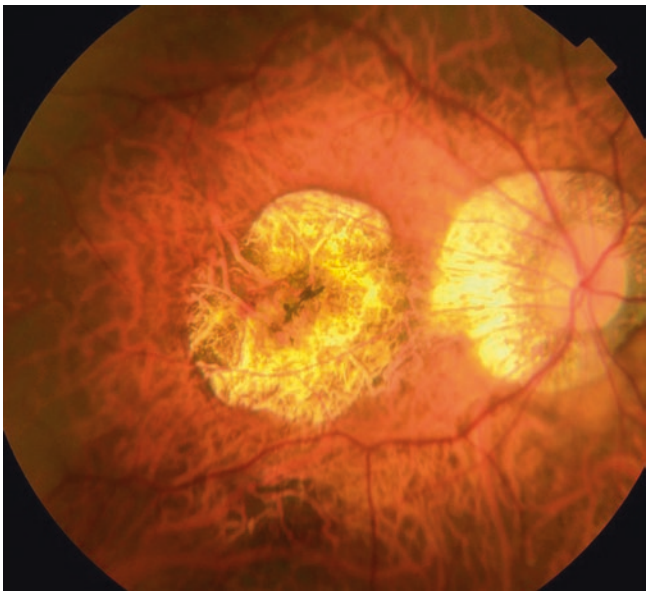

Fig. 5.4 Myopic CNV-related macular atrophy. A well-demarcated area of atrophy is observed centered on the fovea

Since the introduction of anti-VEGF agents in ophthalmology around 10 years ago, anti-angiogenesis treatment with intravitreal anti-VEGF therapy has become the standard-of-care first-line treatment for myopic CNV (Ohno-Matsui et al. 2016a, b; Lai and Cheung 2016). In addition, two large, multi-centered, double-masked, randomized, controlled clinical trials have been performed to evaluate the use of anti-VEGF therapy for myopic CNV (Wolf et al. 2014; Ikuno et al. 2015): the RADIANCE study (intravitreal injection of ranibizumab) and the MYRROR study (intravitreal injection of aflibercept). The results of these two large clinical trials were promising and demonstrated significantly improved visual outcomes of patients with myopic CNV.

However, it is not fully clarified whether anti-VEGF treatments are effective for late complications occurring around the scarred myopic CNV, CNV-related macular atrophy. A recent study using swept-source OCT by Ohno-Matsui et al. showed that CNV-related macular atrophy was also an enlarged hole in BM around the CNV (Ohno-Matsui et al. 2015a, b). To improve the long-term

outcome of anti-VEGF therapies for myopic CNV, the prevention of BM hole enlargement around the CNV is necessary.

Myopic Traction Maculopathy (MTM) (Fig. 5.5)

By using OCT, Takano and Kishi first demonstrated foveal retinal detachment and retinoschisis in severely myopic eyes with posterior staphyloma (Takano and Kishi 1999). Panozzo and Mercanti proposed the term "myopic traction maculopathy (MTM)" to encompass various findings with traction in common by OCT in highly myopic eyes (Panozzo and Mercanti 2004). OCT is an indispensable tool to diagnose MTM, which allows in vivo examination of macular morphology, such as schisis-like inner retinal fluid, schisis-like outer retina fluid, foveal detachment, lamellar or full-thickness macular hole, and/or macular detachment.

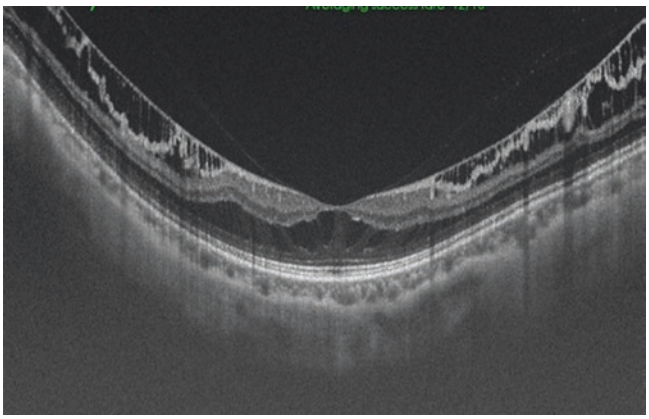

Fig. 5.5 Myopic traction maculopathy. OCT images show the inner and outer retinoschisis

Due to the possible mechanisms involved in the pathogenesis of MTM, vitrectomy is the most common treatment to release all retinal traction, which is caused by cortical vitreous and epiretinal membranes. A foveolar ILM (inner limiting membrane) sparing technique has been used in an attempt to reduce the development of post-vitrectomy macular hole, which was a severe complication and resulted in poor visual recovery (Ho et al. 2012; Shimada et al. 2012).

Posterior Staphyloma

A posterior staphyloma is an outpouching of a limited area of the posterior segment of the eye (Spaide 2014), which is a representative deformity of eyes with PM. Posterior staphyloma is not a lesion of PM maculopathy but is a cause of complications occurring in the macula and in the optic nerve. Earlier studies showed that the presence of staphylomas was significantly correlated with worse vision, more frequent development of myopic macular complications, and optic nerve damage. The sclera protects the central nervous tissues, e.g., the neural retina and the optic nerve, from mechanical insults. Thus, it is reasonable that a deformity of the eye by a staphyloma may result in a mechanical damage of the retina and optic nerve.

Based on ophthalmoscopic observation and fundus drawings, Curtin first classified posterior staphylomas in eyes with pathologic myopia into ten different types (Curtin 1977). Types I to V were considered primary staphylomas, and types VI to X were combined staphylomas. Recently, new imaging modalities that can obtain images of the entire globe, e.g., 3D MRI (Moriyama et al. 2011, 2012; Ohno-Matsui 2014) or ultra-wide fundus imaging (e.g., Optos) have become available. By using a combination of 3D MRI and Optos, Ohno-Matsui (Fig. 5.6)

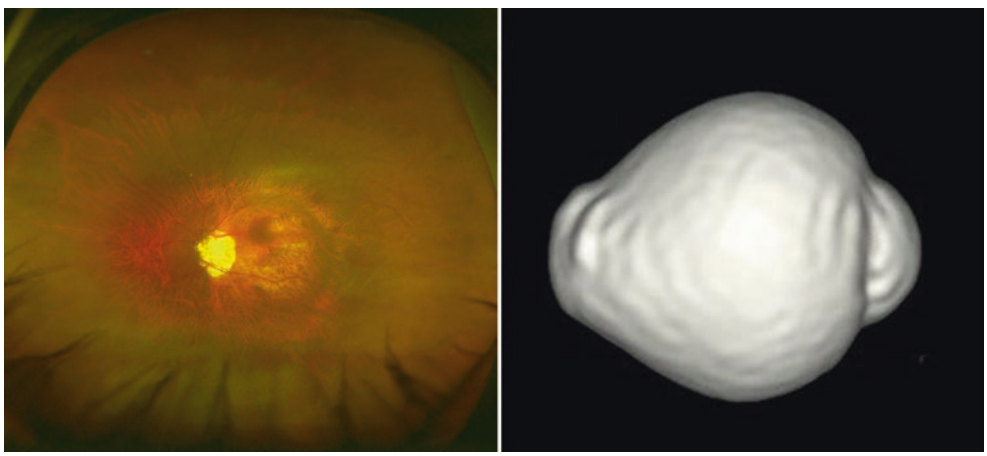

Fig. 5.6 In a wide-field fundus image, the edge of a wide and deep staphyloma is seen. In 3D MRI images from the nasal side, an outpouching of posterior segment of the eye is clearly observed

examined the prevalence and types of posterior staphylomas (Ohno-Matsui 2014). These advances in ocular imaging have made the objective and quantitative evaluations of posterior staphylomas possible.

References

Asakuma T, Yasuda M, Ninomiya T, et al. Prevalence and risk factors for myopic retinopathy in a Japanese population: the Hisayama Study. Ophthalmology. 2012;119:1760–5.

Chang L, Pan CW, Ohno-Matsui K, et al. Myopia-related fundus changes in Singapore adults with high myopia. Am J Ophthalmol. 2013;155:991–9.

Cohen SY, Laroche A, Leguen Y, et al. Etiology of choroidal neovascularization in young patients. Ophthalmology. 1996;103:1241–4.

Curtin BJ. The posterior staphyloma of pathologic myopia. Trans Am Ophthalmol Soc. 1977;75:67–86.

Curtin BJ, Karlin DB. Axial length measurements and fundus changes of the myopic eye. I. The posterior fundus. Trans Am Ophthalmol Soc. 1970;68:312–34.

Grossniklaus HE, Green WR. Pathologic findings in pathologic myopia. Retina. 1992;12:127–33.

Ho TC, Chen MS, Huang JS, et al. Foveola nonpeeling technique in internal limiting membrane peeling of myopic foveoschisis surgery. Retina. 2012;32(3):631–4.

Ikuno Y, Ohno-Matsui K, Wong TY, et al. Intravitreal aflibercept injection in patients with myopic choroidal neovascularization: the MYRROR Study. Ophthalmology. 2015;122:1220–7.

Lai TY, Cheung CM. Myopic choroidal neovascularization: diagnosis and treatment. Retina. 2016;36:1614–21.

Liang YB, Friedman DS, Wong TY, et al. Prevalence and causes of low vision and blindness in a rural Chinese adult population: the Handan Eye Study. Ophthalmology. 2008;115:1965–72.

Morgan IG, Ohno-Matsui K, Saw SM. Myopia. Lancet. 2012;379:1739–48.

Moriyama M, Ohno-Matsui K, Hayashi K, et al. Topographical analyses of shape of eyes with pathologic myopia by high-resolution three dimensional magnetic resonance imaging. Ophthalmology. 2011;118:1626–37.

Moriyama M, Ohno-Matsui K, Modegi T, et al. Quantitative analyses of high-resolution 3D MR images of highly myopic eyes to determine their shapes. Invest Ophthalmol Vis Sci. 2012;53:4510–8.

Neelam K, Cheung CM, Ohno-Matsui K, et al. Choroidal neovascularization in pathological myopia. Prog Retin Eye Res. 2012;31:495–525.

Ohno-Matsui K. Proposed classification of posterior staphylomas based on analyses of eye shape by three-dimensional magnetic resonance imaging and wide-field fundus imaging. Ophthalmology. 2014;121:1798–809.

Ohno-Matsui K. What is the fundamental nature of pathologic myopia? Retina. 2017;37:1043–8.

Ohno-Matsui K, Akiba M, Modegi T, et al. Association between shape of sclera and myopic retinochoroidal lesions in patients with pathologic myopia. Invest Ophthalmol Vis Sci. 2012;53:6046–61.

Ohno-Matsui K, Jonas JB, Spaide RF. Macular Bruch's membrane holes in choroidal neovascularization-related myopic macular atrophy by swept-source optical coherence tomography. Am J Ophthalmol. 2015a;162:133–9.

Ohno-Matsui K, Kawasaki R, Jonas JB, et al. International photographic classification and grading system for myopic maculopathy. Am J Ophthalmol. 2015b;159:877–83.e7.

Ohno-Matsui K, Jonas JB, Spaide RF. Macular Bruch membrane holes in highly myopic patchy chorioretinal atrophy. Am J Ophthalmol. 2016a;166:22–8.

Ohno-Matsui K, Lai TYY, Cheung CMG, Lai CC. Updates of pathologic myopia. Prog Retin Eye Res. 2016b;52:156–87.

Panozzo G, Mercanti A. Optical coherence tomography findings in myopic traction maculopathy. Arch Ophthalmol. 2004;122:1455–60.

Shimada N, Sugamoto Y, Ogawa M, et al. Fovea-sparing internal limiting membrane peeling for myopic traction maculopathy. Am J Ophthalmol. 2012;154(4):693–701

Spaide RF. Staphyloma: part 1. In: Spaide R, Ohno-Matsui K, Yannuzzi L, editors. Pathologic myopia. New York: Springer; 2014.

Steidl SM, Pruett RC. Macular complications associated with posterior staphyloma. Am J Ophthalmol. 1997;123:181–7.

Takano M, Kishi S. Foveal retinoschisis and retinal detachment in severely myopic eyes with posterior staphyloma. Am J Ophthalmol. 1999;128:472–6.

Tokoro T. Types of fundus changes in the posterior pole. In: Tokoro T, editor. Atlas of posterior fundus changes in pathologic myopia. 1st ed. Tokyo: Springer; 1998.

Verkicharla PK, Ohno-Matsui K, Saw SM. Current and predicted demographics of high myopia and an update of its associated pathological changes. Ophthalmic Physiol Opt. 2015;35:465–75.

Wang NK, Wu YM, Wang JP, et al. Clinical characteristics of posterior staphylomas in myopic eyes with axial length shorter than 26.5 mm. Am J Ophthalmol. 2016;162:180–90.

Wolf S, Balciuniene VJ, Laganovska G, et al. RADIANCE: a randomized controlled study of ranibizumab in patients with choroidal neovascularization secondary to pathologic myopia. Ophthalmology. 2014;121:682–92.

Wong YL, Saw SM. Epidemiology of pathologic myopia in Asia and worldwide. Asia Pac J Ophthalmol (Phila). 2016;5:394–402.

Xu L, Wang Y, Li Y, et al. Causes of blindness and visual impairment in urban and rural areas in Beijing: the Beijing Eye Study. Ophthalmology. 2006;113:1134.e1–11.

Yokoi T, Jonas JB, Shimada N, et al. Peripapillary diffuse chorioretinal atrophy in children as a sign of eventual pathologic myopia in adults. Ophthalmology. 2016;123:1783–7.

Yokoi T, Zhu D, Bi HS, et al. Parapapillary diffuse choroidal atrophy in children is associated with extreme thinning of parapapillary choroid. Invest Ophthalmol Vis Sci. 2017;58:901–6.

Yoshida T, Ohno-Matsui K, Yasuzumi K, et al. Myopic choroidal neovascularization: a 10-year follow-up. Ophthalmology. 2003;110:1297–305.

Angioid Streaks

6

Vikram S. Makhijani and Rachel M. Huckfeldt

Abbreviations

BM	Bruch's membrane
CNV	Choroidal neovascularization
FA	Fluorescein angiography
FAF	Fundus autofluorescence
ICGA	Indocyanine green angiography
NIR	Near-infrared reflectance
OCT	Optical coherence tomography
PDT	Photodynamic therapy
PXE	Pseudoxanthoma elasticum
RPE	Retinal pigment epithelium
SD-OCT	Spectral-domain optical coherence tomography

Introduction

Angioid streaks, which appear as jagged lines extending from the optic disc, were first described in 1889 by Doyne and then given their current name by Knapp in 1892 due to their vascular appearance (Clarkson and Altman 1982). They were proposed to occur at the level of Bruch's membrane in 1916 with histopathologic verification several decades later (Clarkson and Altman 1982). Angioid streaks can occur in isolation, but they are also associated with a range of disease processes, most commonly including pseudoxanthoma elasticum (PXE). Advances in retinal imaging have enabled a more detailed view of these defects and facilitated the management of choroidal neovascularization, which is the most commonly encountered complication.

V. S. Makhijani · R. M. Huckfeldt (✉)
Retina Service, Department of Ophthalmology, Massachusetts Eye and Ear Infirmary, Harvard Medical School, Boston, MA, USA
e-mail: rachel_huckfeldt@meei.harvard.edu

Pathogenesis

Histopathologic analysis of globe specimens with angioid streaks demonstrated generalized calcification and thickening of the elastic layers of Bruch's membrane with sharply delineated defects in regions corresponding to the clinical location of angioid streaks (Klien 1947; Verhoeff 1948; Clarkson and Altman 1982; Gibson et al. 1983; Jampol et al. 1987). The breaks, which were attributed to calcification-associated brittleness, were associated with attenuation and hypopigmentation of the overlying retinal pigment epithelium as well as with examples of fibrovascular ingrowth through the defects (Klien 1947; Clarkson and Altman 1982). Correlation was present between the color of angioid streaks on earlier clinical exams and the degree of RPE pigmentation as well as the presence of fibrotic plaque-like growth present in more advanced lesions (Klien 1947).

Disease Associations

Angioid streaks are associated with a variety of systemic disorders, many of which affect mineralization or elastic fibers. Estimates suggest that around 50% of angioid streaks have a systemic association, and of these, PXE is most common (Shields et al. 1975; Clarkson and Altman 1982). The most frequently encountered associated conditions are described below, but other associations include Ehlers-Danlos syndrome.

Pseudoxanthoma Elasticum (PXE)

PXE is a multisystem disease affecting approximately between 1 in 25,000 and 100,000 individuals that is caused by the autosomal recessive inheritance of mutations in the *ABCC6* gene (Ringpfeil et al. 2000; Bergen et al. 2000; Boyd et al. 2000). Dysfunction of the resulting ATP-binding transporter protein leads to ectopic mineralization of elastic fibers, particularly in the skin, eyes, and vasculature, through

I. K. Kim (ed.), *Macular Disorders*, Retina Atlas, https://doi.org/10.1007/978-981-15-3001-2_6

mechanisms that are incompletely understood but likely involve a lack of appropriate suppression (Germain 2017). Systemic associations include characteristic skin papules on the neck and flexural surfaces as well as small and medium artery disease (Germain 2017). Ensuing cardiovascular complications include peripheral artery disease with upper and lower extremity claudication and less commonly aneurysms, angina, ischemic stroke, and myocardial infarction (Germain 2017).

Angioid streaks are the most common ophthalmic finding in PXE, but other retinal manifestations of PXE are well-described. Peau d'orange, which is not specific to PXE, is yellow and near-confluent mottling in the mid-periphery that is thought to represent a transition zone in Bruch's calcification (Fig. 6.1) (Issa et al. 2010). Peau d'orange can be the earliest ocular sign of PXE (Gliem et al. 2013b). Comet lesions are small nodular lesions with white tails of RPE atrophy present within the mid-periphery that are proposed to be pathognomonic of PXE (Gass 2003). Pattern dystrophy-like macular abnormalities as well as vitelliform lesions may also be present, and both of these findings can be accompanied by CNV-independent subretinal fluid that is non-responsive to anti-VEGF therapies (Agarwal 2005; Zweifel et al. 2011; Gliem et al. 2013b). Optic disc drusen may also be present.

Paget's Disease

Paget's disease is a disease of abnormal bone turnover that results in progressive thickening and weakening of bones, in particular the skull and axial skeleton (Ralston et al. 2008). Axial involvement results in osteoarthritis, bone pain, and

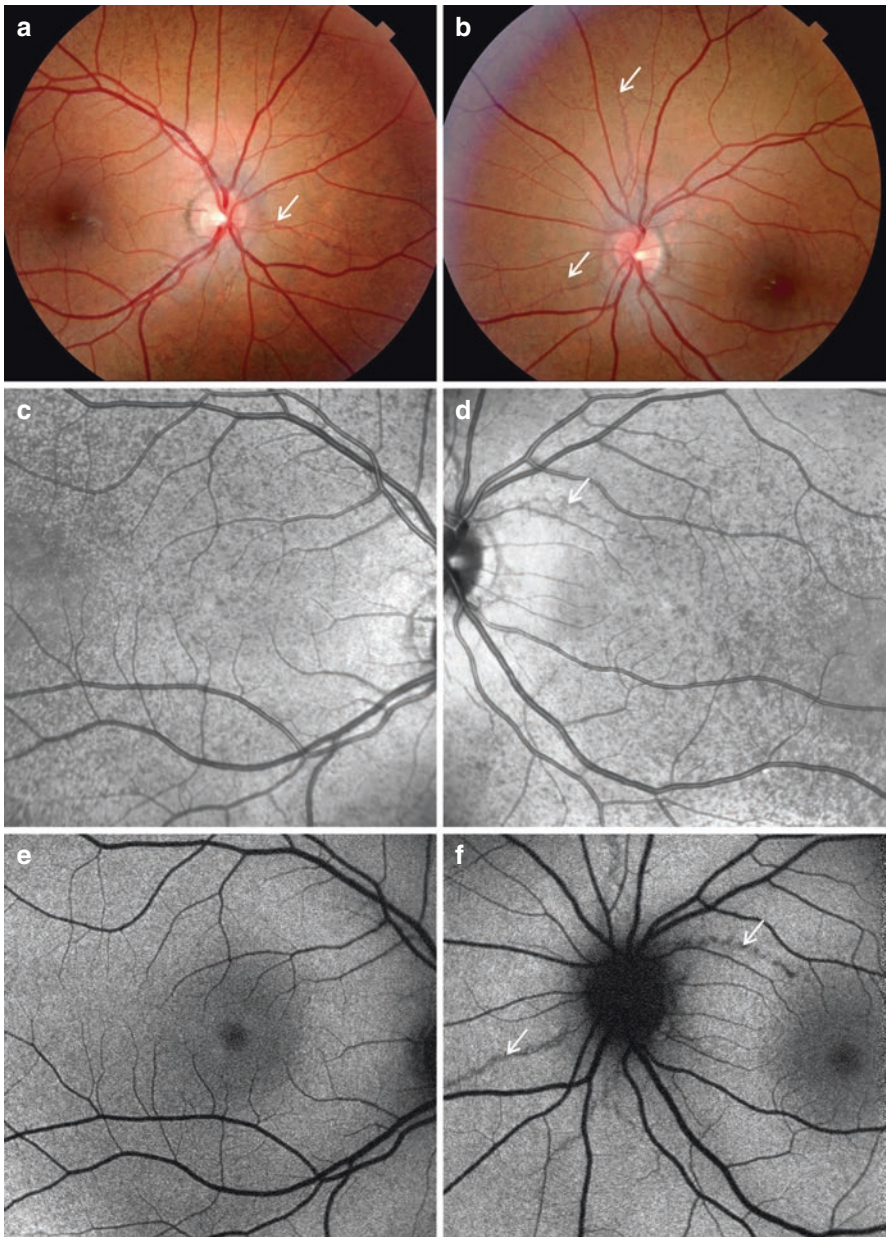

Fig. 6.1 Early presentation of angioid streaks. Fundus photos (**a**, **b**) demonstrate angioid streaks (arrows) in a patient with PXE as well as peau d'orange mottling. These peripapillary streaks are extramacular and visually insignificant to the patient. NIR (**c**, **d**) emphasizes the angioid streaks (arrows) and peau d'orange to a greater extent than FAF (**e**, **f**)

fractures, whereas skull involvement can result in hearing loss, hydrocephalus, pain, and cranial nerve disorders. Angioid streaks are a rare association in Paget's disease but were suggested to occur more frequently in patients with increased skull involvement (Dabbs and Skjodt 1990; Clarkson 1991).

Sickle Cell Disease and Hemoglobinopathies

Angioid streaks are estimated to be present in at least 1–2% of patients with sickle cell disease and possibly much higher numbers in cohorts of older individuals with homozygous sickle cell anemia (Condon and Serjeant 1976; Nagpal et al. 1976). At a mechanistic level, these breaks result from calcification of Bruch's membrane rather than from iron deposition (Jampol et al. 1987). Angioid streaks can also be found in other hemoglobinopathies such as β-thalassemia (Liaska et al. 2016).

Clinical Features

Clinical Exam

Streaks are visible as jagged, vessel-like radial extensions from the peripapillary area that taper toward the periphery and may be connected by circumferential streaks (Fig. 6.1) (Deschweinitz 1896; Clarkson and Altman 1982). The number of streaks in an eye is variable. Early in their natural history, angioid streaks are similar to the color of underlying choroid but can later have obscured margins due to fibrovascular growth through the Bruch's membrane defect, or acquire a whiter hue due to RPE depigmentation (Hagedoorn 1975; De Zaeytijd et al. 2010). The appearance of streaks may be more subtle in areas of associated chorioretinal atrophy (Fig. 6.2) (Gliem et al. 2013b).

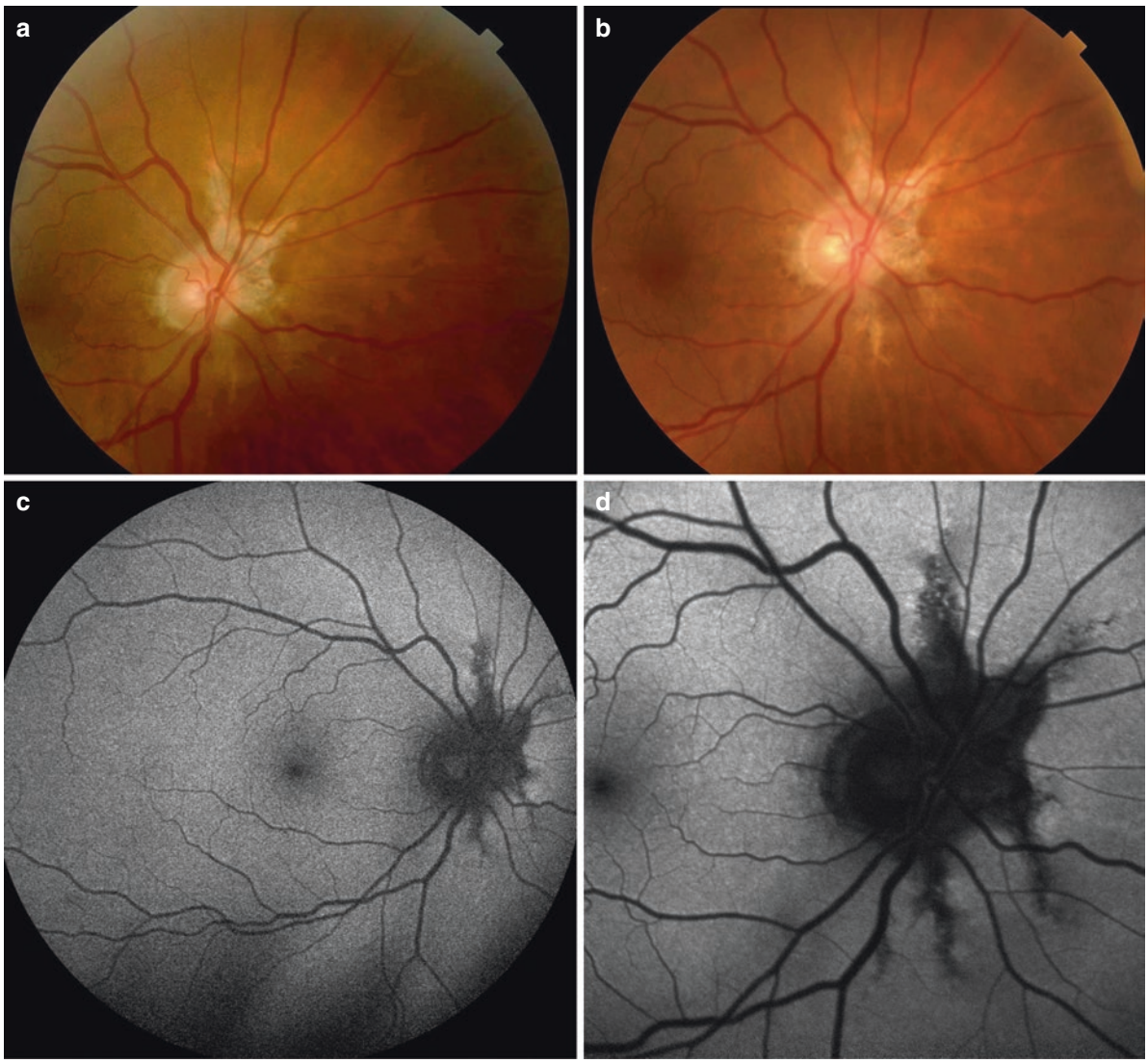

Fig. 6.2 Progression of angioid streaks. Over a 4-year period, fundus photos (**a**: initial, **b**: follow-up) and FAF (**c**: initial, **d**: follow-up) show progressive extension of an angioid streak and atrophic changes inferior to optic nerve

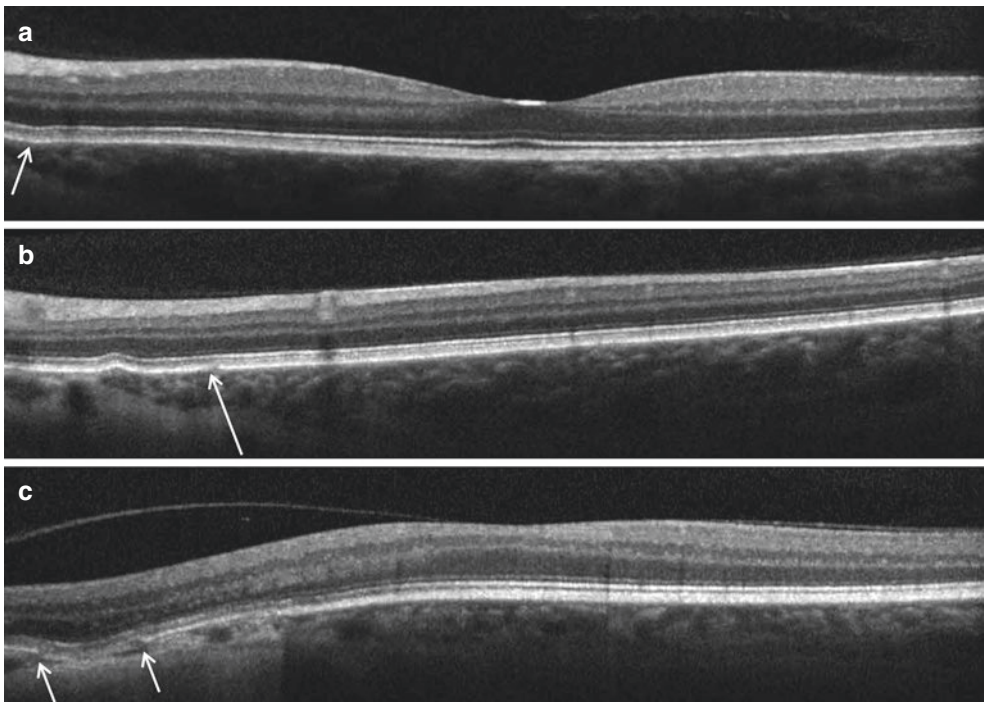

Fig. 6.3 OCT findings associated with angioid streaks including Bruch's membrane undulations (**a**), focal Bruch's membrane break with RPE thinning (**b**), and a more extensive break in Bruch's (**c**). Arrows indicate the relevant finding in each panel

Imaging

SD-OCT provides in vivo confirmation that angioid streaks correspond to breaks in Bruch's membrane (BM) (Charbel Issa et al. 2009). Additional OCT findings include BM undulations, larger dehiscences of BM, and hyperreflective BM dots corresponding to clinically appreciated peau d'orange mottling and proposed to represent calcification (Fig. 6.3) (Charbel Issa et al. 2009; Spaide and Jonas 2015; Marchese et al. 2017). Serial imaging OCT suggests that undulation can lead to breaks and can also document the formation of CNV (Marchese et al. 2017). In the setting of PXE, SD-OCT may reveal subretinal fluid in the absence of CNV that is anti-VEGF resistant and may represent RPE dysfunction (Zweifel et al. 2011; Gliem et al. 2013b). Finally, swept source OCT has demonstrated decreased choroidal thickness in eyes with angioid streak-associated CNV (Ellabban et al. 2012).

En face imaging modalities also offer valuable information (Fig. 6.4). Near-infrared reflectance (NIR) is more effective than fundus autofluorescence (FAF) and fluorescein angiography (FA) in demonstrating angioid streaks and is also more sensitive than clinical exam (Charbel Issa et al. 2009; De Zaeytijd et al. 2010). Angioid streaks appear dark relative to the surrounding fundus with NIR (Charbel Issa et al. 2009). The capabilities of NIR suggest that the reflective powers of the calcified BM are also consistent with the RPE absorbance of the shorter wavelengths used for FAF and FA (Charbel Issa et al. 2009). Angioid streaks appear hypoautofluorescent with FAF with the width of signal abnormality often corresponding to the degree of RPE hypopigmentation surrounding a streak (De Zaeytijd et al. 2010). Variable degrees of hyperautofluorescence can outline the hypoautofluorescent areas (Finger et al. 2009). FAF can also demonstrate patterns of other fundus findings associated with the underlying systemic disease such as comet tails or peau d'orange in PXE (Finger et al. 2009).

Finally, angiography allows the visualization of angioid streaks as well as associated CNV. Angioid streaks are most commonly hyperfluorescent on FA although they cannot always be visualized (Smith et al. 1964; Lafaut et al. 1998; Charbel Issa et al. 2009). Indocyanine green angiography (ICGA) outlines angioid streaks more effectively than FA, and they are most frequently hyperfluorescent in the late venous phases and beyond (Lafaut et al. 1998). FA in particular can enable the detection of angioid streak-associated CNV (Smith et al. 1964; Patnaik and Malik 1971; Lafaut et al. 1998). OCT angiography (OCT-A) will likely prove helpful in these scenarios and has allowed the detection of angioid streak-associated choroidal neovascularization that was stable without exudation over many months (Andreanos et al. 2017). ICGA may also be useful in identifying angioid streak-associated polypoidal lesions.

Natural History

Consistent with the calcification-associated histopathologic mechanism, angioid streaks are thought to be an acquired abnormality with the earliest cases reported late in the first decade of life (Mansour et al. 1993). Evolution of angioid

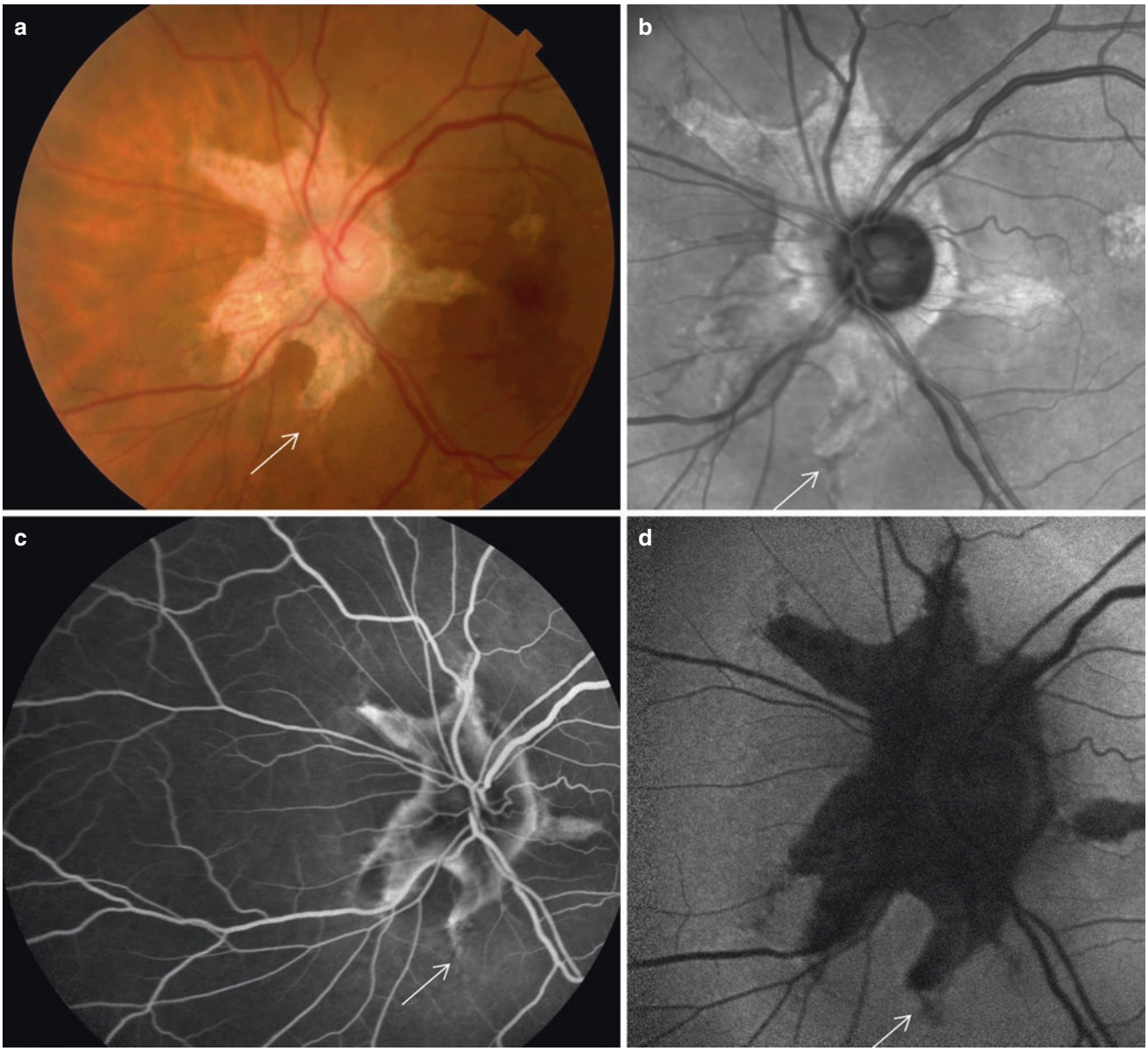

Fig. 6.4 Multimodal imaging of angioid streaks. The fundus photo (**a**) demonstrates angioid streaks (arrow) and associated atrophy. The same angioid streak can be visualized with NIR (**b**), FA (**c**), and FAF (**d**) imaging (arrow in each image). NIR (**b**) demonstrates hyperreflectivity in areas of atrophy with hyporeflective angioid streaks emanating from the peripapillary area. FA (**c**) outlines the atrophic areas but also shows faint hyperfluorescence of streaks. FAF (**d**) demonstrates hypoautofluorescence in the areas of atrophy with subtle hypoautofluorescence beyond these areas corresponding to the angioid streaks

streaks is generally reported to be slow with any change secondary to ongoing mineral deposition in Bruch's membrane weakening its elasticity. Individuals with angioid streaks are usually asymptomatic, unless the streaks have macular involvement or develop choroidal neovascularization-related complications. Choroidal neovascularization (CNV) is a common complication of angioid streaks reported by one study to occur in 73% of eyes from 44 patients who were observed for an average of 3 years (Nakagawa et al. 2013). All forms of CNV have been observed, including polypoidal vasculopathy (PCV), but type 2 CNV is the most common (Nakagawa et al. 2013). Findings of CNV can be obvious (Figs. 6.5 and 6.6) or subtle (Fig. 6.7). Even with treatment, vision loss can result from subretinal hemorrhage and fluid, chorioretinal atrophy, and fibrovascular scarring (Fig. 6.8). Given the relative fragility of Bruch's membrane, mild trauma has been reported to cause hemorrhage, widening of the streaks, and choroidal rupture; non-traumatic hemorrhage can also occur independent of CNV (Fig. 6.9) (Hagedoorn 1975; Mansour et al. 1993).

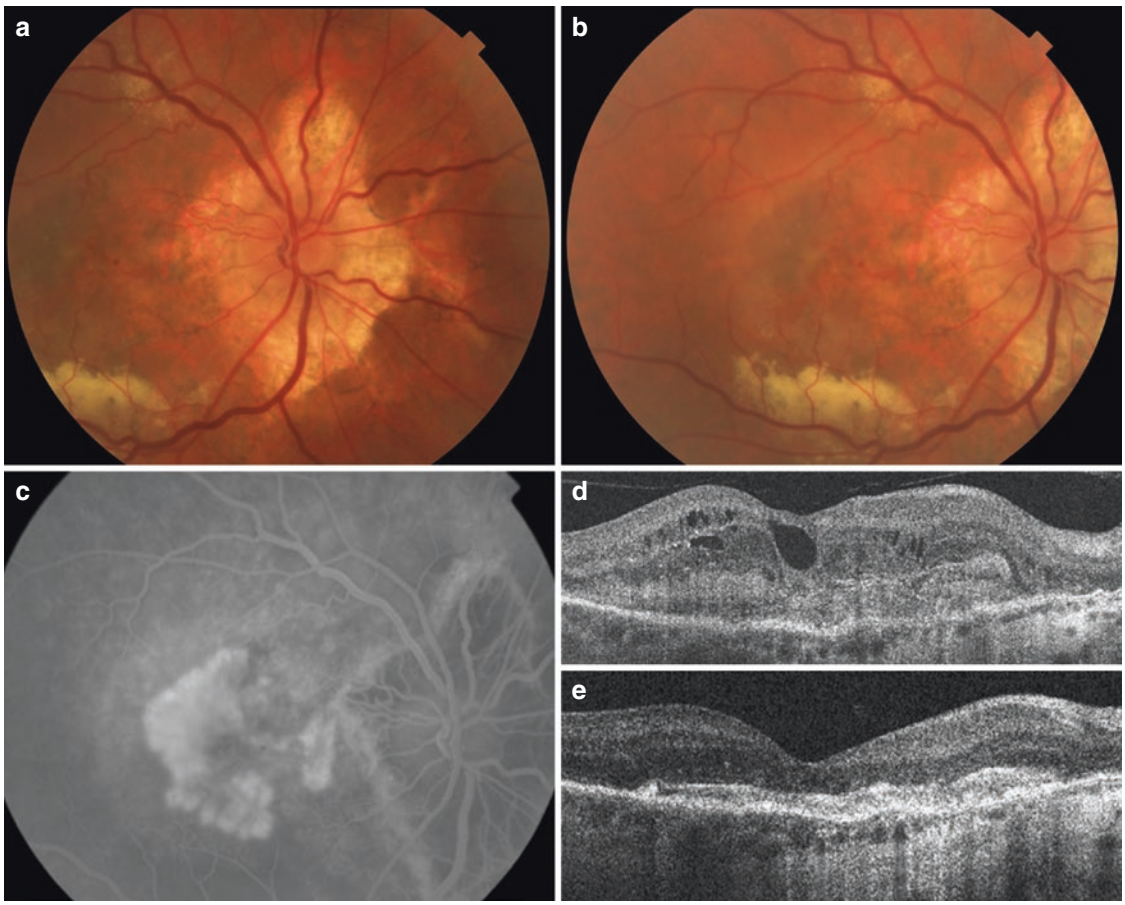

Fig. 6.5 Angioid streaks with CNV. Fundus photos (**a**, **b**) show angioid streaks extending far beyond the peripapillary atrophy as well as a neovascular membrane and significant subretinal fluid and exudate. The extensive neovascular membrane is clearly visualized with FA (**c**). OCT (**d**) shows CNV with intraretinal fluid and subretinal hyperreflective material. A treatment response is present in an OCT (**e**) acquired after a series of 3 monthly intravitreal injections of an anti-VEGF agent

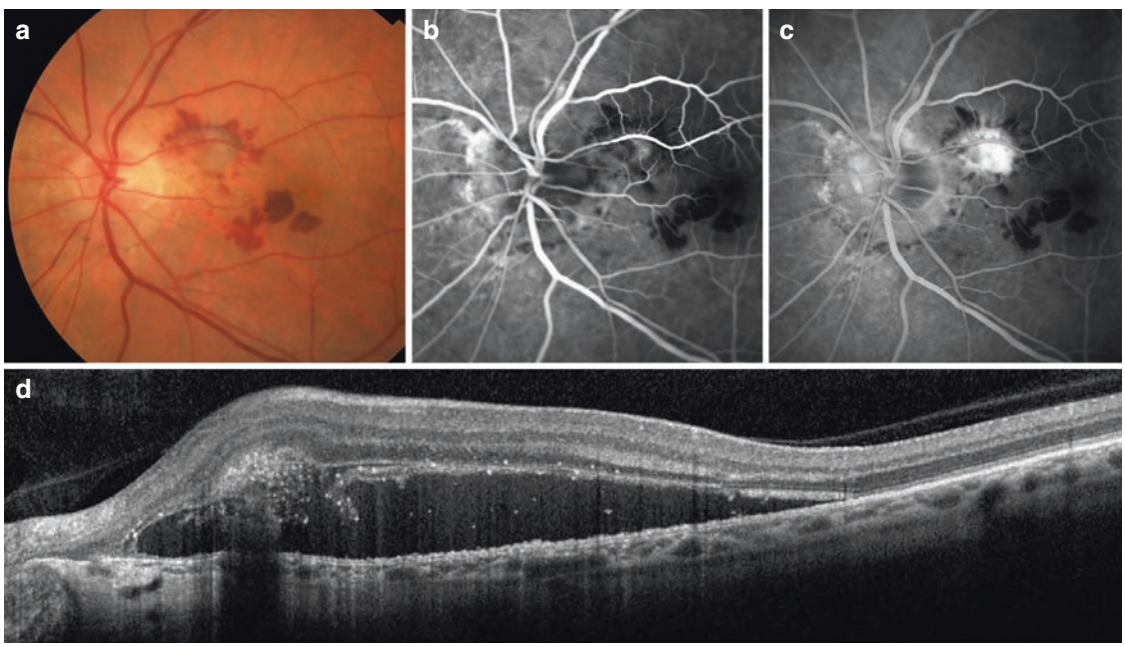

Fig. 6.6 Angioid streaks with CNV and hemorrhage. The fundus photo (**a**) shows angioid streaks with macular hemorrhage due to CNV. FA (**b**, **c**) shows leakage consistent with CNV and blockage from associated hemorrhage. OCT (**d**) shows extensive subretinal fluid

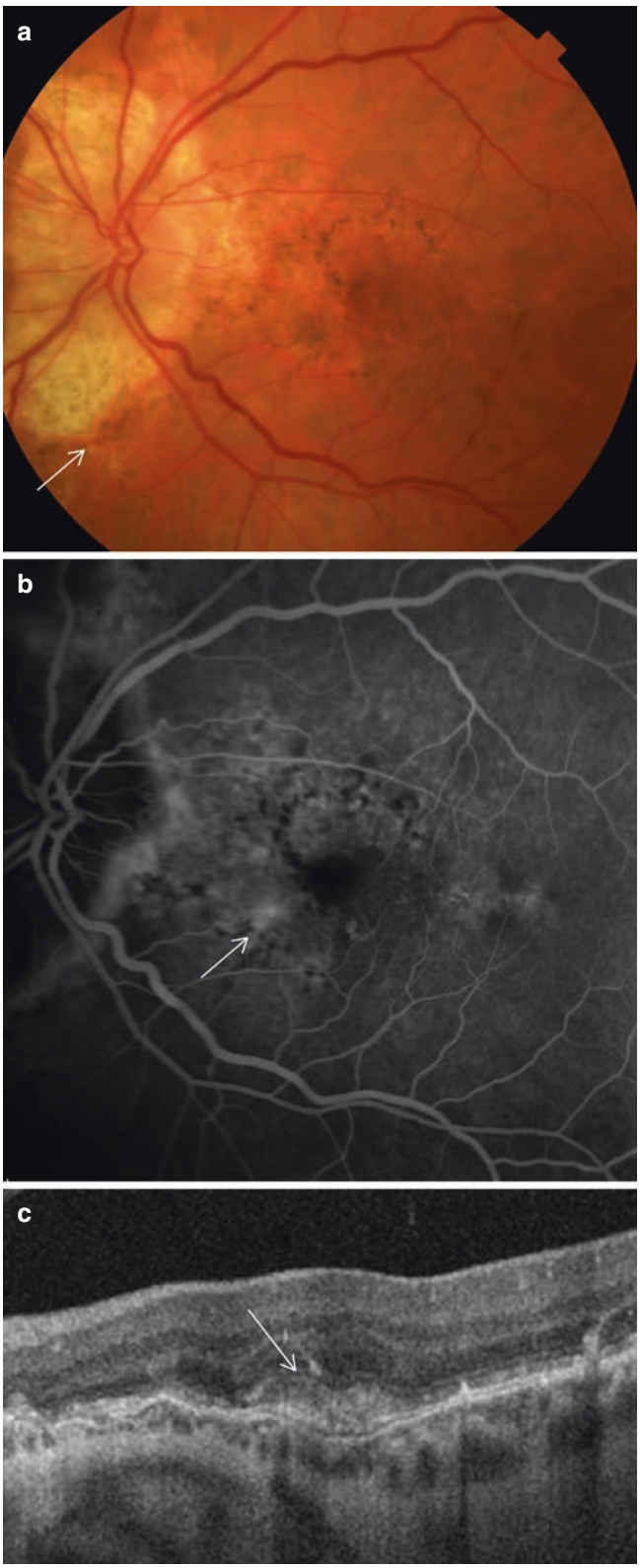

Fig. 6.7 Angioid streaks with subtle CNV. The fundus photo (**a**) demonstrates faint angioid streaks (arrow) emanating from the peripapillary area that are slightly obscured by areas of associated atrophy and pigmentary changes. FA (**b**) shows an area of leakage (arrow). OCT (**c**) shows subretinal hyperreflective material (arrow) corresponding to the leakage that resolved with subsequent anti-VEGF therapy

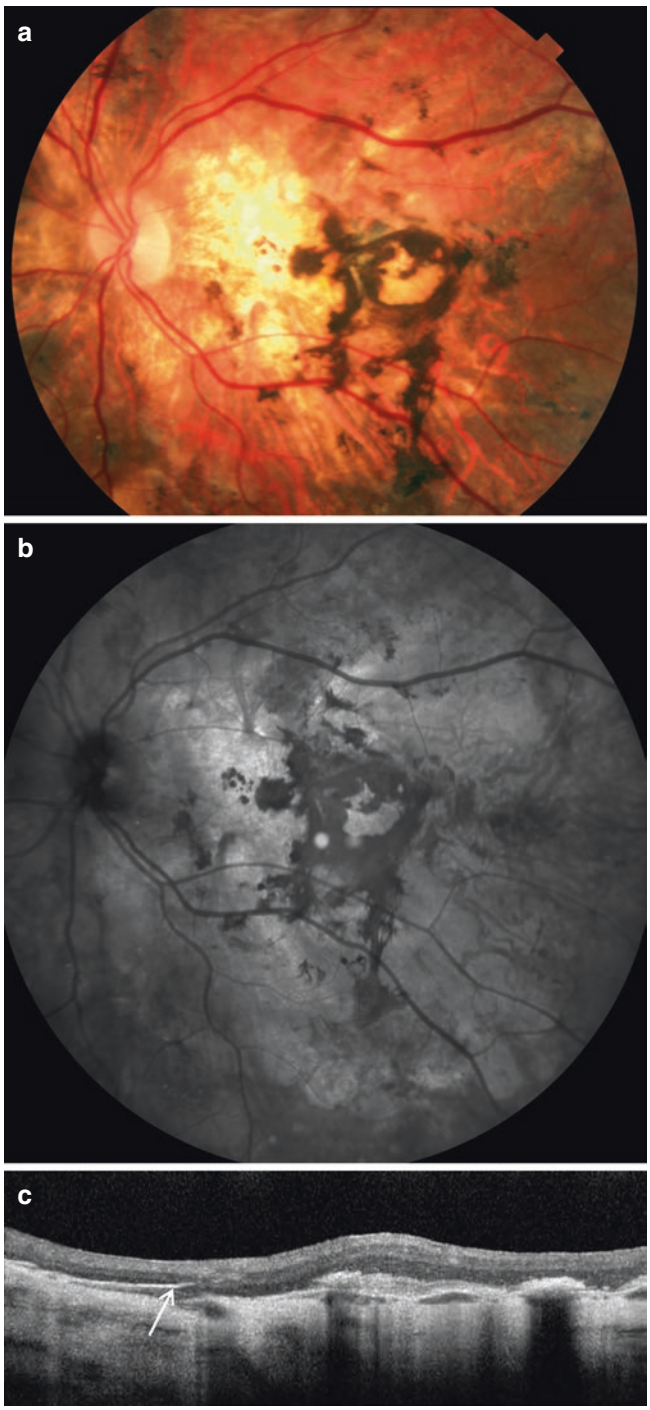

Fig. 6.8 Advanced angioid streaks complicated by CNV. This patient has poor vision and decades of various treatments for CNV and recurrence, including laser photocoagulation. The fundus photo (**a**) shows scarring, pigmentary migration, and atrophy that are also clearly delineated on NIR (**b**). In both images, the angioid streaks are largely obscured by atrophic changes. OCT (**c**) shows atrophy, subretinal hyperreflective material, and a hyperreflective discontinuous Bruch's membrane (arrow)

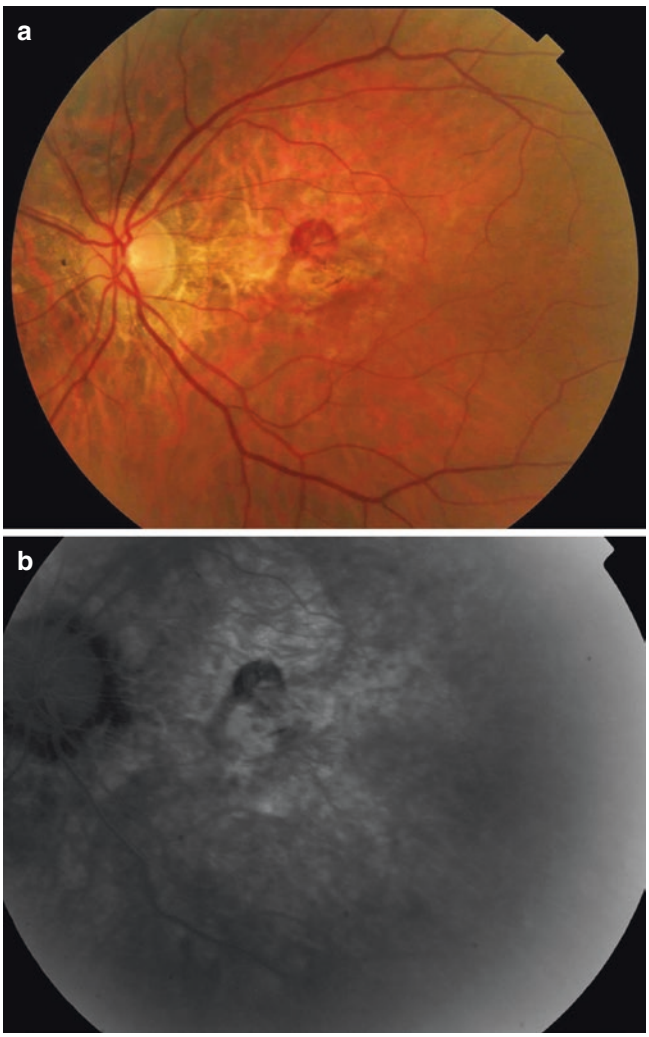

Fig. 6.9 Angioid streaks with non-CNV-associated hemorrhage. The fundus photo (**a**) shows angioid streaks with macular hemorrhage. Neither a late phase FA image (**b**) nor OCT imaging (not shown) demonstrated evidence of CNV

Management

Management of angioid streak-associated disease includes any referrals as appropriate to assess or treat underlying systemic diseases. In addition, patients should be advised to take measures to avoid blunt trauma given the potential for hemorrhage and choroidal rupture. Similarly, avoidance of unnecessary scleral depression is advised by many.

Treatment of ocular complications of angioid streaks is directed at CNV and associated complications. Photodynamic therapy (PDT) and laser photocoagulation may stabilize visual acuity but can be accompanied by an increase in scotoma size with thermal laser, increased lesion size in PDT, and ongoing recurrence (Lim et al. 1993; Pece et al. 1997; Arias et al. 2006; Gliem et al. 2013a). Intravitreal injection of anti-VEGF agents is currently the most widely used treatment for angioid streak-associated CNV and prevention of vision-reducing complications (Fig. 6.5), although laser and PDT may still have a role for non-central CNV (Gliem et al. 2013a). Multiple retrospective series of bevacizumab or ranibizumab for juxtafoveal or subfoveal CNV have shown efficacy in functional gain and reduction of retinal thickness (Sawa et al. 2009; Myung et al. 2010; Finger et al. 2011; Gliem et al. 2013a; Mimoun et al. 2017).

Acknowledgement: Selected images provided courtesy of Drs. Ivana Kim, Joan Miller, and Lucy Young.

References

Agarwal A. Spectrum of pattern dystrophy in pseudoxanthoma elasticum. Arch Ophthalmol. 2005;123:923.

Andreanos KD, Rotsos T, Koutsandrea C, et al. Detection of nonexudative choroidal neovascularization secondary to angioid streaks using optical coherence tomography angiography. Eur J Ophthalmol. 2017;27(5):e140–3.

Arias L, Pujol O, Rubio M, Caminal J. Long-term results of photodynamic therapy for the treatment of choroidal neovascularization secondary to angioid streaks. Graefes Arch Clin Exp Ophthalmol. 2006;244:753–7.

Bergen AAB, Plomp AS, Schuurman EJ, et al. Mutations in ABCC6 cause pseudoxanthoma elasticum. Nat Genet. 2000;25:228–31.

Boyd CD, Le Saux O, Urban Z, et al. Mutations in a gene encoding an ABC transporter cause pseudoxanthoma elasticum. Nat Genet. 2000;25:223–7.

Charbel Issa P, Finger RP, Holz FG, Scholl HPN. Multimodal imaging including spectral domain OCT and confocal near infrared reflectance for characterization of outer retinal pathology in pseudoxanthoma elasticum. Invest Ophthalmol Vis Sci. 2009;50:5913.

Clarkson JG. Paget's disease and angioid streaks: one complication less? Br J Ophthalmol. 1991;75:511.

Clarkson JG, Altman RD. Angioid streaks. Surv Ophthalmol. 1982;26:235–46.

Condon PI, Serjeant GR. Ocular findings of elderly cases of homozygous sickle-cell disease in Jamaica. Br J Ophthalmol. 1976;60:361–4.

Dabbs TR, Skjodt K. Prevalence of angioid streaks and other ocular complications of Paget's disease of bone. Br J Ophthalmol. 1990;74:579–82.

De Zaeytijd J, Vanakker OM, Coucke PJ, et al. Added value of infrared, red-free and autofluorescence fundus imaging in pseudoxanthoma elasticum. Br J Ophthalmol. 2010;94:479–86.

Deschweinitz GE. Angioid streaks in retina. Trans Am Ophthalmol Soc. 1896;7:650–4.

Ellabban AA, Tsujikawa A, Matsumoto A, et al. Macular choroidal thickness and volume in eyes with angioid streaks measured by swept source optical coherence tomography. Am J Ophthalmol. 2012;153:1133–1143.e1.

Finger RP, Charbel Issa P, Ladewig M, et al. Fundus autofluorescence in pseudoxanthoma elasticum. Retina. 2009;29:1496–505.

Finger RP, Issa PC, Schmitz-Valckenberg S, et al. Long-term effectiveness of intravitreal bevacizumab for choroidal neovascularization secondary to angioid streaks in pseudoxanthoma elasticum. Retina. 2011;31:1268–78.

Gass JD. "Comet" lesion: an ocular sign of pseudoxanthoma elasticum. Retina. 2003;23:729–30.

Germain DP. Pseudoxanthoma elasticum. Orphanet J Rare Dis. 2017;12:85.
Gibson JM, Chaudhuri PR, Rosenthal AR. Angioid streaks in a case of beta thalassaemia major. Br J Ophthalmol. 1983;67:29–31.
Gliem M, Finger RP, Fimmers R, et al. Treatment of choroidal neovascularization due to angioid streaks. Retina. 2013a;33:1300–14.
Gliem M, Zaeytijd J, De Finger RP, et al. An update on the ocular phenotype in patients with pseudoxanthoma elasticum. Front Genet. 2013b;4:14.
Hagedoorn A. Angioid streaks and traumatic ruptures of Bruch's membrane. Br J Ophthalmol. 1975;59:267.
Issa PC, Finger RP, Götting C, et al. Centrifugal fundus abnormalities in pseudoxanthoma elasticum. Ophthalmology. 2010;117:1406–14.
Jampol LM, Acheson R, Eagle RC, et al. Calcification of Bruch's membrane in angioid streaks with homozygous sickle cell disease. Arch Ophthalmol. 1987;105:93–8.
Klien BA. Angioid streaks: a clinical and histopathologic study. Am J Ophthalmol. 1947;30:955–68.
Lafaut BA, Leys AM, Scassellati-Sforzolini B, et al. Comparison of fluorescein and indocyanine green angiography in angioid streaks. Graefes Arch Clin Exp Ophthalmol. 1998;236:346–53.
Liaska A, Petrou P, Georgakopoulos CD, et al. β-Thalassemia and ocular implications: a systematic review. BMC Ophthalmol. 2016;16:102.
Lim JI, Bressler NM, Marsh MJ, Bressler SB. Laser treatment of choroidal neovascularization in patients with angioid streaks. Am J Ophthalmol. 1993;116:414–23.
Mansour AM, Ansari NH, Shields JA, et al. Evolution of angioid streaks. Ophthalmologica. 1993;207:57–61.
Marchese A, Parravano M, Rabiolo A, et al. Optical coherence tomography analysis of evolution of Bruch's membrane features in angioid streaks. Eye. 2017;31:1600–5.
Mimoun G, Ebran J-M, Grenet T, et al. Ranibizumab for choroidal neovascularization secondary to pseudoxanthoma elasticum: 4-year results from the PIXEL study in France. Graefes Arch Clin Exp Ophthalmol. 2017;255:1651–60.
Myung JS, Bhatnagar P, Spaide RF, et al. Long-term outcomes of intravitreal antivascular endothelial growth factor therapy for the management of choroidal neovascularization in pseudoxanthoma elasticum. Retina. 2010;30:748–55.
Nagpal KC, Asdourian G, Goldbaum M, et al. Angioid streaks and sickle haemoglobinopathies. Br J Ophthalmol. 1976;60:31–4.
Nakagawa S, Yamashiro K, Tsujikawa A, et al. The time course changes of choroidal neovascularization in angioid streaks. Retina. 2013;33:825–33.
Patnaik B, Malik SR. Fluorescein fundus photography of angioid streaks. Br J Ophthalmol. 1971;55:833–7.
Pece A, Avanza P, Galli L, Brancato R. Laser photocoagulation of choroidal neovascularization in angioid streaks. Retina. 1997;17:12–6.
Ralston SH, Langston AL, Reid IR. Pathogenesis and management of Paget's disease of bone. Lancet. 2008;372:155–63.
Ringpfeil F, Lebwohl MG, Christiano AM, Uitto J. Pseudoxanthoma elasticum: mutations in the MRP6 gene encoding a transmembrane ATP-binding cassette (ABC) transporter. Proc Natl Acad Sci U S A. 2000;97:6001–6.
Sawa M, Gomi F, Tsujikawa M, et al. Long-term results of intravitreal bevacizumab injection for choroidal neovascularization secondary to angioid streaks. Am J Ophthalmol. 2009;148:584–590.e2.
Shields JA, Federman JL, Tomer TL, et al. Angioid streaks. I. Ophthalmoscopic variations and diagnostic problems. Br J Ophthalmol. 1975;59:257–66.
Smith JL, Gass JDM, Justice J. Fluorescein fundus photography of angioid streaks. Br J Ophthalmol. 1964;48:517–21.
Spaide RF, Jonas JB. Peripapillary atrophy with large dehiscences in Bruch membrane in pseudoxanthoma elasticum. Retina. 2015;35:1507–10.
Verhoeff FH. Histological findings in a case of angioid streaks. Br J Ophthalmol. 1948;32:531–44.
Zweifel SA, Imamura Y, Freund KB, Spaide RF. Multimodal fundus imaging of pseudoxanthoma elasticum. Retina. 2011;31:482–91.

Presumed Ocular Histoplasmosis Syndrome

7

William Stevenson, Erica Alvarez, Adnan Mallick, Fatoumata Yanoga, Frederick Davidorf, and Colleen M. Cebulla

Abbreviations

CNV	Choroidal neovascularization
PDT	Photodynamic therapy
POHS	Presumed ocular histoplasmosis syndrome
SST	Submacular surgery trial
VEGF	Vascular endothelial growth factor

Introduction

Presumed ocular histoplasmosis syndrome (POHS), also known as ocular histoplasmosis syndrome, is a multifocal disorder of the choroid and retina that is thought to be caused by *Histoplasma capsulatum*. *H. capsulatum* is a fungal pathogen that is endemic to the Ohio and Mississippi River Valleys. The classic clinical signs of POHS include atrophic chorioretinal scars, peripapillary chorioretinal atrophy, and choroidal neovascularization (CNV) in the absence of vitreous inflammation (Fig. 7.1). The characteristic findings of POHS may be detected in completely asymptomatic individuals; however, the development of CNV can result in a variety of symptoms, including metamorphopsia, paracentral scotomas, and vision loss. Numerous treatment modalities have been employed for POHS, including laser photocoagulation, vitreoretinal surgery, photodynamic therapy (PDT), corticosteroid therapy, and anti-vascular endothelial growth factor (VEGF) therapy, now the dominant treatment in current practice patterns.

W. Stevenson · E. Alvarez · A. Mallick · F. Yanoga · F. Davidorf
C. M. Cebulla (✉)
Department of Ophthalmology and Visual Science, Havener Eye Institute, The Ohio State University Wexner Medical Center, Columbus, OH, USA
e-mail: Colleen.Cebulla@osumc.edu

Etiopathogenesis

In 1906, the autopsy results of a fatal systemic infection were described, and this infection was eventually determined to have been caused by *H. capsulatum* (Darling 1906). *H. capsulatum* is a dimorphic fungus that is typically found in bird and bat droppings and contaminated soil. *H. capsulatum* can be found throughout the world, but it is most commonly found in and around the Ohio and Mississippi River Valleys (Manos et al. 1956). It has been estimated that between 60 and 90% of the people living in and around the Ohio and Mississippi River Valleys have been exposed to *H. capsulatum*. The clinical signs of POHS are thought to become apparent from 10 to 30 years after the primary infection. Most of those diagnosed with POHS in the United States have lived in an endemic area (Smith and Ganley 1971). The prevalence of POHS has been estimated to be as high as 5.3% in endemic areas (Oliver et al. 2005). The diagnosis of POHS is typically made around 36 years of age, with disciform macular scars typically occurring between 30 and 39 years (Smith et al. 1972). The clinical signs of POHS are equally common in men and women. The prevalence of POHS seems to be similar between Caucasians and African Americans; however, disciform scarring is more common in Caucasians (Baskin et al. 1980).

Histoplasmosis typically begins as an asymptomatic pulmonary infection acquired via the inhalation of airborne *H. capsulatum* spores. *H. capsulatum* can subsequently disseminate through the bloodstream to extrapulmonary sites such as the choroid. A self-limiting and largely asymptomatic multifocal choroiditis can develop that is characterized by small yellow or gray choroidal lesions in the midperiphery. The evolution of these choroidal lesions into the characteristic atrophic chorioretinal scars of POHS has been described (Watzke and Claussen 1981). Histopathology of these chorioretinal scars reveals a dense lymphocytic infiltrate at the level of the choroid. These chorioretinal scars can reactivate following repeat exposure to *H. capsulatum* antigens, such as in *Histoplasma* skin testing (Woods and Wahlen 1959). The DNA of *H. capsulatum* has been identified in the chorioretinal

I. K. Kim (ed.), *Macular Disorders*, Retina Atlas, https://doi.org/10.1007/978-981-15-3001-2_7

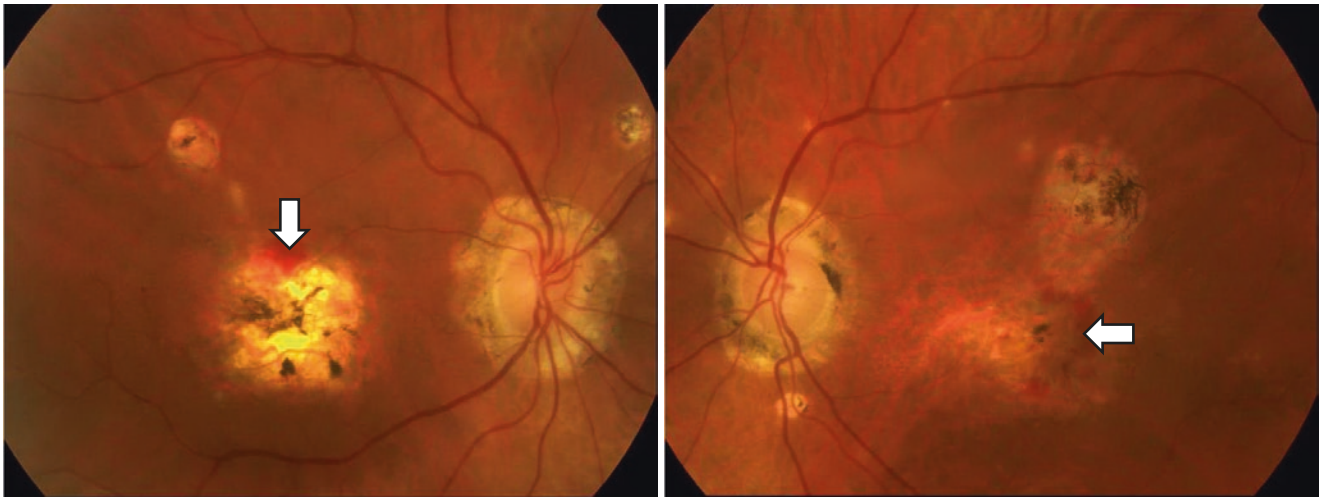

Fig. 7.1 Atrophic chorioretinal scars, peripapillary chorioretinal atrophy, and choroidal neovascularization (arrows) in a patient with bilateral POHS

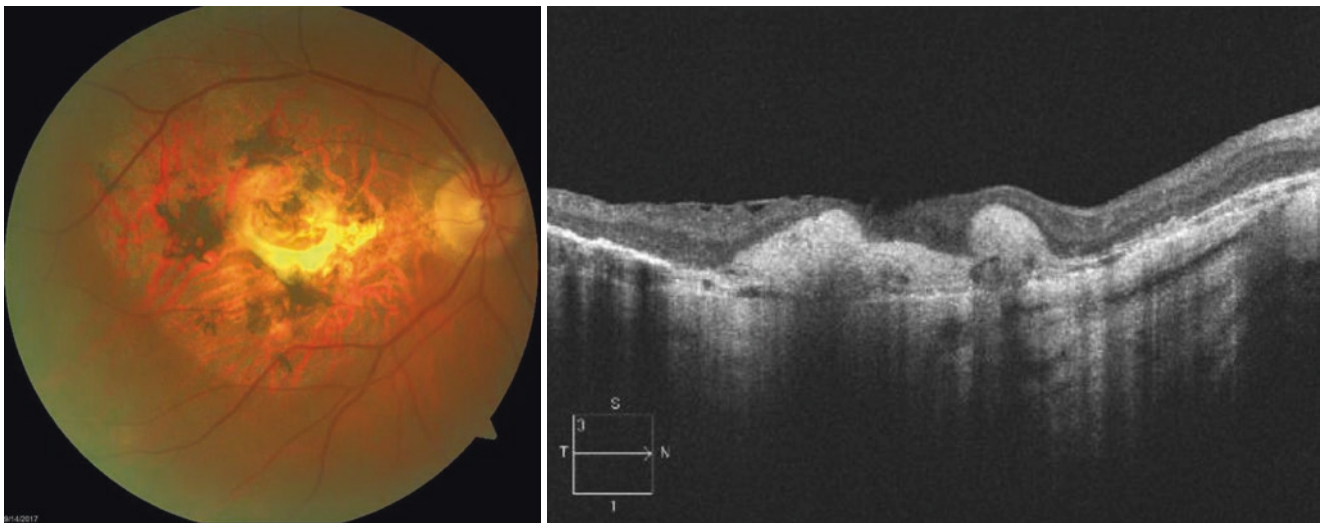

Fig. 7.2 Disciform macular scar as a result of untreated choroidal neovascularization secondary to POHS

scars of an enucleated eye with POHS (Spencer et al. 2003). The chronic presence of latent *H. capsulatum*, *H. capsulatum* antigens, or *H. capsulatum*-specific lymphocytes in these chorioretinal scars may explain their potential to reactivate and progress over time. Interestingly, certain human leukocyte antigens, namely HLA-B7 and HLA-DRw2, have been associated with POHS, indicating a source of genetic susceptibility (Meredith et al. 1980). The chorioretinal lesions in POHS disrupt Bruch's membrane and the retinal pigment epithelium, thereby promoting the development of CNV. This CNV can cause exudative and hemorrhagic retinal detachment with resultant sight-limiting disciform maculopathy (Fig. 7.2).

Clinical and Imaging Findings

A series of landmark clinical studies introduced the classic clinical findings of POHS. In 1942, Reid et al. evaluated a fatal case of histoplasmosis and described "small, white, irregular areas surrounded by hemorrhage—not unlike tubercles" in the patient's fundus (Reid et al. 1942). In 1959, Woods and Wahlen identified 19 patients who were *Histoplasma* skin test positive and exhibited a spectrum of ocular findings, including "discrete, focal spots of atrophic chorioretinitis" and subretinal cysts that could involve secondary hemorrhage, chorioretinal degeneration, and pigmentary gliosis (Woods and Wahlen 1959). In 1966, Schlaegel and Kenney described peripapillary atrophic and pigmentary changes in patients who were *Histoplasma* skin test positive and had the characteristic chorioretinal lesions associated with POHS (Schlaegel and Kenney 1966). The classic clinical findings of POHS are now considered to be: (1) macular and midperipheral atrophic chorioretinal scars, commonly referred to as "Histo spots," (2) peripapillary chorioretinal atrophy and pigmentary changes, and (3) CNV in the absence of vitreous inflammation (Fig. 7.3).

Histo spots are white or yellow atrophic chorioretinal scars with sharp "punched out" borders and varying degrees of pigmentation. Histo spots are typically found in the macula and midperiphery, and they can range in number from 1 to over 100 (Smith and Utz 1972). Although individual Histo spots typically remain stable over time, their size and shape has been noted to change in some cases. Furthermore, new Histo spots have been found to develop in up to 26% of eyes over long-term follow-up (Schlaegel 1975). In approximately 5% of patients, a linear or curvilinear pattern of confluent atrophic chorioretinal scars can be found in the periphery, known as "linear streaks" (Fountain and Schlaegel 1981) (Fig. 7.4). Histo spots typically demonstrate hyperfluorescent window defects on fluorescein angiography. Peripapillary chorioretinal atrophy and pigmentary changes are found in a majority of patients with POHS.

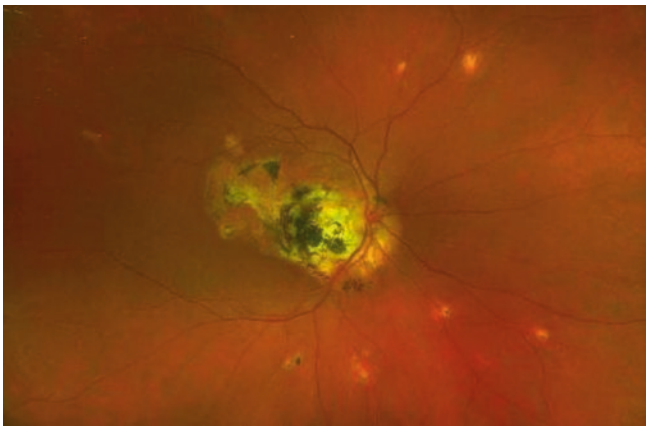

Fig. 7.3 Atrophic chorioretinal scars, peripapillary chorioretinal atrophy, and disciform macular scar in a patient with POHS

CNV has been found to develop in up to 4.5% of patients with POHS (Schlaegel 1975). CNV in POHS elicits the same symptoms as CNV in other conditions, including metamorphopsia, paracentral scotomas, and vision loss. Peripheral CNV lesions can be large and mimic choroidal melanoma. When CNV is suspected, fluorescein angiography can be used to confirm its presence and evaluate its size and location. Fluorescein angiography may demonstrate leakage with increasing intensity and expanding borders or pooling with increasing intensity and stable borders (Fig. 7.5). Indocyanine green angiography can also be used to demonstrate hyperfluorescence as a result of a disorganized choriocapillaris (Diaz et al. 2015). Newer imaging modalities such as optical coherence tomography-angiography can also be used to demonstrate subretinal CNV (Fig. 7.6). Another clinical finding in POHS is the absence of intraocular inflammation. Presumably, there is no inflammation because patients are seen after the initial choroiditis has resolved. This lack of inflammation is important for differentiating POHS from other conditions such as toxoplasmic chorioretinitis and multifocal choroiditis.

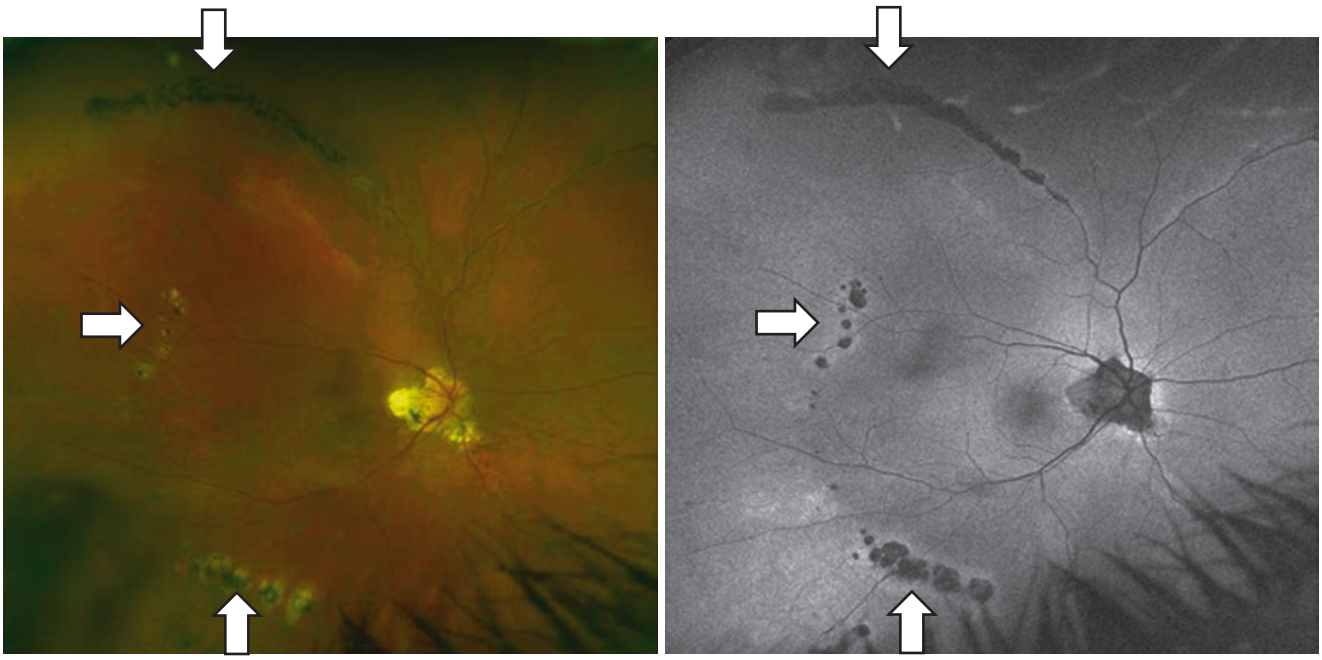

Fig. 7.4 Peripheral curvilinear confluent chorioretinal scars (arrows) known as "linear streaks" in a patient with POHS

Fig. 7.5 Fluorescein angiography demonstrating choroidal neovascularization with progressive leakage in a patient with POHS

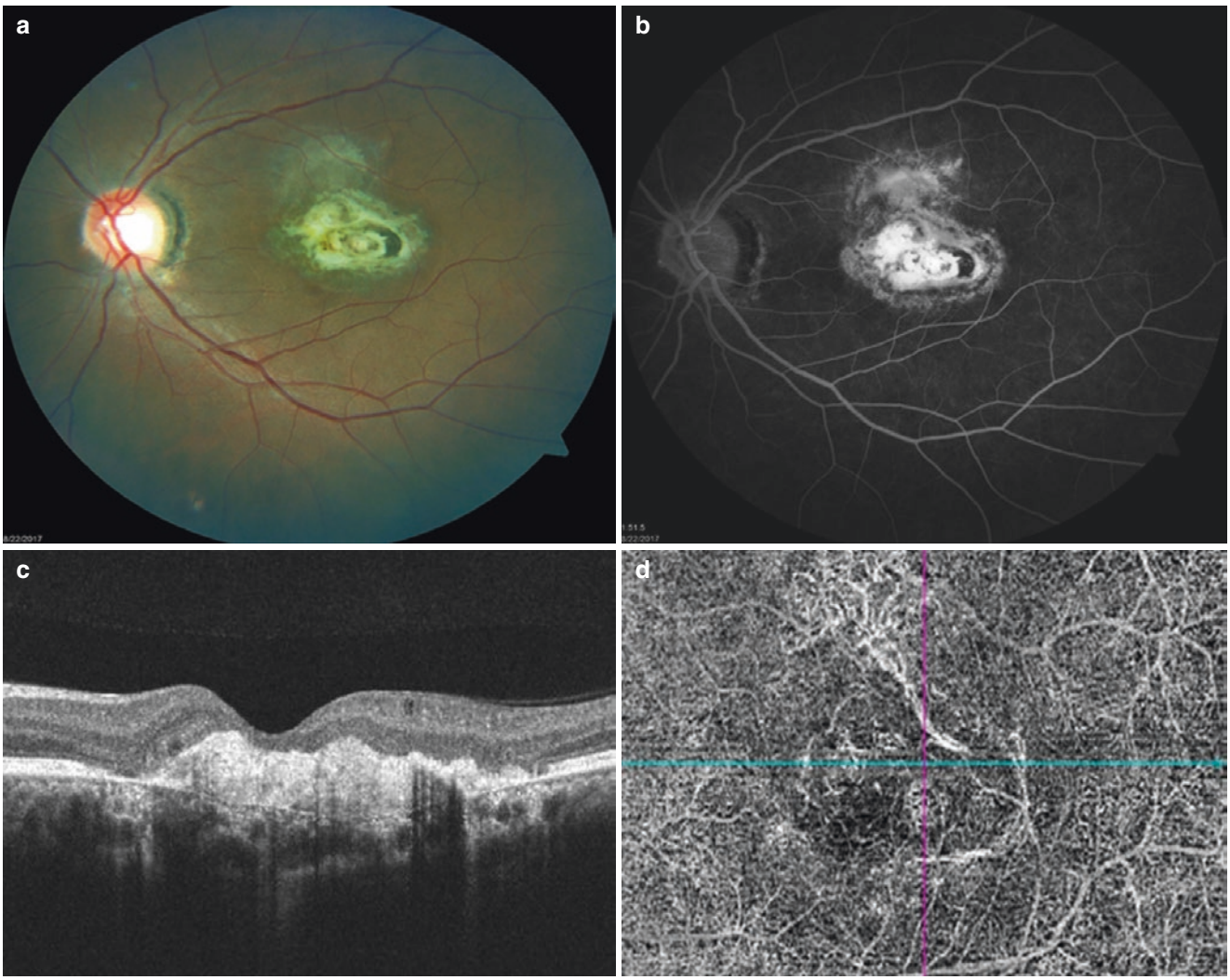

Fig. 7.6 A 32-year-old female with a chronic untreated choroidal neovascularization due to POHS. (**a**) Color fundus photograph showing a macular disciform scar. (**b**) Fluorescein angiography demonstrates hyperfluorescence of the lesion. (**c**) OCT revealing subretinal fibrosis. (**d**) OCT-angiography demonstrating choroidal neovascularization at the level of the choriocapillaris

Management

Observation

The chorioretinal scars and peripapillary pigmentary changes in POHS are generally asymptomatic and may be diagnosed on routine ocular examination. The treatment of active chorioretinal lesions in POHS has been attempted using numerous interventions, including amphotericin B and systemic corticosteroids, with limited benefit (Giles and Falls 1961; Schlaegel 1983). Most of the active chorioretinal lesions in POHS will eventually give rise to chorioretinal scars. Visual impairment in POHS typically occurs secondary to CNV, and no treatment has been shown to prevent the development of CNV (Feman et al. 1982). Patient education, Amsler grid monitoring, and close observation are typically employed until CNV develops.

Laser Photocoagulation

Laser photocoagulation can be used to selectively destroy CNV. The Macular Photocoagulation Study Group performed a series of clinical trials that investigated laser photocoagulation for the treatment of CNV in POHS. In cases of extrafoveal CNV, untreated eyes were found to have a 3.6-fold higher risk of losing six or more lines of visual acuity as compared to laser-treated eyes at 5 years of follow-up (Macular Photocoagulation Study Group 1991). Recurrences were frequent, with 26% of the laser-treated eyes demonstrating persistent or recurrent CNV at 5 years of follow-up. In cases of juxtafoveal CNV, untreated eyes were found to have a 2.6-fold higher risk of losing six or more lines of visual acuity as compared to laser-treated eyes at 5 years of follow-up (Macular Photocoagulation Study Group 1994). In cases of peripapillary CNV, subgroup analysis revealed that 26% of untreated eyes and 14% of laser-treated eyes lost six or more lines of visual acuity at 3 years of follow-up, indicating that a peripapillary location was not a contraindication to laser photocoagulation (Macular Photocoagulation Study Group 1995). Regarding subfoveal CNV, long-term follow-up revealed that 47% of untreated eyes and 22% of laser-treated eyes lost six or more lines of visual acuity after 4 years (Macular Photocoagulation Study Group 1993). Today, laser photocoagulation has largely been supplanted by other treatment modalities, but it can still be an effective adjunctive treatment for extrafoveal CNV.

Vitreoretinal Surgery

In 1988, the surgical removal of submacular hemorrhage and scarring for CNV in age-related macular degeneration was first described (de Juan and Machemer 1988). The Submacular Surgery Trial (SST) was a randomized multicenter prospective clinical trial designed to determine if submacular CNV excision was superior to observation for the treatment of idiopathic and POHS-associated CNV (Flynn and Scott 2004; Sadda et al. 2004; Thuruthumaly et al. 2014). Success was defined as either visual acuity improvement or no more than one line of visual acuity loss at 24 months of follow-up (Flynn and Scott 2004). At 24 months of follow-up, 46% of the observation cohort met this definition of success as compared to 55% of the surgery-treated cohort (Flynn and Scott 2004). Unfortunately, 45% of the surgery-treated patients lost greater than seven letters of visual acuity at 24 months of follow-up (Nielsen et al. 2012). The SST determined that only those patients with baseline visual acuity of 20/100 or worse stood to gain a modest benefit from submacular CNV excision (Almony et al. 2008; Schadlu et al. 2008; Walia et al. 2016). Other studies have demonstrated that the recurrence rate of subfoveal CNV approaches 50%, with over 80% of these patients presenting with a re-bleed within 6 months of surgery (Melberg et al. 1996). With the advent of superior treatments such as anti-VEGF therapy, surgical excision of CNV is now largely obsolete (Flynn and Scott 2004; Diaz et al. 2015).

Photodynamic Therapy

In PDT with verteporfin, verteporfin is delivered to the CNV through the vasculature and activated by a specific wavelength of light, resulting in the production of cytotoxic singlet oxygen that causes blood vessel thrombosis. The utility of PDT in the treatment of CNV in POHS has primarily been demonstrated in retrospective case series. In 2000, a preliminary study involving a single patient with CNV secondary to POHS demonstrated that PDT was well tolerated and yielded a reduction in the area of CNV leakage (Sickenberg et al. 2000). Subsequently, multiple retrospective case series have revealed that PDT stabilized or improved visual acuity in a majority of patients with CNV in POHS (Busquets et al. 2003; Liu et al. 2004; Shah et al. 2005). A relatively small prospective uncontrolled open-label clinical trial demonstrated that PDT improved average visual acuity by six letters and decreased CNV leakage at 2 years of follow-up (Rosenfeld et al. 2004). A retrospective comparative case series found that combination therapy using both PDT and intravitreal bevacizumab was equivalent to intravitreal bevacizumab alone with regards to visual acuity at 3 years of follow-up (Cionni et al. 2012). A large retrospective study reported that combination therapy utilizing bevacizumab and PDT not only decreased the total number of injections required to stabilize or improve visual acuity, but also increased the time to recurrence interval (Cionni et al. 2012; Diaz et al. 2015).

Corticosteroid Therapy

Corticosteroids inhibit CNV by suppressing inflammatory cell recruitment, proinflammatory cytokine expression, and vascular endothelial cell growth (Martidis et al. 1999; Ciulla et al. 2001; Holekamp et al. 2005; Dorrell et al. 2007). Oral administration, sub-Tenon's injection, and intravitreal injection of corticosteroids have all been used to stabilize subfoveal CNV in POHS (Ciulla et al. 2001; Rechtman et al. 2003; Ramaiya et al. 2013; Walia et al. 2016). Favorable visual outcomes have also been observed in juxtafoveal CNV treated with intravitreal triamcinolone at 17 months or more of follow-up (Rechtman et al. 2003; Prasad and Van Gelder 2005). In one study, 70% of patients required only a single intravitreal triamcinolone injection to obtain vision stabilization as compared to 10% and 20% requiring two or more injections, respectively (Prasad and Van Gelder 2005). Fluocinolone acetonide implants used for CNV in POHS have been found to induce visual acuity stabilization or modest improvement for up to 33 months after implantation (Diaz et al. 2015). The most common side effects of steroid use for the treatment of CNV are elevated intraocular pressure and cataract formation, both of which can require surgical intervention (Prasad and Van Gelder 2005; Ramaiya et al. 2013; Diaz et al. 2015).

Anti-vascular Endothelial Growth Factor

The promising outcomes obtained for patients with CNV in exudative age-related macular degeneration paved the way for patients with CNV in POHS to be treated with anti-VEGF agents, including bevacizumab, ranibizumab, and aflibercept. A retrospective case series investigating intravitreal bevacizumab for the treatment of CNV in POHS found that 24 of 28 eyes experienced an improvement or stabilization in visual acuity with an average of 1.8 treatments over an average of 22.4 weeks (Schadlu et al. 2008). Another retrospective case series compared intravitreal bevacizumab monotherapy with combination intravitreal bevacizumab and PDT for the treatment of subfoveal or juxtafoveal CNV in POHS (Cionni et al. 2012). Of the 116 eyes that received intravitreal bevacizumab monotherapy at an average of 4.24 treatments per year, visual acuity improved from an average of 20/83 to 20/54 at 24 months of follow-up. There was no significant difference in visual acuity outcomes between intravitreal bevacizumab monotherapy and combination intravitreal bevacizumab and PDT. A relatively small retrospective case series utilized intravitreal bevacizumab and ranibizumab for the treatment of CNV in POHS and found that both treatments improved visual acuity with an average of 2.6 injections over about 28 months of follow-up (Hu et al. 2014). Interestingly, a comparison of intravitreal ranibizumab and PDT revealed similar changes in visual acuity with 19.6 letters gained in the ranibizumab group and 21 letters gained in the PDT group at 1 year of follow-up; however, all of the PDT-treated patients required rescue intravitreal ranibizumab treatment to obtain this result (Ramaiya et al. 2013). A randomized open-label clinical trial investigating intravitreal aflibercept for the treatment of CNV in POHS with a total of 39 patients demonstrated that treatment as needed was equivalent to a mandatory dosing schedule (Toussaint et al. 2018). Treatment as needed resulted in an average gain of 19 letters and a significant decrease in central subfield thickness at 12 months of follow-up. Early treatment initiation with anti-VEGF agents has been found to confer the best long-term visual acuity outcomes, underscoring the importance of early diagnosis and treatment (Schadlu et al. 2008). Unlike the persistent CNV seen in exudative age-related macular degeneration, the CNV in POHS demonstrates long intervals of quiescence with sudden recurrences and rapid response to intravitreal anti-VEGF treatment (Cionni et al. 2012). For this reason, there is no established treatment regimen for CNV in POHS and close follow-up is advised (Nielsen et al. 2012).

References

Almony A, Thomas MA, Atebara NH, Holekamp NM, Del Priore LV. Long-term follow-up of surgical removal of extensive peripapillary choroidal neovascularization in presumed ocular histoplasmosis syndrome. Ophthalmology. 2008;115:540–545.e545.

Baskin MA, Jampol LM, Huamonte FU, Rabb MF, Vygantas CM, Wyhinny G. Macular lesions in blacks with the presumed ocular histoplasmosis syndrome. Am J Ophthalmol. 1980;89:77–83.

Busquets MA, Shah GK, Wickens J, Callanan D, Blinder KJ, Burgess D, Grand MG, Holekamp NM, Boniuk I, Joseph DP, Thomas MA, Fish E, Bakal J, Hollands H, Sharma S. Ocular photodynamic therapy with verteporfin for choroidal neovascularization secondary to ocular histoplasmosis syndrome. Retina. 2003;23:299–306.

Cionni DA, Lewis SA, Petersen MR, Foster RE, Riemann CD, Sisk RA, Hutchins RK, Miller DM. Analysis of outcomes for intravitreal bevacizumab in the treatment of choroidal neovascularization secondary to ocular histoplasmosis. Ophthalmology. 2012;119:327–32.

Ciulla TA, Piper HC, Xiao M, Wheat LJ. Presumed ocular histoplasmosis syndrome: update on epidemiology, pathogenesis, and photodynamic, antiangiogenic, and surgical therapies. Curr Opin Ophthalmol. 2001;12:442–9.

Darling S. A protozoan general infection producing pseudo tubercles in the lungs and focal necrosis in the liver, spleen, and lymph nodes. JAMA. 1906;46:1.

de Juan E Jr, Machemer R. Vitreous surgery for hemorrhagic and fibrous complications of age-related macular degeneration. Am J Ophthalmol. 1988;105:25–9.

Diaz RI, Sigler EJ, Rafieetary MR, Calzada JI. Ocular histoplasmosis syndrome. Surv Ophthalmol. 2015;60:279–95.

Dorrell M, Uusitalo-Jarvinen H, Aguilar E, Friedlander M. Ocular neovascularization: basic mechanisms and therapeutic advances. Surv Ophthalmol. 2007;52(Suppl 1):S3–19.

Feman SS, Podgorski SF, Penn MK. Blindness from presumed ocular histoplasmosis in Tennessee. Ophthalmology. 1982;89:1295–8.

Flynn HW Jr, Scott IU. Now that we have the results of the subretinal surgery trials, how do we manage the patient? Arch Ophthalmol. 2004;122:1705–6.

Fountain JA, Schlaegel TF. Linear streaks of the equator in the presumed ocular histoplasmosis syndrome. Arch Ophthalmol. 1981;99:246–8.

Giles CL, Falls HF. Further evaluation of amphotericin-B therapy in presumptive histoplasmosis chorioretinitis. Am J Ophthalmol. 1961;51:588–98.

Holekamp NM, Thomas MA, Pearson A. The safety profile of long-term, high-dose intraocular corticosteroid delivery. Am J Ophthalmol. 2005;139:421–8.

Hu J, Hoang QV, Chau FY, Blair MP, Lim JI. Intravitreal anti-vascular endothelial growth factor for choroidal neovascularization in ocular histoplasmosis. Retin Cases Brief Rep. 2014;8:24–9.

Liu JC, Boldt HC, Folk JC, Gehrs KM. Photodynamic therapy of subfoveal and juxtafoveal choroidal neovascularization in ocular histoplasmosis syndrome: a retrospective case series. Retina. 2004;24:863–70.

Macular Photocoagulation Study Group. Argon laser photocoagulation for neovascular maculopathy. Five-year results from randomized clinical trials. Macular Photocoagulation Study Group. Arch Ophthalmol. 1991;109:1109–14.

Macular Photocoagulation Study Group. Laser photocoagulation of subfoveal neovascular lesions of age-related macular degeneration. Updated findings from two clinical trials. Macular Photocoagulation Study Group. Arch Ophthalmol. 1993;111:1200–9.

Macular Photocoagulation Study Group. Laser photocoagulation for juxtafoveal choroidal neovascularization. Five-year results from randomized clinical trials. Macular Photocoagulation Study Group. Arch Ophthalmol. 1994;112:500–9.

Macular Photocoagulation Study Group. Laser photocoagulation for neovascular lesions nasal to the fovea. Results from clinical trials for lesions secondary to ocular histoplasmosis or idiopathic causes. Macular Photocoagulation Study Group. Arch Ophthalmol. 1995;113:56–61.

Manos NE, Ferebee SH, Kerschbaum WF. Geographic variation in the prevalence of histoplasmin sensitivity. Dis Chest. 1956;29:649–68.

Martidis A, Miller DG, Ciulla TA, Danis RP, Moorthy RS. Corticosteroids as an antiangiogenic agent for histoplasmosis-related subfoveal choroidal neovascularization. J Ocul Pharmacol Ther. 1999;15:425–8.

Melberg NS, Thomas MA, Dickinson JD, Valluri S. Managing recurrent neovascularization after subfoveal surgery in presumed ocular histoplasmosis syndrome. Ophthalmology. 1996;103:1064–7; discussion 1067–8.

Meredith TA, Smith RE, Duquesnoy RJ. Association of HLA-DRw2 antigen with presumed ocular histoplasmosis. Am J Ophthalmol. 1980;89:70–6.

Nielsen JS, Fick TA, Saggau DD, Barnes CH. Intravitreal anti-vascular endothelial growth factor therapy for choroidal neovascularization secondary to ocular histoplasmosis syndrome. Retina. 2012;32:468–72.

Oliver A, Ciulla TA, Comer GM. New and classic insights into presumed ocular histoplasmosis syndrome and its treatment. Curr Opin Ophthalmol. 2005;16:160–5.

Prasad AG, Van Gelder RN. Presumed ocular histoplasmosis syndrome. Curr Opin Ophthalmol. 2005;16:364–8.

Ramaiya KJ, Blinder KJ, Ciulla T, Cooper B, Shah GK. Ranibizumab versus photodynamic therapy for presumed ocular histoplasmosis syndrome. Ophthalmic Surg Lasers Imaging Retina. 2013;44:17–21.

Rechtman E, Allen VD, Danis RP, Pratt LM, Harris A, Speicher MA. Intravitreal triamcinolone for choroidal neovascularization in ocular histoplasmosis syndrome. Am J Ophthalmol. 2003;136:739–41.

Reid JD, Schere JH, Herbut PA, Irving H. Systemic histoplasmosis diagnosed before death and produced experimentally in guinea pigs. J Lab Clin Med. 1942;27:419–34.

Rosenfeld PJ, Saperstein DA, Bressler NM, Reaves TA, Sickenberg M, Rosa RH, Sternberg P, Aaberg TM, Verteporfin in Ocular Histoplasmosis Study Group. Photodynamic therapy with verteporfin in ocular histoplasmosis: uncontrolled, open-label 2-year study. Ophthalmology. 2004;111:1725–33.

Sadda SR, Pieramici DJ, Marsh MJ, Bressler NM, Bressler SB. Changes in lesion size after submacular surgery for subfoveal choroidal neovascularization in the submacular surgery trials pilot study. Retina. 2004;24:888–99.

Schadlu R, Blinder KJ, Shah GK, Holekamp NM, Thomas MA, Grand MG, Engelbrecht NE, Apte RS, Joseph DP, Prasad AG, Smith BT, Sheybani A. Intravitreal bevacizumab for choroidal neovascularization in ocular histoplasmosis. Am J Ophthalmol. 2008;145:875–8.

Schlaegel TF. The natural history of histo spots in the disc-macula area. Int Ophthalmol Clin. 1975;15:19–28.

Schlaegel TF. Corticosteroids in the treatment of ocular histoplasmosis. Int Ophthalmol Clin. 1983;23:111–23.

Schlaegel TF, Kenney D. Changes around the optic nervehead in presumed ocular histoplasmosis. Am J Ophthalmol. 1966;62:454–8.

Shah GK, Blinder KJ, Hariprasad SM, Thomas MA, Ryan EH, Bakal J, Sharma S. Photodynamic therapy for juxtafoveal choroidal neovascularization due to ocular histoplasmosis syndrome. Retina. 2005;25:26–32.

Sickenberg M, Schmidt-Erfurth U, Miller JW, Pournaras CJ, Zografos L, Piguet B, Donati G, Laqua H, Barbazetto I, Gragoudas ES, Lane AM, Birngruber R, van den Bergh H, Strong HA, Manjuris U, Gray T, Fsadni M, Bressler NM. A preliminary study of photodynamic therapy using verteporfin for choroidal neovascularization in pathologic myopia, ocular histoplasmosis syndrome, angioid streaks, and idiopathic causes. Arch Ophthalmol. 2000;118:327–36.

Smith RE, Ganley JP. An epidemiologic study of presumed ocular histoplasmosis. Trans Am Acad Ophthalmol Otolaryngol. 1971;75:994–1005.

Smith JW, Utz JP. Progressive disseminated histoplasmosis. A prospective study of 26 patients. Ann Intern Med. 1972;76:557–65.

Smith RE, Ganley JP, Knox DL. Presumed ocular histoplasmosis. II. Patterns of peripheral and peripapillary scarring in persons with nonmacular disease. Arch Ophthalmol. 1972;87:251–7.

Spencer WH, Chan CC, Shen DF, Rao NA. Detection of histoplasma capsulatum DNA in lesions of chronic ocular histoplasmosis syndrome. Arch Ophthalmol. 2003;121:1551–5.

Thuruthumaly C, Yee DC, Rao PK. Presumed ocular histoplasmosis. Curr Opin Ophthalmol. 2014;25:508–12.

Toussaint BW, Kitchens JW, Marcus DM, Miller DM, Kingdon ML, Holcomb D, Ivey K. Intravitreal aflibercept injection for choroidal neovascularization due to presumed ocular histoplasmosis syndrome: the Handle Study. Retina. 2018;38:755–63.

Walia HS, Shah GK, Blinder KJ. Treatment of CNV secondary to presumed ocular histoplasmosis with intravitreal aflibercept 2.0 mg injection. Can J Ophthalmol. 2016;51:91–6.

Watzke RC, Claussen RW. The long-term course of multifocal choroiditis (presumed ocular histoplasmosis). Am J Ophthalmol. 1981;91:750–60.

Woods AC, Wahlen HE. The probable role of benign histoplasmosis in the etiology of granulomatous uveitis. Trans Am Ophthalmol Soc. 1959;57:318–43.

Macular Telangiectasis Type 2

8

Richard F. Spaide

Abbreviations

CNTF	Ciliary neurotrophic factor
MacTel 2	Macular telangiectasia Type 2
MCT	Mono-carboxylate transporters
OCT	Optical coherence tomography
OCTA	Optical coherence tomography angiography
PEDF	Pigment epithelium-derived factor
RPE	Retinal pigment epithelial
sFlt-1	Soluble fms-like tyrosine kinase-1
TGF	Transforming growth factor
TSP-1	Thrombospondin-1
VRAS	Volume rendered angiographic and structural

Introduction

Macular telangiectasia Type 2 (MacTel 2) is a simplified terminology (Yannuzzi et al. 2006) referring to idiopathic juxtafoveolar telangiectasia Type 2 as originally described by Gass in the 1977 edition of his atlas and subsequently in a publication with Oyakawa (Gass 1977; Gass and Oyakawa 1982). Patients with this condition can have graying and decreased transparency of the parafoveolar retina, crystalline deposits in the inner retina, a migration of hyperplastic retinal pigment epithelium, a lack of macular pigment, and progressive abnormalities of the juxtafoveolar retinal vessels (Charbel Issa et al. 2008, 2009, 2013; Helb et al. 2008; Wu et al. 2013; Gass 1997; Gass and Blodi 1993). Additional retinal vascular abnormalities include right angle veins, proliferation of vessels in the outer retina and subretinal space, and in some patients, obliteration of the foveal avascular zone (Park et al. 1997; Koizumi et al. 2007a). Fluorescein angiography shows ectatic vessels with hyperfluorescence in the involved regions. Gass proposed there was early fluorescein staining of thickened capillary walls that accounted for the appearance of telangiectatic vessels (Gass 1997). Judgments about the vascular changes in MacTel 2 have been based on fluorescein angiography, a modality shown to have poor ability to visualize two of the three main vascular layers in the retina (Spaide et al. 2015b). In particular, the deep capillary plexus is not imaged well by fluorescein angiography.

Imaging Findings

The features of MacTel 2 were first described with a combination of color fundus photography and fluorescein angiography. The eyes show a characteristic loss of transparency and graying, usually starting in the temporal juxtafoveal macula (Figs. 8.1, 8.2, and 8.3). There can be angular gnarly capillaries, creating the appearance of telangiectasis, but the hallmark of telangiectasia, the microaneurysm, is not commonly found. Although the graying and telangiectasia may start in the temporal macula, there is a widespread loss of macular pigment early in the disease. Curiously, the macular graying becomes less prominent upon exposure to light (Jindal et al. 2015). Characteristic findings of MacTel 2 seen in optical coherence tomography (OCT), developed after Gass's original classification, showed some confirmatory and many new findings. Macular thinning and cavitation in the inner retina, outer retina, or both, are common findings. A minority progress to developing full-thickness macular holes with little or no observable vitreous traction, suggesting a failure of the intrinsic macular tissue (Cohen et al. 2007; Olson and Mandava 2006; Koizumi et al. 2007a, b). Gass proposed the telangiectatic vessels had altered structure of the capillary walls that impeded metabolic exchange (Gass 1997). The resultant low-grade chronic nutritional damage was posited to cause degeneration and atrophy of not only the Müller cells, but also of the associated photoreceptor cells (Charbel Issa et al. 2013). Eyes with MacTel 2 were proposed to have decreased macular pigment (Spaide

R. F. Spaide (✉)
Vitreous, Retina, Macula Consultants of New York, New York, NY, USA

I. K. Kim (ed.), *Macular Disorders*, Retina Atlas, https://doi.org/10.1007/978-981-15-3001-2_8

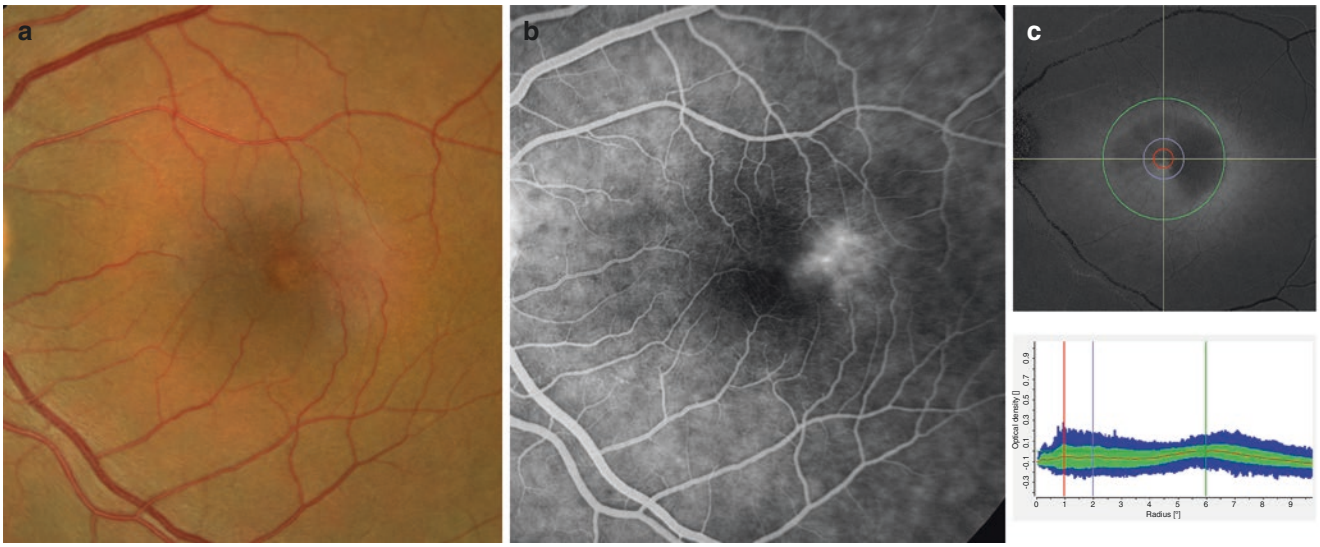

Fig. 8.1 Macular telangiectasis Type 2 with early involvement. (**a**) There is minimal opacification of the temporal juxtafoveal macula. Note how the vessels in the inferotemporal macula arch toward the fovea. (**b**) Fluorescein angiogram showing angular microvessels with leakage in the temporal juxtafoveal macula. (**c**) Even though there is mild disease, the macula lacks macular pigment as shown by the two wavelength autofluorescence image (top) and the radial profile shows a nearly flat profile (bottom)

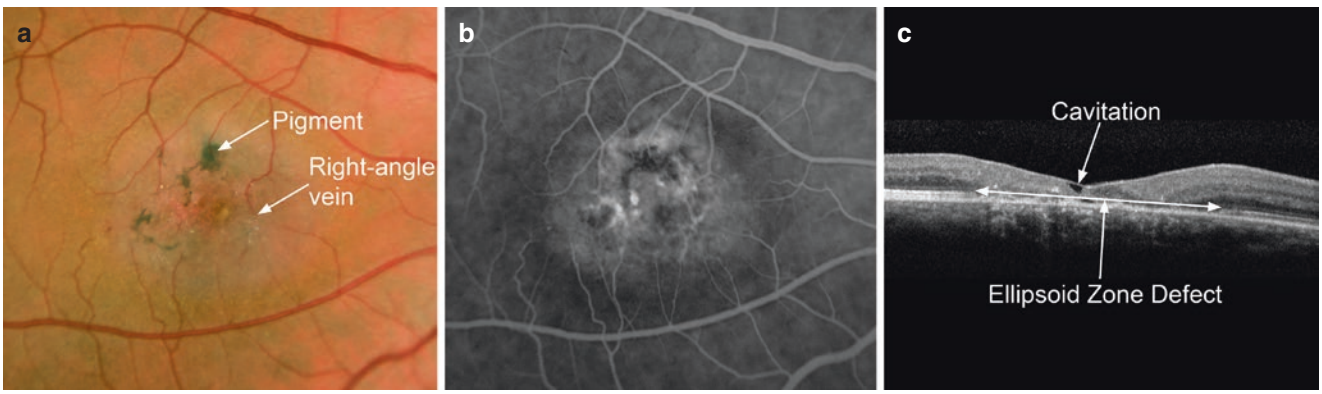

Fig. 8.2 MacTel 2. (**a**) This patient has more advanced disease than the eye in Fig. 8.1. There are multiple collections of pigment and a right-angle vein visible. (**b**) There is widespread leakage and staining of the central macula. At one time there was controversy about the nature of the leakage in this condition, but dye accumulation in the avascular fovea demonstrates dye accumulation in the substance of the retina. (**c**) The patient has cavitations with intact overlying internal limiting membrane and a large defect in the ellipsoid zone

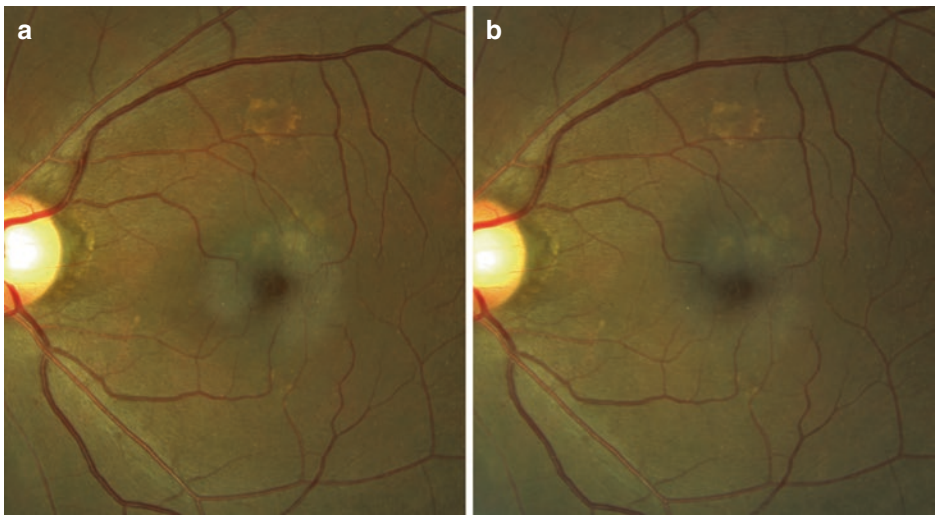

Fig. 8.3 Change in macular opacity with light exposure. (**a**) Note the perifoveal opacification in the first fundus photograph. (**b**) Immediately after the first photograph the patient had this photograph. There is less macular opacification. With patching the opacification would return

1999), which was shown when imaged by blue reflectance and two wavelength autofluorescence (Charbel Issa et al. 2008; Helb et al. 2008; Wong et al. 2009).

Optical coherence tomography angiography (OCTA) has the potential to image all vascular layers of the retina, as compared with the more limited ability of fluorescein angiography. OCTA provides depth-resolved images of retinal vascular flow. Initial OCTA descriptions by Thorell et al. and Spaide and colleagues of MacTel 2 highlighted the invasion of vessels into deeper layers of the retina (Thorell et al. 2014; Spaide et al. 2015a, b). Coexistent abnormalities of both the deep and inner plexus of the retinal vasculature were evident in more advanced cases. In both studies, the OCT data was segmented into layers using an "en-face" strategy in which anatomic layers of the retina were used to create slabs of tissue data, and flow information from those layers was derived from changes in reflectance amplitude. The problem with OCTA en face imaging is that it relies on segmentation. Since there is loss of the macular tissue and disruption of laminations, segmentations performed by OCTA instruments are frequently incorrect. This produces images of vessels where potentially more than one layer is merged; additionally, images may show lack of vessels in regions where the segmentation deviates outside of regions that do not ordinarily contain vessels. Finally, en face imaging does not show structural changes occurring in tissue.

Volume rendering allows the use of all layers of the imaging data and does not strictly depend on segmentation (Spaide et al. 2015a, b). Often an element of segmentation is introduced by adding color to highlight different vascular layers in the retina. Volume rendered angiographic and structural (VRAS) OCT is a newer approach that integrates the structural abnormalities from the reflectance OCT with flow information derived from OCT angiography (Spaide 2015; Spaide et al. 2017; Balaratnasingam et al. 2015). Since the angiographic data is derived from the structural OCT, the scaling, dimensions, and depth interrelationships are maintained. This allows visualization of the associations among vascular abnormalities and structural changes and provides an opportunity to study pathological changes occurring in MacTel 2. VRAS-OCT can be combined with more conventional imaging methods as an extension of the multimodal imaging approach.

MacTel 2 is a difficult disease to understand when evaluating data obtained only from fluorescein angiography and OCT. The additional information supplied by OCTA, especially using volume rendering techniques, has made the disease easier to mentally visualize and understand, despite newer findings being seen. The main findings are contraction of parafoveolar tissue, formation of cavitations and microcavitations, tissue loss, vascular invasion, and fluorescein leakage, and potential for sub-retinal pigment epithelial (RPE) vascular invasion (Figs. 8.4 and 8.5) (Balaratnasingam et al. 2015). These will be discussed in turn.

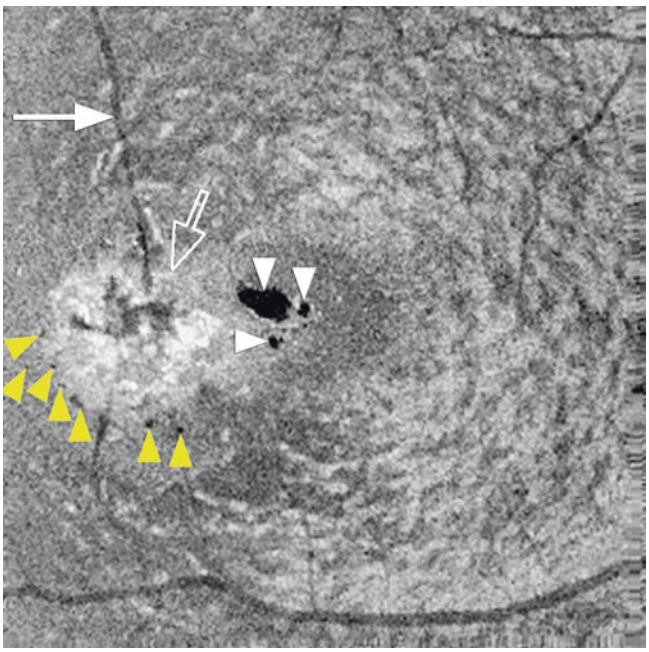

Fig. 8.4 Structural optical coherence tomography scan, 10-microns thick, of right eye of the same patient shown in Fig. 8.2. There is entry of right angle veins at the superior and inferior margin of a hyperreflective zone (open arrow). This zone is ringed temporally and inferiorly by a series of microcavitations (yellow arrowheads). In the fovea are larger cystoid spaces (white arrowheads) and some smaller microcavitations

Tissue Contraction

Although tissue contraction may be a secondary phenomenon in the disease, it produces many of the more salient features of the disease (Spaide et al. 2017, 2018). In eyes with MacTel 2, right angle veins are part of a larger complex that includes a centripetal tissue contraction that appears to distort the surrounding vessels, particularly in the temporal macula. In some eyes, the foveal avascular zone was diminished in size, and was nearly obliterated. The angular distortions of the vessels contribute to the telangiectatic appearance of the vessels. Careful examination of the vessels in the region of a right angle vein shows capillaries bent to form shapes resembling the caret symbol (^) or the apex of a triangle. The apices of these angular figures pointed to a common epicenter, which was not occupied by a vessel. It is possible that this angular character may enhance the appearance of telangiectasis. The contraction occurred in the lateral direction, which may explain the diminution of the foveal avascular zone as has been noted earlier. When fundus photographs taken over many years are evaluated the vascular dragging is readily evident (Figs. 8.6 and 8.7) (Spaide et al. 2018).

The structural OCTs show increased reflectivity of the retinal parenchyma in regions surrounding the origin of right angle veins. Since only part of the increased reflectivity is occupied

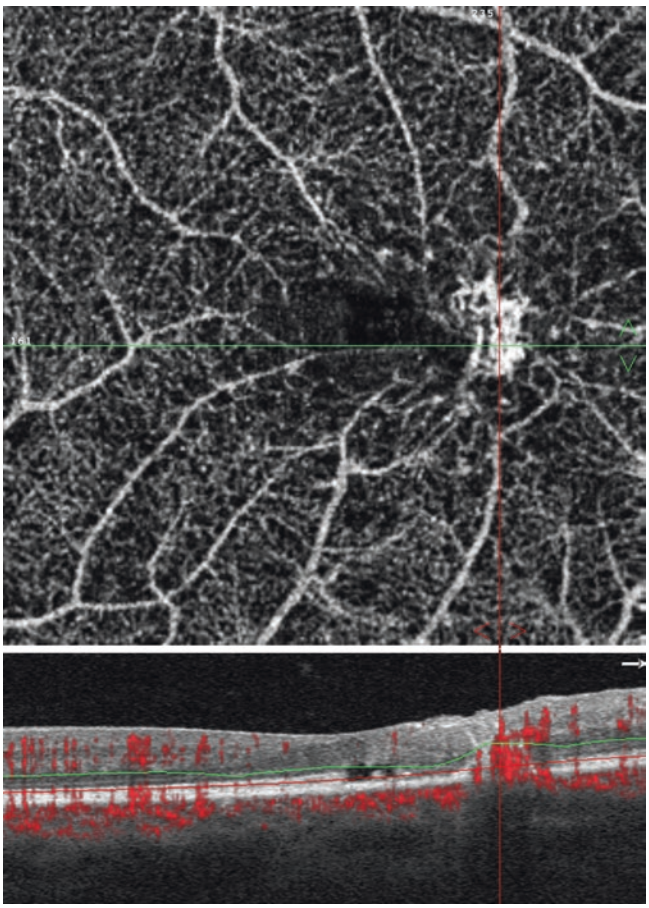

Fig. 8.5 Same eye as shown in Fig. 8.2c. Top, en-face and bottom B-scan with flow overlay in red shows subretinal proliferation of vessels extending through the outer nuclear layer

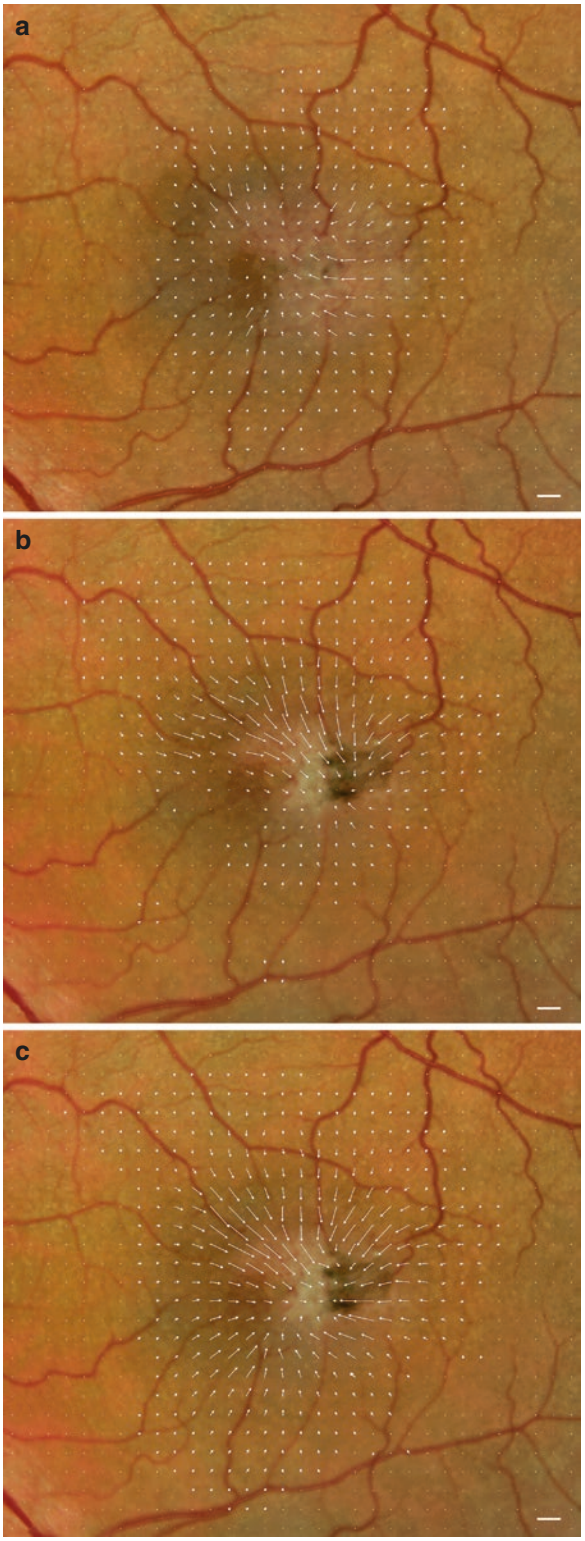

Fig. 8.6 Vector fields illustrating the tissue distortion that occurred with follow-up. (**a**) This is the vector field for the first 6 years of follow-up. The directions of the arrows point to the temporal juxtafoveal macula. (**b**) This is the vector field of the tissue warping from the sixth to the seventh year of follow-up. Note the arrows generally point toward the area of retinal pigmentation. (**c**) The vector field for the entire 7 years of follow-up. The white bar on the lower right of each picture represents 250 μm

by vessels, the implication is the increased reflectivity is caused by alterations in the tissue in which the vessels are embedded (Spaide et al. 2018). Increased reflectivity conceivably can be caused by changes in the architecture of the tissue whereby the ordinarily relatively transparent character of the retinal tissue would have greater scattering properties because of tissue disorganization. It is also possible that normal retinal tissue components could respond in ways that lead to both increased backscatter and tissue contracture. According to the current understanding of the disease process, Müller cell dysfunction or loss is one of the early steps leading to MacTel 2 (Gass 1997; Powner et al. 2010, 2013). In response to a number of stimuli and as an integral part of important ocular diseases, Müller cells can show hypertrophy, proliferation, migration, cytokine production (Brooks et al. 1998; Jingjing et al. 1999), and expression of intermediate filaments and alpha smooth muscle actin (Lewis et al. 1989; Guidry 1997; Guidry et al. 2003). They modulate the inner blood-retina barrier formed by the junctions of retinal vascular endothelial cells (Reichenbach and Bringmann 2010) and are implicated, along with vascular cells, in important disease processes such as proliferative diabetic

retinopathy and proliferative vitreoretinopathy, which can have a vascular component (Bai et al. 2009).

Cavitations and Microcavitations

Cavitations are optically empty spaces within the tissue of the macula related to MacTel 2 (Paunescu et al. 2006). Cavitations are typically found in the temporal fovea adjacent to regions of tissue contraction. The cavitations are likely formed by loss of cellular elements such as Müller cells and photoreceptors. Loss of both of these elements has been documented in histologic evaluation of MacTel 2. The internal limiting membrane initially appears to be intact and may be seen to drape across defects within the fovea. The residual tissue in the parenchyma of the retina is remaining Müller cells and photoreceptors, which may be in various stages of degeneration. A curious finding was the alteration of cavitations from one examination to the next (Spaide et al. 2017). The long-term changes in MacTel 2 appear to be degeneration and atrophy of the macula, but the pronounced changes in structure with appearance and disappearance of cavities and voids imply a more dynamic process. Although there may be degenerative decline, it is possible there are simultaneous reorganization of cell location and reparative processes at work. This may help explain how outer retinal defects can form and heal. Given there appear to be neighboring contractile forces associated with a right angle vein complex, the macular tissue may be under tensile stress. In a study of fracture in material science (Rogers 1960), plastic deformation of ductile materials under stress leads to void formation and under continuing stress the voids can coalesce. Although the cavitations in the macula can eventually contribute to structural failure, an extreme example of which is macular hole formation, which occurs in MacTel 2 (Koizumi et al. 2007a, b), the process seems more complex than failure in ductile materials (Rogers 1960) because the cavities can resolve from one examination to the next. This would imply a healing process that may occur in parallel with tissue deformation and cavitation in this disease. This reorganization of retinal layers may help explain, in part, the abnormal laminations seen in the macula in MacTel 2.

The reactive changes in response to tissue injury caused by the disease may contribute to the altered architecture of the macula; the laminations ordinarily visible in the macula become more indistinct and regions of altered reflectivity appear along with structural changes such as loss of the ellipsoid layer. Of course loss of Müller cells and photoreceptors occur and contribute to the loss of laminations ordinarily seen in the retina. The alteration in expected architecture may belie the cellular composition. Some patients with MacTel 2 have loss of the normal architecture, but retain relatively good visual acuity. This implies there are still functional photoreceptors present.

Outside of the fovea, patients with MacTel may develop many small optically empty spaces, which have been named microcavitations (Figs. 8.4, 8.8, and 8.9). These were found within the ovoid area commonly affected by MacTel, even in regions without apparent vascular involvement, and are typically 50–100 μm in diameter. Green and coworkers found thickening and edema was present in the temporal macular region of their case, with a few "microcavities" present in the retinal tissue (Green et al. 1980). It is possible the microcavitations seen in the present series are similar to those seen by Green et al., except the distribution is different. The microcavitations seen in the present series occupied the "MacTel zone," even in areas with no apparent thickening or edema,

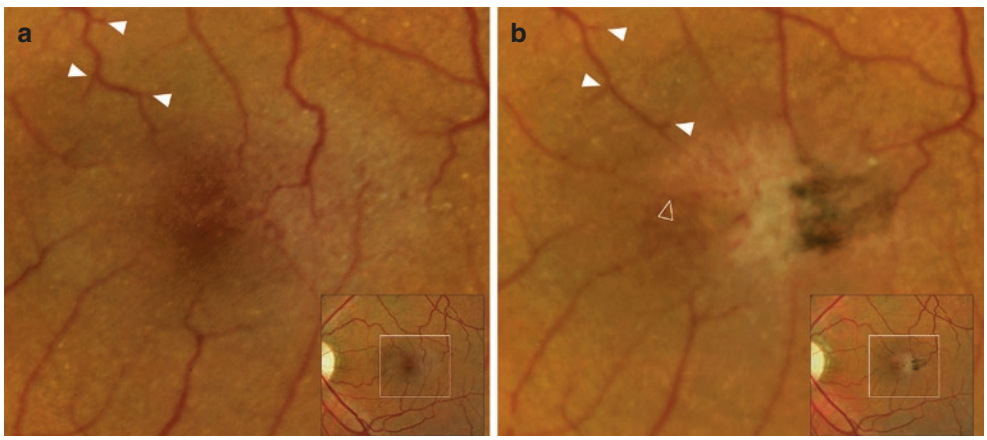

Fig. 8.7 Comparison of vascular morphology over a 7-year follow-up in MacTel 2. This is the same patient illustrated in Fig. 8.1. (**a**) Image at baseline; the inset shows the region from which this magnified was obtained. (**b**) The matched image 7 years later. Note the vascular traction with straightening of vessels. Some of the vessels were pulled into the foveal avascular zone (open arrowhead). In (**a**) branching points of a retinal venule are highlighted with arrowheads. In (**b**) the same branching points are highlighted with arrowheads; note the displacement that has occurred over the intervening time

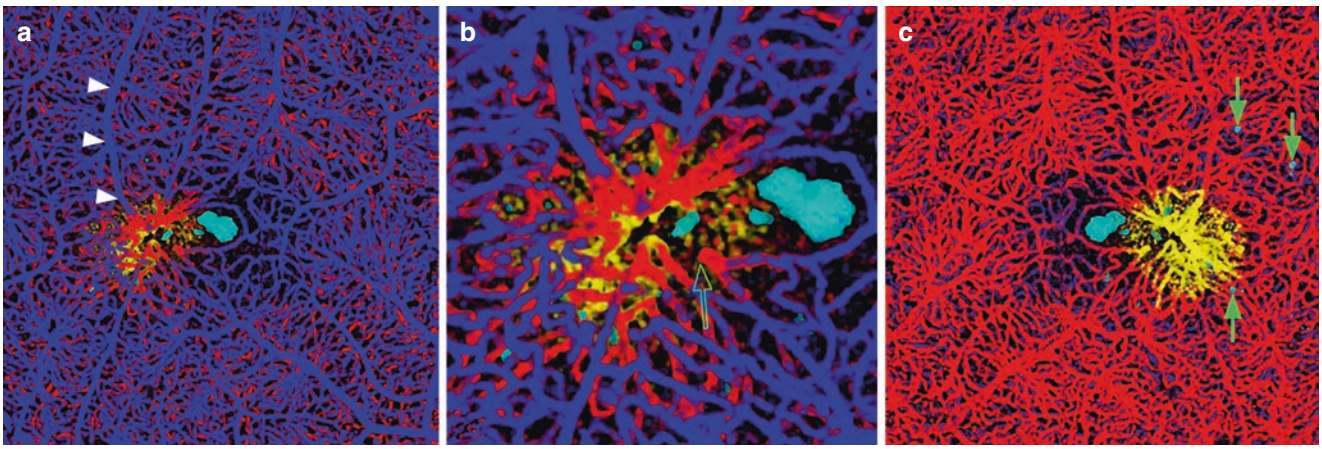

Fig. 8.8 (**a**) MacTel 2 in a 58-year-old with right angle veins, the most prominent of which are shown by the white arrowheads. The vessels on the temporal side of the foveal avascular zone are red, which signifies they are at the level of the deep plexus. In this temporal juxtafoveal region there are no vessels at the level of the inner plexus. Since they are vessels that would ordinarily be at the level of the inner plexus, the implication is that they are being displaced posteriorly. There are cavitations in the fovea. (**b**) The foveal avascular zone is smaller and displaced toward the central focus of the vascular lesion in the temporal macula. Note the vessels of the perifoveal ring are drawn toward the center of the vascular aggregate and form angular figures and their apices (one of which is shown by the open arrow) point toward the center of the vascular aggregate. (**c**) Viewed from the choroidal side, the vessels deeper than the deep plexus are shown in yellow. There are several microcavitations, as shown by the green arrows

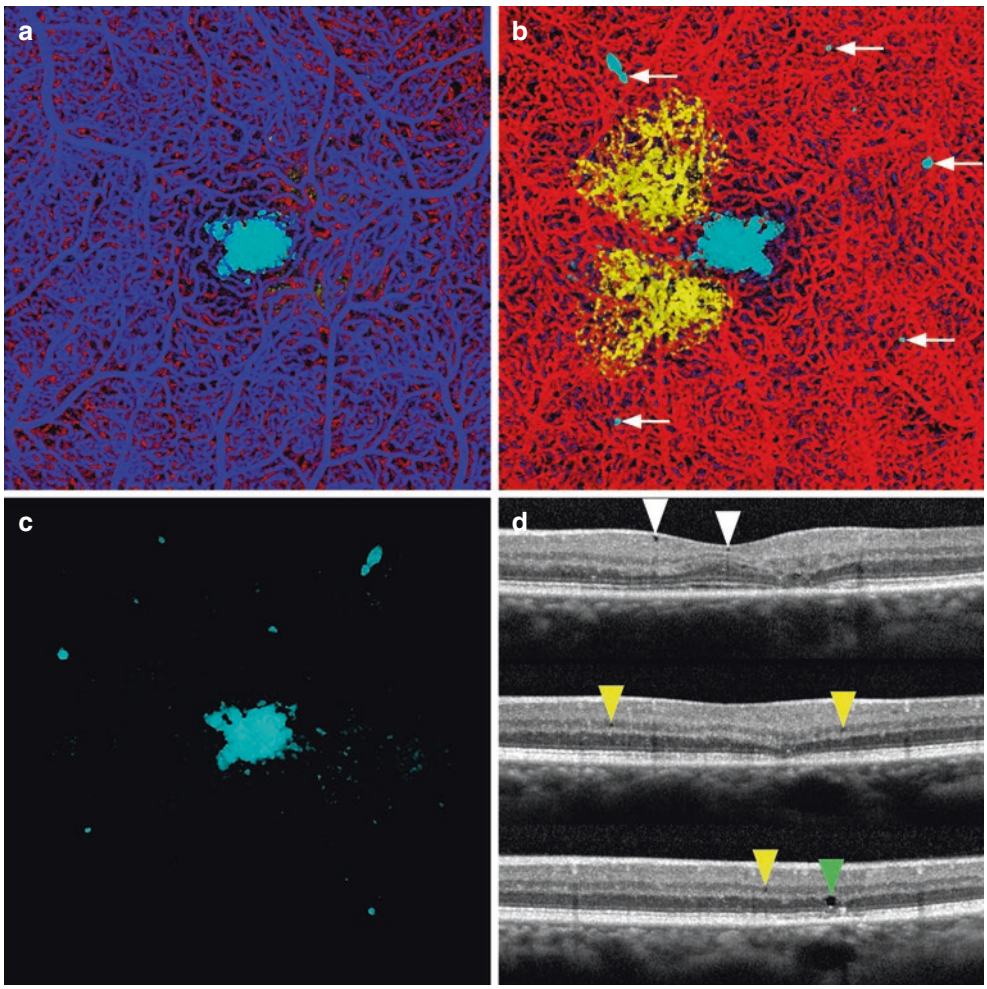

Fig. 8.9 Volume rendered angiographic and structural optical coherence tomography in a 44-year-old with MacTel 2. (**a**) There is a large cavitation in the foveal region. (**b**) When viewed from the choroidal side, the abnormal vessels deep to the deep vascular plexus are shown in yellow. There are numerous microcavitations (arrows). (**c**) The macular cavitations were shown without the accompanying retinal vessels. (**d**) Optical coherence tomography B-scans showing microcavitations in the ganglion cell layer (white arrowheads, top), in the inner nuclear layer (yellow arrowheads, middle) and in Henle's fiber layer (green arrowhead, bottom)

whereas those seen in Green et al. were in the temporal macula. The microcavitations in the present series were typically found in the ganglion cell, inner nuclear, and Henle's fiber layers. The specific reason for this observation is not known, although Müller cells span all three of these layers.

Fluorescein Leakage

There is loss and remodeling of foveal tissue in MacTel 2. If the vessels in the deep plexus descend toward the RPE deeper than the deep plexus, they appear to leak fluorescein (Spaide et al. 2015a, b, 2017). A second mechanism by which vessels show leakage is if the vessels proliferate deeper than the deep vascular plexus into the outer nuclear layer. Both of these appear to occur in later phases of the disease where there has been loss of tissue and remodeling of the remaining tissue. Müller cells appear to be important in the control of retinal vasculature in embryology through adulthood by producing pro- and anti-angiogenic substances (Eichler et al. 2004). The anti-angiogenic substances Müller cells produce include transforming growth factor (TGF)-beta2, pigment epithelium-derived factor (PEDF), and thrombospondin-1 (TSP-1) (Eichler et al. 2004; Yafai et al. 2014). Müller cells produce endogenous vascular endothelial growth factor, as does the retinal pigment epithelium. Photoreceptors produce a soluble receptor, soluble fms-like tyrosine kinase-1, more commonly known as sFlt-1 (Luo et al. 2013). This binds to free VEGF in the outer retina and helps maintain the outer retina as an avascular zone. Loss of photoreceptors in MacTel 2 (Powner et al. 2013) could lead to decreased levels of sFlt-1 in the outer retina, with subsequent vascular abnormalities induced by unbridled VEGF. The possible cytokines and other substances in the retina that influence vessel proliferation and maintenance are present in complicated and changing gradients and relative proportions as cell depletion and possible rearrangement occur, and the interaction of these factors are likely to contribute to the abnormal vascularization seen in MacTel 2.

Potential for Choroidal Neovascularization

In some eyes, the vessels appear to penetrate deeper than the RPE, and grow in the outer retina and sub-RPE space (Figs. 8.10 and 8.11). These vessels have a different character than the vessels in the subretinal space (Fig. 8.12) (Balaratnasingam et al. 2015). Many times the patients have signs of increasing exudation and some have had pigment epithelial detachments. Thus, end-stage MacTel 2 appears to have signs resembling later phases of Type 3 neovascularization.

VRAS-OCT provided images that showed three-dimensional relationships among vessels and cystoid spaces within the substance of the retina. The possible forces causing contracture of tissue in the temporal macula and appreciation of both cavitations and microcavitations were made possible by this extension of conventional OCT angiographic imaging. This allowed generation of a theoretical model that could explain many manifestations of the disease.

Pathology

There are very few reported cases of MacTel 2 and so our knowledge of the disease is incomplete. The early reports by Green and Gass highlighted the vascular abnormalities of the disease. In 1980, Green et al. reported an eye exenterated because of a squamous carcinoma. The retina was reported to show no telangiectasis, but the capillaries were reported to have thickened basement membrane. Perhaps because of a shift in disease concepts, at least by some, the focus of more ideas shifted to MacTel 2 being a neurodegenerative disease, with the vascular changes being secondary, recent papers have concentrated on Müller cells and photoreceptors. There is a depletion of Müller cells in MacTel 2 as well as photoreceptors. No mention was made concerning corresponding vascular changes in the later publications.

Pathogenesis

The pathogenesis of MacTel 2 is not known at present, but clues from epidemiologic and genetic association studies have led to interesting suggestions. Patients with MacTel 2 were found to have an increased prevalence of diabetes mellitus, obesity, hypertension, and history of cardiovascular disease as compared with age and sex-matched controls from the general population (Clemons et al. 2013). There is a slight female preponderance.

A genome-wide analysis identified common variants that were associated with MacTel 2 (Scerri et al. 2017). One locus is known to associate with retinal vascular diameter. The other two were associated with the glycine/serine metabolic pathway. Testing of patients showed they had decreased serum levels of glycine and serine than controls.

Retina Metabolism as a Possible Pathophysiologic Pathway

The metabolism of the retina and RPE is both complex and interesting. The retina consumes glucose and uses nearly all

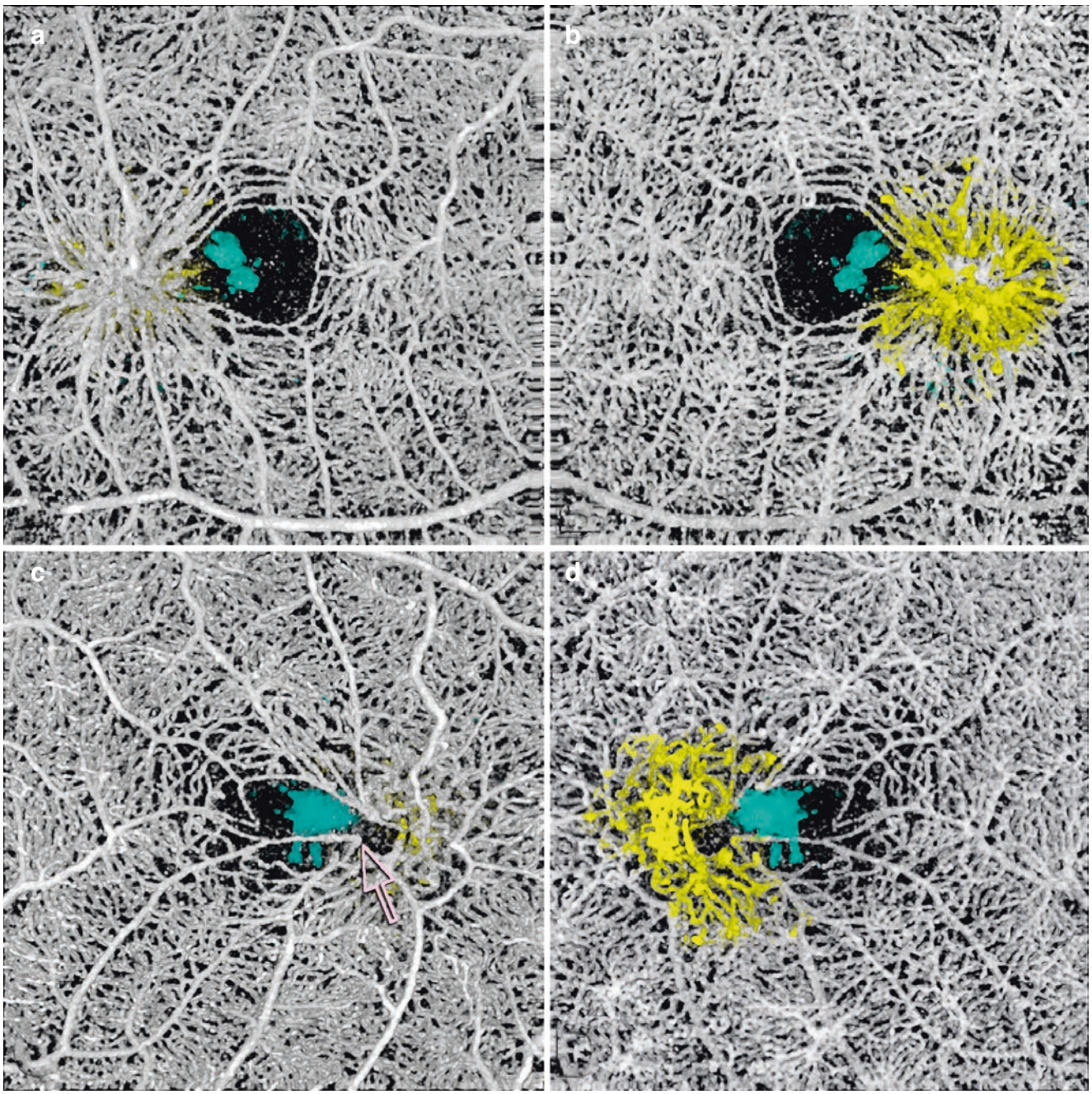

Fig. 8.10 This 64-year-old male with MacTel 2 had a visual acuity of 20/30 in each eye. There are prominent right-angle veins in each eye. (**a**) The exit point of the right-angle vein from the substance of the retina in the right eye is at the nexus of a network of vessels, which appear to be drawn into a central focus. Retinal arterioles, venules, and small order vessels appear to be involved. The foveal avascular zone is distorted and appears to be pulled toward the temporal macula. There is a group of neighboring (and in the image, overlapping) foveal cavitations (cyan) that are on the temporal side of the foveal avascular zone. (**b**) Viewed from the choroidal side, the deeper penetrating vessels appear as yellow. This region corresponded to the area of late fluorescein staining. (**c**) More prominent traction on the vessels are evident in the left eye with pulling of the perifoveal vessels into an apex of a triangle (open arrow). (**d**) Viewed from the choroidal side the vessels deep to the deep vascular plexus are shown in yellow. The cystoid space in the left eye (cyan) has a complex outer boundary

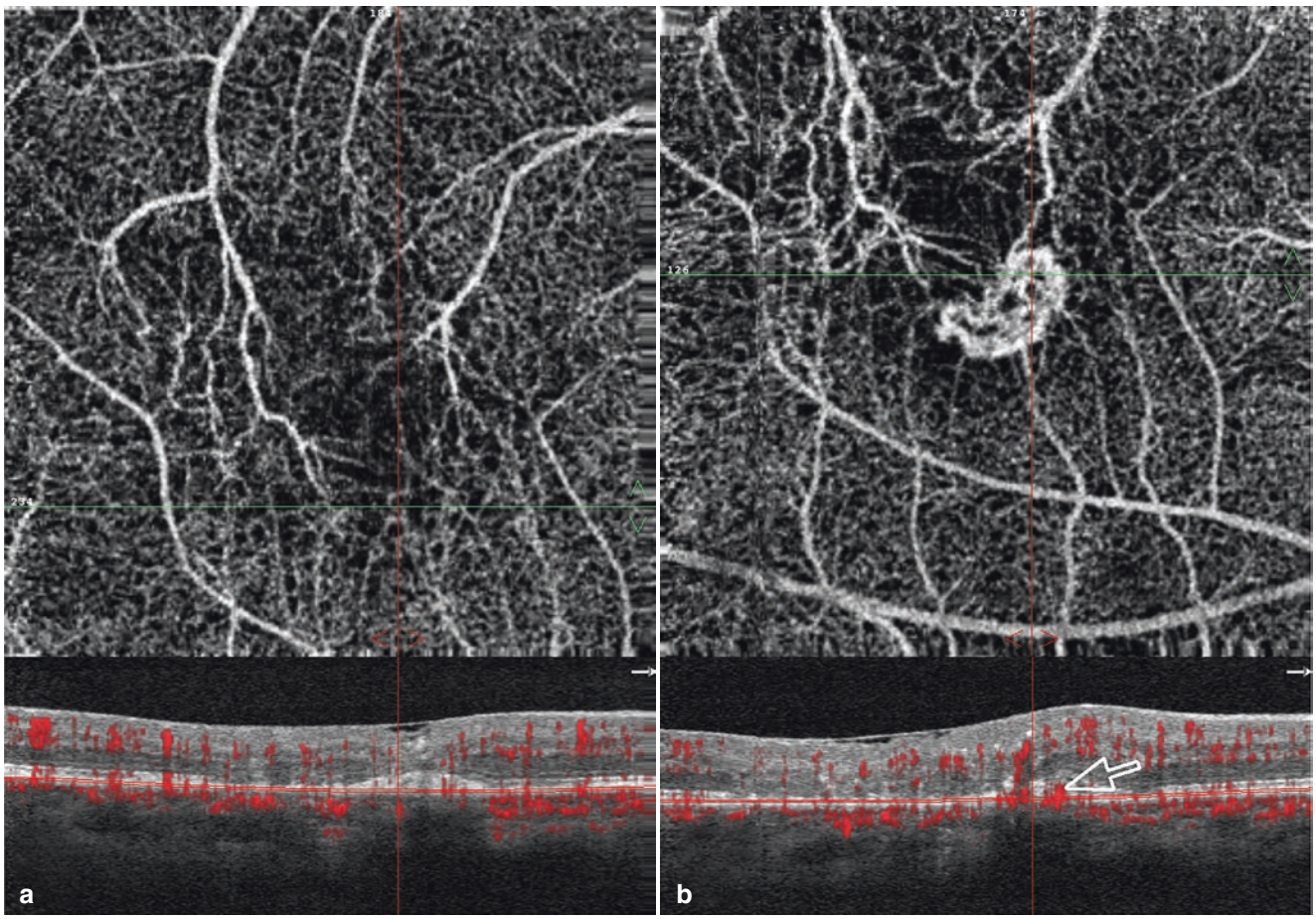

Fig. 8.11 The right eye of a 54-year-old with MacTel 2. Seven months after being imaged and found to have no subretinal neovascularization (**a**), the patient returned with complaints of altered vision. (**b**) Top shows the en-face view, which shows a vascular net. Bottom, the B-scan with flow overlay in red shows proliferation of vessels deep with prominent flow in the outer retina (open arrow)

the oxygen delivered from the choriocapillaris in the ellipsoid layer of the inner segments of the photoreceptors. This produces metabolic water and carbon dioxide, transport of both out of the outer retina is helped by the water pumping ability and carbonic anhydrase of the RPE. Most of the glucose used by the outer segments is metabolized in the glycolytic pathway to produce energy and lactic acid. The photoreceptors produce copious amounts of lactate and this is transported by the RPE cells with mono-carboxylate transporters (MCT). While the removal of lactic acid helps manage the pH of the outer retina, it appears to have another important effect. When RPE cells are exposed to lactate, they decrease their usage of glucose, thus seemingly preserving it for photoreceptor usage (Kanow et al. 2017). The transport of glucose by the RPE may be increased by lactate as well. Thus, the retina and RPE make up a metabolic ecosystem. It is possible that with disease the proportion of glucose used by RPE is increased, leaving less for the retina.

Another cell involved in processing photoreceptor-derived lactate is the Müller cell. Müller cell survival is increased by exposure to lactate and this effect was abolished by MCT inhibition (Vohra et al. 2018). Glycolytic metabolism produces oxidative damage (which may seem counterintuitive). One important mechanism used in cellular antioxidative protection involves single carbon metabolism. This is a complex metabolic network, dependent on folate, that uses serine and glycine to, among other things, generate NADPH. The NADPH in turn is used in reactions to regenerate cellular antioxidant mechanisms. Müller cells exposed to mild oxidative stress shown much greater damage when serine metabo-

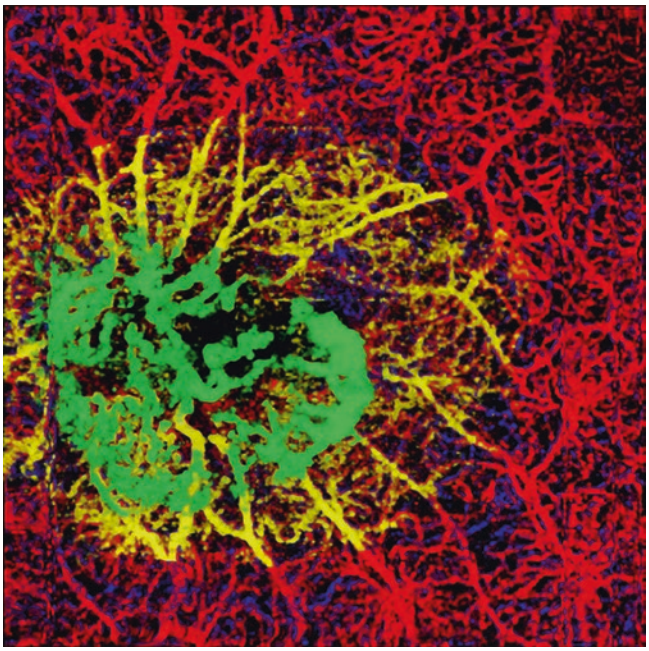

Fig. 8.12 Volume rendered structural and angiographic OCT of a case of MacTel 2 with vascular proliferation. The vessels at the level of the superficial plexus are blue, deep plexus, red, below the deep plexus, yellow and below the RPE, green. Note the different character of the sub-RPE vessels. (View from the choroidal side)

lism is inhibited (Zhang et al. 2018). The cellular damage could be partially reversed by supplementation with exogenous serine and glycine.

Viewed in the context of Müller cell, photoreceptor, and potentially RPE cell metabolism, the genetic association with variants in the serine/glycine pathway and decreased serum levels of both, becomes very interesting. One possible treatment for MacTel 2 may be to use high levels of serine as a supplement. There is a very important reason to be cautious about this approach. The other known tissues that depend heavily on glycolysis are tumor cells. NADPH production via the one carbon pathway is extremely important for mitochondrial redox homeostasis in tumors (Ye et al. 2014). Serine can be generated from the glycolytic intermediate, 3-phosphoglycerate, by the serine synthesis pathway. Cancer cells that do not have upregulation of serine synthesis pathway enzymes require extracellular sources of serine for survival (Possemato et al. 2011). Serine increases tumor growth and serine starvation reduces tumor cell proliferation (Maddocks et al. 2013). Increased activation of the serine synthesis pathway correlates with tumorigenesis (Locasale 2013), and may do so via interlinked metabolic and epigenetic programming (Kottakis 2016). In this context, loading with large doses of serine to try to treat MacTel 2 may carry risks of producing, or accelerating, tumor growth.

Treatment

The natural history of MacTel 2 (Clemons et al. 2010) is characterized by a decrease of 1.07 letters per year as seen during a 5-year follow-up study (Vujosevic et al. 2018). There are several main drivers for vision loss. Atrophy of the retina, reorganization of the central macular tissue, and subretinal and choroidal neovascularization are the main features of the disease that are associated with more significant visual acuity losses. Visual function is affected in two main ways, decreased acuity and development of a scotoma in the central 5 × 8-degree area (Vujosevic et al. 2018). The scotomas that develop in MacTel 2 are related to ellipsoid zone loss by OCT imaging (Peto et al. 2018; Heeren et al. 2018). Implantation of device using encapsulated cell therapy that released ciliary neurotrophic factor (CNTF) was first tested in a Phase 1 trial in seven subjects (Chew et al. 2015). A larger Phase 2 study of 99 eyes of 67 patients showed the area of ellipsoid zone loss over a 24-month period was lower in the CNTF treated eyes as compared with sham-treated eyes ($P = 0.04$) (Chew et al. 2019). The difference was only 0.065 mm^2, however. That is approximately one-half the area of the period at the end of this sentence. There was a less of a decline in reading speed in treated patients (-13.9 words per minute) as compared to controls (-1.3 words per minute) ($P = 0.02$).

Patients may also show two different forms of neovascularization. A common subtype is subretinal neovascularization, which is a proliferation of blood vessels under the retina and they are supplied and drained by the retinal circulation. In some patients, there may be sub-RPE proliferation that can anastomose with the choroidal circulation. In both situations, intravitreal injection of anti-VEGF agents can cause a decrease in exudation.

References

Bai Y, Ma JX, Guo J, et al. Müller cell-derived VEGF is a significant contributor to retinal neovascularization. J Pathol. 2009;219:446–54.

Balaratnasingam C, Yannuzzi LA, Spaide RF. Possible choroidal neovascularization in macular telangiectasia type 2. Retina. 2015;35:2317–22.

Brooks SE, Gu X, Kaufmann PM, et al. Modulation of VEGF production by pH and glucose in retinal Müller cells. Curr Eye Res. 1998;17:875–82.

Charbel Issa P, Berendschot TT, Staurenghi G, Holz FG, Scholl HP. Confocal blue reflectance imaging in type 2 idiopathic macular telangiectasia. Invest Ophthalmol Vis Sci. 2008;49:1172–7.

Charbel Issa P, van der Veen RL, Stijfs A, Holz FG, Scholl HP, Berendschot TT. Quantification of reduced macular pigment optical density in the central retina in macular telangiectasia type 2. Exp Eye Res. 2009;89:25–31.

Charbel Issa P, Gillies MC, Chew EY, et al. Macular telangiectasia type 2. Prog Retin Eye Res. 2013;34:49–77.

Chew EY, et al. Ciliary neurotrophic factor for macular telangiectasia type 2: results from a phase 1 safety trial. Am J Ophthalmol. 2015;159:659–666.e1.
Chew EY, et al. Effect of ciliary neurotrophic factor on retinal neurodegeneration in patients with macular telangiectasia type 2. Ophthalmol. 2019;126(4):540–49.
Clemons TE, et al. Baseline characteristics of participants in the natural history study of macular telangiectasia (MacTel) MacTel Project Report No. 2. Ophthalmic Epidemiol. 2010;17:66–73.
Clemons TE, et al. Medical characteristics of patients with macular telangiectasia type 2 (MacTel Type 2) MacTel project report no. 3. Ophthalmic Epidemiol. 2013;20:109–13.
Cohen SM, Cohen ML, El-Jabali F, Pautler SE. Optical coherence tomography findings in nonproliferative group 2a idiopathic juxtafoveal retinal telangiectasis. Retina. 2007;27:59–66.
Eichler W, Yafai Y, Wiedemann P, et al. Angiogenesis-related factors derived from retinal glial (Müller) cells in hypoxia. Neuroreport. 2004;15:1633–7.
Gass JDM. Stereoscopic atlas of macular diseases. Diagnosis and treatment. St. Louis: C.V. Mosby Company; 1977. p. 268.
Gass JDM. Stereoscopic atlas of macular diseases: diagnosis and treatment, vol. 1. 4th ed. St. Louis: Mosby; 1997.
Gass JD, Blodi BA. Idiopathic juxtafoveolar retinal telangiectasis. Update of classification and follow-up study. Ophthalmology. 1993;100:1536–46.
Gass JD, Oyakawa RT. Idiopathic juxtafoveolar retinal telangiectasis. Arch Ophthalmol. 1982;100:769–80.
Green WR, Quigley HA, De la Cruz Z, Cohen B. Parafoveal retinal telangiectasis. Light and electron microscopy studies. Trans Ophthalmol Soc U K. 1980;100(Pt 1):162–70.
Guidry C. Tractional force generation by porcine Müller cells. Development and differential stimulation by growth factors. Invest Ophthalmol Vis Sci. 1997;38:456–68.
Guidry C, Bradley KM, King JL. Tractional force generation by human Müller cells: growth factor responsiveness and integrin receptor involvement. Invest Ophthalmol Vis Sci. 2003;44:1355–63.
Heeren TFC, Kitka D, et al. Longitudinal correlation of ellipsoid zone loss and functional loss in macular telangiectasia Type 2. Retina. 2018;38(Suppl 1):S20–6.
Helb HM, Charbel Issa P, Van Der Veen RL, Berendschot TT, Scholl HP, Holz FG. Abnormal macular pigment distribution in type 2 idiopathic macular telangiectasia. Retina. 2008;28:808–16.
Jindal A, et al. A novel clinical sign in macular telangiectasia type 2. Ophthalmic Surg Lasers Imaging Retina. 2015;46(1):134–6.
Jingjing L, Xue Y, Agarwal N, Roque RS. Human Müller cells express VEGF183, a novel spliced variant of vascular endothelial growth factor. Invest Ophthalmol Vis Sci. 1999;40:752–9.
Kanow MA, Giarmarco MM, Jankowski CS, et al. Biochemical adaptations of the retina and retinal pigment epithelium support a metabolic ecosystem in the vertebrate eye. Elife. 2017;6. pii: e28899.
Koizumi H, Cooney MJ, Leys A, Spaide RF. Centripetal retinal capillary proliferation in idiopathic parafoveolar telangiectasis. Br J Ophthalmol. 2007a;91:1719–20.
Koizumi H, Slakter JS, Spaide RF. Full-thickness macular hole formation in idiopathic parafoveal telangiectasis. Retina. 2007b;27:473.
Kottakis F. LKB1 loss links serine metabolism to DNA methylation and tumorigenesis. Nature. 2016;539:390–5.
Lewis GP, Erickson PA, Guérin CJ, et al. Changes in the expression of specific Müller cell proteins during long-term retinal detachment. Exp Eye Res. 1989;49:93–111.
Locasale JW. Serine, glycine and one-carbon units: cancer metabolism in full circle. Nat Rev Cancer. 2013;13:572–83.
Luo L, Uehara H, Zhang X, et al. Photoreceptor avascular privilege is shielded by soluble VEGF receptor-1. Elife. 2013;2:e00324.
Maddocks OD, Berkers CR, et al. Serine starvation induces stress and p53-dependent metabolic remodelling in cancer cells. Nature. 2013;493:542–6.
Olson JL, Mandava N. Macular hole formation associated with idiopathic parafoveal telangiectasia. Graefes Arch Clin Exp Ophthalmol. 2006;244:411–2.
Park DW, Schatz H, McDonald HR, Johnson RN. Grid laser photocoagulation for macular edema in bilateral juxtafoveal telangiectasis. Ophthalmology. 1997;104:1838–46.
Paunescu LA, Ko TH, Duker JS, et al. Idiopathic juxtafoveal retinal telangiectasis: new findings by ultrahigh-resolution optical coherence tomography. Ophthalmology. 2006;113:48–57.
Peto T, Heeren TFC, et al. Correlation of clinical and structural progression with visual acuity loss in macular telangiectasia Type 2: MacTel Project Report No. 6-The MacTel Research Group. Retina. 2018;38(Suppl 1):S8–S13.
Possemato R, Marks KM, et al. Functional genomics reveal that the serine synthesis pathway is essential in breast cancer. Nature. 2011;476:346–50.
Powner MB, Gillies MC, et al. Perifoveal Müller cell depletion in a case of macular telangiectasia type 2. Ophthalmology. 2010;117:2407–16.
Powner MB, Gillies MC, Zhu M, et al. Loss of Müller's cells and photoreceptors in macular telangiectasia type 2. Ophthalmology. 2013;120:2344–52.
Reichenbach A, Bringmann A. Müller cells in the healthy retina. In: Müller cells in the healthy and diseased retina. New York: Springer Science + Business Media, LLC; 2010.
Rogers HC. The tensile fracture of ductile metals. Trans Metall Soc AIME. 1960;218:498–506.
Scerri TS, Quaglieri A, et al. Genome-wide analyses identify common variants associated with macular telangiectasia type 2. Nat Genet. 2017;49:559–67.
Spaide RF. Aneurysms and telangiectasias. In: Spaide RF, editor. Diseases of the retina and vitreous. Philadelphia: WB Saunders Company; 1999.
Spaide RF. Volume-rendered angiographic and structural optical coherence tomography. Retina. 2015;35:2181–7.
Spaide RF, Klancnik JM Jr, Cooney MJ, Yannuzzi LA, Balaratnasingam C, Dansingani KK, Suzuki M. Volume-rendering optical coherence tomography angiography of macular telangiectasia type 2. Ophthalmology. 2015a;122:2261–9.
Spaide RF, Klancnik JM Jr, Cooney MJ. Retinal vascular layers in macular telangiectasia type 2 imaged by optical coherence tomographic angiography. JAMA Ophthalmol. 2015b;133:66–73.
Spaide RF, Suzuki M, Yannuzzi LA, Matet A, Behar-Cohen F. Volume-rendered angiographic and structural optical coherence tomography angiography of macular telangiectasia type 2. Retina. 2017;37:424–35.
Spaide RF, Marco RD, Yannuzzi LA. Vascular distortion and dragging related to apparent tissue contraction in macular telangiectasis type 2. Retina. 2018;38(Suppl 1):S51–60.
Thorell MR, Zhang Q, Huang Y, et al. Swept-source OCT angiography of macular telangiectasia type 2. Ophthalmic Surg Lasers Imaging Retina. 2014;45:369–80.
Vohra R, Aldana B, et al. Essential roles of lactate in Müller cell survival and function. Mol Neurobiol. 2018;55:9108–21.
Vujosevic S, Heeren TFC, et al. Scotoma characteristics in macular telangiectasia Type 2: MacTel Project Report No. 7-The MacTel Research Group. Retina. 2018;38(Suppl 1):S14–9.

Wong WT, Forooghian F, Majumdar Z, Bonner RF, Cunningham D, Chew EY. Fundus autofluorescence in type 2 idiopathic macular telangiectasia: correlation with optical coherence tomography and microperimetry. Am J Ophthalmol. 2009;148:573–83.

Wu L, Evans T, Arevalo JF. Idiopathic macular telangiectasia type 2 (idiopathic juxtafoveolar retinal telangiectasis type 2A, Mac Tel 2). Surv Ophthalmol. 2013;58:536–59.

Yafai Y, Eichler W, Iandiev I, et al. Thrombospondin-1 is produced by retinal glial cells and inhibits the growth of vascular endothelial cells. Ophthalmic Res. 2014;52:81–8.

Yannuzzi LA, Bardal AM, Freund KB, Chen KJ, Eandi CM, Blodi B. Idiopathic macular telangiectasia. Arch Ophthalmol. 2006;124:450–60.

Ye J, Fan J, et al. Serine catabolism regulates mitochondrial redox control during hypoxia. Cancer Discov. 2014;4:1406–17.

Zhang T, Gillies MC, et al. Disruption of de novo serine synthesis in Müller cells induced mitochondrial dysfunction and aggravated oxidative damage. Mol Neurobiol. 2018;55:7025–37.

Perifoveal Exudative Vascular Anomalous Complex (PEVAC)

9

Riccardo Sacconi, Eleonora Corbelli, Lea Querques, Eric H. Souied, Francesco Bandello, and Giuseppe Querques

Abbreviations

AMD	Age-related macular degeneration
CME	Cystoid macular edema
CNV	Choroidal neovascularization
DCP	Deep capillary plexus
FA	Fluorescein angiography
GCC	Ganglion cell complex
ICGA	Indocyanine green angiography
INL	Inner nuclear layer
IPL	Inner plexiform layer
OCT	Optical coherence tomography
OCT-A	OCT angiography
OPL	Outer plexiform layer
PEVAC	Perifoveal exudative vascular anomalous complex
RPE	Retinal pigment epithelium
SCP	Superficial capillary plexus
VEGF	Vascular endothelial growth factor

Introduction

Perifoveal exudative vascular anomalous complex (PEVAC) is a peculiar and rare clinical entity that does not fit into any other previously described macular disease, defined by the presence of a unilateral, isolated perifoveal aneurysm in otherwise healthy patients. By definition, PEVAC occurs in subjects without any signs of arterial hypertension, diabetes, or any other systemic or local vasculopathy; however, eyes with PEVAC may manifest other macular diseases including age-related macular degeneration (AMD) (40% of cases) or pathological myopia (13% of cases). No other coincident retinal diseases have been detected. Age of diagnosis is variable; both young people, and more frequently, aged subjects could be affected (mean age at onset is 71 ± 13 years) (Sacconi et al. 2017).

In 2011, Querques and colleagues first reported two cases of isolated PEVAC in an 82-year-old woman and in a 52-year-old man, describing the angiographic and optical coherence tomography (OCT) features (Querques et al. 2011). More recently, in 2017, Sacconi and associates have provided a detailed analysis of PEVAC, reporting the baseline multimodal imaging findings in 15 patients, including OCT angiography (OCT-A), and analyzing follow-up in several cases (Sacconi et al. 2017). They identified peculiar features to distinguish this rare disorder from other retinal diseases that are characterized by the presence of perifoveal retinal vascular abnormalities, including diabetic retinopathy, hypertensive retinopathy, venous occlusion, inflammatory diseases, and blood dyscrasias. In addition, PEVAC should be distinguished also from type 3 neovascularization, although, infrequently, the two entities may be concomitant.

The main symptom in subjects with PEVAC is the visual decline caused by the presence of cystoid macular edema (CME), although, in rare cases, patients could be asymptomatic without signs of exudation.

The clinical course of the disease is stable and no significant improvement is obtained after anti-vascular endothelial growth factor (VEGF) therapy.

Etiopathogenesis

PEVAC is an idiopathic large perifoveal aneurysm without a known origin. The pathogenesis remains unclear, although multimodal imaging has provided a better understanding of the pathophysiological mechanisms. On the basis of the

R. Sacconi · E. Corbelli · L. Querques · F. Bandello
G. Querques (✉)
Department of Ophthalmology, University Vita-Salute, IRCCS Ospedale San Raffaele, Milan, Italy

E. H. Souied
Department of Ophthalmology, Hospital Intercommunal de Creteil, University Paris Est Creteil, Creteil, France

I. K. Kim (ed.), *Macular Disorders*, Retina Atlas, https://doi.org/10.1007/978-981-15-3001-2_9

clinical and imaging findings and the absence of capillary ischemia or inflammation, the main hypothesis is that PEVAC may be the result of a focal and progressive endothelial cell injury in patients without other retinal vascular diseases. This could explain the unresponsiveness to anti-VEGF treatments (Sacconi et al. 2017).

Clinical Features

At the diagnosis, PEVAC is typically associated with visual decline due to the presence of CME identified by OCT analysis. However, in few cases, PEVAC is diagnosed during a routine clinical examination without any symptoms reported by the patients. A multimodal imaging approach is mandatory to discern between PEVAC and other retinal diseases.

Multimodal Imaging Features

Fundus color pictures/multicolor imaging. PEVAC typically appears as a large, unilateral, perifoveal, aneurysmal abnormality affecting healthy people, usually unifocal, although rarely two lesions have been described in the same eye, in association with small retinal hemorrhages, intraretinal exudation, and, in some cases, hard exudates (Fig. 9.1). The lesion is usually located less than 500 μm from the center of the fovea but, in some cases, it could be located between 500 and 1500 μm from the center.

Fluorescein angiography (FA) and indocyanine green angiography (ICGA). FA displays a well-defined hyperfluorescent lesion, characterized by isolated aneurysmal dilatation, with variable leakage during the late phase (Fig. 9.2). ICGA usually reveals the same hyperfluorescence identified by FA but without leakage in the late frame of the exam (Fig. 9.2).

Structural OCT. PEVAC appears as a round hyperreflective lesion characterized in detail by a reflective wall surrounding a dark lumen with variably reflective material (Figs. 9.3, 9.4 and 9.5). In most cases, PEVAC is located between the outer plexiform layer (OPL) and the inner nuclear layer (INL), but sometimes it is also in the inner plexiform layer (IPL) with extension to the ganglion cell complex (GCC). Intraretinal cystic spaces usually surround PEVAC. On the contrary, subretinal fluid under the lesion has been rarely reported. Signs of choroidal neovascularization (CNV) are notably absent from structural OCT.

OCT-angiography. OCT-A is a new noninvasive tool able to provide depth-resolved analysis of retinal vascular flow and differentiation of the various retinal capillary plexuses. It shows PEVAC as an isolated large dilated aneurysmal abnormality with detectable flow in the superficial capillary plexus (SCP) in 17% of cases, in the deep capillary plexus (DCP) in 33% of cases, in both SCP and DCP in 33% of cases, and in the DCP and the avascular slab in the remaining 17% of cases (Figs. 9.6 and 9.7). In addition, PEVAC is characterized by rarefaction of retinal capillaries in the perilesional area. Anomalous flow is absent and no signs of anastomosis between the retinal capillary plexuses and the choriocapillaris are detected by OCT-A. A shadow effect is constantly present in the choriocapillaris segmentation (Fig. 9.7). No other macular abnormalities are present on OCT-A outside the area of the lesion.

Differential Diagnosis

PEVAC is defined as an isolated large perifoveal aneurysm, in the absence of retinal vascular or inflammatory diseases. Indeed, it is well known that macroaneurysm may be associated with other retinal vascular disorders such as retinal vein occlusion, diabetic retinopathy, and inflammatory diseases

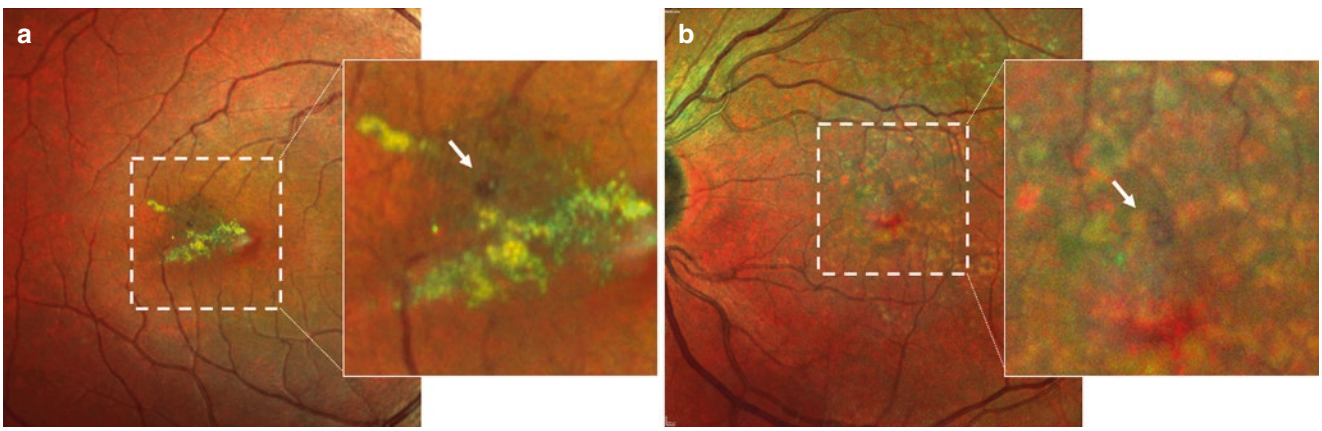

Fig. 9.1 Multicolor imaging showing a perifoveal isolated aneurysmal lesion in two different patients. (**a**) Healthy patient affected by PEVAC with large hard exudates and without any other retinal disease. (**b**) Patient affected by concomitant age-related macular degeneration and PEVAC

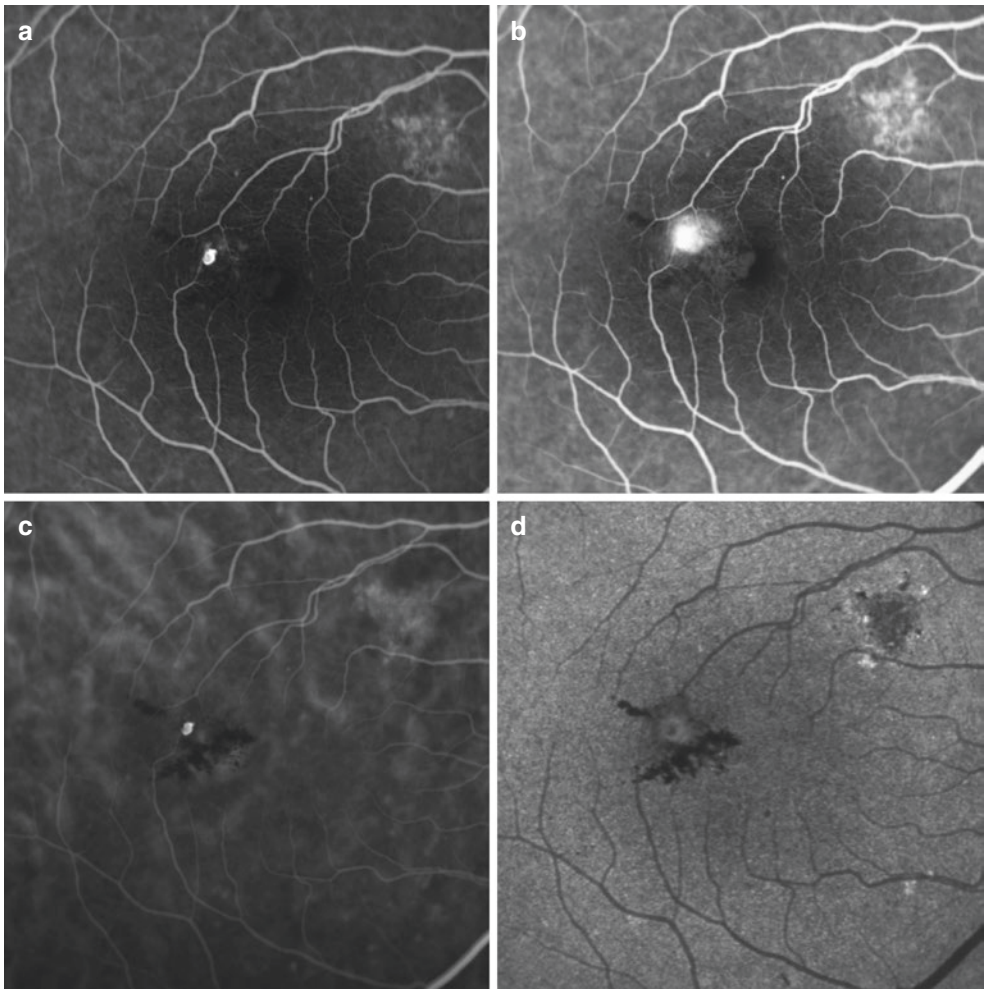

Fig. 9.2 Fluorescein angiography (FA) (**a**, **b**) and indocyanine green angiography (ICGA) (**c**, **d**) showing a well-defined hyperfluorescent lesion with leakage in the late frame of FA examination (**b**) and no leakage at ICGA (**d**)

(Verougstraete et al. 2001; Yamanaka et al. 2004; Bourhis et al. 2010). Therefore, aneurysms that occur in these kinds of patients should not be included in the PEVAC definition.

PEVAC may be classified in the spectrum of idiopathic retinal vascular abnormalities of the macula. However, PEVAC should not be misdiagnosed as type 1 macular telangiectasia (or a subtype). Group 1B macular telangiectasia, also defined as "Visible, Exudative and Focal Idiopathic Juxtafoveolar Retinal Telangiectasis" by Gass and Blodi (Gass and Blodi 1993), is characterized by focal exudative telangiectasia limited to 2 clock hours or less in the juxtafoveal area with intraretinal microangiopathy affecting both the superficial and deep capillary plexus. By contrast, PEVAC is characterized by an isolated and well-defined aneurysmal abnormality with rarefaction of the retinal capillaries in the perilesional area but without adjacent capillary aneurysms and/or telangiectasia. Furthermore, type 1 macular telangiectasia usually affects young patients and responds to anti-VEGF treatment (Gamulescu et al. 2008). On the other hand, PEVAC affects older patients and it is typically unresponsive to anti-VEGF therapy, such as ranibizumab or aflibercept intravitreal injections (Sacconi et al. 2017).

PEVAC could be confused also with nascent type 3 lesion, typically associated with no exudation (Sacconi et al. 2018), or with stage 1 of type 3 neovascularization, typically associated with slight intraretinal fluid (Su et al. 2016). However, these early stages of type 3 neovascularization are almost always associated with downward growth toward the retinal pigment epithelium (RPE) with progressive exudation (Su et al. 2016). In fact, RPE invasion may serve as the substrate for a greater exudative process. On the contrary, PEVAC tends to remain confined to the retinal layers and it is unresponsive to anti-VEGF injections (Sacconi et al. 2017), whereas type 3 neovascularization responds briskly to anti-VEGF (Kuehlewein et al. 2015; Phasukkijwatana et al. 2017). Furthermore, structural OCT displays a very different morphology of PEVAC versus type 3 neovascularization.

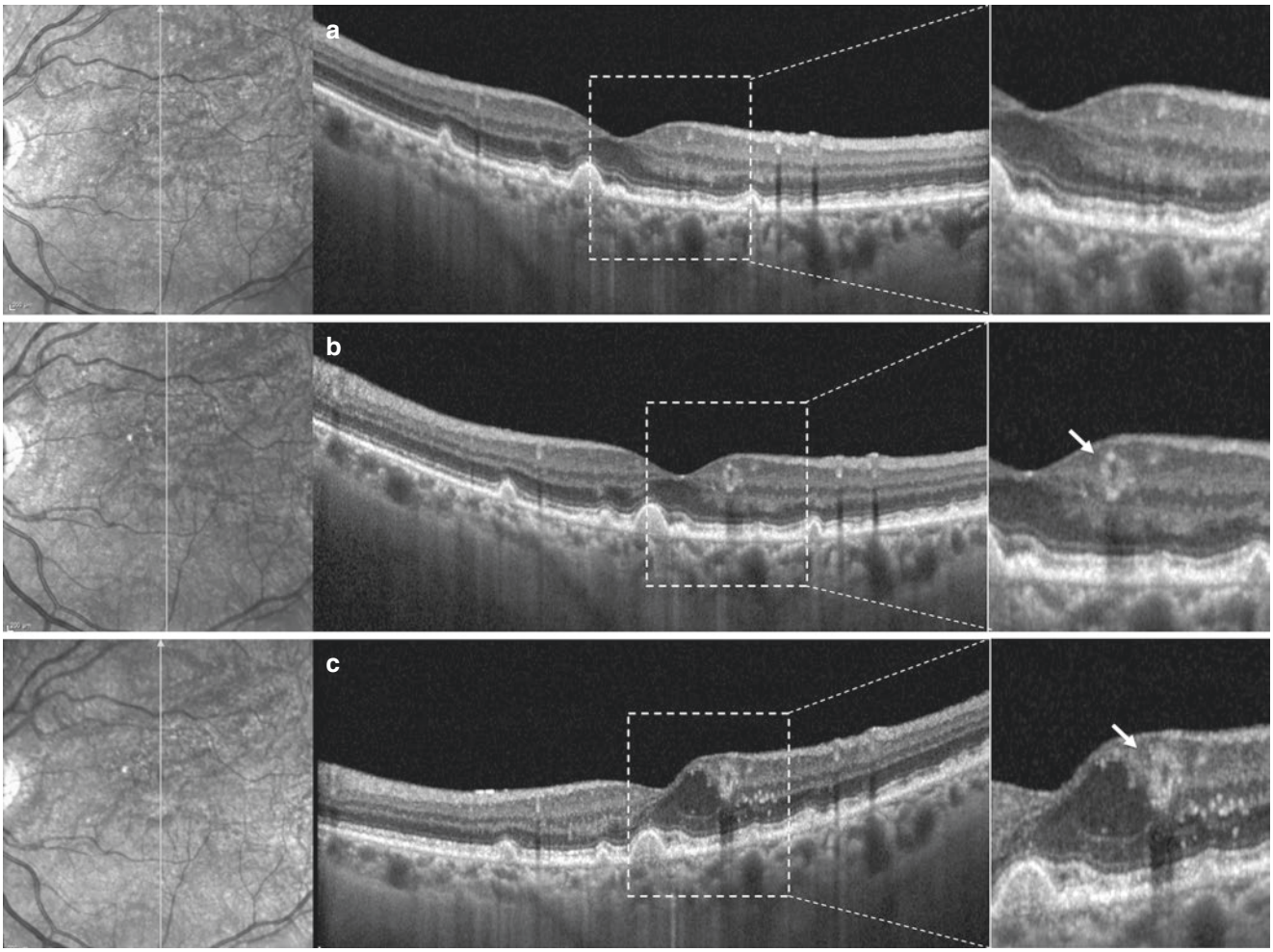

Fig. 9.3 Vertical structural OCT passing through the fovea showing the development of a PEVAC in a patient affected by concomitant age-related macular degeneration and PEVAC. (**a**) At baseline, no lesion was disclosed. (**b**, **c**) At 6-month follow-up, structural OCT showed a round lesion with a hyperreflective wall (**b**) that developed intraretinal cystic spaces and hard exudates after 6 months (**c**)

A PEVAC lesion appears as an aneurysmal abnormality, i.e., an isolated round lesion with a reflective wall surrounding a lumen containing variably reflective material (Figs. 9.3, 9.4 and 9.5), whereas type 3 neovascularization appears as a hyperreflective lesion that displays downward growth from the deep capillary plexus to the RPE (Sacconi et al. 2018).

Interestingly, sometimes PEVAC develops in AMD patients and is rarely associated with a concomitant nascent type 3 neovascularization remote from the lesion. However, the authors believe that the development of type 3 neovascularization in the reported cases was related only to AMD and not strictly related to PEVAC, because of the considerable distance between the two lesions (Sacconi et al. 2017).

Management

Because of the rarity of the disease, little is known about the correct management and treatment of PEVAC.

Observation

The disease displays a stable clinical course, with no significant improvement or worsening in functional and anatomical outcomes at the end of 1-year follow-up without any medical or surgical treatment (Sacconi et al. 2017). However, some cases could display a partial spontaneous resolution of CME during the follow-up (Fig. 9.4).

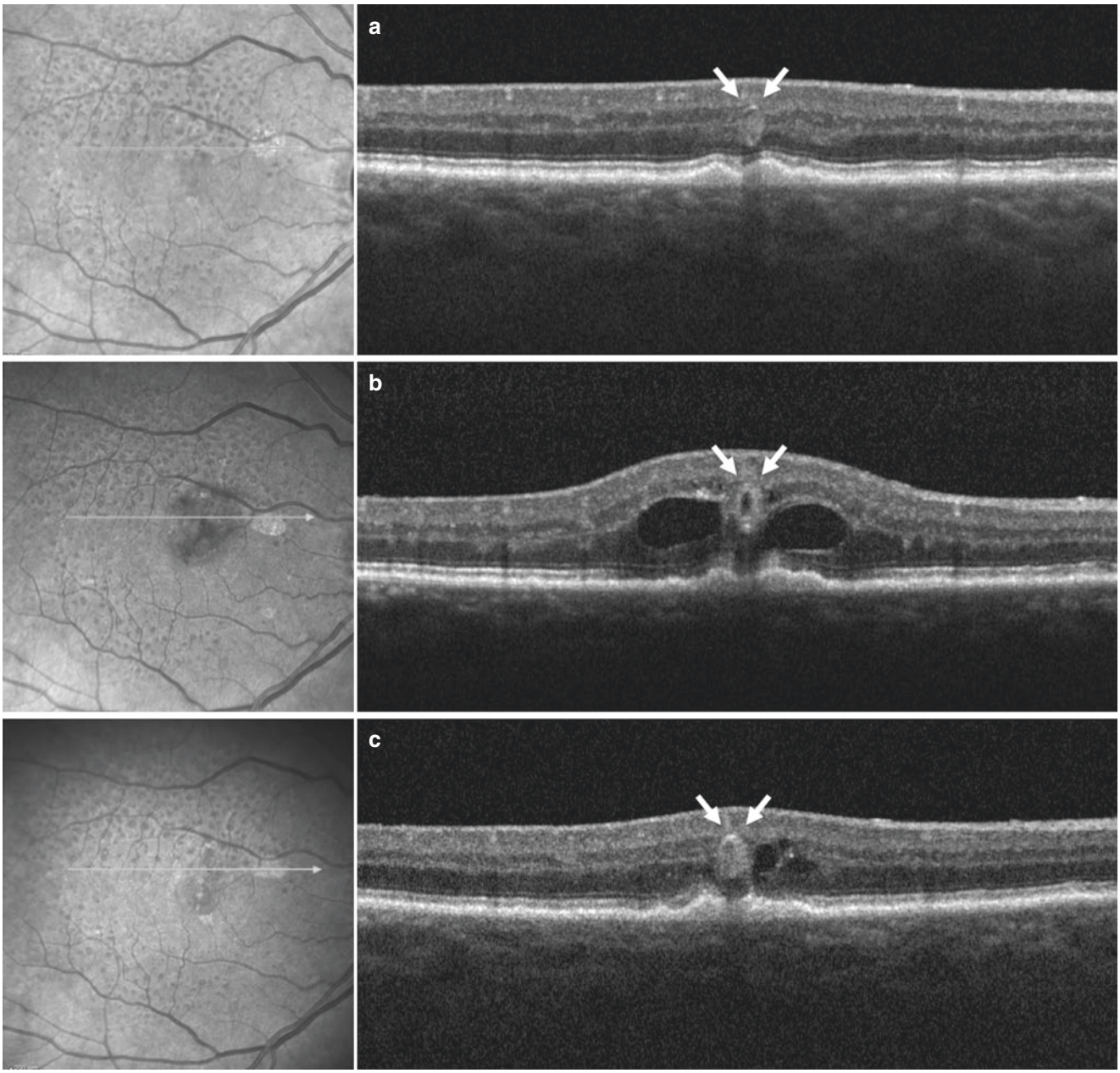

Fig. 9.4 Horizontal structural OCT scans passing through the PEVAC at baseline and at all follow-up examinations. Structural OCT revealed a round lesion with a hyperreflective wall matching PEVAC without intraretinal cystic spaces at baseline (**a**) which appeared at 8-month follow-up (**b**). A partial spontaneous resolution of intraretinal cystic spaces was recorded at 11-month follow-up (**c**)

Medical Therapy

There is no evidence that anti-VEGF injections are effective in the treatment of PEVAC (Fig. 9.5). In the series reported by Sacconi and associates (Sacconi et al. 2017), three patients were treated with anti-VEGF injections (two patients underwent three Ranibizumab injections and one patient three Aflibercept injections) and all patients illustrated the persistence of PEVAC at the follow-up. Furthermore, CME persisted in all three patients, and no evidence of functional or anatomic improvement was disclosed.

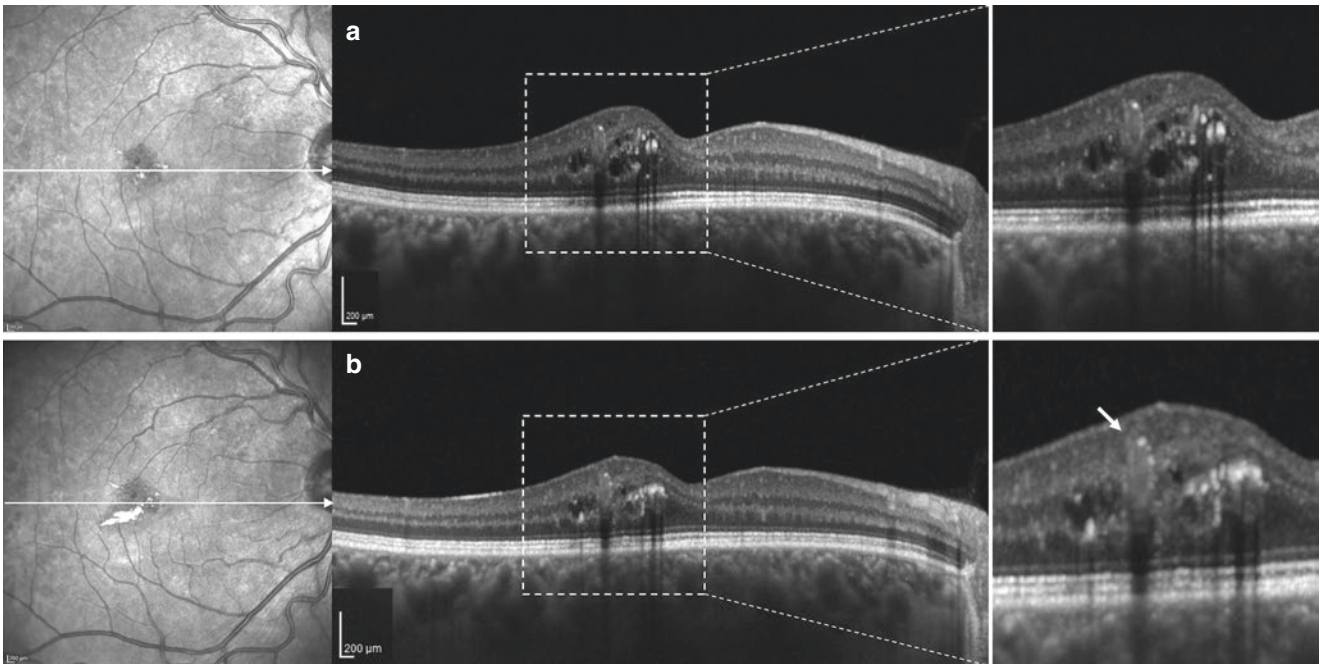

Fig. 9.5 Horizontal structural OCT scans passing through the PEVAC at baseline and at 4-month follow-up after three ranibizumab injections. Structural OCT showed a round lesion with a hyperreflective wall, intraretinal cystic spaces and hard exudates at baseline (**a**) and after the treatment (**b**), without significant improvement

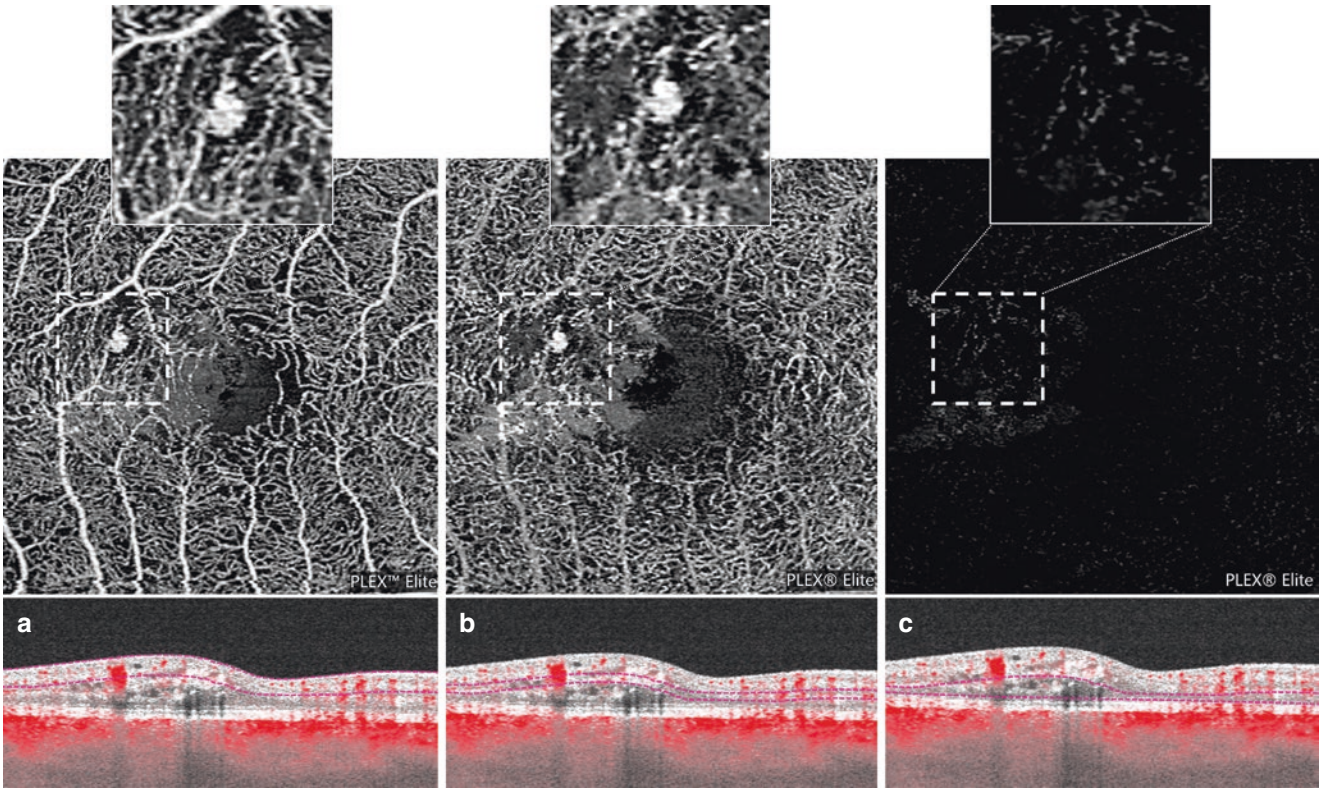

Fig. 9.6 Optical coherence tomography angiography images (PLEX® Elite 9000, Carl Zeiss Meditec Inc., Dublin, CA, USA) and corresponding B-scans with flow nicely disclose an isolated large dilation matching PEVAC with detectable flow in superficial capillary plexus (**a**), deep capillary plexus (**b**) and no flow in the avascular slab (**c**)

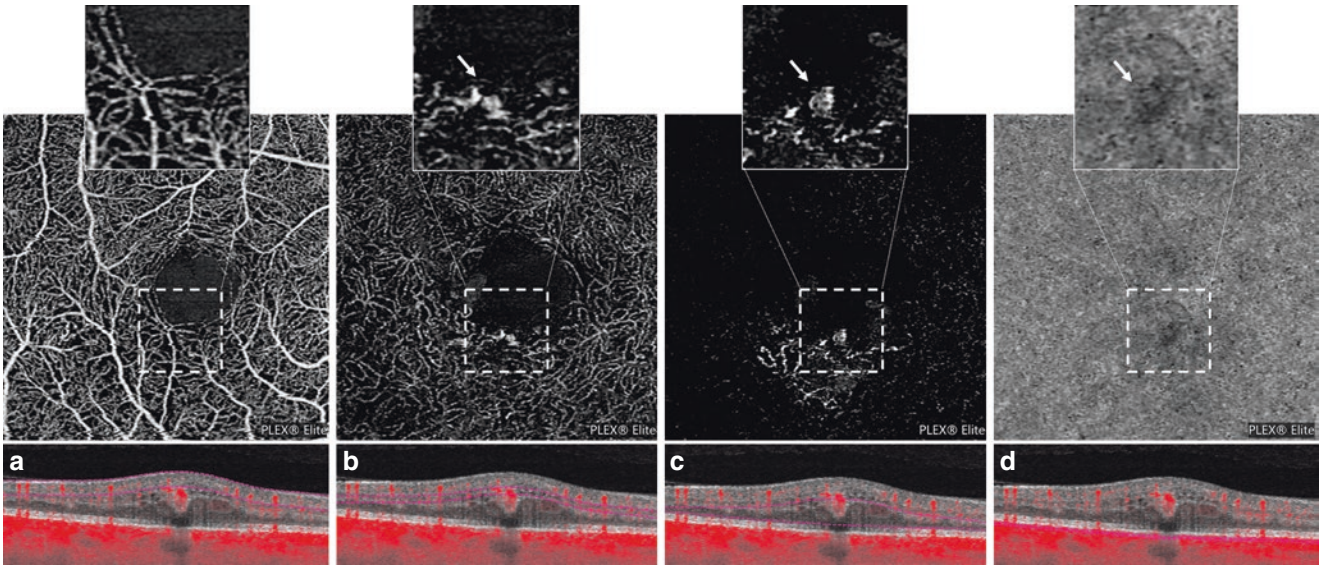

Fig. 9.7 Optical coherence tomography angiography images (PLEX® Elite 9000, Carl Zeiss Meditec Inc., Dublin, CA, USA) and corresponding B-scans with flow disclose an isolated large dilation matching PEVAC with no detectable flow in superficial capillary plexus (**a**), detectable flow in the deep capillary plexus (**b**) and the avascular slab (**c**), and a shadow effect in the choriocapillaris segmentation (**d**)

References

Bourhis A, Girmens JF, Boni S, et al. Imaging of macroaneurysms occurring during retinal vein occlusion and diabetic retinopathy by indocyanine green angiography and high resolution optical coherence tomography. Graefes Arch Clin Exp Ophthalmol. 2010;248:161–6.

Gamulescu MA, Walter A, Sachs H, Helbig H. Bevacizumab in the treatment of idiopathic macular telangiectasia. Graefes Arch Clin Exp Ophthalmol. 2008;246:1189–93.

Gass JD, Blodi BA. Idiopathic juxtafoveolar retinal telangiectasis. Update of classification and follow-up study. Ophthalmology. 1993;100:1536–46.

Kuehlewein L, Dansingani KK, de Carlo TE, et al. Optical coherence tomography angiography of type 3 neovascularization secondary to age-related macular degeneration. Retina. 2015;35:2229–35.

Phasukkijwatana N, Tan ACS, Chen X, Freund KB, Sarraf D. Optical coherence tomography angiography of type 3 neovascularisation in age-related macular degeneration after antiangiogenic therapy. Br J Ophthalmol. 2017;101:597–602.

Querques G, Kuhn D, Massamba N, Leveziel N, Querques L, Souied EH. Perifoveal exudative vascular anomalous complex. J Fr Ophtalmol. 2011;34:559.e1–4.

Sacconi R, Freund KB, Yannuzzi LA, et al. The expanded spectrum of perifoveal exudative vascular anomalous complex. Am J Ophthalmol. 2017;184:137–46.

Sacconi R, Sarraf D, Garrity S, et al. Nascent type 3 neovascularization in age-related macular degeneration. Ophthalmol Retina. 2018;2:1097–106.

Su D, Lin S, Phasukkijwatana N, et al. An updated staging system of type 3 neovascularization using spectral domain optical coherence tomography. Retina. 2016;36(Suppl 1):S40–9.

Verougstraete C, Snyers B, Leys A, Caspers-Velu LE. Multiple arterial ectasias in patients with sarcoidosis and uveitis. Am J Ophthalmol. 2001;131:223–31.

Yamanaka E, Ohguro N, Kubota A, Yamamoto S, Nakagawa Y, Tano Y. Features of retinal arterial macroaneurysms in patients with uveitis. Br J Ophthalmol. 2004;88:884–6.

Photic Retinopathy

10

Priya Sharma and Caroline Baumal

Abbreviations

CNV	Choroidal neovascularization
ELM	External limiting membrane
FA	Fluorescein angiography
FDA	Food and Drug Administration
IR	Infrared
OCT	Optical coherence tomography
RPE	Retinal pigment epithelium
UV	Ultraviolet

Introduction

Light interaction with the retina can result in mechanical damage to the retina, known as photic retinopathy. Photic retinopathy encompasses an array of disorders in which light produces damage to the retina, and the source of the inciting light can come from varied sources, including solar rays, laser pointers, welding arcs, and even ophthalmic equipment. The severity of damage is often related to the duration and wavelength of exposure and the intensity of the light source, and visual recovery can be variable. There can also be differences in severity of photic retinopathy based on iris pigmentation, pupillary constriction, and absorption of the target tissue. We herein aim to discuss various mechanisms of photic retinopathy, their clinical features, and methods of prevention.

Characteristics of Light and Mechanisms of Light-Induced Damage

Visible light ranges from 400 to 760 nm, but damage often occurs in the ultraviolet (UV, 200–400 nm) and infrared (IR, >760 nm) wavelengths. Intrinsic ocular defenses against light-induced damage include corneal absorption of ultraviolet and infrared radiation, lens absorption of ultraviolet and visible blue radiation, and xanthophyll absorption of ultraviolet and blue light (Mainster 1987; Boettner and Wolter 1962). Choroidal thermoregulation and pupillary miosis are additional defense mechanisms against photic damage (Mainster 1987). Younger patients are at higher risk of photic retinopathy due to presence of a clear lens leading to an unobstructed visual pathway for the incoming light source.

There are three major ways in which light causes damage to the retina—photodisruption, photocoagulation, and photochemical. Overall, the tissue effects of light are determined by the wavelength of light, duration of exposure, irradiance (W/cm^2), and absorption of target tissue (Mainster et al. 1983). **Photodisruption** is a type of mechanical injury that results from short-duration, high-irradiance exposure in the nanosecond (10^{-9}) to picosecond (10^{-12}) range, which disintegrates the tissue into plasma. Photodisruption is the primary mechanism of action of the neodymium:yttrium-aluminum-garnet (Nd:YAG) laser which is used to create posterior capsular openings after cataract surgery and for peripheral iris puncture (also known as iridectomy) in angle-closure glaucoma. **Photothermal** tissue damage occurs with moderate irradiance and moderate exposure to a light source, which results in a temperature rise in the target tissue. This temperature rise produces protein denaturation and cellular necrosis (White et al. 1971; Priebe et al. 1975). An example of photothermal tissue effects is produced with retinal photocoagulation, which is the primary mechanism of action to induce retinal tissue destruction for proliferative retinovascular diseases. The final mechanism of light damage is **photochemical**. This occurs with low-to-moderate irradiances and with shorter wavelengths, in particular ultraviolet light. Short-wavelength light causes a photochemical reaction in the target tissue by producing an excited molecular state from photon absorption. This is the mechanism of action for photodynamic therapy which couples a systemic photosensitizing agent such as verteporfin with low energy light to induce retinal tissue effects. These methods of light-induced damage are

P. Sharma (✉) · C. Baumal
Retina Service, New England Eye Center, Tufts Medical Center, Tufts University School of Medicine, Boston, MA, USA

I. K. Kim (ed.), *Macular Disorders*, Retina Atlas, https://doi.org/10.1007/978-981-15-3001-2_10

used intentionally by some forms of ophthalmic lasers as described above. However, unregulated light sources can also produce permanent retinal damage using these same photic mechanisms described. More than one mechanism of light damage may also be produced after photic exposure. For example, solar damage may produce retinal damage by photothermal as well as photochemical mechanisms.

Clinical Features

The features of photic retinopathy are variable and depend on host factors (pigmentation, body temperature, photosensitizing agents, integrity of preexisting intrinsic ocular defenses against photic damage) and the characteristics of the photic exposure (wavelength, duration, irradiance, area). Mild photic retinopathy may be asymptomatic. An individual typically presents for evaluation for a decline in vision, scotoma, or erythropsia following exposure to an inciting light source. Patients with minor or subclinical photic exposure may not present at all due to lack of symptoms. Clinical examination may reveal retinal pigment epithelium (RPE) changes and/or a foveal defect, although this finding may not be visible for hours to days after the inciting event and occasionally is so subtle that it is not visible on clinical examination. Optical coherence tomography (OCT) is the most sensitive modality to demonstrate photic damage. Multiple high-resolution OCT scans should be directed at the area of interest to show subtle changes. OCT typically shows disruption of the outer retina that may involve the external limiting membrane (ELM), interdigitation zone, and/or ellipsoid layer. Visual recovery is possible, although it varies based on severity of initial injury. Patients on photosensitizing agents such as tetracycline derivatives and psoralen may be more susceptible to damage.

Solar Retinopathy

Solar retinopathy describes photic damage from indirect or direct visualization of solar rays. This has been associated with religious sungazing, psychiatric and psychotropic disorders, and prolonged sunlight exposure without eye protection, such as in skiing or sailing. There is a threshold for which solar viewing can cause retinal damage, due to the temperature rise in retinal tissue from the direct image of the sun that is focused on the fovea. Solar viewing through a 3 mm pupil produces a 4 °C increase in temperature, which is below the threshold for retinal damage. Conversely, solar observation through a dilated pupil produces a 22 °C increase in temperature, which is above the threshold for retinal damage (White et al. 1971). Solar retinopathy is often more pronounced with large pupillary diameters, as larger pupils allow for unimpeded entry of light into the eye (White et al. 1971).

Symptoms usually develop shortly after the inciting event and are often bilateral. Acute symptoms often manifest up to several hours after exposure and cause distortion in vision, scotomata in the center of vision, and/or blurred vision. Clinical exam can be unremarkable or, in more severe cases, can reveal subfoveal RPE changes (Fig. 10.1a, b). Fluorescein angiography (FA) can show a small foveal window defect without leakage. OCT often shows subfoveal ellipsoid disruption without intraretinal edema (Figs. 10.1c, d and 10.2a, b). Vision often slowly improves over the following months, although subtle permanent distortion and visual sequelae can persist. Chronic RPE mottling can be seen in patients with multiple prior episodes of sungazing.

A well-known subset of solar retinopathy includes eclipse retinopathy. A solar eclipse occurs when the moon passes between the Earth and sun, blocking the sunlight and casting a shadow on a part of the Earth. This spectacular phenomenon is often enticing to view, but viewing the eclipse directly with the unprotected eye can cause solar retinopathy, due to the duration of exposure and the intensity of the light. The most recent total solar eclipse occurred in the United States on August 21, 2017, which was preceded by an extensive public awareness campaign to avoid solar viewing without proper approved ocular protection. Eclipse retinopathy presents similarly to solar retinopathy, usually with mild perifoveal changes on examination and outer retinal disruption visible on OCT (Fig. 10.3).

Lasers and Handheld Laser Pointer Injury

Lasers can produce sudden visual loss when inadvertently directed into the eye, producing retinal injury. There are different variations of laser injuries, and the severity and long-term outcome depend on the mechanism of injury. The first type is related to industrial lasers, which are often high-powered and produce photocoagulation injury to the retina. This usually results from exposure without safety glasses or secondary to misalignment of the laser. The second kind of laser injury involves handheld lasers that may not comply with the strict regulations set forth by the American National Standards Institute (ANSI) and can be of higher energy than these regulations allow. These types of lasers are often obtained from abroad or on the Internet. The last kind of laser injury is related to laser pointers that fully comply with ANSI regulations, but are incorrectly used.

Laser energy has been shown to have a predilection for retinal injury due to absorption by the RPE and the combination of photochemical and photothermal damage (Alsulaiman et al. 2014). Symptoms of laser pointer maculopathy include unilateral or bilateral blurred vision with or without central scotomata (Weng et al. 2015). There have been cases of audible popping sounds and temporary pain at the time of laser pointer exposure, possibly due to sudden rapid expansion of

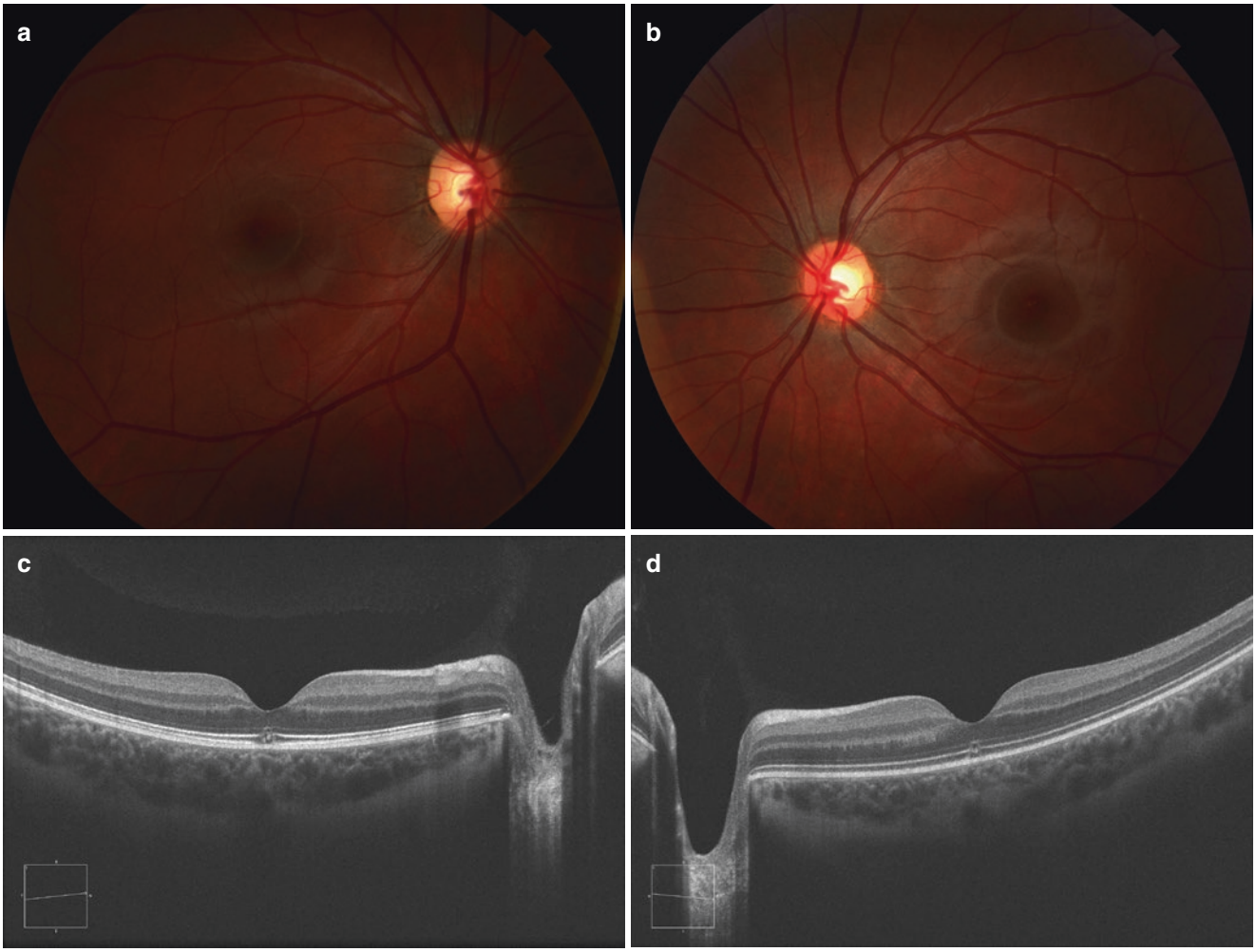

Fig. 10.1 Fundus photograph of the right (**a**) and left (**b**) eyes in a 13-year-old girl who presented with blurred vision 10 days after direct prolonged solar (sun) viewing. Examination revealed subtle subfoveal RPE changes. OCT of the right (**c**) and left (**d**) eyes showed focal foveal ellipsoid disruption extending between the RPE and the ELM without overlying retinal edema

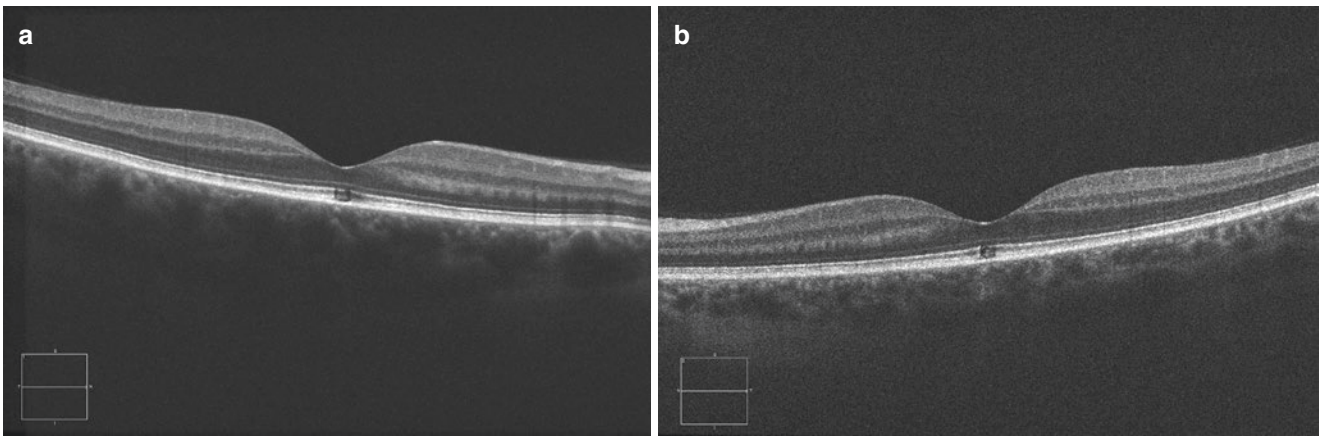

Fig. 10.2 OCT of the right (**a**) and left (**b**) eyes of a 47-year-old female with history of narcotic and benzodiazepine use, who admitted to prolonged episodes of sungazing. OCT shows hyporeflective disruptions in the ellipsoid layer without overlying retinal edema, consistent with solar retinopathy

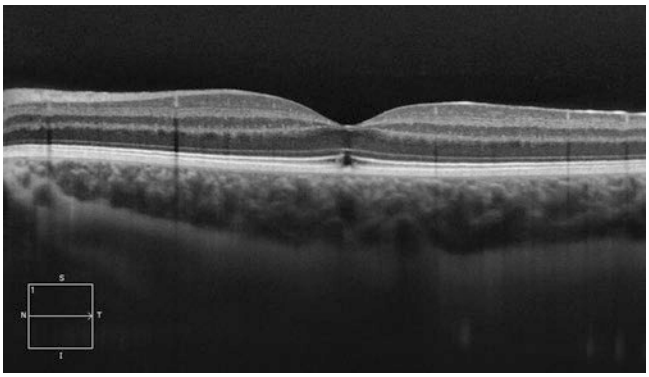

Fig. 10.3 OCT of the left eye acutely after eclipse exposure revealed outer retinal disruption and ellipsoid loss in the left eye

the chorioretinal tissues due to thermal expansion in higher-energy lasers (Weng et al. 2015). Fundus examination acutely reveals RPE changes in the fovea. Tissue disruption or hemorrhage may also be visible. OCT after acute exposure typically reveals focal disruption in the outer retina extending from Bruch's membrane to the external limiting membrane, involving RPE destruction and ellipsoid disruption (Fig. 10.4a, b). Opacification of Henle's layer may be visible in the region of tissue disruption. The OCT changes typically improve over time, although some of OCT findings may persist, including ellipsoid attenuation and RPE irregularity. Fluorescein angiography may demonstrate foveal window defects at the area of RPE damage (Fig. 10.4c–e), and fundus autofluorescence can show hypoautofluorescence in these same areas (Weng et al. 2015). There have also been reports of laser pointer injury causing full-thickness macular hole or subretinal hemorrhage, thought to be related to high-energy laser sources held within 2 m of the eye (Alsulaiman et al. 2015; Dhoot and Xu 2014).

The severity of injury from laser pointers depends on power of the laser, wavelength of the laser, duration of exposure, and degree of retinal pigmentation (Barkana and Belkin 2000). Therefore, primary prevention of laser pointer-induced retinopathy is cautious use of laser pointers with care to point the laser beam away from the eyes. However, given the prevalence of laser pointers and the possibility of inadvertent exposure, it is important to ensure that all laser pointers are of low-energy that is below the threshold of retinal toxicity.

Lasers are regulated by the Food and Drug Administration (FDA), in order to ensure safety. The FDA classifies lasers according to the hazard posed by the amount and type of light they emit, according to the standard set forward in the Code of Federal Regulations. Hazard classes range from Classes I to IV, with Class IV lasers being the most hazardous. Laser pointers are classified into Class IIIa and are limited to a maximal 5 mW output power in the visible wavelength range from 400 to 710 nm, which at this level poses negligible risk of ocular damage with correct pointer use (FDA 2017). However, given the ease of global purchasing and the lack of regulations overseas, laser can be erroneously advertised as pointers that exceed these requirements and can pose considerable risk of injury to the people exposed (Weng et al. 2015). Furthermore, there is no regulatory board monitoring labeling of lasers obtained from outside of the United States (Lee et al. 2014). Additionally, improper use of Class IIIa laser pointers such as with prolonged direct viewing may produce retinal damage (Lee et al. 2014).

Ophthalmology Equipment Related

With technological advances, operating microscopes have morphed over the years to provide clear intraoperative views with high levels of illumination. However, photic retinopathy has been reported from prolonged high-intensity intraoperative light exposure after both anterior segment surgery and vitreoretinal surgery (Michels and Sternberg Jr 1990). Unobstructed high-intensity light can cause photochemical and photothermal damage to the retina, particularly when unobstructed due to pupillary dilation, aphakia, or direct endoillumination during vitrectomy. Symptoms often present similarly to that of solar retinopathy, although oftentimes there is little to no clinical evidence of macular pathology immediately after the exposure. Within 48 h, a yellow lesion measuring around 0.5–2.0 disc diameters may develop at the level of the RPE, with overlying retinal edema. Fluorescein angiography will show dye leakage at the level of the RPE. The acute retinal edema will resolve, but chronic findings of RPE clumping and atrophy, ellipsoid loss, and window defects on fluorescein angiography can persist. Typically, symptoms present in the postoperative period and are more common in patients with prolonged operative times and patients on photosensitizing medications or with the use of high-intensity light sources. Severity of vision loss can also vary, as the area of damage depends on the shape and exposure of the illuminating source, and so damage can occur outside of the fovea. Diagnosis is often delayed, as vision is often limited in the early postoperative period from normal postoperative corneal edema, refractive changes, and/or intraocular gas. Symptoms and clinical findings often improve with observation, although there can be subtle residual deficits.

Arc Welding

Welding-induced retinopathy occurs due to exposure to ultraviolet, near ultraviolet, and blue light, without appropriate eye protection. More commonly, arc welding will cause a

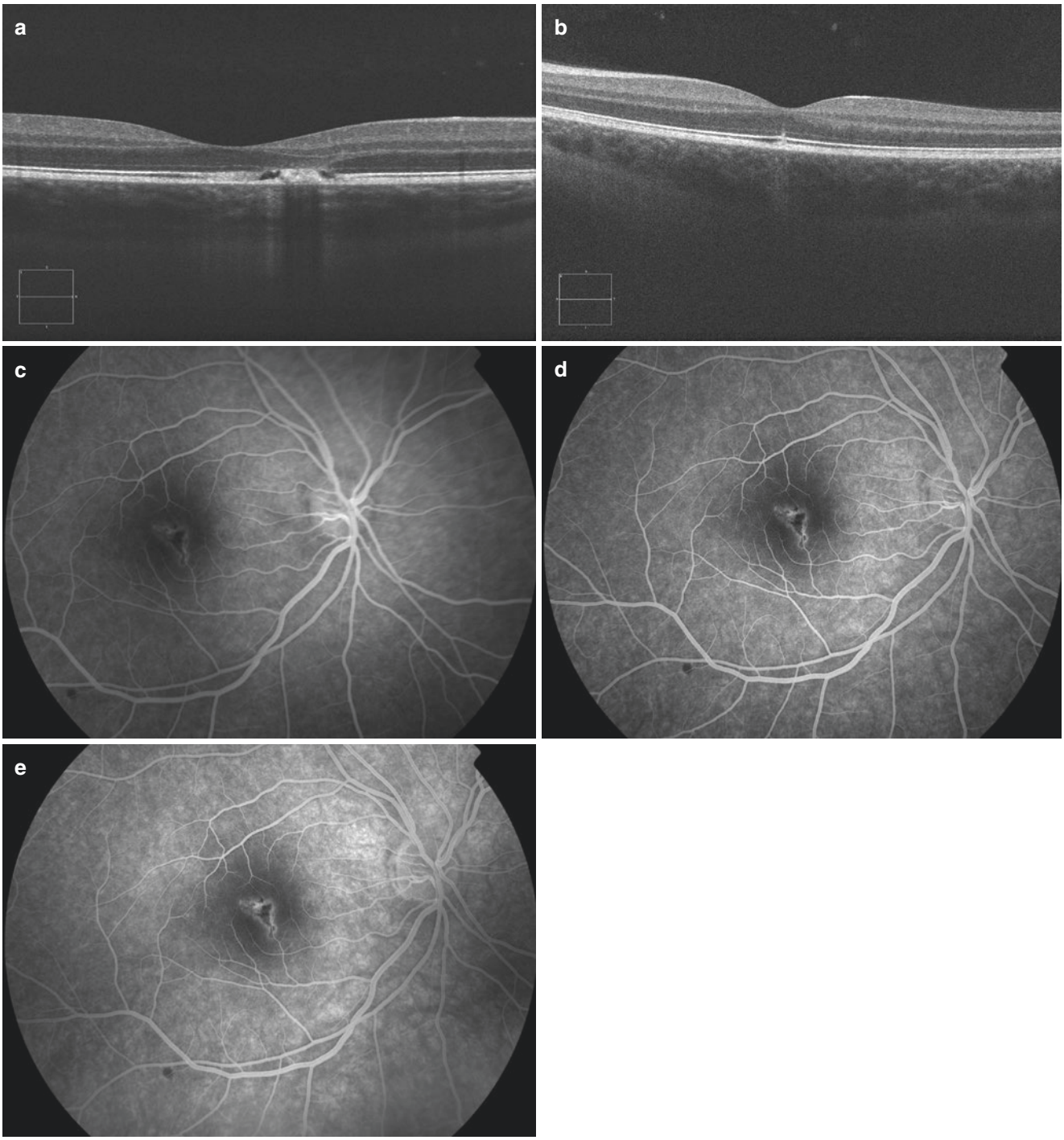

Fig. 10.4 OCT of the right (**a**) and left (**b**) eyes in an 11-year-old boy who briefly viewed a laser pointer directed into a mirror. OCT right eye shows RPE and outer retinal disruption, hyperreflectivity in the region of damage, and subtle opacification of Henle's layer. In the left eye, there is small hyperreflective foci in the fovea. Fluorescein angiography of the right eye at 46 s (**c**) and at 2 min (**d**) showed parafoveal hyperfluorescence corresponding to region of outer retinal damage. Fluorescein angiogram of the right eye at 7 min (**e**) shows stable window defect hyperfluorescence without evidence of leakage

temporary photokeratitis known as "welder's flash," which often resolves spontaneously with the addition of lubricating eye drops. However, in more severe cases, arc welding can also cause photic retinopathy. Clinical examination often reveals subfoveal RPE changes, OCT ellipsoid disruption, and oftentimes a subfoveal RPE window defect on fluorescein angiography (Choi et al. 2006), similar to other forms of photic retinopathy such as solar retinopathy.

Prevention of Photic Injury to the Retina

Prevention is the major factor to avoid most instances of photic retinal damage. The general principles include education, avoidance of hazardous exposure, use of proper eye protection, following most recent regulations to ensure that equipment is safely used, and minimizing duration of surgical light exposure.

Primary prevention of solar retinopathy includes avoidance of any sungazing. Furthermore, avoidance of photosensitizing agents such as tetracycline and psoralen is important, particularly when involved in activities with sun exposure. Direct viewing of a solar eclipse without eye protection should be avoided. Special regulated filters are required for eclipse viewing. These filters transmit less than 0.003% of visible light (380–780 nm) and a maximum of 0.5% of the near-infrared radiation (780–1400 nm). These filters are typically labeled as International Organization for Standardization (ISO) 12312-2 certified (Emerson and Wong 2017).

Prevention of welding ocular damage requires wearing appropriate ocular protection. However, there have been case reports of photic retinopathy during arc welding despite protective eyewear due to insufficient range of protection from all wavelengths of light emitted during arc welding (Choi et al. 2006), highlighting the need to ensure that eye protection is updated and accurate.

Laser pointers are ubiquitous and widely available, but are not always from reputable sources, and are differently regulated among different countries. Be aware lasers from the Internet may not comply with ANSI standards, may be marketed as a pointer but have much higher outputs capable of photocoagulation if misused, and may also be mislabeled as demonstrated in the case by Lee and associates (Lee et al. 2014). Whether handheld laser or laser pointer, laser light should never be directly viewed or pointed into a mirror. Laser pointers also should not be used by minors or given to a minor for recreational use.

In the medical field, Class IIIb lasers are often used for procedures. Improper use of these lasers could similarly cause permanent ocular damage. Therefore, it is imperative that any medical professional required to operate or assist in any laser-based therapy get mandatory laser safety training. It is also important to wear protective eyewear around lasers, and it is critical to ensure that the frequency of the laser and the filtration of the protective eyewear match, to ensure optimal protection.

Avoidance of iatrogenic photic retinopathy related to ophthalmologic equipment is critical, as this could otherwise permanently affect a patient's vision, even in the setting of perfect surgical technique. Recommended measures to avoid this complication include using the lowest light output necessary for the procedure and minimizing the total duration of surgery. Furthermore, filters incorporated into operative microscopes are used to reduce the amounts of ultraviolet, blue, and infrared light output. Placement of a corneal cover during extraocular procedures can be helpful to act as a barricade against inadvertent intraocular light exposure, and placement of an air bubble in the anterior chamber can be helpful to defocus incoming light. In vitrectomy surgery, careful use of the light pipe is crucial, and therefore maximizing light pipe distance from the retina and using eccentric endoillumination techniques can help to avoid photic retinopathy.

Treatment of Photic Retinal Injury

No specific therapy exists for photic retinopathy. In the majority of cases, observation with cessation of further unprotected solar, laser pointer, or arc welding exposure is recommended. However there are instances where medical or surgical therapy may be indicated.

Medical therapy with corticosteroids has been reported in some cases of solar retinopathy (Choi et al. 2006; Moran and O'Donoghue 2013). The rationale for this is that systemic corticosteroids have been shown to reduce laser-induced retinal damage in the primate model (Ishibashi et al. 1985). Some practitioners use a short course of oral steroids in hopes that it will help resolve acute changes more rapidly and have a beneficial effect in visual acuity (Turaka et al. 2012). However, due to the infrequency of these cases, there has been no large randomized trial comparing systemic corticosteroid for photic retinal injury to an untreated control group. Additionally, spontaneous resolution often occurs without treatment. A short course of oral corticosteroids may be considered in cases where there is retinal edema, severe visual loss related to the photic damage, or bilateral visual loss. A rare complication of handheld laser injury is choroidal neovascularization (CNV) typically related to laser-induced damage to Bruch's membrane, and anti-VEGF agents may be utilized.

Surgical closure of accidental blue laser-induced full-thickness macular hole may be indicated. In a review of 17 patients with laser pointer-induced full-thickness macular holes, 14 eyes underwent 23 gauge pars plana vitrectomy, with a success rate of 78.6% (11/14 eyes). Although closure of these macular holes resulted in anatomic success, persistent outer retinal abnormalities persisted in 73% (8/11 eyes). Outer retinal abnormalities can be persistent after full-thickness macular hole closure (Alsulaiman et al. 2015).

Summary

In summary, photic retinopathy can occur after exposure to varied sources, including solar rays, eclipse rays, laser pointers, welding arcs, and even ophthalmic equipment. Prevention of photic retinopathy is critical and includes avoidance of sungazing, appropriate eye protection, regulations on equipment that can cause permanent visual changes, and judicious use of lighting during ophthalmic surgery. Once photic retinopathy occurs, management involves observation and prevention of further exposure to the inciting source. Severity of photic retinopathy depends on duration and intensity of exposure, and most cases can have some resolution, although the amount of resolution and the remaining visual sequelae can vary.

References

Alsulaiman S, Alrushood A, Almasaud A, et al. High-power handheld blue laser-induced maculopathy. Ophthalmology. 2014;121:566–72.

Alsulaiman SM, Abdulaza AA, Almasaud J, et al. Full-thickness macular hole secondary to high-power handheld blue laser: natural history and management outcomes. Am J Ophthalmol. 2015;160:107–13.

Barkana Y, Belkin M. Laser eye injuries. Surv Ophthalmol. 2000;44:459–78.

Boettner EA, Wolter JR. Transmission of the ocular media. Invest Ophthalmol. 1962;1:776–83.

Choi SW, Chun KI, Lee SJ, Rah SH. A case of photic retinal injury associated with exposure to plasma arc welding. Korean J Ophthalmol. 2006;20:250–3.

Dhoot DS, Xu D. High-powered laser pointer injury resulting in macular hole formation. J Pediatr. 2014;164:668.

Emerson GG, Wong RW. Special safety edition: 2017 Great American Eclipse. ASRS Retina Health Series; 2017. https://www.asrs.org/patients/retinal-diseases/special-safety-edition-2017-great-american-eclipse. Accessed 25 Sept 2017.

FDA. Important information for laser pointer manufacturers radiation emitting products and procedures 2017. Food and Drug Administration; 2017. https://www.fda.gov/RadiationEmittingProducts/RadiationEmittingProductsandProcedures/HomeBusinessandEntertainment/LaserProductsandInstruments/default.htm. Accessed 12 Oct 2017.

Ishibashi T, Miki K, Sorgente N, et al. Effects of intravitreal administration of steroids on experimental subretinal neovascularization in the subhuman primate. Arch Ophthalmol. 1985;103:708–11.

Lee GD, Baumal CR, Lally D, et al. Retinal injury after inadvertent handheld laser exposure. Retina. 2014;34:2388–96.

Mainster M. Light and macular degeneration: a biophysical and clinical perspective. Eye. 1987;1:304–10.

Mainster MA, Ham WT, DeLori FC. Potential retinal hazards. Instrument and environmental light sources. Ophthalmology. 1983;90:927–32.

Michels M, Sternberg P Jr. Operating microscope-induced retinal phototoxicity: pathophysiology, clinical manifestations and prevention. Surv Ophthalmol. 1990;34:237–52.

Moran S, O'Donoghue E. Solar retinopathy secondary to sungazing. BMJ Case Rep. 2013;2013:bcr2012008402.

Priebe LA, Cain CP, Welch AJ. Temperature rise required for the production of minimal lesions in the *Macaca mulatta* retina. Am J Ophthalmol. 1975;79:405–43.

Turaka K, Bryan JS, Gordon AJ, et al. Laser pointer induced macular damage: case report and mini review. Int Ophthalmol. 2012;32:293–7.

Weng C, Baumal CR, Albini TA, Berrocal AM. Self-induced laser maculopathy in an adolescent boy utilizing a mirror. Ophthalmic Surg Lasers Imaging Retina. 2015;46:485–8.

White TJ, Mainster MA, Wilson PW, et al. Chorioretinal temperature increases from solar observation. Bull Math Biophys. 1971;33:1–17.

Postsurgical Cystoid Macular Edema

11

Anna Marmalidou and John B. Miller

Abbreviations

AMD	Age-related macular degeneration
BAB	Blood-aqueous barrier
BRB	Blood-retinal barrier
CNVM	Choroidal neovascularization membrane
DME	Diabetic macular edema
ERM	Epiretinal membrane
FA	Fluorescein angiography
IOL	Intraocular lens
IOP	Intraocular pressure
IVFA	Intravenous fluorescein angiography
IVTA	Intravitreal triamcinolone acetonide
NSAIDs	Nonsteroidal anti-inflammatory drugs
OCT	Optical coherence tomography
PCME	Postsurgical cystoid macular edema
PPV	Pars plana vitrectomy
RVO	Retinal vein occlusion
VMT	Vitreomacular traction

Introduction

Postsurgical cystoid macular edema (PCME) was first described by Hruby in 1950 in a patient presenting after cataract surgery, followed shortly by a similar report by Irvine in 1953 (Hruby 1950; Irvine 1953). Gass and Norton later concluded that this condition was caused by marked macular edema with a classic appearance of perifoveal petalloid staining with late leakage from the optic nerve on intravenous fluorescein angiography (IVFA) (Gass and Norton 1966). Due to these early descriptions by Irvine and Gass, this entity became known as Irvine-Gass syndrome, which is recognized as a common cause of impaired vision following cataract surgery.

Postsurgical cystoid macular edema can occur after any intraocular surgery but is most commonly described after cataract surgery. The reported incidence for PCME is variable, depending on the specific surgical technique for cataract extraction (intracapsular or extracapsular cataract extraction, phacoemulsification). The incidence also varies depending on the method of clinical evaluation (visual acuity, fluorescein angiography, optical coherence tomography). With regard to surgical approach, studies suggest an incidence of angiographic PCME of about 60% following intracapsular cataract extraction, 20% after extracapsular cataract surgery, and 20–30% with small-incision phacoemulsification (Stark et al. 1984; Flach 1998; Ursell et al. 1999; Gulkilik et al. 2006). Following modern phacoemulsification, the rate of PCME as seen on OCT may be as low as 4–11% and as high as 41% depending on the study (Belair et al. 2009; Perente et al. 2007; Lobo et al. 2004). Given the contemporary trends away from intracapsular cataract extraction to almost exclusively extracapsular and phacoemulsification techniques, the incidence of CME resulting from cataract extraction has decreased. The incidence rates of clinically significant PCME are much lower and are estimated to range from 2% to 12% and 0.1% to 2.35% following uncomplicated extracapsular cataract extraction and phacoemulsification, respectively (Bradford et al. 1988; Henderson et al. 2007).

Risk Factors

Various ocular and systemic risk factors have been associated with PCME. Proposed risk factors include diabetes mellitus, hypertension, history of central retinal vein occlusion, recent history of uveitis, pre-existing epiretinal membrane, or complicated cataract surgery (Flach 1998; Henderson et al. 2007). In particular, patients with diabetes mellitus are

A. Marmalidou · J. B. Miller (✉)
Retina Service, Department of Ophthalmology, Massachusetts Eye and Ear Infirmary, Harvard Medical School, Boston, MA, USA
e-mail: John_Miller@meei.harvard.edu

I. K. Kim (ed.), *Macular Disorders*, Retina Atlas, https://doi.org/10.1007/978-981-15-3001-2_11

at increased risk of PCME, likely due to the predisposition to macular edema in diabetic eye disease (Jiramongkolchai et al. 2011). Schmier et al. reported a statistically significant increase in PCME incidence from 1.73 to 3.05% in patients with diabetes mellitus (Schmier et al. 2007).

Like diabetic retinopathy, epiretinal membrane (ERM) and retinal vein occlusion (RVO) can lead to macular edema even in the absence of cataract surgery (Fig. 11.1). A history of ERM or RVO was associated with an increased risk for PCME in a large series by Henderson et al. who reviewed 1659 cataract surgeries (Henderson et al. 2007).

The inflammation associated with uveitis can also predispose to macular edema and confer an increased risk of PCME. In a prospective study comparing 41 eyes with uveitis with 52 controls, the incidence of PCME on OCT was 8% versus 0% at 3 months postoperatively. That study also found that the incidence decreased from 27 to 4% after treating patients with perioperative oral corticosteroids (Belair et al. 2009). Furthermore, Ram and colleagues observed high incidence rates (~21%) of clinical CME following phacoemulsification with intraocular lens implantation in patients with prior uveitis (Ram et al. 2010).

Intraoperative complications considered a risk factor for PCME include vitreous loss, vitreous traction at incision sites, vitreous incarceration, pars plana vitrectomy (PPV) for retained lens fragment, iris trauma, posterior capsule rupture, dislocation of intraocular lens (IOL), early postoperative capsulotomy, and use of iris-fixated or anterior chamber IOLs (Flach 1998; Cohen et al. 2006).

The role of perioperative glaucoma has been unclear in PCME. Although perioperative glaucoma has been implicated as a risk factor for PCME, a retrospective study by Law et al. evaluating glaucoma as a risk factor in the development of PCME reported no increased prevalence of clinical PCME in glaucoma patients undergoing uncomplicated cataract surgery (Law et al. 2010).

Beyond the disease of glaucoma itself, topical antiglaucoma medications may be a risk factor for PCME. A study by Arcieri et al. demonstrated that glaucoma patients treated with prostaglandin analogs were more likely to develop angiographic PCME compared with controls. Fortunately in this study, the PCME resolved after discontinuation of the prostaglandin analogs and treatment with topical diclofenac in all cases (Arcieri et al. 2005).

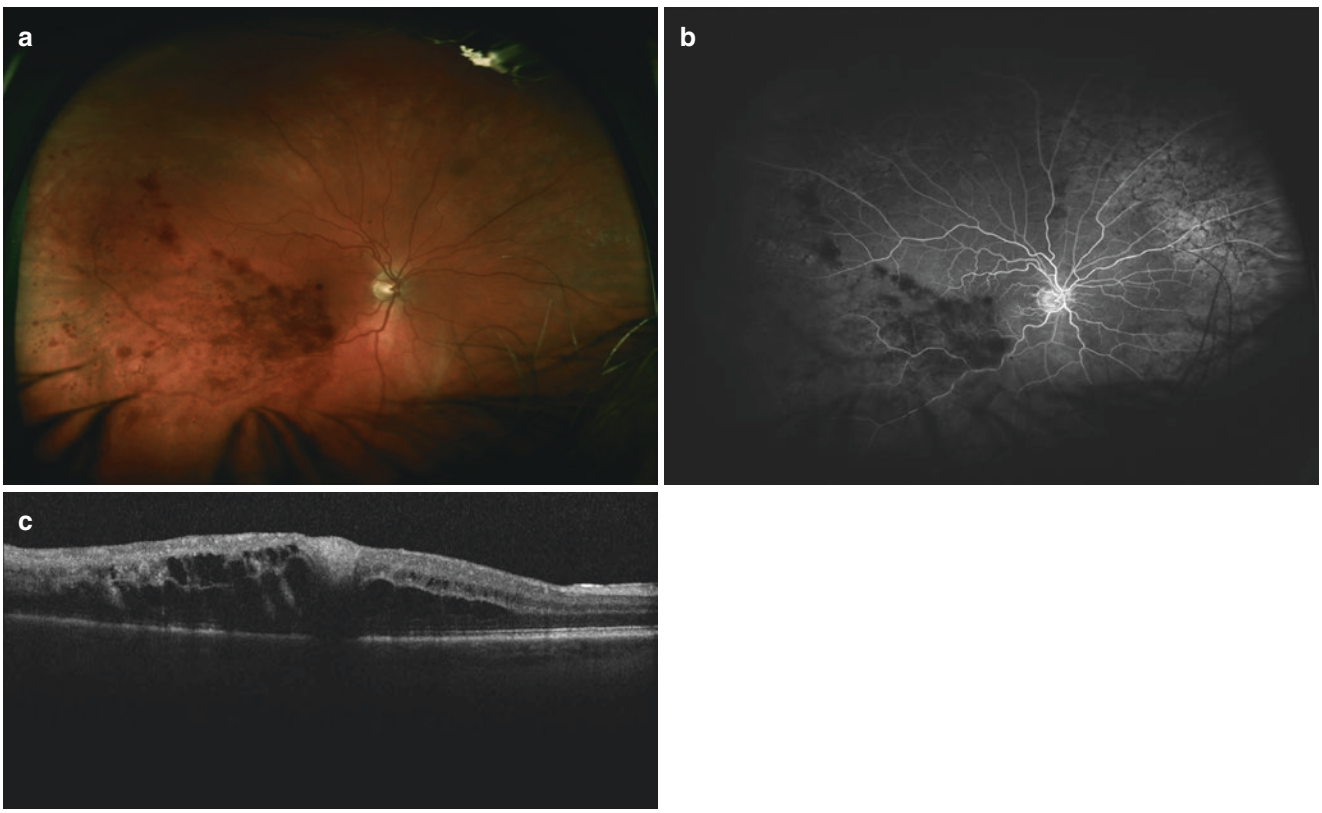

Fig. 11.1 (**a**) Fundus photo of a patient with a branch retinal vein occlusion with sectoral inferior retinal hemorrhages. (**b**) Fluorescein angiography of the same patient with relative blocking of the fluorescence due to overlying retinal hemorrhages. Note the absence of petaloid staining and optic disc leakage as would typically be seen in PCME. (**c**) OCT of the same patient shows diffuse intraretinal edema with posterior shadowing from overlying hemorrhages and intraretinal fluid

Pathogenesis

Postsurgical cystoid macular edema occurs as a sequela of many different surgical procedures, including cataract surgery, vitrectomy, scleral buckling, laser capsulotomy, penetrating keratoplasty, and panretinal photocoagulation (Shimura et al. 2009; Irvine 1976).

The pathogenesis of postsurgical cystoid macular edema is most likely inflammatory, although other contributing factors such as light toxicity or mechanical irritation have been suggested (Schubert 1989; Henry et al. 1977; Miyake and Ibaraki 2002). The release of inflammatory mediators such as prostaglandins and the subsequent disruption of the blood-aqueous barrier (BAB) and blood-retinal barrier (BRB) promote vascular permeability and leakage from perifoveal capillaries and pooling of fluid in the outer retinal layers (Ursell et al. 1999; Yonekawa and Kim 2012; Kent et al. 2000). This increased permeability may be further exacerbated by the previously discussed ocular conditions that can be a risk factor for PCME (Henderson et al. 2007; Miyake et al. 2001; Ray and D'Amico 2002).

Histopathology

Pathological sections of eyes with postsurgical cystoid macular edema demonstrate eosinophilic transudate in the inner nuclear and outer plexiform layers of the retina. The intraretinal fluid results in formation of cystoid spaces that may coalesce into perifoveal cysts. The photoreceptor layer below the cysts usually appears thinner. More severe cases will typically progress to fluid within most retinal layers including the subretinal space (Flach 1998; Ray and D'Amico 2002; Zur and Loewenstein 2017).

Clinical Diagnosis

CME may develop in association with several pathological conditions ranging from ocular to generalized systemic etiologies. Therefore, the correct diagnosis requires a thorough medical and ocular history, ocular examination, and ancillary testing. A proper evaluation may help to reveal and treat the underlying associated disease.

The most common clinical presentation of PCME is decreased visual acuity in the initial postoperative period, most frequently 4–6 weeks after cataract surgery (Yonekawa and Kim 2012). Less common clinical features include decreased contrast sensitivity, central scotomas, metamorphopsias, and mild photophobia (Zur and Loewenstein 2017; Ibanez et al. 1993).

A complete ophthalmic examination is necessary to screen for the many risk factors and associated diseases. In particular, it is important to look for signs of uveitis, IOL dislocation or displacement, and incarceration of vitreous to the cataract wound on the anterior segment exam (Ray and D'Amico 2002). Posteriorly, biomicroscopic fundoscopy will classically show macular thickening and/or loss of foveal depression (Yonekawa and Kim 2012). In addition to the CME findings, one may see associated findings of risk factors or other diseases including ERM, retinal hemorrhage, and optic disc swelling. Use of red-free light can be useful to detect intraretinal cystoid spaces, which may fuse to form larger foveal cysts in chronic cases (Zur and Loewenstein 2017).

Ancillary ophthalmic imaging tests such as fluorescein angiography (FA) and optical coherence tomography (OCT) are valuable in confirming the diagnosis. FA remains the gold standard in differentiating PCME from other conditions. FA demonstrates early staining from the small perifoveal capillaries followed by pooling in the outer plexiform layer resulting in the classic appearance of perifoveal petaloid leakage. Late leakage and staining of the optic nerve due to capillary leakage is also a common finding (Fig. 11.2). Notably, clinical improvement has been reported to correlate with decreased optic nerve staining (Zur and Loewenstein 2017).

The advent of OCT has allowed for noninvasive detection of macular edema beyond what can be typically seen on fundoscopy. OCT demonstrates macular thickening, loss of foveal depression, and hyporeflective cystic spaces more prominently in the inner nuclear and outer plexiform layers, occasionally with subfoveal fluid (Yonekawa and Kim 2012; Kim et al. 2008; Sigler et al. 2016) (Fig. 11.3).

Differential Diagnosis

The differential diagnosis of PCME is quite broad.

Other common causes of cystoid macular edema:

- Diabetic macular edema (DME)
- RVO-related macular edema
- Vitreomacular traction (VMT)
- Epiretinal membrane (ERM)
- Wet age-related macular degeneration (AMD)
- Choroidal neovascularization membrane (CNVM)
- Choroidal hemangioma
- Uveitis
- Hypertensive retinopathy
- Radiation retinopathy

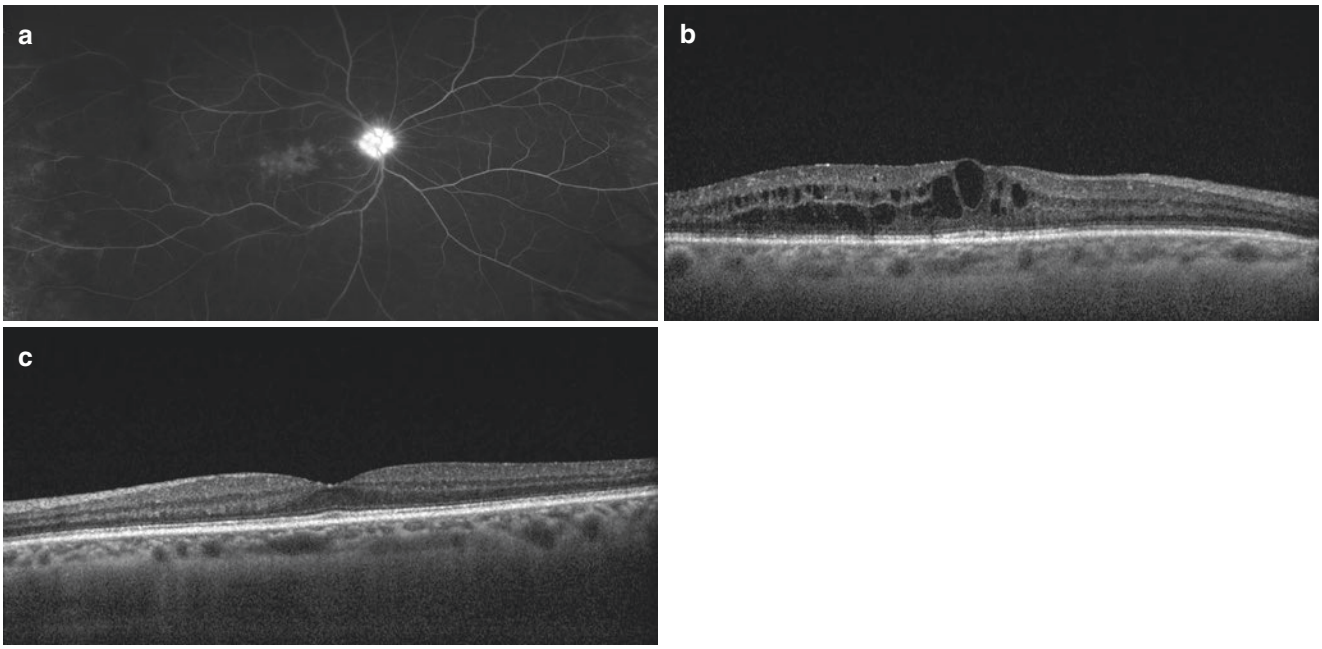

Fig. 11.2 Fluorescein angiography and OCT images of a patient with pseudophakic CME. (**a**) Note macular hyperfluorescence in a petalloid shape and late staining of the optic nerve. (**b**) OCT of the same patient shows intraretinal fluid accumulation of cystoid spaces in the inner retinal layers at the initial presentation. (**c**) Three months after treatment with topical agents, OCT demonstrates resolution of the CME and restoration of the foveal contour

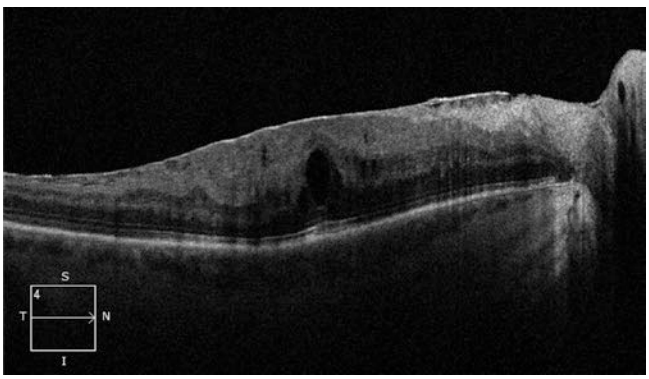

Fig. 11.3 An OCT of a patient with cystoid macular edema secondary to a mild ERM after cataract surgery and retinal detachment repair

More rare causes of macular edema:

- Coats' disease
- Retinopathy of prematurity
- Retinitis pigmentosa
- X-linked hereditary retinoschisis
- Goldmann-Favre disease
- Nicotinic acid maculopathy

Medical history, retinal examination, FA, and OCT can be helpful in distinguishing these etiologies from PCME in the acute phase.

Management

The efficacy of different treatment options in PCME can be difficult to determine given the high proportion of cases that resolve spontaneously (Jacobson and Dellaporta 1974). Often a stepwise approach to management is chosen. Least invasive options are used first with topical therapies, followed by injectable agents, and occasionally surgery in chronic or refractory cases (Zur and Loewenstein 2017).

Topical Medications

Medical therapy aims to suppress inflammation caused by prostaglandin and leukotriene synthesis, thus reducing macular edema. Therapeutic options for topical treatment of PCME include topical nonsteroidal anti-inflammatory drugs (NSAIDs) and corticosteroids.

NSAIDs work by inhibiting the cyclooxygenase enzyme, which is responsible for converting arachidonic acid into prostaglandins during the inflammatory process. Topical NSAIDs are the mainstay for perioperative PCME prophylaxis and treatment and thus are routinely prescribed for all cataract surgeries (Yavas et al. 2007; Almeida et al. 2008). Several ophthalmic preparations can be used including ketorolac, indomethacin, diclofenac, bromfenac, and nepafenac.

Nepafenac is a prodrug which is converted to the more active metabolite amfenac by intraocular hydrolases in vascular ocular tissue and acts as a potent inhibitor of COX-1 and COX-2 activity (Yonekawa and Kim 2012; Hariprasad et al. 2009).

Topical NSAIDs have been successfully used in treatment and prophylaxis of PCME in uncomplicated cases (Miyake et al. 2007; Warren and Fox 2008). The use of topical NSAIDs has also been supported for prevention of PCME in patients with complicated ocular surgery or high-risk patients such as those with a history of diabetes and topical prostaglandin analog use (Henderson et al. 2007; Miyake et al. 1999). Topical nepafenac or bromfenac added benefit to intravitreal anti-VEGF and steroid treatment in chronic cases of PCME (Warren et al. 2010).

In addition to NSAIDs, corticosteroids are commonly used to both manage and prevent macular edema associated with inflammation through their anti-inflammatory actions. Corticosteroids inhibit phospholipase A2 during the arachidonic acid cascade resulting in decreased prostaglandin synthesis, block macrophage and neutrophil migration, and decrease capillary permeability and vasodilation (Simone and Whitacre 2001).

There is little evidence regarding the use of topical NSAIDs alone. Combination therapy with topical corticosteroids has been shown to be superior in treatment or prophylaxis of PCME than either agent alone (Wolf et al. 2007; Heier et al. 2000; Wittpenn et al. 2008) (Fig. 11.4). Few comparative studies support the notion that topical NSAIDs are more effective in preventing PCME compared with topical corticosteroids (Miyake et al. 2007; Asano et al. 2008; Kessel et al. 2014). However, others report similar prophylactic efficacy (Demco et al. 1997; el-Harazi et al. 1998).

Periocular and Intravitreal Therapies

If topical therapy fails, injectable medications may be used.

Sub-Tenon's or Periocular Corticosteroids

Sub-Tenon's and periocular corticosteroids are commonly employed in cases refractory to topical treatments (Zur and Loewenstein 2017). Both retrobulbar and sub-Tenon's corticosteroid injections are effective in treating PCME with improvement in visual acuity but are complicated by low rates of increased intraocular pressure (IOP) (Thach et al. 1997) (Fig. 11.5).

Intravitreal Corticosteroids

Intravitreal triamcinolone acetonide (IVTA) has been shown to be effective for the management of refractory PCME with significant improvement in visual acuity and macular thickness (Conway et al. 2003; Benhamou et al. 2003; Boscia et al. 2005; Koutsandrea et al. 2007; Jonas et al. 2003). In three studies, IVTA caused an increase in IOP in one third of cases, yet all cases gained IOP control with topical antiglaucoma medications (Conway et al. 2003; Koutsandrea et al. 2007; Jonas et al. 2003). Intravitreal dexamethasone corticosteroid implants, which slowly release 0.7 mg of dexamethasone for up to 6 months, have also been used successfully (Khurana et al. 2015; Brynskov et al. 2013; Meyer and Schonfeld 2011). A comparative study between IVTA and dexamethasone implants showed similar efficacy in improving visual acuity and macular thickness. The use of IVTA was found to be associated with the need for repeat injections within 6 months and more frequent and prolonged intraocular hypertension compared with dexamethasone (Dang et al. 2014).

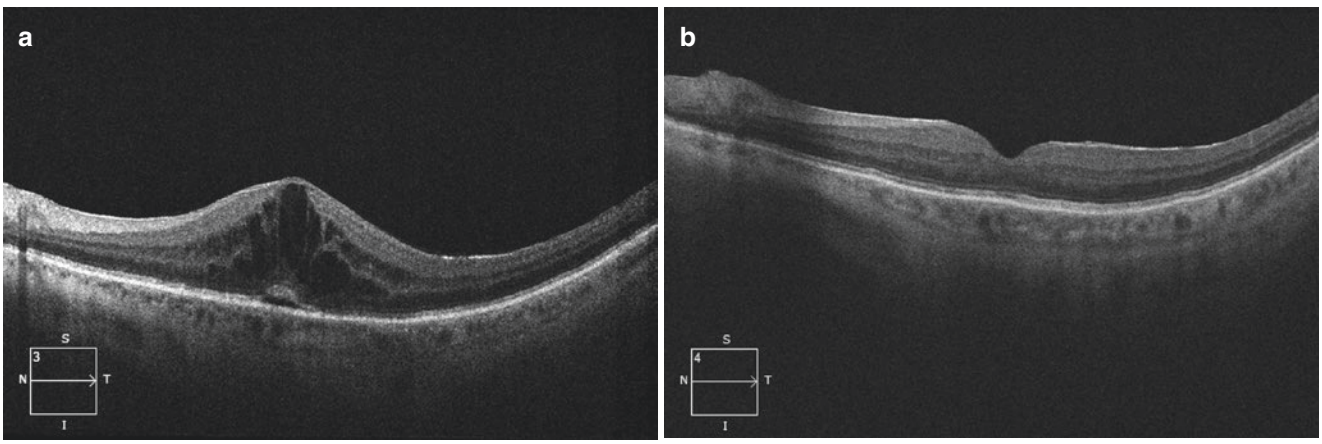

Fig. 11.4 (**a**) OCT demonstrating CME in a patient with history of retinal detachment and anterior chamber IOL. (**b**) OCT demonstrating resolution of CME after treatment with topical steroid and NSAID

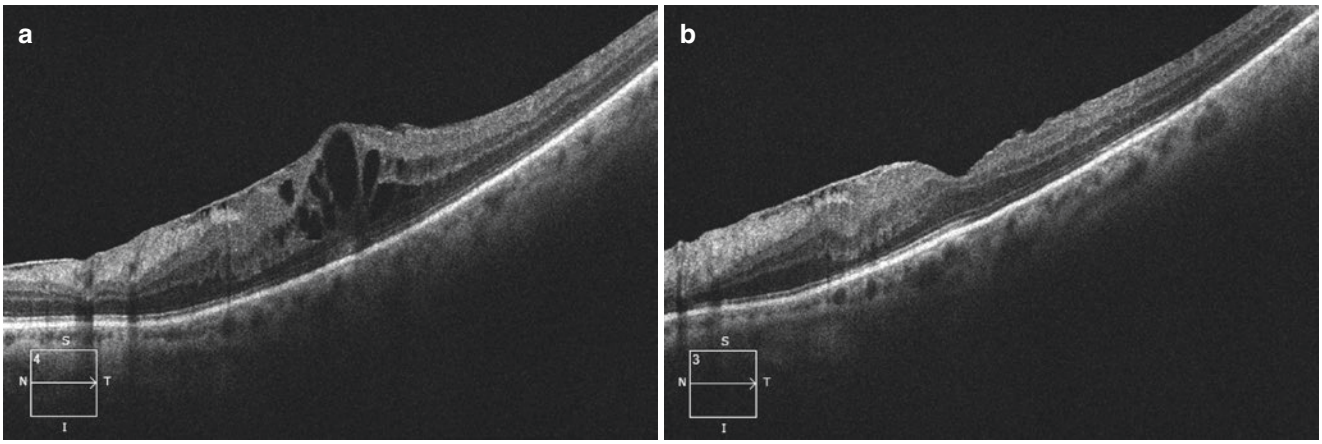

Fig. 11.5 (**a**) OCT showing CME in a patient with ERM and history of retinal detachment. (**b**) OCT after sub-Tenon's injection of triamcinolone showing significant improvement in CME with restoration of foveal contour

Surgical Management

PPV may be considered for PCME complicated by vitreoretinal traction or retained lens fragments (Harbour et al. 1995; Margherio et al. 1997; Rossetti and Doro 2002). A few studies support the use of PPV in some cases of chronic PCME in the absence of vitreoretinal traction (Pendergast et al. 1999). PPV may be considered for PCME refractory to medical treatment for more than 1 year. Internal limiting membrane peeling does not seem to add benefit to PPV (Yonekawa and Kim 2012), but there is only limited data in the literature.

Conclusion

PCME is a rare but significant secondary complication of intraocular surgeries, most commonly cataract extraction. It is an important cause of decreased postoperative vision. Various risk factors have been described for PCME including diabetes mellitus, hypertension, history of central retinal vein occlusion and uveitis, pre-existing epiretinal membrane, and complicated cataract surgery. The clinical diagnosis can be made by the classic petalloid staining pattern and optic disc leakage on FA, intraretinal cystic changes on OCT, and macular thickening on dilated fundus examination. The majority of cases resolve spontaneously. A medical approach is the primary therapeutic option for cases that fail to resolve. Topical NSAIDs are the mainstay in prevention and management of PCME. Topical, periocular, and intravitreal corticosteroids can be useful as monotherapy or as adjunct to NSAIDs. For cases that do not respond to medical therapy or are complicated by vitreomacular traction or retained lens material, surgical intervention may be considered.

References

Almeida DR, Johnson D, Hollands H, et al. Effect of prophylactic nonsteroidal antiinflammatory drugs on cystoid macular edema assessed using optical coherence tomography quantification of total macular volume after cataract surgery. J Cataract Refract Surg. 2008;34:64–9.

Arcieri ES, Santana A, Rocha FN, Guapo GL, Costa VP. Blood-aqueous barrier changes after the use of prostaglandin analogues in patients with pseudophakia and aphakia: a 6-month randomized trial. Arch Ophthalmol. 2005;123:186–92.

Asano S, Miyake K, Ota I, et al. Reducing angiographic cystoid macular edema and blood-aqueous barrier disruption after small-incision phacoemulsification and foldable intraocular lens implantation: multicenter prospective randomized comparison of topical diclofenac 0.1% and betamethasone 0.1%. J Cataract Refract Surg. 2008;34:57–63.

Belair ML, Kim SJ, Thorne JE, et al. Incidence of cystoid macular edema after cataract surgery in patients with and without uveitis using optical coherence tomography. Am J Ophthalmol. 2009;148:128–35.e2.

Benhamou N, Massin P, Haouchine B, Audren F, Tadayoni R, Gaudric A. Intravitreal triamcinolone for refractory pseudophakic macular edema. Am J Ophthalmol. 2003;135:246–9.

Boscia F, Furino C, Dammacco R, Ferreri P, Sborgia L, Sborgia C. Intravitreal triamcinolone acetonide in refractory pseudophakic cystoid macular edema: functional and anatomic results. Eur J Ophthalmol. 2005;15:89–95.

Bradford JD, Wilkinson CP, Bradford RH Jr. Cystoid macular edema following extracapsular cataract extraction and posterior chamber intraocular lens implantation. Retina. 1988;8:161–4.

Brynskov T, Laugesen CS, Halborg J, Kemp H, Sorensen TL. Longstanding refractory pseudophakic cystoid macular edema resolved using intravitreal 0.7 mg dexamethasone implants. Clin Ophthalmol. 2013;7:1171–4.

Cohen SM, Davis A, Cukrowski C. Cystoid macular edema after pars plana vitrectomy for retained lens fragments. J Cataract Refract Surg. 2006;32:1521–6.

Conway MD, Canakis C, Livir-Rallatos C, Peyman GA. Intravitreal triamcinolone acetonide for refractory chronic pseudophakic cystoid macular edema. J Cataract Refract Surg. 2003;29:27–33.

Dang Y, Mu Y, Li L, et al. Comparison of dexamethasone intravitreal implant and intravitreal triamcinolone acetonide for the treatment of pseudophakic cystoid macular edema in diabetic patients. Drug Des Devel Ther. 2014;8:1441–9.

Demco TA, Sutton H, Demco CJ, Raj PS. Topical diclofenac sodium compared with prednisolone acetate after phacoemulsification-lens implant surgery. Eur J Ophthalmol. 1997;7:236–40.

el-Harazi SM, Ruiz RS, Feldman RM, Villanueva G, Chuang AZ. A randomized double-masked trial comparing ketorolac tromethamine 0.5%, diclofenac sodium 0.1%, and prednisolone acetate 1% in reducing post-phacoemulsification flare and cells. Ophthalmic Surg Lasers. 1998;29:539–44.

Flach AJ. The incidence, pathogenesis and treatment of cystoid macular edema following cataract surgery. Trans Am Ophthalmol Soc. 1998;96:557–634.

Gass JD, Norton EW. Cystoid macular edema and papilledema following cataract extraction. A fluorescein fundoscopic and angiographic study. Arch Ophthalmol. 1966;76:646–61.

Gulkilik G, Kocabora S, Taskapili M, Engin G. Cystoid macular edema after phacoemulsification: risk factors and effect on visual acuity. Can J Ophthalmol. 2006;41:699–703.

Harbour JW, Smiddy WE, Rubsamen PE, Murray TG, Davis JL, Flynn HW Jr. Pars plana vitrectomy for chronic pseudophakic cystoid macular edema. Am J Ophthalmol. 1995;120:302–7.

Hariprasad SM, Akduman L, Clever JA, Ober M, Recchia FM, Mieler WF. Treatment of cystoid macular edema with the new-generation NSAID nepafenac 0.1%. Clin Ophthalmol. 2009;3:147–54.

Heier JS, Topping TM, Baumann W, Dirks MS, Chern S. Ketorolac versus prednisolone versus combination therapy in the treatment of acute pseudophakic cystoid macular edema. Ophthalmology. 2000;107:2034–8; discussion 9.

Henderson BA, Kim JY, Ament CS, Ferrufino-Ponce ZK, Grabowska A, Cremers SL. Clinical pseudophakic cystoid macular edema. Risk factors for development and duration after treatment. J Cataract Refract Surg. 2007;33:1550–8.

Henry MM, Henry LM, Henry LM. A possible cause of chronic cystic maculopathy. Ann Ophthalmol. 1977;9:455–7.

Hruby K. Spaltlampenmikroskopie des hinteren Augenabschnittes. Wien: Urban & Schwarzenberg; 1950.

Ibanez HE, Lesher MP, Singerman LJ, Rice TA, Keep GF. Prospective evaluation of the effect of pseudophakic cystoid macula edema on contrast sensitivity. Arch Ophthalmol. 1993;111:1635–9.

Irvine SR. A newly defined vitreous syndrome following cataract surgery. Am J Ophthalmol. 1953;36:599–619.

Irvine AR. Cystoid maculopathy. Surv Ophthalmol. 1976;21:1–17.

Jacobson DR, Dellaporta A. Natural history of cystoid macular edema after cataract extraction. Am J Ophthalmol. 1974;77:445–7.

Jiramongkolchai K, Lalezary M, Kim SJ. Influence of previous vitrectomy on incidence of macular oedema after cataract surgery in diabetic eyes. Br J Ophthalmol. 2011;95:524–9.

Jonas JB, Kreissig I, Degenring RF. Intravitreal triamcinolone acetonide for pseudophakic cystoid macular edema. Am J Ophthalmol. 2003;136:384–6.

Kent D, Vinores SA, Campochiaro PA. Macular oedema: the role of soluble mediators. Br J Ophthalmol. 2000;84:542–5.

Kessel L, Tendal B, Jorgensen KJ, et al. Post-cataract prevention of inflammation and macular edema by steroid and nonsteroidal anti-inflammatory eye drops: a systematic review. Ophthalmology. 2014;121:1915–24.

Khurana RN, Palmer JD, Porco TC, Wieland MR. Dexamethasone intravitreal implant for pseudophakic cystoid macular edema in patients with diabetes. Ophthalmic Surg Lasers Imaging Retina. 2015;46:56–61.

Kim SJ, Belair ML, Bressler NM, et al. A method of reporting macular edema after cataract surgery using optical coherence tomography. Retina. 2008;28:870–6.

Koutsandrea C, Moschos MM, Brouzas D, Loukianou E, Apostolopoulos M, Moschos M. Intraocular triamcinolone acetonide for pseudophakic cystoid macular edema: optical coherence tomography and multifocal electroretinography study. Retina. 2007;27:159–64.

Law SK, Kim E, Yu F, Caprioli J. Clinical cystoid macular edema after cataract surgery in glaucoma patients. J Glaucoma. 2010;19:100–4.

Lobo CL, Faria PM, Soares MA, Bernardes RC, Cunha-Vaz JG. Macular alterations after small-incision cataract surgery. J Cataract Refract Surg. 2004;30:752–60.

Margherio RR, Margherio AR, Pendergast SD, et al. Vitrectomy for retained lens fragments after phacoemulsification. Ophthalmology. 1997;104:1426–32.

Meyer LM, Schonfeld CL. Cystoid macular edema after complicated cataract surgery resolved by an intravitreal dexamethasone 0.7-mg implant. Case Rep Ophthalmol. 2011;2:319–22.

Miyake K, Ibaraki N. Prostaglandins and cystoid macular edema. Surv Ophthalmol. 2002;47(Suppl 1):S203–18.

Miyake K, Ota I, Maekubo K, Ichihashi S, Miyake S. Latanoprost accelerates disruption of the blood-aqueous barrier and the incidence of angiographic cystoid macular edema in early postoperative pseudophakias. Arch Ophthalmol. 1999;117:34–40.

Miyake K, Ota I, Ibaraki N, et al. Enhanced disruption of the blood-aqueous barrier and the incidence of angiographic cystoid macular edema by topical timolol and its preservative in early postoperative pseudophakia. Arch Ophthalmol. 2001;119:387–94.

Miyake K, Nishimura K, Harino S, et al. The effect of topical diclofenac on choroidal blood flow in early postoperative pseudophakias with regard to cystoid macular edema formation. Invest Ophthalmol Vis Sci. 2007;48:5647–52.

Pendergast SD, Margherio RR, Williams GA, Cox MS Jr. Vitrectomy for chronic pseudophakic cystoid macular edema. Am J Ophthalmol. 1999;128:317–23.

Perente I, Utine CA, Ozturker C, et al. Evaluation of macular changes after uncomplicated phacoemulsification surgery by optical coherence tomography. Curr Eye Res. 2007;32:241–7.

Ram J, Gupta A, Kumar S, Kaushik S, Gupta N, Severia S. Phacoemulsification with intraocular lens implantation in patients with uveitis. J Cataract Refract Surg. 2010;36:1283–8.

Ray S, D'Amico DJ. Pseudophakic cystoid macular edema. Semin Ophthalmol. 2002;17:167–80.

Rossetti A, Doro D. Retained intravitreal lens fragments after phacoemulsification: complications and visual outcome in vitrectomized and nonvitrectomized eyes. J Cataract Refract Surg. 2002;28:310–5.

Schmier JK, Halpern MT, Covert DW, Matthews GP. Evaluation of costs for cystoid macular edema among patients after cataract surgery. Retina. 2007;27:621–8.

Schubert HD. Cystoid macular edema: the apparent role of mechanical factors. Prog Clin Biol Res. 1989;312:277–91.

Shimura M, Yasuda K, Nakazawa T, et al. Panretinal photocoagulation induces pro-inflammatory cytokines and macular thickening in high-risk proliferative diabetic retinopathy. Graefes Arch Clin Exp Ophthalmol. 2009;247:1617–24.

Sigler EJ, Randolph JC, Kiernan DF. Longitudinal analysis of the structural pattern of pseudophakic cystoid macular edema using multimodal imaging. Graefes Arch Clin Exp Ophthalmol. 2016;254:43–51.

Simone JN, Whitacre MM. Effects of anti-inflammatory drugs following cataract extraction. Curr Opin Ophthalmol. 2001;12:63–7.

Stark WJ Jr, Maumenee AE, Fagadau W, et al. Cystoid macular edema in pseudophakia. Surv Ophthalmol. 1984;28(Suppl):442–51.

Thach AB, Dugel PU, Flindall RJ, Sipperley JO, Sneed SR. A comparison of retrobulbar versus sub-Tenon's corticosteroid therapy for cystoid macular edema refractory to topical medications. Ophthalmology. 1997;104:2003–8.

Ursell PG, Spalton DJ, Whitcup SM, Nussenblatt RB. Cystoid macular edema after phacoemulsification: relationship to blood-aqueous barrier damage and visual acuity. J Cataract Refract Surg. 1999;25:1492–7.

Warren KA, Fox JE. Topical nepafenac as an alternate treatment for cystoid macular edema in steroid responsive patients. Retina. 2008;28:1427–34.

Warren KA, Bahrani H, Fox JE. NSAIDs in combination therapy for the treatment of chronic pseudophakic cystoid macular edema. Retina. 2010;30:260–6.

Wittpenn JR, Silverstein S, Heier J, Kenyon KR, Hunkeler JD, Earl M. A randomized, masked comparison of topical ketorolac 0.4% plus steroid vs steroid alone in low-risk cataract surgery patients. Am J Ophthalmol. 2008;146:554–60.

Wolf EJ, Braunstein A, Shih C, Braunstein RE. Incidence of visually significant pseudophakic macular edema after uneventful phacoemulsification in patients treated with nepafenac. J Cataract Refract Surg. 2007;33:1546–9.

Yavas GF, Ozturk F, Kusbeci T. Preoperative topical indomethacin to prevent pseudophakic cystoid macular edema. J Cataract Refract Surg. 2007;33:804–7.

Yonekawa Y, Kim IK. Pseudophakic cystoid macular edema. Curr Opin Ophthalmol. 2012;23:26–32.

Zur D, Loewenstein A. Postsurgical cystoid macular edema. Dev Ophthalmol. 2017;58:178–90.